frontiers | Research Topics

# Tumor immune microenvironment topographies for prediction and evaluation: Unlock the mystery of the therapeutic effects and adverse events of tumor immunotherapy

**Edited by**
Xiaoran Yin, Siying Chen, Sidney Fu and Yuyan Wang

**Published in**
Frontiers in Immunology
Frontiers in Oncology

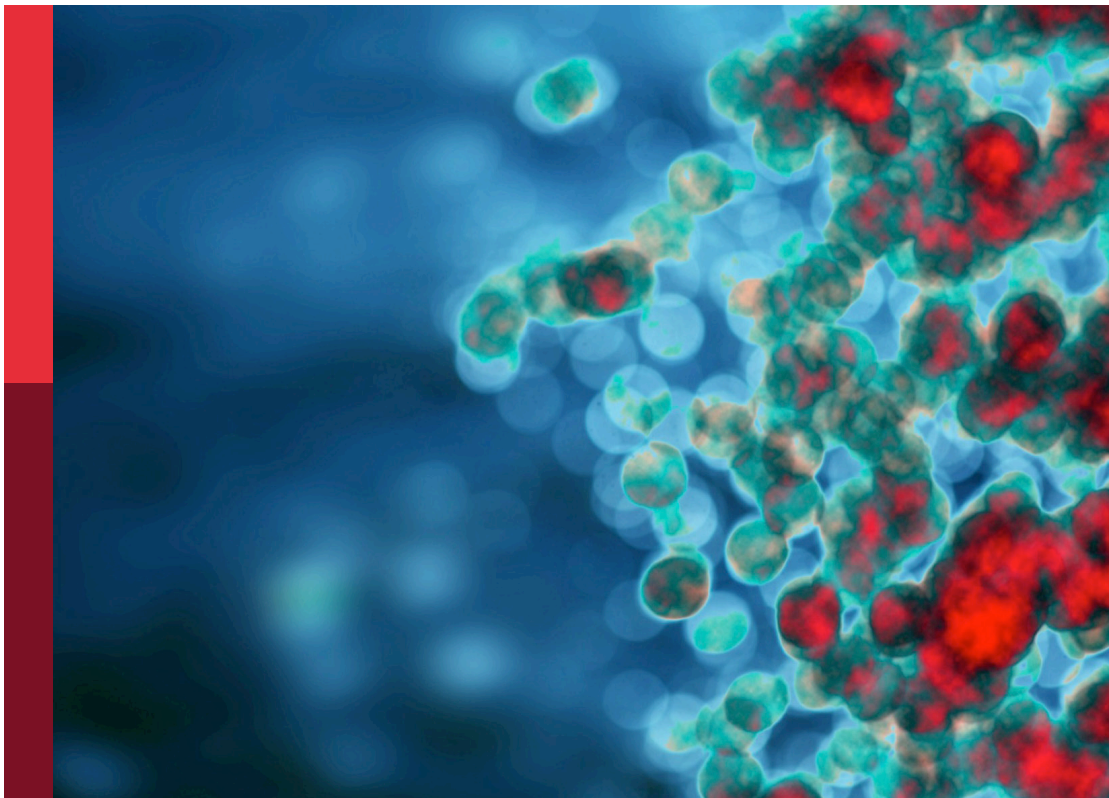

ISSN 1664-8714
ISBN 978-2-8325-3950-7
DOI 10.3389/978-2-8325-3950-7

## About Frontiers

Frontiers is more than just an open access publisher of scholarly articles: it is a pioneering approach to the world of academia, radically improving the way scholarly research is managed. The grand vision of Frontiers is a world where all people have an equal opportunity to seek, share and generate knowledge. Frontiers provides immediate and permanent online open access to all its publications, but this alone is not enough to realize our grand goals.

## Frontiers journal series

The Frontiers journal series is a multi-tier and interdisciplinary set of open-access, online journals, promising a paradigm shift from the current review, selection and dissemination processes in academic publishing. All Frontiers journals are driven by researchers for researchers; therefore, they constitute a service to the scholarly community. At the same time, the *Frontiers journal series* operates on a revolutionary invention, the tiered publishing system, initially addressing specific communities of scholars, and gradually climbing up to broader public understanding, thus serving the interests of the lay society, too.

## Dedication to quality

Each Frontiers article is a landmark of the highest quality, thanks to genuinely collaborative interactions between authors and review editors, who include some of the world's best academicians. Research must be certified by peers before entering a stream of knowledge that may eventually reach the public - and shape society; therefore, Frontiers only applies the most rigorous and unbiased reviews. Frontiers revolutionizes research publishing by freely delivering the most outstanding research, evaluated with no bias from both the academic and social point of view. By applying the most advanced information technologies, Frontiers is catapulting scholarly publishing into a new generation.

## What are Frontiers Research Topics?

Frontiers Research Topics are very popular trademarks of the *Frontiers journals series*: they are collections of at least ten articles, all centered on a particular subject. With their unique mix of varied contributions from Original Research to Review Articles, Frontiers Research Topics unify the most influential researchers, the latest key findings and historical advances in a hot research area.

Find out more on how to host your own Frontiers Research Topic or contribute to one as an author by contacting the Frontiers editorial office: frontiersin.org/about/contact

# Tumor immune microenvironment topographies for prediction and evaluation: Unlock the mystery of the therapeutic effects and adverse events of tumor immunotherapy

**Topic editors**

Xiaoran Yin — Second Affiliated Hospital of Xi'an Jiaotong University, China
Siying Chen — The First Affiliated Hospital of Xi'an Jiaotong University, China
Sidney Fu — George Washington University, United States
Yuyan Wang — Beijing Cancer Hospital, China

**Citation**

Yin, X., Chen, S., Fu, S., Wang, Y., eds. (2023). *Tumor immune microenvironment topographies for prediction and evaluation: Unlock the mystery of the therapeutic effects and adverse events of tumor immunotherapy*. Lausanne: Frontiers Media SA. doi: 10.3389/978-2-8325-3950-7

# Table of contents

frontiers | Frontiers in Oncology

TYPE Editorial
PUBLISHED 01 November 2023
DOI 10.3389/fonc.2023.1301340



OPEN ACCESS

EDITED AND REVIEWED BY
Peter Brossart,
University of Bonn, Germany

*CORRESPONDENCE
Xiaoran Yin
yinxiaoran@163.com
Sidney W. Fu
sidney.fu@nih.gov
Yuyan Wang
wangyuyan1219@aliyun.com
Siying Chen
ychen0326@163.com

RECEIVED 24 September 2023
ACCEPTED 09 October 2023
PUBLISHED 01 November 2023

CITATION
Yin X, Feng Y, Zhang B, Mao X, Chen S, Wang Y and Fu SW (2023) Editorial: Tumor immune microenvironment topographies for prediction and evaluation: unlock the mystery of the therapeutic effects and adverse events of tumor immunotherapy. *Front. Oncol.* 13:1301340.
doi: 10.3389/fonc.2023.1301340



# Editorial: Tumor immune microenvironment topographies for prediction and evaluation: unlock the mystery of the therapeutic effects and adverse events of tumor immunotherapy

Xiaoran Yin[1]*, Yan Feng[2], Bowen Zhang[1], Xueyan Mao[3], Siying Chen[4]*, Yuyan Wang[5]* and Sidney W. Fu[6]*

[1]Department of Oncology, The Second Affiliated Hospital of Xi'an Jiaotong University, Xi'an, Shaanxi, China, [2]Department of Gastroenterology, The First Affiliated Hospital of Xi'an Jiaotong University, Xi'an, Shaanxi, China, [3]Department of Medical Intensive Care Unit, The First Affiliated Hospital, Sun Yat-sen University, Guangzhou, Guangdong, China, [4]Department of Pharmacy, The First Affiliated Hospital of Xi'an Jiaotong University, Xi'an, Shaanxi, China, [5]Key Laboratory of Carcinogenesis and Translational Research (Ministry of Education/Beijing), Department of Thoracic Medical Oncology, Peking University Cancer Hospital & Institute, Beijing, China, [6]Division of Cancer Prevention (Cancer Biomarkers Research Group), National Cancer Institute, Rockville, MD, United States

KEYWORDS

**tumor microenvironment, immune landscape, computational technology, tumor immunotherapy, prognostic model**

Editorial on the Research Topic
Tumor immune microenvironment topographies for prediction and evaluation: unlock the mystery of the therapeutic effects and adverse events of tumor immunotherapy

The tumor microenvironment (TME) constitutes a dynamic system comprising tumor cells, stromal cells and inflammatory cells, among others. Within this milieu, tumor cells adapt, exerting profound influence on antitumor immunity, drug resistance, metastasis, and immune evasion. Immunotherapy harnesses the host's immune system to prevent and combat tumors. Although immunotherapy has achieved notable success, some patients exhibit resistance to treatment, and the mechanisms are poorly elucidated. Confronting these challenges represents a formidable undertaking that requires a deeper understanding of the intricate interplay among these components. The potential for enhancing immunotherapy and reshaping clinical outcomes in pan-tumor therapies lies in the remodeling and recognition of individual TME characteristics (Figure 1).

The compilation of ten manuscripts delves into the Research Topic of "*Prediction and Evaluation of Tumor Immune Microenvironment Topographies*." The main objective of this research is to enhance our comprehension of how to create a topographic map for the immune TME. The investigators discussed the pending issues associated with this ground-breaking field including basic research findings to novel computational approaches, clinic case reports, and research summaries. We aim to open potential translational venues and novel platforms for

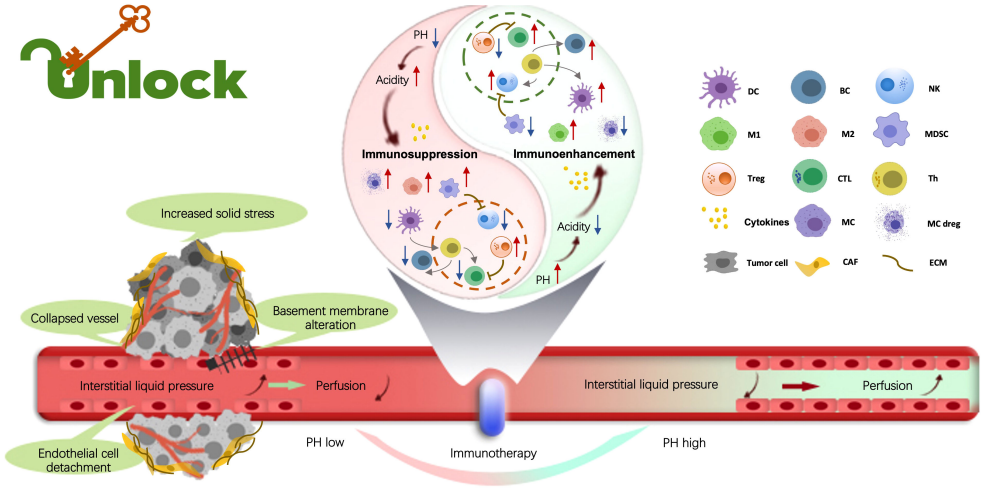


FIGURE 1
Within the tumor microenvironment (TME), the biological, chemical, and mechanical factors influence tumor promotion, metastasis, drug resistance, and immune evasion. Tumor-infiltrating immune cells (TIICs) play the crucial role in regulating these processes. By exploring the distinct attributes of TIICs, the topic offers the potential to unveil novel approaches and cutting-edge technologies, driving the advancement of tumor immunotherapies. Indeed, understanding the multifaceted landscape of the immune TME is essential to develop breakthrough strategies for fighting malignant tumors. (By Xueyan Mao and Xiaoran Yin).

exploring the mystery of the therapeutic effects and adverse events (AEs) of tumor immunotherapy. This Research Topic includes (i) comprehensive reviews on biomarkers utilized for predicting patient response and prognosis when undergoing immunotherapies; (ii) illuminating viewpoints on examining the mechanism of the immune landscape associated with tumors in the TME; (iii) clinical case summaries and reports detailing the therapeutic outcomes and AEs of various forms of tumor immunotherapies; and (iv) original research on creating prognostic models with cutting-edge computational technologies based on clinical characteristics and big data of patients for predicting the responses and side effects of immunotherapies.

Notably, immunotherapy has achieved remarkable advancements through various treatment modalities, including immune checkpoint inhibitors (ICIs), cytokines, tumor vaccines, and cellular therapies, among others. Among all these approaches ICIs have demonstrated remarkable success in the treatment of different types of malignant tumors. Recent studies have unveiled the promising clinical efficacy of perioperative immunotherapy involving ICIs. Precise classification of perioperative treatment strategies based on their specific implementation methods is of paramount importance. Peng et al. conducted an extensive investigation into neoadjuvant therapies and biomarkers to identify the optimal approach to perioperative immunotherapy for non-small cell lung cancer (NSCLC). Their findings highlight that patients receiving a combination of immunotherapy and chemotherapy during the perioperative phase achieved enhanced outcomes with the favorable safety profile. Furthermore, for the optimization of patient outcomes, clinicians should meticulously consider the ideal time interval between neoadjuvant immunotherapy and surgical intervention. Despite significant progress in biomarker research, further in-depth exploration is imperative to refine personalized selection criteria for perioperative immunotherapy.

The effectiveness of immunotherapy is intricately linked to various factors pertaining to both tumor cells and the TME. However, our understanding of the interactions between tumor-infiltrating immune cells (TIICs) and tumors, as well as tumor cells' influence on shaping the TME, remains elusive. The primary challenge lies in eliciting a robust anti-tumor immune response within a conducive TME, while overcoming the barriers of immunosuppression and immune exclusion. Consequently, the reconfiguration of the immune TME emerges as a viable strategy. Martínez et al. conducted an investigation into TME treatment, focusing on rectal cancer patients who underwent various neoadjuvant therapies, including chemotherapy, chemoradiotherapy (RCT), long-interval radiotherapy (LRT), and short-interval radiotherapy (SRT). Their research unveiled that patients with PIK3CA-mutated tumors exhibited elevated infiltration rates of tumor dendritic cells (DCs). Moreover, in comparison to conventional radiotherapy, LRT engendered a higher presence of interstitial helper T cells within the TME. Furthermore, the study observed that, relative to LRT, RCT resulted in diminished numbers of interstitial B cells and stromal T helper cells (Ths), regulatory T cells (Tregs), and cytotoxic T cells (CTLs), alongside an increased presence of swollen DCs in TME. Additionally, it was noted that local therapies such as radiotherapy elicited a more consistent overall immune response in comparison to no treatment or chemotherapy alone. These findings underscore the importance of discerning the divergent immune landscape induced by specific treatments, facilitating more individualized treatment decisions for rectal cancer patients in the future.

Metabolism research have provided invaluable insights into the intricate biological intricacies and the challenges associated with tumor immunotherapy. Several chemical compounds have been identified as potential targets for immunotherapy due to their influence on the progression of tumors within the immune system. One particular promising avenue of investigation is the dysregulated polyamine metabolism. Polyamines have emerged as key players in modulating the behavior of immune cells to mount an effective anti-

tumor response, positioning them as compelling candidate for anti-tumor treatment. However, it is worth noting that polyamines may also exert immunosuppressive effects, promoting the development and progression of tumor cells by aiding them in evading immune surveillance. In a comprehensive study conducted by Lian et al., the effects of polyamines on the immune TME were meticulously examined, revealing a two-fold regulatory impact on both tumor cells and immune cells. This research unveiled that inhibiting polyamines can effectively reshape the immune landscape of TME. Furthermore, the findings from this study suggest that polyamines play a pivotal role in immunomodulation, contributing to tumor evasion. Consequently, polyamines are emerging as a promising avenue for advancing tumor immunotherapy. In a study by Liu et al., it was demonstrated that polyamines have a detrimental effect on the activity of DCs, NKTs, $CD8^+$ TILs, and Th1 cells, while concurrently enhancing the function of Treg cells. Notably, polyamines exhibit a dual role in the context of NKs. Despite a range of preclinical trials involving inhibitors of polyamine metabolism, the clinical applications remain somewhat restricted and require further investigation to unlock their full potential in anti-tumor therapy.

Precision immunotherapy for tumors relies on the analysis of each patient's genetic biomarkers to select the most appropriate individualized therapeutic regimen. Advancements in data mining and digital modeling have enabled researchers to leverage big data platforms and integrate various genome, proteome, and metabolic data to construct visual models. These models are increasingly finding application in clinical settings, aiding in the evaluation of treatment effectiveness, potential side effects, and overall prognosis, thereby ensuring accurate and reliable treatment for malignant tumor patients. In the realm of anti-tumor therapy, prognostic models provide a critical role in guiding clinical decisions for patients undergoing different combined strategies. Liang et al. developed an immune-related gene (IRGPI), to assess the effectiveness of immunotherapy in colorectal carcinoma (CRC). The index consists of 11 genes derived from transcriptome datasets and clinical data, accurately predicting survival rates, characterizing the immune TME, and gauging sensitivity to immunotherapy in CRC patients. Validation of the IRGPI's utility was further confirmed through the CRC mouse model. Additionally, accumulating evidence underscores the intricate interplay between various factors that profoundly orchestrate tumor fate. Methylthioadenosine (MTA) phosphorylase (MTAP), a key enzyme in the methionine synthesis pathway, plays a pivotal role. The accumulation of MTA selectively inhibits the activity of protein arginine methyltransferase 5 (PRMT5) enzyme, resulting in increased sensitivity to PRMT5 inhibition in MTAP-deficient tumors. Notably, MTAP is closely located to the tumor suppressor CDKN2A on chromosome 9p21, leading to frequent genomic alterations involving MTAP/CDKN2A co-occurrence. Xu et al. discovered a connection between MTAP/CDKN2A deficiency and sarcomatous dedifferentiation in renal cell carcinoma (RCC), a finding that can predict aggressive disease progression, poor prognosis, primary resistance to targeted therapy, and potential favorable responses to immune checkpoint blockade. In the future, novel therapeutic options, such as immunotherapies or synthetic PRMT5 inhibitors, may offer new hope to RCC patients with *MTAP/CDKN2A*$^{MUT}$.

In addition, cuproptosis refers to copper-induced cell death, often accompanied by heightened mitochondrial-dependent energy metabolism and an increase in reactive oxygen species (ROS). Research suggested that an excess of copper is associated with various types of malignant tumors. Genes associated with cuproptosis could impact the development, progression, and metastasis of cancerous cells. Cai et al. developed a signature based on 43 cuproptosis-related genes to predict immune cell infiltration and evaluate the efficacy of immune checkpoint blockade (ICB) for individual patients. The cuproptosis risk score derived from this signature indicated that patients with kidney renal clear cell carcinoma (KIRC) who had higher risk scores experienced worse survival outcomes. This finding holds significant value in predicting the prognosis and facilitating precision therapy. Similarly, Wang et al. identified two distinct cuproptosis regulatory subtypes in hepatocellular carcinoma (HCC), each exhibiting unique immune cell infiltration characteristics. Differential gene expression between the two cuproptosis clusters was used to develop a risk signature model. This model revealed that patients in the high-risk group exhibited increased levels of immune and stromal cell infiltration and had a poorer prognosis. The regulatory patterns of cuproptosis may significantly contribute to the diversity of immune cell infiltration, enabling the quantification of individual patient risk and offering novel avenues for personalized anti-tumor immunotherapy in HCC patients.

There are still lots of puzzles in managing AEs in immunotherapy of pan-tumors. Thus, the management of those AEs, such as treatment-related adverse events (trAEs) and immune-related adverse reactions (irAEs), can pose a significant challenge. In a recent meta-analysis led by Kou et al., 21 randomized controlled trials were scrutinized to evaluate the trAEs associated with ICIs. Their findings indicated promising results for various perioperative immunotherapy strategies, notably in patients with operable NSCLC. Nevertheless, the quest for optimal dosing regimens and biomarkers persists, with the aim of tailoring treatments to individual needs and enhancing clinical practice. Fortunately, most AEs can be reversed with appropriate interventions. However, some trAEs can be serious, underscoring the importance of monitoring and comprehending AEs of ICIs therapy for safety outcomes. Among the most prevalent AEs for ICIs are skin-related reactions, with Stevens-Johnson syndrome being a potentially life-threatening cutaneous reaction. A case study by Li et al. documented the experience of a 76-year-old male patient with poorly differentiated metastatic lung adenocarcinoma. Following 9 weeks of sintilimab exposure (3 doses) combined with paclitaxel liposome subsequent to CRT, the patient developed Stevens-Johnson syndrome, affecting the limbs, trunk, lips, and oral mucosa. Skin tissue biopsy revealed infiltration of $CD4^+$ and $CD8^+$ T lymphocytes. However, studies evaluating discontinuation and restart strategies based on efficacy and AEs have not yielded definitive answers. Additionally, determining the optimal duration of ICIs treatment remains an ongoing challenge. The most recent research on customizing the length of immune checkpoint inhibitors (ICIs), as outlined by Yin et al., suggests ICIs tailoring treatment duration of according to an individual's response patterns, tumor stage, and irAEs. This approach incorporates key assessments such as PET-CT, liquid biopsy (e.g.,

ctDNA), or tissue biopsy to guide discontinuation decisions. Moreover, ongoing prospective studies are expected to offer additional insights into the ideal duration of ICIs in the coming years.

Immunotherapy, an epoch-defining treatment, has revolutionized the way for the treatment of malignant tumors. It has significantly enhanced treatment efficacy, prognosis, and tolerability when compared to traditional therapies, providing new hope for patients. A crucial aspect of this approach involves analyzing the TME. The scientific insights gained from this field have yielded a wealth of knowledge on how to predict treatment responses and minimize AEs, thereby providing invaluable guidance for individualized therapy. This dynamic has prompted the establishment of a dedicated platform, fostering the identification and evaluation of the most efficacious immunotherapies while prioritizing patient safety. Although there remains a considerable learning curve concerning optimal dosing and the identification of biomarkers, the potential benefits of personalized treatment approaches are genuinely exhilarating, offering renewed hope to those in need of effective anti-tumor therapeutic strategies.

## Author contributions

XY: Writing – review & editing, Supervision, Writing – original draft. YF: Writing – original draft. BZ: Writing – original draft. XM: Writing – original draft. SC: Writing – original draft. YW: Writing – review & editing. SF: Writing – review & editing.

## Funding

The author(s) declare financial support was received for the research, authorship, and/or publication of this article. This work was supported by the National Natural Science Foundation of China (NSFC) (81802453), the Key Research and Development Program of Shaanxi Province (2019SF-093), and the Basic Scientific Research Interdisciplinary and Cooperation Project of Xi'an Jiaotong University (1119293853).

## Conflict of interest

The authors declare that the research was conducted in the absence of any commercial or financial relationships that could be construed as a potential conflict of interest.

## Publisher's note

frontiers | Frontiers in Immunology

TYPE Original Research
PUBLISHED 01 August 2022
DOI 10.3389/fimmu.2022.953721



OPEN ACCESS

EDITED BY
Xiaoran Yin,
Second Affiliated Hospital of Xi'an Jiaotong University, China

REVIEWED BY
Jianfeng Yang,
Shanghai University of Traditional Chinese Medicine, China
Guiming Zhang,
The Affiliated Hospital of Qingdao University, China
Jun Wang,
Sun Yat-sen University Cancer Center (SYSUCC), China

*CORRESPONDENCE
Dingwei Ye
dwyelie@163.com
Hailiang Zhang
zhanghl918@163.com
Yuanyuan Qu
quyy1987@163.com
Jianyuan Zhao
zhaojy@fudan.edu.cn

†These authors have contributed equally to this work

SPECIALTY SECTION
This article was submitted to Cancer Immunity and Immunotherapy, a section of the journal Frontiers in Immunology

RECEIVED 26 May 2022
ACCEPTED 05 July 2022
PUBLISHED 01 August 2022

CITATION
Xu W, Anwaier A, Liu W, Wei G, Su J, Tian X, Xia J, Qu Y, Zhao J, Zhang H and Ye D (2022) Genomic alteration of MTAP/CDKN2A predicts sarcomatoid differentiation and poor prognosis and modulates response to immune checkpoint blockade in renal cell carcinoma.
*Front. Immunol.* 13:953721.
doi: 10.3389/fimmu.2022.953721

# Genomic alteration of MTAP/CDKN2A predicts sarcomatoid differentiation and poor prognosis and modulates response to immune checkpoint blockade in renal cell carcinoma

Wenhao Xu[1†], Aihetaimujiang Anwaier[1†], Wangrui Liu[2,3†], Gaomeng Wei[3†], Jiaqi Su[1], Xi Tian[1], Jing Xia[4], Yuanyuan Qu[1*], Jianyuan Zhao[5*], Hailiang Zhang[1*] and Dingwei Ye[1*]

[1]Department of Urology, Fudan University Shanghai Cancer Center, Shanghai, China, [2]Department of Interventional Oncology, Renji Hospital, Shanghai Jiao Tong University School of Medicine, Shanghai, China, [3]Affiliated Hospital of Youjiang Medical University for Nationalities, Baise, China, [4]The Medical Department, 3D Medicines Inc., Shanghai, China, [5]Institute for Developmental and Regenerative Cardiovascular Medicine, MOE-Shanghai Key Laboratory of Children's Environmental Health, Xinhua Hospital, Shanghai Jiao Tong University School of Medicine, Shanghai, China

Sarcomatoid differentiation is a highly aggressive pathological characteristic of renal cell carcinoma (RCC) and is characterized by susceptibility to progression and extremely poor prognosis. In this study, we included all genomic alteration events that led to a loss of protein function of MTAP and CDKN2A, and enrolled 5,307 RCC patients with genomic sequencing data from Western and Chinese cohorts. Notably, *MTAP/CDKN2A*$^{MUT}$ occurred in the Chinese population ~2 times more frequently than in the Western cohort and showed significant co-mutation trends. We found significantly higher proportions of sarcomatoid-positive patients with *MTAP*$^{MUT}$ or *CDKN2A*$^{MUT}$ compared with *MTAP/CDKN2A* wild-type (WT) patients ($P < 0.001$). Of the 574 RCC samples from the FUSCC cohort and 3,563 RCC samples from 17 independent cohorts, the *MTAP/CDKN2A*$^{MUT}$ significantly predicted extremely poor outcomes ($P < 0.0001$). The Western cohort suggested a concordant relationship between *MTAP/CDKN2A*$^{MUT}$ and sarcomatoid differentiation in RCC. Moreover, although *MTAP/CDKN2A*$^{MUT}$ RCC may be insensitive to targeted therapy, the high degree of tumor heterogeneity and higher PD-L1 and CXCL13 expression characterizations reflected that *MTAP/CDKN2A*-deficient features could benefit from immunotherapy for patients with RCC. This study utilized RCC samples from large-scale, global, multicenter sequencing cohorts and first proved that *MTAP/CDKN2A* deficiency significantly correlates with

sarcomatoid differentiation in RCC and predicts aggressive progression, poor prognosis, and primary resistance to targeted therapy and potential favorable responses to immune checkpoint blockade. Unlike conventional targeted therapies, emerging drugs such as immunotherapies or synthetic lethal PRMT5 inhibitors may become novel therapeutic options for patients with *MTAP/CDKN2A*$^{MUT}$ RCC.

KEYWORDS

renal cell carcinoma, sarcomatoid differentiation, immunotherapy, genomic alteration, MTAP, CDKN2A, tumor microenvironment

## Introduction

Renal cell carcinoma (RCC) is one of the most common genitourinary malignancies (1), accounting for 3% of all malignant tumors, and its incidence is increasing at a rate of 3% every year (2). The incidence rate in major domestic cities of China, such as Beijing, Shanghai, and Hangzhou, has reached more than 8/100,000, which is more than double that of 10 years ago (3, 4). Clear cell renal cell carcinoma (ccRCC) is the predominant pathological type of kidney cancer, which accounts for about 78% of all RCC in adults. Nearly one-third of ccRCC patients encountered lymphatic, bone, or organ metastases at initial diagnosis, and the 5-year survival rate of patients with advanced ccRCC is less than 20% (5, 6). Although classic histological heterogeneity has been widely explored in the research of ccRCC, the latest advances in genomic technologies have demonstrated prominent molecular subtypes, which have assisted in elucidating the precise typing and treatment of ccRCC as well as mechanisms underlying the inevitable occurrence and development essence (7, 8). Therefore, the multi-omics approach from molecular and genomic levels have become important research techniques in the systematic study of tumor occurrence and treatment efficacy improvement for patients with ccRCC.

Sarcomatoid differentiation is a highly aggressive pathological and extremely uncommon characteristic of RCC and is characterized by susceptibility to metastasis and recurrence and extremely poor prognosis. Renal cell carcinoma with sarcomatoid dedifferentiation (sRCC) is insensitive to chemoradiotherapy and targeted therapy, and radical resection is the preferred treatment. Patients who have clear cell histology and a higher percentage of sarcomatoid differentiation may have worse outcomes with VEGF-targeted therapy (9). In addition, the more sarcoma components, the worse the prognosis of the patient. Even with active treatment, the median postoperative survival for patients with sRCC was still not optimistic (10). For example, with over 42 months of median follow-up, RCC patients with sarcomatoid histology who received nivolumab plus ipilimumab still had median overall survival that was not yet reached [(25.2–not estimable); $n = 74$] versus those who received sunitinib [14.2 months (9.3–22.9); $n = 65$; $P = 0.0004$] (11). Meanwhile, the JAVELIN Renal 101 trial enrolled 108 RCC patients with sarcomatoid histology (47 patients in the avelumab plus axitinib arm and 61 in the sunitinib arm), and patients with sRCC in the combination arm had improved efficacy outcomes versus those in the sunitinib arm (12). The median progression-free survival (PFS) was 7.0 months (95% CI, 5.3–13.8 months) versus 4.0 months (95% CI, 2.7–5.7 months), respectively. Although researchers keep on exploring the unique molecular pathogenesis and driver mutation spectrum of sRCC, the need for individual diagnostic or effective treatment options is urgent (13).

Methylthioadenosine (MTA) phosphorylase (MTAP) is a key enzyme of the methionine remediation synthesis pathway. In MTAP-deficient cancers, MTA accumulation selectively inhibits protein arginine methyltransferase 5 (PRMT5) enzyme activity and increases PRMT5 inhibition sensitivity (14). Precisely because of this synthetic lethal mechanism, the development and application of drugs targeting PRMT5 have led to new treatment options for patients with MTAP deletion tumors (15). Since *MTAP* is located on chromosome 9p21, close to the tumor suppressor *CDKN2A*, genomic alteration of *MTAP*/*CDKN2A* co-occurrence is frequent. At the EAU2021 conference, Necchi et al. compared genomic differences between sRCC and clear

**Abbreviations:** ccRCC, clear cell renal cell carcinoma; DEGs, differentially expressed genes; DFS, disease-free survival; DSS, disease-specific survival; FUSCC, Fudan University Shanghai Cancer Center; GEO, Gene Expression Omnibus; MTAP, methylthioadenosine phosphorylase; PRMT5, protein arginine methyltransferase; OS, overall survival; TIME, tumor immune microenvironment; TME, tumor microenvironment; PFS, progression-free survival; RCC, renal cell carcinoma; sRCC, renal cell carcinoma with sarcomatoid dedifferentiation; TCGA, The Cancer Genome Atlas.

cell RCC (ccRCC). The authors found a significant increase in *MTAP*/*CDKN2A* loss in sRCC and proposed a potential role of anti-PRMT5 drugs in MTAP-deficient advanced sRCC (16). However, the lack of clinical data and the small sample size were major limitations.

In this study, we included all genomic alteration (GA) events that led to a loss of protein function in the statistical analysis. The study included 574 Chinese patients with RCC from the Fudan University Shanghai Cancer Center (FUSCC); 3,563 RCC samples from 17 independent cohorts were integrated (Western). *MTAP*/*CDKN2A* alteration frequency, clinicopathological features, and prognosis were depicted in the FUSCC and Western cohorts. Finally, we included 1,170 Chinese RCC patients from the 3D cohort with panel sequencing data. The relationship of *CDKN2A* mutations with therapeutic markers was further explored. We hypothesized that *MTAP*/*CDKN2A*-deficient features significantly correlate with sarcomatoid differentiation in RCC and predict poor outcomes, inactive targeted treatment responsiveness, and favorable responses to immune checkpoint blockade in patients with RCC.

# Methods

## Data collection and preprocessing from the discovery, testing, and validation sets

In the Chinese training cohort, 574 patients with available whole-exome sequencing (WES) data from the FUSCC (Shanghai, China) were included. In the Western testing cohort, the WES sequencing data of 3,563 ccRCC Caucasian patients were obtained from the cBioPortal for Cancer Genomics database (http://www.cbioportal.org/) with gene IDs converted from Ensembl ID to gene symbol matrix. The combined 3D medicine cohort included WES data of DNA extracted from clinically annotated tumor specimens and from whole blood (as the matched germline source) from a total of 1,170 Chinese RCC patients.

## Genetic variation analysis

The somatic mutation data were processed using the "maftools" R package to screen and present the genes with the top 20 mutation frequencies. The chi-square test was implemented to analyze the differences in the mutation frequencies of the high-frequency mutant genes among the three cohorts. We counted all genomic alterations (specifically the focal loss of 9p21) to the *MTAP* and *CDKN2A* genes that sit next to each other on chromosome 9p21 and referred to the altered status as "MUT."

## Clinicopathological subgroup analysis

We divided patients into different subgroups based on different clinicopathological features, including neoplasm histological grade, cancer metastasis, cancer lymph node stage, neoplasm clinical stage, and race category; different hemogram features, including the levels of hemoglobin, platelet, WBC, and serum calcium; and different clinical therapy data, including individual neoplasm status, sunitinib treatment after operation, new neoplasm event after initial therapy indicator, and response to systematic first-line targeted therapy. The Fisher test was used to compare the differences in different clinical subgroups between the *MTAP*/*CDKN2A*-altered and *MTAP*/*CDKN2A*-unaltered groups.

## Differential gene expression analysis and functional enrichment analysis

To explore the potential biological differences between the *MTAP*/*CDKN2A*-altered and *MTAP*/*CDKN2A*-unaltered patterns, the "limma" R package was used to identify differentially expressed genes (DEGs), and the threshold value was set as $P < 0.05$, $|\log FC| \geq 3.37$. Functional enrichment analyses were carried out to explore the potential functions of the genomic alteration of *MTAP*/*CDKN2A* in patients with RCC using the Gene Ontology (GO), Kyoto Encyclopedia of Genes and Genomes (KEGG), and Reactome databases (17).

## Hematoxylin and eosin and immunohistochemistry staining analysis

Hematoxylin and eosin staining was conducted according to routine protocols. Briefly, after deparaffinization and rehydration, tissue sections were stained with hematoxylin solution and eosin solution (ZSGB-BIO, China), followed by dehydration with graded alcohol and clearing in xylene. The mounted slides were then examined and photographed using a LEICA DM3000 LED (Leica DMshare (v3), Germany) following the manufacturer's protocols and previously described procedure (8). IHC was performed to evaluate the expression level of CXCL13 (1:1,000 dilution; ab246518; Abcam, USA) and PD-L1 (1:300 dilution; No. 19313684, CST, China) in ccRCC samples from the FUSCC according to standard procedures as previously described (8). Staining score and sarcomatoid differentiation features were independently measured by two experienced clinical pathologists.

## Statistical analysis

In the statistical analyses, the Wilcoxon test was used to compare the differences between the two groups of samples. The survival curve was analyzed using Kaplan–Meier, and the log-rank test was used to assess the significance for disease-specific survival (DSS), disease-free survival (DFS), overall survival (OS), and PFS. The "survminer" R package was utilized to take the best cutoff value for all survival analyses. A *P*-value less than 0.05 was considered statistically significant.

# Results

## Clinical value of MTAP/CDKN2A$^{MUT}$ in sarcomatoid and prognosis of 574 patients with RCC from the FUSCC cohort

First, we summarized the mutation frequencies of *MTAP/CDKN2A* in the three cohorts, namely, the discovery set (FUSCC cohort, $n$ = 574), the testing set (Western cohort, $n$ = 3,563), and the validation cohort (3D medicine cohort, $n$ = 1,170) (Figure 1A). The results showed the highest frequency of *MTAP*$^{MUT}$ and *CDKN2A*$^{MUT}$ (2.96% and 5.75%, respectively) in the FUSCC cohort, and the *MTAP*$^{MUT}$ frequency was approximately half of *CDKN2A*$^{MUT}$ frequency. Notably, *MTAP/CDKN2A*$^{MUT}$ occurred in the Chinese population ~2 times more frequently than in the Western cohort and showed significant co-mutation trends.

To verify the relationship between *MTAP/CDKN2A* mutations and sarcomatoid differentiation, we evaluated the pathological features of 574 samples from the FUSCC cohort and found significantly higher proportions of sarcomatoid-positive patients with *MTAP*$^{MUT}$ or *CDKN2A*$^{MUT}$ compared with *MTAP/CDKN2A* wild-type (WT) patients ($P$ < 0.001; Figure 1B). The majority of *MTAP/CDKN2A*$^{MUT}$ samples showed sarcomatoid pathological features (Figure 1C). Of the 574 RCC samples, the *MTAP/CDKN2A*$^{MUT}$ significantly predicted extremely poor PFS [hazard ratio (HR)=7.705, $P$ < 0.0001] and OS (HR = 6.369, $P$ < 0.0001; Figure 1D). Taken together, we found that *MTAP/CDKN2A*$^{MUT}$ could significantly predict sarcomatoid differentiation and prognosis in RCC.

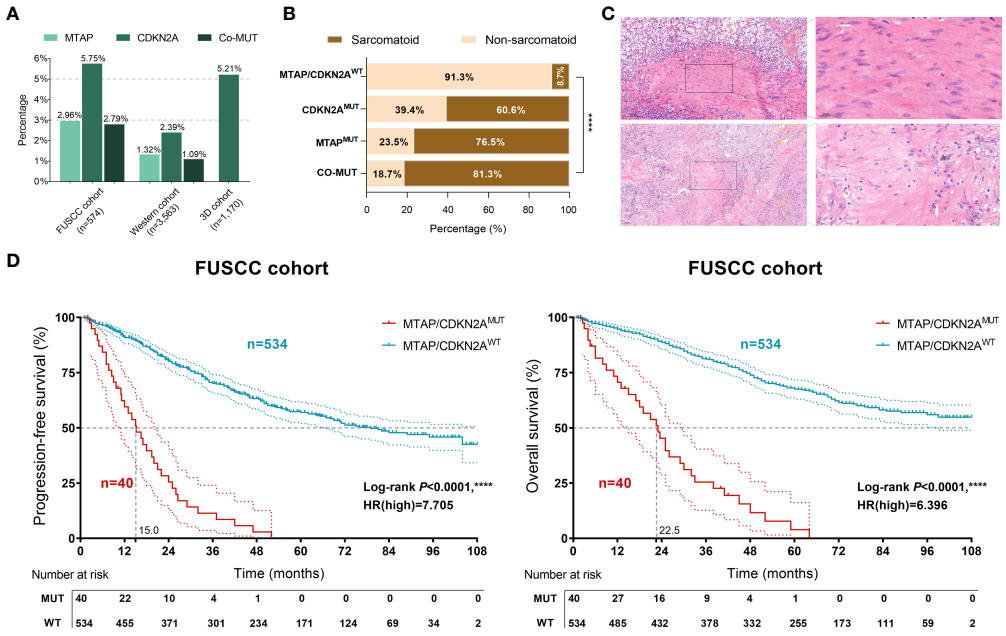


FIGURE 1
Clinical value of *MTAP/CDKN2A*$^{MUT}$ in sarcomatoid and the prognosis of 574 patients with renal cell carcinoma (RCC) from the discovery set of the Fudan University Shanghai Cancer Center (FUSCC) cohort. **(A)** Genomic alteration frequency of *MTAP* and *CDKN2A* in 574 Chinese patients with RCC from the FUSCC cohort; 3,563 RCC samples from 17 independent cohorts were integrated (Western cohort), and 1,170 Chinese patients with RCC were included from the 3D medicine cohort with panel sequencing data. **(B)** The proportion of sarcomatoid pathological features in 574 patients with RCC from the FUSCC cohort in different mutation groups. **(C)** The representative images of sarcomatoid pathological features in *MTAP/CDKN2A*$^{MUT}$ samples. **(D)** Classified by the *MTAP/CDKN2A*$^{MUT}$, progression-free survival (PFS) and overall survival (OS) of 574 RCC patients from the FUSCC cohort using Kaplan–Meier curve analysis. ****, P<0.0001.

## MTAP/CDKN2A$^{MUT}$ in histopathological subtypes and sarcomatoid differentiation of 3,563 patients with RCC from the Western cohort

To further test our hypothesis, we then explored *MTAP/CDKN2A*$^{MUT}$ frequencies in 3,563 RCC samples from the Western cohort. As shown in Figure 2A, *MTAP/CDKN2A*$^{MUT}$ is more common in non-ccRCC, and the frequency of progression and mortality events was significantly increased in the GA group. The frequency of *MTAP/CDKN2A*$^{MUT}$ in different RCC datasets is shown in Figure 2B. The results revealed that *MTAP/CDKN2A*$^{MUT}$ is more common in non-ccRCC histopathological subtypes, which is consistent with the consensus that sarcomatoid differentiation occurs more frequently in non-ccRCC. Interestingly, we found remarkable sarcomatoid differentiation in patients with both *MTAP*$^{MUT}$ and *CDKN2A*$^{MUT}$ (Figure 2C). Overall, the results from the Western cohort suggest a concordant relationship between *MTAP/CDKN2A*$^{MUT}$ and sarcomatoid differentiation in RCC.

## Implications of MTAP/CDKN2A$^{MUT}$ in prognosis, clinicopathological features, and sensitivity to therapy of 3,563 patients with RCC from the Western cohort

Next, we collected RCC samples with available survival and mutation information from the Western cohort. Significantly, the genomic alteration of *MTAP* prominently predicted shorter DSS ($P < 0.0001$, HR=5.675), PFS ($P < 0.0001$, HR = 6.000), DFS ($P < 0.0001$, HR = 6.008), and OS ($P < 0.0001$, HR = 3.669) in patients with RCC from the Western testing cohort (Figure 3A). Moreover, the genomic alteration of *CDKN2A* was also significantly associated with shorter DSS ($P < 0.0001$, HR = 7.415), PFS ($P < 0.0001$, HR = 6.441), DFS ($P < 0.0001$, HR = 5.902), and OS ($P < 0.0001$, HR = 4.837) in 3,563 patients with RCC from the Western cohort (Figure 3B).

Additionally, the results revealed that *MTAP/CDKN2A*$^{MUT}$ significantly predicted poor DSS ($P < 0.0001$, HR = 6.921), PFS ($P < 0.0001$, HR = 6.295), DFS ($P < 0.0001$, HR = 5.919), and OS

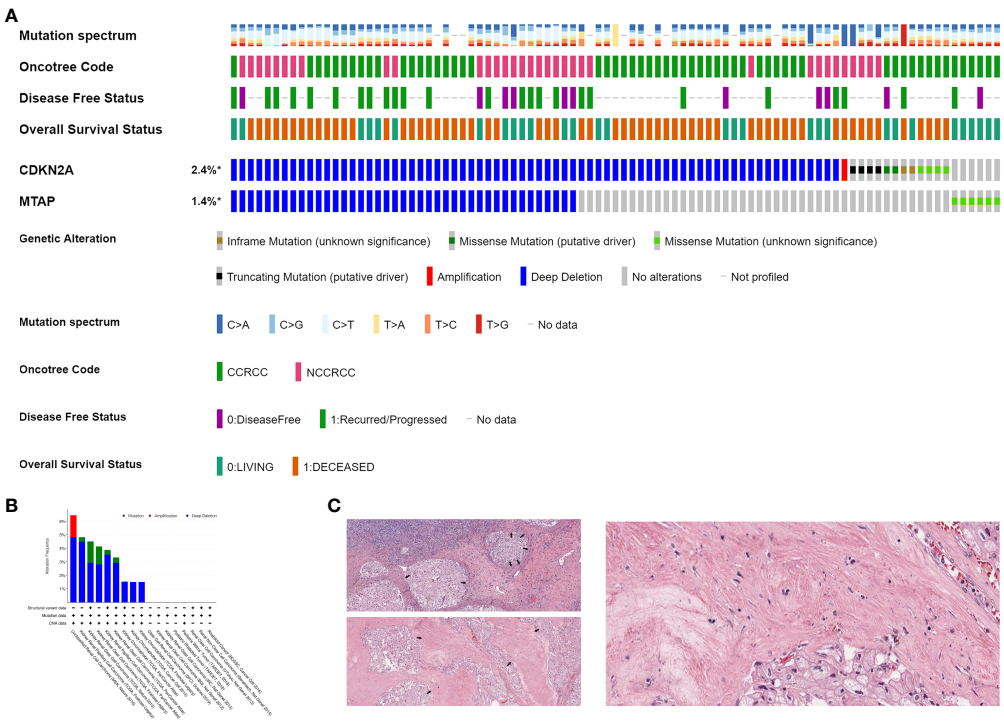


FIGURE 2
*MTAP/CDKN2A*$^{MUT}$ in histopathological subtypes and sarcomatoid differentiation of 3,563 patients with RCC from the Western cohort. **(A)** Relationship between *MTAP/CDKN2A*$^{MUT}$ and histopathological subtypes of RCC, disease-free status, and OS status in 3,563 RCC samples from the Western cohort. **(B)** The frequency of *MTAP/CDKN2A* genomic alterations in different RCC datasets. **(C)** Remarkable sarcomatoid differentiation in patients with both *MTAP*$^{MUT}$ and *CDKN2A*$^{MUT}$ from The Cancer Genome Atlas. * Ratio is calculated as altered/profiled.

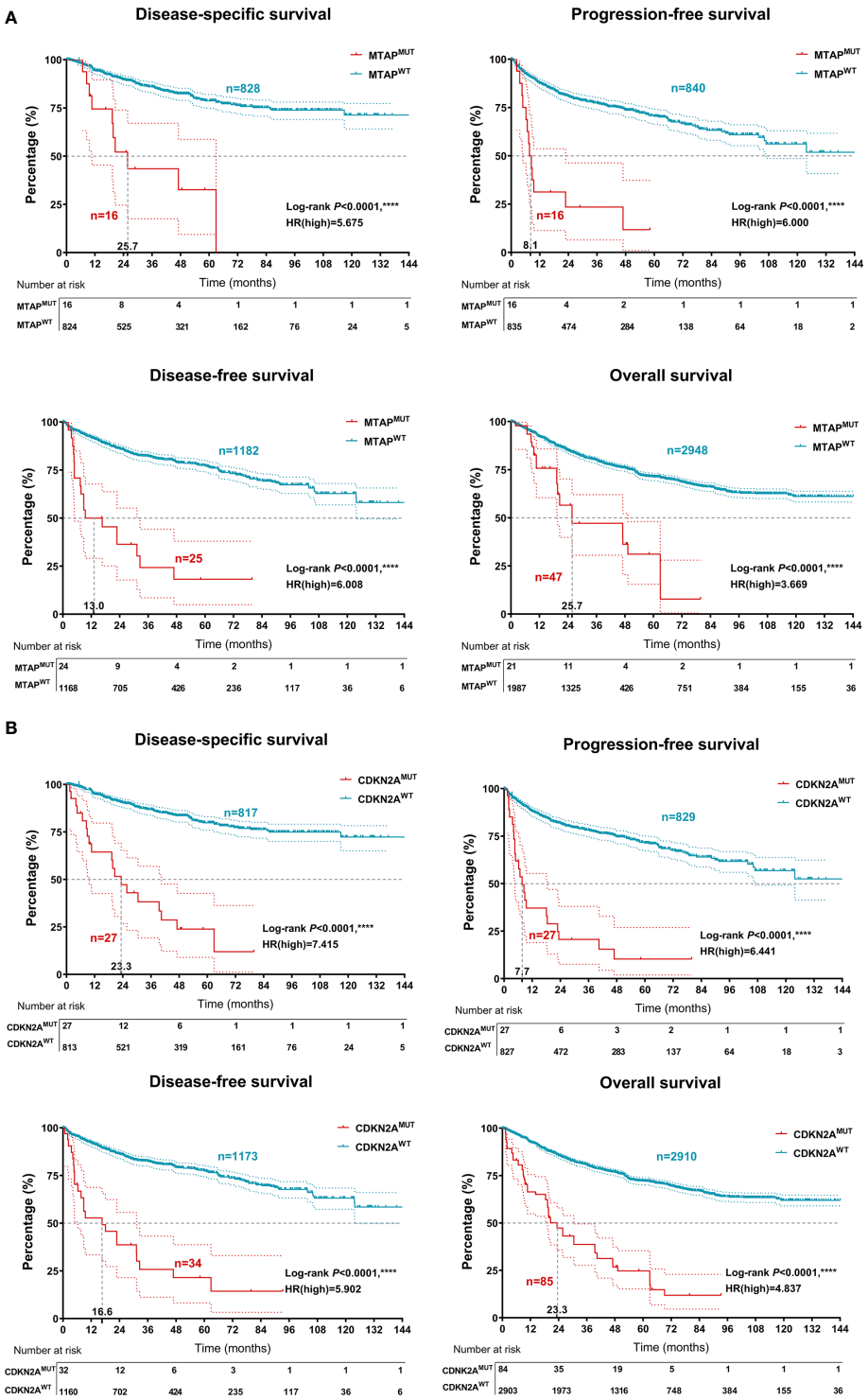


FIGURE 3
Prognostic implications of *MTAP*$^{MUT}$ and *CDKN2A*$^{MUT}$ 3,563 patients with RCC from the testing set of the Western cohort. **(A)** Classified by the *MTAP*/*CDKN2A*$^{MUT}$, disease-specific survival, PFS, disease-free survival, and OS of RCC patients from the Western cohort using Kaplan–Meier survival analysis. **(B)** Association between *MTAP*/*CDKN2A*$^{MUT}$ and clinicopathological characteristics, association between *MTAP*/*CDKN2A*$^{MUT}$ and hemogram, and association between *MTAP*/*CDKN2A*$^{MUT}$ and clinical therapeutic efficacy. ****, P<0.0001.

($P < 0.0001$, HR = 4.564) in patients with RCC from the testing set (Figure 4A). Moreover, RCC patients with *MTAP/CDKN2A*$^{MUT}$ showed significantly higher pathology grades (95.8% were G3–G4) and clinical stages (92.5% were III–IV; Figure 4B). Consistently, we found a significantly higher frequency of Asian subjects in the GA group than in the unaltered group. Additionally, patients in the GA group exhibited lower hemoglobin and leukocyte levels and higher platelet and blood calcium levels, reflecting a higher IMDC stage and a higher treatment primary tolerance. Additionally, in the GA group, the proportion of patients with unresectable tumors was 63.5%; 50% of the patients received postoperative sunitinib therapy, and approximately 40% of patients carried new neoplasm events after initial therapy. These findings suggested that patients in the GA group are primarily resistant to conventional targeted therapy (Figures S1A, B). Overall, to our knowledge, this is the first verification of the prominent relationship between *MTAP/CDKN2A*$^{MUT}$ and sRCC. *MTAP/CDKN2A*$^{MUT}$ could significantly predict progression, long-term survival, and treatment efficacy in RCC patients.

## MTAP/CDKN2A$^{MUT}$ predicts higher tumor heterogeneity, tumor microenvironment characterizations, and active responses to immune checkpoint blockade of RCC patients

The above findings aroused our interest regarding the impact of *MTAP/CDKN2A*$^{MUT}$ on RCC malignant biological functions. Therefore, we analyzed genotype differences in the Western cohort using the "limma" R package with a threshold of $Log^{10}$($q$-value) >2. A total of 363 significantly upregulated genes in the *MTAP/CDKN2A*$^{MUT}$ group were identified (Figure 5A). Functional enrichment suggested that *MTAP/CDKN2A*$^{MUT}$ response genes participate in the aggregation and activation of immune cells in the tumor microenvironment (TME). Similarly, pathway enrichment results revealed a marked involvement in the JAK–STAT, interferon, and mTOR signaling pathways, suggesting that *MTAP/CDKN2A*$^{MUT}$ may activate the anti-tumor immune response in the TME of RCC (Figure 5B). Notably, the 3D cohort showed significantly elevated tumor mutation burden (TMB) and PD-L1 levels in the *CDKN2A*$^{MUT}$ group (Figure 5C).

To further portray intratumoral immunophenotypes according to genomic alterations of MTAP and CDKN2A, we evaluated the expression levels of the immune checkpoint molecule, PD-L1, and the key lymphokine that recruits tertiary lymphoid structures, CXCL13, in ccRCC samples with available genomic data from the discovery set of the FUSCC cohort. The relative expression of PD-L1 and CXCL13 was defined as strong, moderate, and absent/weak staining according to the staining density and intensity of each section. Interestingly, significantly higher PD-L1 and CXCL13 expression was found in 30 RCC samples with *MTAP/CDKN2A*$^{MUT}$ compared with 88 patients in the *MTAP/CDKN2A*$^{WT}$ group ($P < 0.01$; Figures 5D, E). In general, these results demonstrated that although *MTAP/CDKN2A*$^{MUT}$ RCC may be insensitive to targeted therapy, the high degree of tumor heterogeneity and immune-excluded TME reflected that *MTAP/CDKN2A*$^{MUT}$ patients could benefit from immunotherapies.

# Discussion

The advancement of cancer genome analyses has revealed the detailed genomic landscapes of cancer. Targeted therapies based on the characteristics of the tumor genome are increasingly being offered to patients with cancers (18–20). Our study has essential implications for the design and analysis of molecular epidemiology studies in patients with sarcomatoid differentiation of RCC as well as the somatic characterization of genomes for the Chinese population. Among the Chinese and Caucasian populations, we assessed the mutation landscape and found the highest frequency of *MTAP*$^{MUT}$ and *CDKN2A*$^{MUT}$ (2.96% and 5.75%, respectively) in the FUSCC cohort, and the *MTAP*$^{MUT}$ frequency was approximately half of *CDKN2A*$^{MUT}$ frequency. Notably, *MTAP/CDKN2A*$^{MUT}$ occurred in the Chinese population ~2 times more frequently than in the Western cohort and showed significant co-mutation trends.

A previous study identified *VHL* mutations as the most common gene mutation (72%), followed by *PBRM1* (45%), *SETD2* (34%), and *BAP1* mutations (17%) in 29 Caucasian patients with advanced ccRCC (21). It is also suggested that *BAP1*, *SETD2*, and *PBRM1* are prevalent co-drivers of tumor grade and invasion of ccRCC and associated with aggressive progression (21–23). However, PBRM1-mutant patients tended to have a higher TMB and might evoke immunotherapy sensitivity (24). Furthermore, Malouf et al. detected genomic profiling, underpinning renal cell carcinoma with sarcomatoid dedifferentiation, and identified *TP53* (42.3%), *VHL* (34.6%), *CDKN2A* (26.9%), and *NF2* (19.2%) as the most frequently altered genes for sRCC (12, 25). Approaches and strategies are needed for other malignancies driven by the loss of CDKN2 and NF2, as revealed by genomic features in the course of clinical management for patients with sRCC. This study speculated that although the initiating mutation in sRCC is similar to other types of RCC, the acquisition of other driver alterations, such as TP53 or NF2, may lead to the generation of the sarcomatoid phenotype. Therefore, understanding the distinct genomic alteration background of the Chinese population with sarcomatoid differentiation of RCC will guide targeted therapies and immunotherapies, paving the way for the clinical practice of precision medicine in this highly lethal cancer.

Previous studies have revealed the unique molecular classification of ccRCC predicting prognosis in Caucasian patients treated with targeted therapies, specifically the TKIs (26). The

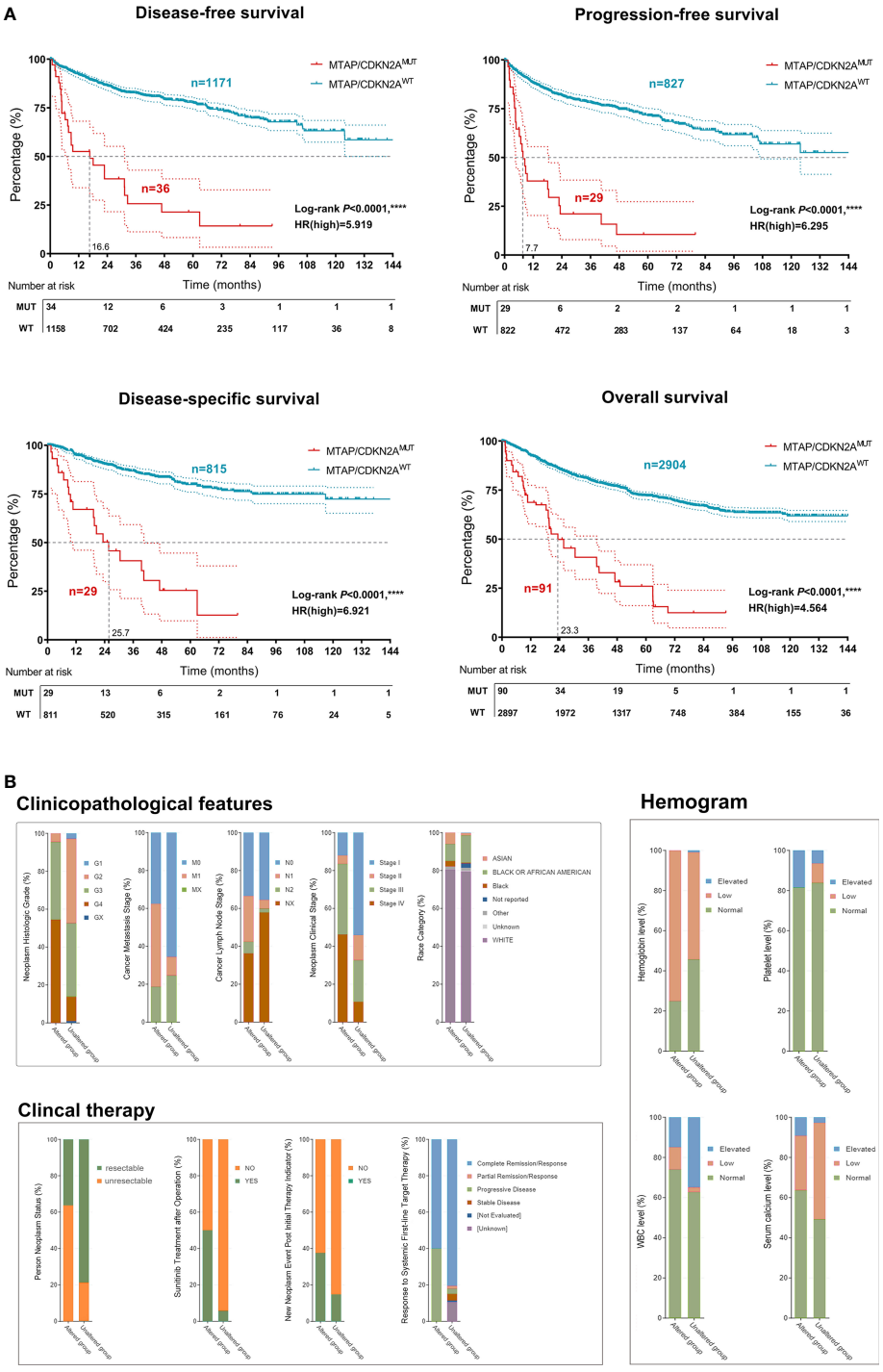


FIGURE 4
Implications of *MTAP*/*CDKN2A*$^{MUT}$ in prognosis, clinicopathological features, and sensitivity to therapy of 3,563 patients with RCC from the Western cohort. **(A)** Classified by the *MTAP*$^{MUT}$, DSS, PFS, DFS, and OS of RCC patients from the Western cohort using Kaplan–Meier survival analysis and log-rank test. **(B)** Classified by the *CDKN2A*$^{MUT}$, DSS, PFS, DFS, and OS of RCC patients from the Western cohort using Kaplan–Meier survival analysis and log-rank test. ****, P<0.0001.

10.3389/fimmu.2022.953721

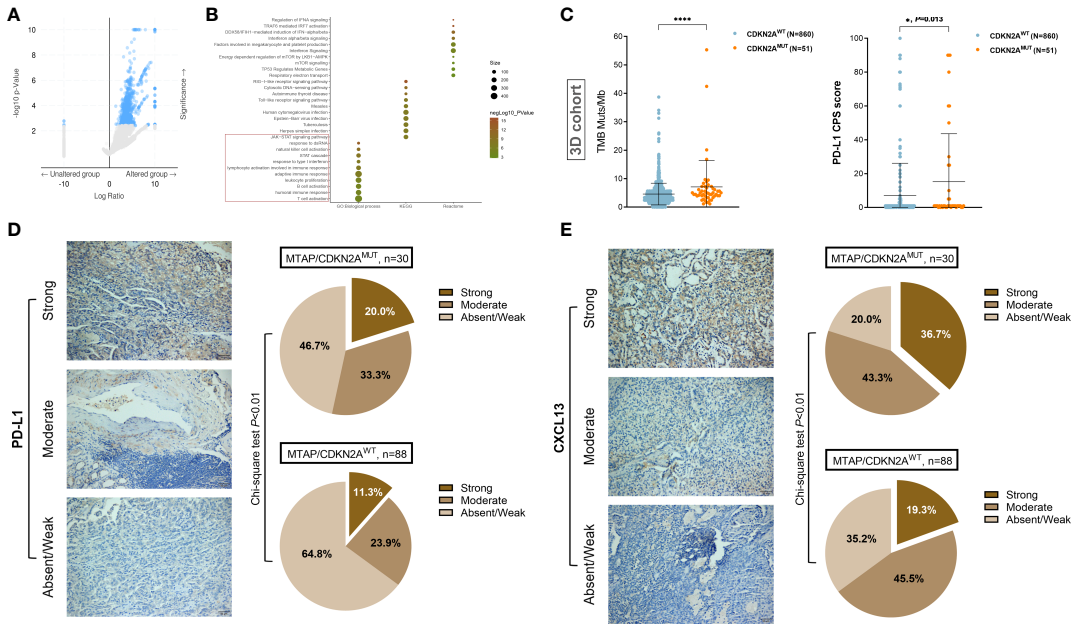


FIGURE 5
*MTAP/CDKN2A*$^{MUT}$ predicts tumor heterogeneity and TME characterizations of RCC patients from the 3D and FUSCC cohorts. **(A)** Identification of differential altered genes between *MTAP/CDKN2A*$^{MUT}$ and unaltered groups in the Western cohort using the "limma" R package with a threshold of Log$^{10}$(*q*-value) >2. **(B)** Gene Ontology (GO), Kyoto Encyclopedia of Genes and Genomes (KEGG), and Reactome functional enrichment analyses were performed to speculate on the biological functions and tumor environment changes involved in *MTAP/CDKN2A*$^{MUT}$. **(C)** Tumor mutation burden (TMB) and PD-L1 levels in the *CDKN2A*$^{MUT}$ group compared with the *CDKN2A*$^{WT}$ group in 1,170 Chinese patients with RCC from the 3D medicine cohort. **(D, E)** Protein expression levels of immune checkpoint molecule, PD-L1, and the key lymphokine that recruits tertiary lymphoid structures, CXCL13, were evaluated in ccRCC samples with available genomic data from the discovery set of the FUSCC cohort. The relative expression of PD-L1 and CXCL13 was defined as strong, moderate, and absent/weak staining according to the staining density and intensity of each section. The chi-square test was used to compare differences between groups. *, P<0.05; ****, P<0.0001.

molecular classification (ccRCC1–4) suggested a high predictive value for favorable outcomes in patients with advanced ccRCC treated with sunitinib (27). This study identified the clusters with *MTAP/CDKN2A*-altered and *MTAP/CDKN2A*-unaltered groups with distinct levels of genomic alteration, clinicopathological features, and immune infiltration in patients with RCC. Moreover, RCC patients with *MTAP/CDKN2A*$^{MUT}$ showed significantly higher pathology grades (95.8% were G3–G4) and clinical stages (92.5% were III–IV). Consistently, we found a significantly higher frequency of Asian subjects in the GA group than in the unaltered group. Additionally, patients in the GA group exhibited lower hemoglobin and leukocyte levels and higher platelet and blood calcium levels, reflecting a higher IMDC stage and a higher treatment primary tolerance. Additionally, in the GA group, the proportion of patients with unresectable tumors was 63.5%; 50% of the patients received postoperative sunitinib therapy, and approximately 40% of patients carried new neoplasm events after initial therapy.

The loss of MTAP expression has been linked to a tumor-promoting effect in multiple cancers, and MTAP may serve as a tumor suppressor (28–30). For example, in 2021, Han et al. found that 9p21 loss, normally CDKN2A (13.5%) and MTAP (9.3%), confers a cold tumor immune microenvironment, poor clinical outcomes, and primary resistance to immune checkpoint therapy for cancers (31). However, this study did not explore the clinicopathological significance of 9p21 deletion in RCC, let alone its impact on the dysregulation of TME. Despite the frequent loss of MTAP expression in high-grade gliomas, MTAP did not appear to be associated with a deteriorating outcome, and *in-vitro* models demonstrated that MTAP did not affect proliferation, invasion, and migration (32). Unlike in other tumors, non-synonymous mutations, neoantigens, insertions, or deletions caused by chromosomal structural changes and somatic copy number variations were not in significant consistency with the response to immune checkpoint therapies (ICTs) in ccRCC (33). Moreover, the elevated expression of PD-L1 correlated with poor OS, which was also observed in the pro-tumorigenic *MTAP/CDKN2A*$^{MUT}$ cluster (34, 35).

A previous study pointed out that genetic alteration of CDKN2A was correlated with reduced benefits from ICTs and changes in the TME of urothelial carcinoma (36). Furthermore, CDKN2A deletion and BAP1 mutations, as well as increased

expression of MYC transcriptional programs, have been identified as genomic features of aggressive behavior for sarcomatoid and rhabdoid RCC (37). In this study, the relatively immune-infiltrated *MTAP/CDKN2A*$^{MUT}$ cluster showed a transcriptional signature indicative of pro-tumorigenic immune infiltration in tumors and prominently higher TMB values based on 1,170 Chinese patients with RCC. Interestingly, we identified the mutually exclusive aggressive tumor phenotypes in ccRCC. Through phenotypic analysis, favorable clinical response to ICTs, elevated expression of immune checkpoints, increased abundance of tumor-infiltrated lymphocyte infiltration, and elevated TMB and PD-L1 expression were observed in the *MTAP/CDKN2A*$^{MUT}$ cluster. However, just as not all solid tumors with high TMB are sensitive to ICTs, patients with high neoantigens are not necessarily accompanied by an elevated level of $CD8^+$ T-cell infiltration in the TME of ccRCC (38). Therefore, under a paradigm of targeted therapies, such as TKIs, two of the clusters that are "immune-infiltrated TME" exerted poorer prognosis but might be uniquely responsive to immune checkpoint blockade, thereby improving treatment outcomes for ccRCC patients. Further tumor type-specific studies are warranted in investigating biomarkers for ICTs.

## Conclusion

This study utilized RCC samples from large-scale, global, multicenter sequencing cohorts and first proved that genomic alteration of *MTAP/CDKN2A* significantly correlates with sarcomatoid differentiation in RCC and predicts aggressive progression, poor prognosis, primary resistance to targeted therapy, and potential favorable responses to immune checkpoint blockade. Unlike conventional targeted therapies, emerging drugs such as immunotherapies or synthetic lethal PRMT5 inhibitors may become novel therapeutic options for patients with *MTAP/CDKN2A*$^{MUT}$ RCC.

## Data availability statement

The original contributions presented in the study are included in the article/Supplementary Material. Further inquiries can be directed to the corresponding authors.

## Ethics statement

The studies involving human participants were reviewed and approved by ethics committee of Fudan University Shanghai Cancer Center (ID: 050432-4-1805C, Shanghai, China). The patients/participants provided their written informed consent to participate in this study.

## Author contributions

Conceptualization: WX, AA, GW, and WL. Data curation and formal analysis: WX, WL, AA, GW, JX, W Shi, JS, and XT. Funding acquisition: WX, YQ, HZ, and DY. Investigation and methodology: WX, AA, WL, GW, JZ, and HZ. Resources and software: JZ, YQ, HZ, and DY. Supervision: JZ, HZ, and DY. Validation and visualization: WX, AA, WL, and JS. Original draft: WX, AA, WL, and GW. Editing: JZ, HZ, and DY. All authors contributed to the article and approved the submitted version.

## Funding

This work was supported by grants from the "Eagle" Program of Shanghai Anticancer Association (No. SHCY-JC-2021105), the Natural Science Foundation of Shanghai (No. 20ZR1413100). and Shanghai Municipal Health Bureau (No. 2020CXJQ03).

## Acknowledgments

We are grateful to all patients for their dedicated participation in the current study. We expressed our sincere gratitude to Ms. Zoo for editing the figures for this study.

## Conflict of interest

Author JX was employed by The Medical Department, 3D Medicines Inc., Shanghai, China.

The remaining authors declare that the research was conducted in the absence of any commercial or financial relationships that could be construed as a potential conflict of interest.

## Publisher's note



## Supplementary material

The Supplementary Material for this article can be found online at: https://www.frontiersin.org/articles/10.3389/fimmu.2022.953721/full#supplementary-material

# References

1. Hsieh JJ, Purdue MP, Signoretti S, Swanton C, Albiges L, Schmidinger M, et al. Renal cell carcinoma. *Nat Rev Dis Primers* (2017) 3:17009. doi: 10.1038/nrdp.2017.9

2. Siegel R, Miller K, Jemal A. Cancer statistics, 2020. *CA: Cancer J Clin* (2020) 70:7–30. doi: 10.3322/caac.21590

3. Cao W, Chen HD, Yu YW, Li N, Chen WQ. Changing profiles of cancer burden worldwide and in China: a secondary analysis of the global cancer statistics 2020. *Chin Med J (Engl)* (2021) 134:783–91. doi: 10.1097/CM9.0000000000001474

4. Zheng R, Zhang S, Zeng H, Wang S, Sun K, Chen R, et al. Cancer incidence and mortality in China, 2016. *J Natl Cancer Center* (2022) 2:1–9. doi: 10.1016/j.jncc.2022.02.002

5. Miller K, Nogueira L, Mariotto A, Rowland J, Yabroff K, Alfano C, et al. Cancer treatment and survivorship statistics, 2019. *CA: Cancer J Clin* (2019) 69:363–85. doi: 10.3322/caac.21565

6. Gerlinger M, Rowan A, Horswell S, Math M, Larkin J, Endesfelder D, et al. Intratumor heterogeneity and branched evolution revealed by multiregion sequencing. *New Engl J Med* (2012) 366:883–92. doi: 10.1056/NEJMoa1113205

7. Xu W, Anwaier A, Ma C, Liu W, Tian X, Su J, et al. Prognostic immunophenotyping clusters of clear cell renal cell carcinoma defined by the unique tumor immune microenvironment. *Front Cell Dev Biol* (2021) 9:785410. doi: 10.3389/fcell.2021.785410

8. Xu W, Ma C, Liu W, Anwaier A, Tian X, Shi G, et al. Prognostic value, DNA variation and immunologic features of a tertiary lymphoid structure-related chemokine signature in clear cell renal cell carcinoma. *Cancer Immunol Immunother* (2022) 71:1923–35. doi: 10.1007/s00262-021-03123-y

9. Golshayan AR, George S, Heng DY, Elson P, Wood LS, Mekhail TM, et al. Metastatic sarcomatoid renal cell carcinoma treated with vascular endothelial growth factor-targeted therapy. *J Clin Oncol* (2009) 27:235–41. doi: 10.1200/JCO.2008.18.0000

10. Pichler R, Comperat E, Klatte T, Pichler M, Loidl W, Lusuardi L, et al. Renal cell carcinoma with sarcomatoid features: Finally new therapeutic hope? *Cancers (Basel)* (2019) 11:(422–6). doi: 10.3390/cancers11030422

11. Tannir NM, Signoretti S, Choueiri TK, McDermott DF, Motzer RJ, Flaifel A, et al. Efficacy and safety of nivolumab plus ipilimumab versus sunitinib in first-line treatment of patients with advanced sarcomatoid renal cell carcinoma. *Clin Cancer Res* (2021) 27:78–86. doi: 10.1158/1078-0432.CCR-20-2063

12. Choueiri TK, Larkin J, Pal S, Motzer RJ, Rini BI, Venugopal B, et al. Efficacy and correlative analyses of avelumab plus axitinib versus sunitinib in sarcomatoid renal cell carcinoma: *post hoc* analysis of a randomized clinical trial. *ESMO Open* (2021) 6:100101. doi: 10.1016/j.esmoop.2021.100101

13. Wang Z, Kim TB, Peng B, Karam J, Creighton C, Joon A, et al. Sarcomatoid renal cell carcinoma has a distinct molecular pathogenesis, driver mutation profile, and transcriptional landscape. *Clin Cancer Res* (2017) 23:6686–96. doi: 10.1158/1078-0432.CCR-17-1057

14. Mavrakis KJ, McDonald ER3rd, Schlabach MR, Billy E, Hoffman GR, deWeck A, et al. Disordered methionine metabolism in MTAP/CDKN2A-deleted cancers leads to dependence on PRMT5. *Science* (2016) 351:1208–13. doi: 10.1126/science.aad5944

15. Mulvaney KM, Blomquist C, Acharya N, Li R, Ranaghan MJ, O'Keefe M, et al. Molecular basis for substrate recruitment to the PRMT5 methylosome. *Mol Cell* (2021) 81:3481–3495.e3487. doi: 10.1016/j.molcel.2021.07.019

16. Necchi A, Grivas P, Spiess P, Jacob J, Schrock A, Madison R, et al. Methylthioadenosine phosphorylase (MTAP) deletion is more common in sarcomatoid (srcRCC) than in clear cell renal cell carcinoma (ccRCC). *Eur Urol* (2021) 79:S868–9. doi: 10.1016/S0302-2838(21)01008-3

17. Xu W, Liu WR, Xu Y, Tian X, Anwaier A, Su JQ, et al. Hexokinase 3 dysfunction promotes tumorigenesis and immune escape by upregulating monocyte/macrophage infiltration into the clear cell renal cell carcinoma microenvironment. *Int J Biol Sci* (2021) 17:2205–22. doi: 10.7150/ijbs.58295

18. Zhou H, Liu J, Zhang Y, Huang Y, Shen J, Yang Y, et al. PBRM1 mutation and preliminary response to immune checkpoint blockade treatment in non-small cell lung cancer. *NPJ Precis Oncol* (2020) 4:6. doi: 10.1038/s41698-020-0112-3

19. Okamura R, Kato S, Lee S, Jimenez RE, Sicklick JK, Kurzrock R, et al. ARID1A alterations function as a biomarker for longer progression-free survival after anti-PD-1/PD-L1 immunotherapy. *J Immunother Cancer* (2020) 8:e000438(1-6). doi: 10.1136/jitc-2019-000438

20. Zaretsky JM, Garcia-Diaz A, Shin DS, Escuin-Ordinas H, Hugo W, Hu-Lieskovan S, et al. Mutations associated with acquired resistance to PD-1 blockade in melanoma. *N Engl J Med* (2016) 375:819–29. doi: 10.1056/NEJMoa1604958

21. Reig Torras O, Mishra A, Christie A, McKenzie T, Onabolu O, Singla N, et al. Molecular genetic determinants of shorter time on active surveillance in a prospective phase 2 clinical trial in metastatic renal cell carcinoma. *Eur Urol* (2021) 81:555–8. doi: 10.1016/j.eururo.2021.12.003

22. Espana-Agusti J, Warren A, Chew SK, Adams DJ, Matakidou A. Loss of PBRM1 rescues VHL dependent replication stress to promote renal carcinogenesis. *Nat Commun* (2017) 8:2026. doi: 10.1038/s41467-017-02245-1

23. Linehan WM, Ricketts CJ. The cancer genome atlas of renal cell carcinoma: findings and clinical implications. *Nat Rev Urol* (2019) 16:539–52. doi: 10.1038/s41585-019-0211-5

24. Huang Y, Wang J, Jia P, Li X, Pei G, Wang C, et al. Clonal architectures predict clinical outcome in clear cell renal cell carcinoma. *Nat Commun* (2019) 10:1245. doi: 10.1038/s41467-019-09241-7

25. Malouf GG, Ali SM, Wang K, Balasubramanian S, Ross JS, Miller VA, et al. Genomic characterization of renal cell carcinoma with sarcomatoid dedifferentiation pinpoints recurrent genomic alterations. *Eur Urol* (2016) 70:348–57. doi: 10.1016/j.eururo.2016.01.051

26. Beuselinck B, Verbiest A, Couchy G, Job S, de Reynies A, Meiller C, et al. Pro-angiogenic gene expression is associated with better outcome on sunitinib in metastatic clear-cell renal cell carcinoma. *Acta Oncol (Stockholm Sweden)* (2018) 57:498–508. doi: 10.1080/0284186x.2017.1388927

27. Verbiest A, Couchy G, Job S, Zucman-Rossi J, Caruana L, Lerut E, et al. Molecular subtypes of clear cell renal cell carcinoma are associated with outcome during pazopanib therapy in the metastatic setting. *Clin Genitourinary Cancer* (2018) 16:e605–12. doi: 10.1016/j.clgc.2017.10.017

28. Laera L, Guaragnella N, Giannattasio S, Moro L. 6-thioguanine and its analogs promote apoptosis of castration-resistant prostate cancer cells in a BRCA2-dependent manner. *Cancers (Basel)* (2019) 11:(945–59). doi: 10.3390/cancers11070945

29. Bertino JR, Waud WR, Parker WB, Lubin M. Targeting tumors that lack methylthioadenosine phosphorylase (MTAP) activity: current strategies. *Cancer Biol Ther* (2011) 11:627–32. doi: 10.4161/cbt.11.7.14948

30. Christopher SA, Diegelman P, Porter CW, Kruger WD. Methylthioadenosine phosphorylase, a gene frequently codeleted with p16 (cdkN2a/ARF), acts as a tumor suppressor in a breast cancer cell line. *Cancer Res* (2002) 62:6639–44.

31. Han G, Yang G, Hao D, Lu Y, Thein K, Simpson BS, et al. 9p21 loss confers a cold tumor immune microenvironment and primary resistance to immune checkpoint therapy. *Nat Commun* (2021) 12:5606. doi: 10.1038/s41467-021-25894-9

32. Menezes WP, Silva VAO, Gomes INF, Rosa MN, Spina MLC, Carloni AC, et al. Loss of 5'-methylthioadenosine phosphorylase (MTAP) is frequent in high-grade gliomas; nevertheless, it is not associated with higher tumor aggressiveness. *Cells* (2020) 9:(492–515). doi: 10.3390/cells9020492

33. Braun DA, Hou Y, Bakouny Z, Ficial M, Sant' Angelo M, Forman J, et al. Interplay of somatic alterations and immune infiltration modulates response to PD-1 blockade in advanced clear cell renal cell carcinoma. *Nat Med* (2020) 26:909–18. doi: 10.1038/s41591-020-0839-y

34. Darrow JJ, Avorn J, Kesselheim AS. FDA Approval and regulation of pharmaceuticals, 1983-2018. *JAMA* (2020) 323:164–76. doi: 10.1001/jama.2019.20288

35. Black JRM, McGranahan N. Genetic and non-genetic clonal diversity in cancer evolution. *Nat Rev Cancer* (2021) 21:379–92. doi: 10.1038/s41568-021-00336-2

36. Adib E, Nassar AH, Akl EW, Abou Alaiwi S, Nuzzo PV, Mouhieddine TH, et al. CDKN2A alterations and response to immunotherapy in solid tumors. *Clin Cancer Res* (2021) 27:4025–35. doi: 10.1158/1078-0432.CCR-21-0575

37. Bakouny Z, Braun DA, Shukla SA, Pan W, Gao X, Hou Y, et al. Integrative molecular characterization of sarcomatoid and rhabdoid renal cell carcinoma. *Nat Commun* (2021) 12:808. doi: 10.1038/s41467-021-21068-9

38. McGrail DJ, Pilie PG, Rashid NU, Voorwerk L, Slagter M, Kok M, et al. High tumor mutation burden fails to predict immune checkpoint blockade response across all cancer types. *Ann Oncol* (2021). doi: 10.1016/j.annonc.2021.02.006

frontiers | Frontiers in Immunology

TYPE Review
PUBLISHED 02 September 2022
DOI 10.3389/fimmu.2022.912279



OPEN ACCESS

EDITED BY
Mohd Wajid Ali Khan,
University of Hail, Saudi Arabia

REVIEWED BY
Bruno Ramos-Molina,
Biomedical Research Institute of Murcia (IMIB), Spain
Morteza Gholami,
Golestan University, Iran

*CORRESPONDENCE
Jincheng Zeng
zengjc@gdmu.edu.cn
Xianxiu Qiu
bmsqiu@gdmu.edu.cn

†These authors have contributed equally to this work

SPECIALTY SECTION
This article was submitted to Cancer Immunity and Immunotherapy, a section of the journal Frontiers in Immunology

RECEIVED 05 April 2022
ACCEPTED 15 August 2022
PUBLISHED 02 September 2022

CITATION
Lian J, Liang Y, Zhang H, Lan M, Ye Z, Lin B, Qiu X and Zeng J (2022) The role of polyamine metabolism in remodeling immune responses and blocking therapy within the tumor immune microenvironment. *Front. Immunol.* 13:912279. doi: 10.3389/fimmu.2022.912279



# The role of polyamine metabolism in remodeling immune responses and blocking therapy within the tumor immune microenvironment

Jiachun Lian[1,2†], Yanfang Liang[3†], Hailiang Zhang[1,2†], Minsheng Lan[1], Ziyu Ye[1,3,4], Bihua Lin[1,5,6], Xianxiu Qiu[1,5,6*] and Jincheng Zeng[1,4,5,6*]

[1]Guangdong Provincial Key Laboratory of Medical Molecular Diagnostics, The First Dongguan Affiliated Hospital, Guangdong Medical University, Dongguan, China, [2]Institute of Laboratory Medicine, School of Medical Technology, Guangdong Medical University, Dongguan, China, [3]Department of Pathology, Dongguan Hospital Affiliated to Jinan University, Binhaiwan Central Hospital of Dongguan, Dongguan, China, [4]Dongguan Metabolite Analysis Engineering Technology Center of Cells for Medical Use, Guangdong Xinghai Institute of Cell, Dongguan, China, [5]Key Laboratory of Medical Bioactive Molecular Research for Department of Education of Guangdong Province, Collaborative Innovation Center for Antitumor Active Substance Research and Development, Zhanjiang, China, [6]Department of Biochemistry and Molecular Biology, School of Basic Medicine, Guangdong Medical University, Zhanjiang, China

The study of metabolism provides important information for understanding the biological basis of cancer cells and the defects of cancer treatment. Disorders of polyamine metabolism is a common metabolic change in cancer. With the deepening of understanding of polyamine metabolism, including molecular functions and changes in cancer, polyamine metabolism as a new anti-cancer strategy has become the focus of attention. There are many kinds of polyamine biosynthesis inhibitors and transport inhibitors, but not many drugs have been put into clinical application. Recent evidence shows that polyamine metabolism plays essential roles in remodeling the tumor immune microenvironment (TIME), particularly treatment of DFMO, an inhibitor of ODC, alters the immune cell population in the tumor microenvironment. Tumor immunosuppression is a major problem in cancer treatment. More and more studies have shown that the immunosuppressive effect of polyamines can help cancer cells to evade immune surveillance and promote tumor development and progression. Therefore, targeting polyamine metabolic pathways is expected to become a new avenue for immunotherapy for cancer.

KEYWORDS

**polyamine, tumor immune microenvironment, metabolism, T cell, immunotherapy, innate immune, adaptive immune**

# 1 Introduction

Polyamines, including putrescine, spermidine and spermine, are polycationic alkylamine that present in mammalian cells in millimolar concentrations (1). They can interact with negatively charged biological macromolecules such as nucleic acids and neurotransmitter under physiological pH conditions (1) (Figure 1). Polyamines are reported to be involved in regulation of DNA synthesis and stability, transcription, ion channel transport, and protein phosphorylation (2–5). In mammals, polyamines play important roles in diverse physiological processes, including immunity, aging, hair growth, and wound healing (1). The intracellular concentration of polyamines varies greatly depending on cell types, cellular context and the surrounding microenvironment (6, 7). Polyamines are necessary for normal cell growth, and their consumption results in cell stasis. In the early stages of tumor transformation and progression, multiple carcinogenic pathways lead to the dysregulation of polyamine demand and metabolism, indicating that elevated levels of polyamines are necessary for transformation and tumor progression (8, 9).

Human diet and gut microbiota are also important sources of polyamines (10–12). Polyamines are present in all types of foods in a wide range of concentrations (13). The predominant polyamine in plant-derived foods is spermidine, whereas animal-derived foods have higher levels of spermine (13). Studies have shown that dietary polyamines intake is associated with cardiovascular, intestinal development, cancer progression, and anticancer immunity (14, 15). Oral supplementation of spermidine in mice can prolong life span, enhance cardiac autophagy, and improves the mechanical elastic properties of cardiomyocytes (16). Exogenous spermidine supplementation also reduces transplantable tumor growth, stimulates anticancer immune surveillance in combination with chemotherapy, and inhibits tumorigenesis in mice caused by chemical injury (17). Furthermore, Carlos Gómez-Gallego et al. reported that formula-fed mice supplemented with polyamines were similar to normal breast-fed mice in terms of microbial communities, lymphocyte numbers, and immune-related gene expression throughout the gastrointestinal tract (18). Gut microbial-derived polyamines are another important source of host polyamine reservoirs. Gut microbes can synthesize putrescine, spermine, and spermidine in milligram concentrations and use polyamines for cell-to-cell communication, cell signaling, and cell differentiation (19). Bacteria colonizing the gut produce polyamines, primarily through the transamination of ingested amino acids by catalytic enzymes, especially arginine (20, 21). Studies have shown that supplementation with arginine and/or *Bifidobacterium animalis subsp. lactis* LKM512 increases the content of polyamines in the intestine of mice and significantly prolongs lifespan, which is related to the down-regulation of inflammation-related genes and the improvement of intestinal barrier function (22, 23). With the in-depth study of polyamines derived from gut microbes, the presence of probiotics was found to increase the concentration of polyamines in the gut (24). Studies have shown that consuming yogurt containing the probiotic strain *B. animalis subsp. Lactis* LKM512 can increase the concentration of polyamines in human intestine, which is beneficial to improve intestinal health, prolong life and quality of life (25–27). Moreover, consumption of LKM512 yogurt can improve the intestinal environment and induce T-helper type 1 cytokine (IFN-gamma) in atopic dermatitis (AD) patients (25), which also suggests the potential role of probiotic-derived polyamines in immune regulation.

Tumors are complicated multicellular systems characterized by the sophisticated interaction between cancer cells and the tumor microenvironment (TME) (28). TME consists of extracellular matrix (ECM) and various noncancerous cell types, including immune cells, endothelial cells, pericytes, and fibroblasts (29). In tumor immune microenvironment (TIME), including various T helper cells, monocytes/macrophages, natural killer (NK) cells, neutrophils, and dendritic cells, have multifaceted roles during carcinogenesis and progression (30). TME, characterized by either elevated and chronic inflammation or immunosuppression, is considered as one of the hallmarks of cancer (31). In order to survive and proliferate in TIME, tumor cells need to evade immune surveillance and avoid being killed by cytotoxic lymphocytes. This is achieved by shaping the TIME into a tolerable and immunosuppressive environment, which is characterized by impaired production of tumoricidal cytokines and chemokines, decreased infiltration of activated T lymphocytes, cytotoxic $CD8^+$T cells, and NK cells, and increased infiltration of immature myeloid derived suppressor cells (MDSC), regulatory T cells (Tregs), and other immunosuppressive cells (32–36).

Increased polyamine metabolism is commonly observed in various types of cancer. Elevated levels of polyamines stimulate cell proliferation and angiogenesis in tumors, thereby promoting tumorigenesis and development (37–40). Multiple oncogenes and tumor suppressors regulate tumor polyamine metabolism, which not only increased polyamine biosynthesis but also increased cellular uptake of polyamines *via* an upregulated polyamine transport system (41, 42). To date, many reports have suggested that polyamines play a functional role in immune-modulation, and participate in anti-tumor immune response by regulating the proliferation, differentiation and function of immune cells. Polyamines are essential for the activation and proliferation of mouse $CD4^+$ and $CD8^+$ T lymphocytes (43). In mouse bone marrow derived macrophages, spermidine-dependent OXPHOS metabolism may be beneficial to the alternative activation of ARG1 expression and inhibition of pro-inflammatory cytokine expression, which reduces the infiltration of autoimmune $CD4^+$

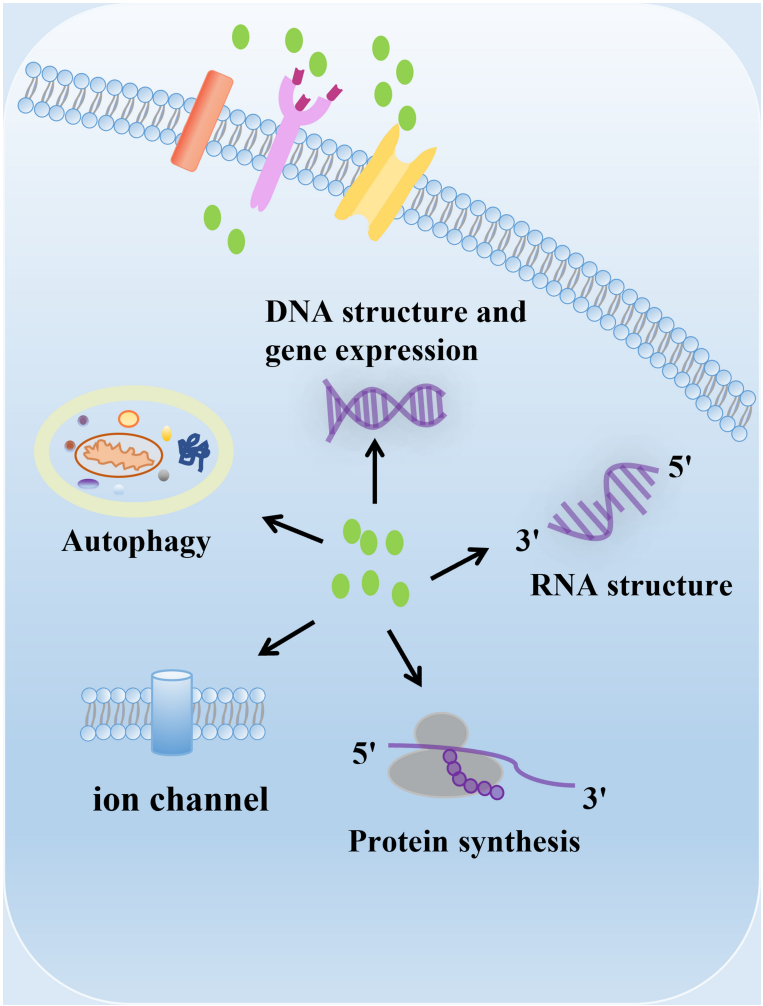


FIGURE 1
The biological function of polyamines. Polyamines have multiple roles in cells, including regulation of gene expression, RNA structure, protein synthesis, ion channel flux, and autophagy. Polyamines are required for growth and play important roles in a variety of physiological processes, including immunity, aging, hair growth, and wound healing.

and $CD8^+$ T lymphocytes into the central nervous system and the clinical score of experimental autoimmune encephalomyelitis (44, 45). Polyamines can also improve anti-cancer immunity through autophagy, a cellular metabolic process necessary for T cell activation, function and survival (46–50). However, polyamines have also been reported to exert immunosuppressive effects, which may contribute to the multiple complex mechanisms by which cancer cells escape from immune responses. Myeloid-derived suppressor cells (MDSC) in the tumor microenvironment utilize polyamines to invoke their suppressive activations and support their metabolism (51–56). Polyamines also inhibit lymphocyte proliferation, reduce neutrophil locomotion and NK cell activity, and suppress macrophage-mediated tumoricidal activity through reprogramming proinflammatory M1 to anti-inflammatory M2 phenotypes (57–61). Taken together, polyamine metabolism and its metabolic molecules, play a complex role in the differentiation and function of various immune cells under both physiological and pathological conditions.

Metabolic regulation is a key component of coordinating the immune response (62). Targeting polyamine metabolism has long been an attractive approach for cancer chemotherapy. In animal experiments, polyamine deprivation enhances the production of chemokines, reverses the inhibitory activity of cytotoxic cells induced by tumor inoculation, and prevent tumor-induced immunosuppression (59, 63). Some studies have shown that inhibition of ornithine decarboxylase (ODC), and/or treatment of polyamine transport inhibitors (PTIs), significantly reduces the tumor growth rate due to the

enhanced anti-tumor immunity (64–66). Moreover, polyamine blocking therapy (PBT) reduces polyamine-mediated immunosuppression in the tumor microenvironment and activates tumor-killing T cells (67). Since accumulating evidence supports that polyamines contribute important roles to immune evasion of tumor cells, polyamines might be added to the list of immunosuppressive metabolites (68). In this review, we outline the relationship between polyamines and immune cell function. We also discuss the impact of polyamines on the tumor immune microenvironment, and the dual regulatory functions of polyamines in cancer and immune cells. Finally, we provide insights on targeting polyamine metabolism as a novel avenue for cancer immunotherapy.

# 2 Polyamine metabolism

Under normal physiological conditions, the intracellular concentration of polyamines is strictly regulated by biosynthesis, catabolism and transport mechanisms (7, 69, 70). While polyamine pathways, which are modulated by several important oncogenic pathways, are often dysregulated in cancer. As such, polyamine metabolism may serve as a promising target for anticancer therapies (9).

## 2.1 Polyamine biosynthesis

Polyamines are produced from arginine and ornithine, which are controlled by *de novo* synthesis and diet (71, 72) (Figure 2). Ornithine is produced from arginine by arginase 1 (ARG1) and metabolized by ornithine decarboxylase (ODC) to produce putrescine, which is the first mammalian polyamine (73). Methionine is metabolized by methionine adenosyltransferase (MAT2) to produce s-adenosylmethionine (SAM), which is the main methyl donor for cell methylation (74). SAM is decarboxylated by adenosylmethionine decarboxylase 1 (AMD1) to produce decarboxylated SAM (dcSAM), which is a substrate for polyamine synthesis (72). In inflammatory and autoimmune diseases, intracellular methylation modification affects immune dysfunction in the body, including $CD4^+$T lymphocytes, $CD8^+$T lymphocytes, B lymphocytes, macrophages, and regulatory T cells (75). Therefore, in addition to playing an important role in the synthesis of polyamines, AMD1 may also affect the methylation reaction by affecting the availability of SAM, and even play a role in immune function (75). Decarboxylated SAM (dcSAM) is the aminopropyl donor, which is added to the reactions catalyzed by spermidine synthase (SPDSY, coded by SRM) and spermine synthase (SPMSY, coded by SMS) to

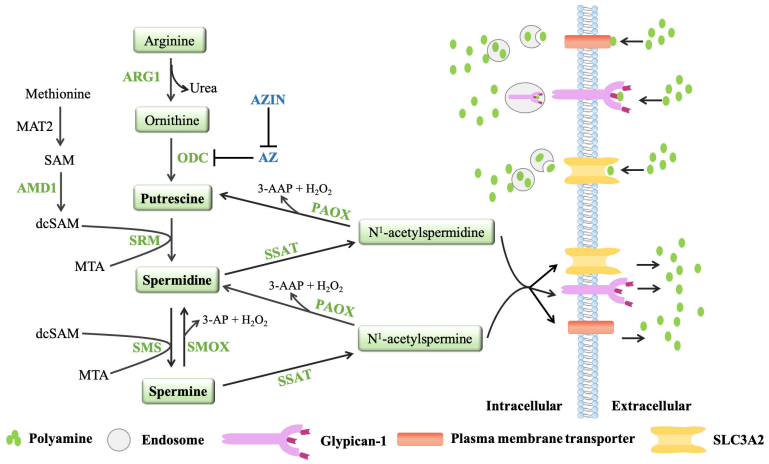


FIGURE 2
The polyamine metabolic pathway and transport way. Polyamine biosynthesis involves the conversion of ornithine to putrescine by ornithine decarboxylase (ODC), followed by the formation of spermidine *via* spermidine synthase (SRM) and decarboxylated s-adenosylmethionine (dcSAM, formed by AMD1). The aminopropyl fragment required for putrescine to produce spermidine was provided by dcSAM. In a similar manner, spermine is produced from the conversion of spermidine by spermine synthase (SMS) and AMD1. The polyamine catabolism process occurs through the action of amine oxidase, mainly polyamine oxidase (PAOX) and spermine oxidase (SMOX). PAOX and SMOX can generate a large amount of reactive oxygen species (ROS) during the process of decomposing polyamines, causing oxidative damage. Currently, three models of polyamine transport systems have been proposed. Although the molecules involved in the polyamine transport system have not been fully recognized, it is known that the polyamine transport system is energy dependent and substrate selective. ODC antienzymes (AZs) and antizyme inhibitors (AZINs) also play important roles in polyamine transport. ODC monomers have a higher affinity for AZs. When the intracellular polyamine concentration is high, AZs binds to ODC monomers, preventing ODC activity and promoting the binding of ODC monomers to the 26S proteasome for degradation in a ubiquitin (Ub)-independent manner (only AZ1 induces ODC degradation). However, the binding of AZs to ODC can be blocked by AZINs.

convert putrescine into polyamine metabolites (73, 76). Spermidine synthase (SRM) catalyzes putrescine and dcSAM to produce spermine and methylthioadenosine (MTA). Spermidine can react with the second dcSAM molecule through the action of spermine synthase (SMS) to produce spermine and another MTA molecule (69).

## 2.2 Polyamine catabolism

Polyamine catabolism is another key factor in maintaining polyamine homeostasis (Figure 2). The aminopropyltransferase reaction to form spermidine and spermine is irreversible, but the interconversion of polyamines in cells can occur through the action of amine oxidase, which are mainly polyamine oxidase (PAOX) and spermine oxidase (SMOX) (77). The activity of PAOX is limited by the availability of acetylation products produced by spermidine/spermine N1-acetyltransferase 1 (SSAT, which is encoded by SAT1). SSAT is a highly inducible enzyme, which is regulated in response to the free polyamine concentration to maintain polyamine homeostasis (78). SSAT forms N1-acetylspermine and N1-acetylspermidine by adding acetyl group to the N1 position of spermine or spermidine from acetyl-coenzyme A. Depending on the initial substrate, these acetylated polyamines can be excreted from the cell or converted to 3-acetylaminopropanal, $H_2O_2$ and spermidine or putrescine by PAOX (78). SMOX is an FAD-dependent enzyme with high homology to PAOX and exists in the cytoplasm and nucleus. Unlike PAOX, SMOX directly oxidizes spermine to generate 3-aminopropanal, $H_2O_2$ and spermidine (77). These catabolic pathways can prevent excessive concentrations of polyamines in cells. PAOX and SMOX can generate a large amount of reactive oxygen species (ROS) during the process of decomposing polyamines, causing oxidative damage (77, 79).

## 2.3 Polyamine transport

In addition to polyamine synthesis and catabolism, polyamine transport also plays an important role in maintaining an appropriate level of intracellular polyamines. Completely protonated at physiological pH, polyamines do not passively diffuse across cell membranes. Currently, three models of polyamine transport systems have been proposed (80) (Figure 2). One proposed model relies on a highly selective membrane permease to allow polyamines to be rapidly internalized into endosomes, where they can be dispersed throughout the cell as needed (81). In a second model, polyamines are internalized by endocytosis which bound to heparin sulfate moieties in glypican-1 at the cell surface. Polyamines are internalized into the endosomes and then released through an oxidation mechanism mediated by nitric oxide (82). The third model proposes that polyamine transport is mediated by endocytosis and solute carrier transport mechanisms in the gastrointestinal tract, especially SLC3A2 (82).

Ornithine decarboxylase (ODC) and ODC antizymes (AZs) also play an important role in polyamine transport (83, 84). ODC is active as a homodimer, but the ODC monomer has a higher affinity for AZ. There are three main members of the antizyme family: AZ1, AZ2 and AZ3 (85). Studies have shown that AZ2 is expressed at much lower levels compared to AZ1. However, AZ2 shows higher evolutionary conservation, which may indicate increased functional value (86, 87). AZ3 is tissue-specific and is mainly expressed in the testis during certain stages of spermatogenesis (88, 89). Moreover, AZ1, AZ2, AZ3 are able to inhibit ODC activity and polyamine uptake, only AZ1 induces ODC degradation (90). AZs negatively regulate the uptake activity of polyamines. When the intracellular polyamine concentrations are high, polyamines transport will be blocked because AZs can bind to ODC monomers to inhibit ODC activity and chaperon the ODC monomers to the 26S proteasome for degradation in a non-ubiquitin (Ub) manner. When the intracellular polyamine concentrations are low, the full-length AZ cannot be translated, so it cannot inhibit ODC activity or block the transport of polyamines (83, 84). AZ can also bind to and inhibit polyamine-specific transporters on the plasma membrane to affect the transport of polyamines (91). AZs and polyamine synthesis were also affected by the antizyme inhibitors (AZINs), which are proteins highly homologous to ODC (90), and retain no ornithine-decarboxylating activity (92, 93). In contrast to ODC, AZINs are degraded by the proteasome through a ubiquitin-dependent mechanism (94). Two subtypes of antizyme inhibitors, AZIN1 and AZIN2, have been reported. AZIN1 is required for normal embryonic development and is associated with cell proliferation, but AZIN2 is predominantly expressed in the human brain and testis, and AZIN2 may play a role in terminal differentiation rather than cell proliferation (95). Since only transfection experiments have shown that AZIN2 affects ODC activity and polyamine uptake, and little is known about the effect of AZIN2 on polyamine levels *in vivo* (96, 97), the AZIN described in this article refers to AZIN1. AZIN1 interacts with AZ more efficiently than ODC, counteracting the negative effects of AZ on intracellular polyamine biosynthesis (98, 99). And when AZIN1 is tightly bound to AZ, AZIN1 does not degrade as fast as ODC. Conversely, AZ binding stabilizes AZIN1 by preventing AZIN1 ubiquitination (94, 100). Notably, AZIN1 can also increase extracellular polyamine uptake, presumably by binding to and sequestering AZ, thereby preventing negative regulation of polyamine transport by AZ (96). Studies have shown that AZIN is overexpressed in a variety of malignancies (gastric cancer, lung cancer, prostate cancer, liver cancer and ovarian cancer) and has carcinogenic effects (101–104). Increased AZIN1 expression correlates with elevated polyamine levels, which promote tumor cell proliferation (100, 105). Although AZ is a tumor suppressor and its expression can prevent cell growth and

tumorigenesis, AZIN1 competes with ODC to release ODC from the ODC-AZ complex based on the stronger binding ability of AZIN1 and AZ, which is conducive to the polyamine synthesis pathway and promotes cancer progression (100, 106). With the deepening of research, it is found that the cancer-promoting effect of AZIN1 can also affect the secretion of cytokines in the tumor microenvironment, such as IL-8 and TGF-β (107, 108). Studies have shown that AZIN1 can up-regulate IL-8 and promote tumor angiogenesis. IL-8 has been reported to contribute to cancer progression and metastasis through different mechanisms, including preangiogenic and cancer stem cell maintenance, but its ability to attract and regulate neutrophils and macrophages is arguably one of the most important factors (107, 109). Although there is no direct evidence that AZIN can play a role in the tumor immune microenvironment, AZIN may affect the tumor immune microenvironment by regulating the secretion of cytokines.

## 2.4 Polyamine metabolites

### 2.4.1 Putrescine

Putrescine is the precursor of spermidine and spermine, produced from ornithine by ornithine decarboxylase (ODC) (73). Putrescine regulates DNA structure, mRNA translation and protein activity, and plays an important role in promoting cell proliferation and migration (2–5). Putrescine has been shown to promote the proliferation of colon cancer cells, even be used as a biochemical marker for malignant brain tumors (110, 111). It is worthy to note that putrescine exerts anti-inflammatory function by inhibiting IL-8 and TNF-α in a LPS-stimulated inflammation model, which may provide a survival mechanism for tumor cells to evade immune response (112). Meanwhile, putrescine derived from macrophages induces 5-FU resistance in colorectal cancer (113). In addition, putrescine can also inhibit the maturation of cytolytic T lymphocyte (CTL), which may impair anti-tumor immunity (114).

### 2.4.2 Spermidine

Spermidine is a metabolite of putrescine converted by spermidine synthase (SRM), or an oxidized product of spermine catalyzed by SMOX. Spermidine can interact with polyanions such as nucleic acid and protein to maintain DNA genome homeostasis and regulate cellular autophagy, apoptosis, oxidative stress and so on (115). There have been many reports suggest that spermidine prolongs the life span across species in an autophagy-dependent manner, and fights cancer and age-related diseases (such as cardiovascular disease, neurodegeneration) (16, 17, 45, 116). In the tumor microenvironment, spermidine can exert multiple functions, e. g. the cell-autonomous inhibitory effect on proliferation or induction of apoptosis of cancer cells by releasing $H_2O_2$ and reactive aldehydes, impeding communication between cancer cells and immune monitoring effector cells, suppressing the function of immunosuppressive cells and promoting the polarization of M2-like tumor associated macrophages (TAMs) (117). In addition, spermidine can also increase the autophagy-dependent release of ATP to facilitate immune monitoring (117).

### 2.4.3 Spermine

Spermine is converted from spermidine by spermine synthase. Spermine also regulates cell proliferation, differentiation, and apoptosis (7, 118). Spermine is more effective against reactive oxygen species and other stresses than spermidine and has been shown to be involved in the maturation of the body's immune system and induction of autophagy to delay brain aging (119–121). In addition, spermine has been reported to regulate T cell function (122), and dietary supplementation of spermine reduces inflammatory response, enhances immune function, and regulates gene expression of inflammation-related signal molecules (123).

# 3 Roles of polyamines in the innate immune cell responses in TIME

## 3.1 Regulation of macrophage polarization by targeting polyamine-eIF5A-hypusine axis

Macrophage are professional phagocytic cells that internalize large particles such as debris, apoptotic cells, pathogens, and maintain a stable environment in the body (124). According to their functions, macrophages can be classified into two categories: classically activated or inflammatory M1 macrophages and alternately activated or anti-inflammatory M2 macrophages (125, 126). The cytokines released by cancer cells in the tumor immune microenvironment (TIME) affect the polarization of macrophages. In the early stages of tumor formation, M1 macrophages in TIME initiate inflammation and exert anti-tumor immunity (126). However, in established tumors, M1 macrophages can be reprogrammed into M2-like TAMs by cytokines enriched in TIME, such as IL-10, IL-4, and IL-13, etc. (125). M2 macrophages have anti-inflammatory effects and can promote angiogenesis and fibrosis, so they have immunosuppressive activity (124). The macrophages located around the TIME are often called TAMs. However, TAMs are mostly M2 macrophages, which play an important role in the establishment of immunosuppressive tumor microenvironment, metastasis, therapy-resistance, and recurrence of cancer (127–131). Therefore, macrophages represent a group of cells with high plasticity, which can

constantly shift their functional states in response to subtle changes in tissue physiology or environmental challenges (132–137).

Numerous studies have implicated the involvement of polyamines in regulating polarization and functions of macrophages, particularly, in regulating tumor immunity (138). For instance, putrescine has been shown to inhibit M1 macrophage activation (112, 138) through downregulating IL-8 and TNF-α expression in a LPS-stimulated inflammation model, thus implying the contribution of M1 macrophage inhibition to immune evasion of tumor cells (138). Spermidine inhibits M1 macrophages by reducing the expression of co-stimulatory molecules (CD80 and CD86) in macrophages and the production of pro-inflammatory cytokines (45). Moreover, spermidine induces the expression of ARG1 in macrophages and promotes the polarization of macrophages to M2 phenotype through inducing mitochondrial superoxide-dependent AMPK activation, Hif-1α up-regulation and autophagy (45, 139). In addition, spermine inhibits iNOS in macrophages activated by Helicobacter pylori to prevent the antibacterial effect of NO, leading to the persistence of cellular bacteria and an increased risk of gastric cancer (140). Spermine also induces the autophagy of liver-resident macrophages (Kupffer cells) by upregulating ATG5 expression, thereby inhibiting the pro-inflammatory M1 polarization and promoting the anti-inflammatory M2 polarization of macrophages (141).

The role of key enzymes in polyamine metabolism on the polarization and the immune functions of macrophages should not be underestimated. In tuberculosis, highly expression of ARG1 in macrophages leads to collagen deposition and lung damage, which drives to inflammation by inhibiting Th1 cells (142). In colitis, ODC in macrophages exacerbates colitis and promotes the occurrence of colitis-related colon cancer by impairing the immune response of M1 macrophages (143). During the occurrence and development of human esophageal squamous cell carcinoma (ESCC), the activation of ODC can increase the secretion of IL-33 in the tumor site, thereby promoting the polarization of macrophages to the anti-inflammatory M2 phenotype (144). Moreover, MTA accumulates in MTAP-deficient tumor cells, blocks the activation of macrophages and inhibits the production of TNF-α through adenosine A2 receptor and TLR receptor after LPS stimulation, which promotes the differentiation of M2 macrophages with immunosuppressive effect (145).

According to the recent research reports, polyamines can regulate the activation and function of macrophages largely depends on the arginase-eIF5A-hypusine axis. The researchers activated mouse bone marrow-derived macrophages with IL-4 [referred to M(IL-4)], and found that $eIF5A^H$ (eIF5A Hypusination) was induced upon activation with IL-4. Significantly increased $eIF5A^H$ in M(IL-4) correlated with enrichment of hypusinating enzymes (ODC, DHPS, DOHH) expression in these cells. It was also observed that increased arginine in M(IL-4) promoted putrescine production by ODC and increased flux of putrescine to spermidine, which could be used to synthesize hypusine. These data may imply that even if the expression of polyamine-hypusine enzymes is not altered, hypusine synthesis might increase due to the increased availability of ornithine, putrescine and spermidine, followed by changes in $eIF5A^H$ levels in immune cells (44). In conclusion, various links in the polyamine pathway play important roles in the immunomodulatory function of macrophages, especially the activation of macrophages, thereby promoting the establishment of an immunosuppressive tumor microenvironment.

## 3.2 Excessive polyamines in cancer cells confer immunosuppressive properties on DCs

Dendritic cells(DCs) are bone marrow-derived cells that present in all tissues (146–148), and are sentinels of the immune system, which play a central role in linking innate and adaptive immune responses (146). The function of DCs is determined by the integration of environmental signals, which are sensed *via* the surface expression and intracellular receptors of cytokines, pathogen-associated molecular patterns (PAMPs) and damage-associated molecular patterns (DAMPs) (149). Dendritic cells can capture tumor antigens released from live or dead tumor cells, and cross-present these antigens to T cells in the tumor draining lymph nodes, thus leading to the generation of tumor-specific CTLs (150, 151). However, signals from the TIME can prevent antigen presentation and the establishment of tumor-specific immune responses *via* a variety of mechanisms. For example, the anti-inflammatory cytokine IL-10 secreted by immunosuppressive cells can inhibit the maturation of DCs, leading to antigen-specific anergy (152, 153). In addition, the tumor antigens, e. g. glycoproteins carcinoembryonic antigen (CEA) and mucin 1(MUC1), can be endocytosed by DCs and confined to the early endosomes, thus preventing their effective processing and presentation to T cells (154). Polyamines also play an important role in the maturation and functional regulation of DCs. ARG1, a key enzyme of polyamine biosynthesis, is highly expressed in DCs, and is one of the most important immune checkpoints that allow tumor immune escape (155–158). It has been reported that DCs metabolize local arginine to produce local arginine starvation and prevent the progression of T cell cycle in the G0-G1 phase by impairing the expression of the T cell receptor (TCR) CD3-ξ chain in human and mouse cells (159, 160). In the psoriatic inflammatory circuit, lack of Pp6 in keratinocytes causes ARG1 accumulation and drives polyamine production, which promotes self-RNA sensing by dendritic cells, leading to increased inflammation (161). Adding putrescine to the microenvironment of DCs will hinder their ability to effectively cross-prime exogenous antigens, indicating that

their immunogenic functions are reduced (162). Spermidine activates the Src kinase and confers IDO1-dependent immunosuppressive properties in DCs (163). Moreover, spermine and spermidine may convert immunogenic DCs into tolerant DCs by promoting the production of IL-10, thereby inducing anergic cytotoxic $CD8^+$T cells (164–166). Spermidine may also inhibit the differentiation and maturation of DCs by promoting the production of VEGF (167–169). In addition, ROS is released during polyamine catabolism (77, 79). High levels of ROS in the tumor microenvironment may inhibit the function of DCs. ROS can enter DCs through diffusion across the plasma membrane or extracellular vesicles released by tumor cells, which gives the tumor microenvironment more opportunities to inhibit DC function (170). Therefore, the ROS generated during the catabolism of polyamines may not only inhibit the cross-presentation of DCs, but also inhibit the maturation of DCs through endoplasmic reticulum stress (171, 172).

## 3.3 Polyamines for NK cells: A double-edged sword

NK cells are the first subtype of innate lymphoid cells (ILCs) characterized by a surface marker profile $CD3^-CD56^+NKp46^+$ in humans, exerting natural cytotoxicity against primary tumor cells and metastasis by inhibiting proliferation, migration and colonization to distant tissues (173). The detection of abnormal cells by NK cells is determined by the integration of complex signals such as IL-12, IL-15, and IL-18, as well as the balance between activation and inhibition signals and the interaction of MHC-I on the surface of target cells (174–176). During infection and inflammation, NK cells are recruited and activated within a short period of time, proliferate rapidly and largely contribute to the innate and adaptive immune response (177, 178). NK cell activation is inhibited by the binding of inhibitory receptors to class I HLA (MHC I) molecules. However, many cancer cells downregulate the expression of the MHC I molecules to evade the detection of cytotoxic $CD8^+$T cells. Therefore, due to the lack of MHC I-induced signaling *via* inhibitory receptors and the subsequent increase in activation signaling, NK cells can recognize and respond to cells of this missing-self phenotype, and ultimately lead to target cell lysis (179).

Despite their activity in controlling tumor growth, NK cells are susceptible to multiple immunosuppressive mechanisms in TIME. Many cancer-related soluble immunosuppressive molecules have negative effects on NK cell function, including TGF-β, IL-10, indoleamine 2,3-dioxygenase, prostaglandin E2 (PGE2) and macrophage migration inhibitory factor (MIF) (180). In addition to immunosuppressive cytokines, accumulation of tumor-derived metabolites in TIME, including polyamines, also exerts immunosuppressive effects on NK cells (37–40, 68, 181). Polyamines act as a double-edged sword in regulating NK cell functions. According to reports, polyamines act as natural immunosuppressive agents by reducing the cytolytic properties of NK cells, which protect tumors from the host's immune response (182), while polyamine deprivation stimulates NK cell activity (59). Polyamines can also inhibit the expression of NK1.1 receptors of NK cells and the production of perforin and IFN-γ, thus attenuating NK cell-mediated tumor cell recognition and cytolysis, and such effects could be reversed by treatment with DFMO, rosuvastatin, and their combination (182). Adhesion molecules have been shown to promote NK cell activation (183). Lymphocyte function-associated antigen 1 (LFA-1) is expressed on NK cells and interacts with intercellular adhesion molecules (ICAM) on target cells. The combination of LFA-1 and ICAM-1 can enhance NK cell-mediated cytotoxicity by enhancing the polarization of the cytoskeleton mechanism, which is necessary for effective delivery of cytotoxic particles (183). However, spermine, a natural polyamine, can negatively affect the expression of LFA-1 and attenuate the binding of LFA-1 and ICAM-1, thus resulting in a decrease in NK cell-mediated cytotoxicity and ineffective delivery of cytotoxic particles (183, 184). On the other hand, polyamines may participate in the differentiation of NK cells, contribute to their maturation and protect their viability. It is well known that IL-2 can induce the proliferation of NK cells and improve their cytolytic activity (185). Polyamine biosynthesis can increase IL-2 production, thus enhancing the cytotoxicity of NK cells (186). In addition, polyamines, particularly spermidine and spermine, reverse immune senescence through translational control of autophagy (121, 187). Autophagy is necessary for the differentiation of mature NK cells from bone marrow-derived HSC (188, 189), and is essential for NK cells to clear the virus and enhance the memory formation of NK cells (188–190). Therefore, polyamines are involved in regulating the differentiation process of NK cells, even play an important role in tumor immunity.

## 3.4 Polyamines, activators of type I NKT cells

NKT cells, subtypes of innate-like T lymphocytes, can quickly respond to antigen stimulation and produce a large amount of various cytokines and chemokines, thus serving as a key player in connecting the innate immune system and the adaptive immune system (191–194). Unlike the TCR of traditional T cells, which only recognizes one (or at most a few) epitopes, a single TCR of NKT cells can react with a large number of antigens, including self and foreign antigens. Therefore, in a T cell environment specific to an antigen, their numbers are high enough to initiate a significant immune response, although the absolute frequency of NKT cells is low (e.g., about 1% in mouse spleen) (195–197). According to the heterogeneity of TCR rearrangement, NKT cells are divided into

two types, type I or type II NKT cells with different roles in tumor immunity (198). Usually, type I NKT cells promote tumor immunity, while type II NKT cells inhibit tumor immunity. Under normal conditions, an immunomodulatory axis exists between type I and type II NKT cells, wherein they have opposite polar functions and counteract each other (198).

In tumor immune surveillance, NKT cells can directly kill malignant cells. For example, both mouse and human NKT cells can directly lyse tumor cells through a perforin-dependent mechanism, and the expression of granzyme B also enhances the killing effect of NK cells (199, 200). However, polyamines can inhibit the production of perforin, making it unable to effectively lyse tumor cells (182). Polyamine blocking therapy (PBT) has been shown to increase the production of granzyme B in immune cells, thus enhancing the killing effect of NKT cells (67). It is reported that IL-12 is an effective inducer of IFN-γ (201), the main mechanism by which NKT cells act against cancer cells and induce other downstream effector cell functions (especially NK cells and $CD8^+$ T cells) to produce more IFN-γ to mediate tumor lysis (202, 203). Polyamines have been shown to reduce the production of IL-12 and IFN-γ in immune cells (164, 182), thus contributing to the inhibition of the killing function of NKT cells and NKT-mediated induction and activation of NK cells, DCs cells, and other immune cells. A main factor of type II NKT cells-mediated tumor immunosuppression is the increased production of IL-13 and IL-4 cytokines, which tilt immune response mainly toward the Th2 type with pro-tumor functions (204). In immune cells, IL-4 and IL-13 can increase polyamine levels (68, 205) that may also contribute to type II NKT cell-mediated tumor immunosuppression. In addition to lipid antigens, type I NKT cells can also be activated through toll-like receptor (TLR)-mediated signaling (206). Polyamines have been reported to affect immune system function by participating in the expression of Toll like Receptors (TLRs). Therefore, polyamines may play an important role in regulating the recruitment and activation of type I NKT cells through TLRs (207).

### 3.5 Polyamine-PD-L1-γδ T cells: A novel immune checkpoint pathway

Gamma delta (γδ) T cells are a unique lymphocyte population that mediate natural immunity against various infections and play a unique role in immune monitoring and tissue homeostasis (208). Since γδ T cells can quickly identify infected and transformed cells, they are considered as the first line of defense against infection and malignancy (209). The main pathway of γδ T cell activation involves γδ TCR. γδ TCR can bind to soluble or membrane proteins, such as tetanus toxoid, bacterial protein, viral protein and heat shock protein (210–212). According to the TCRδ chain usage, human γδ T cells are generally divided into 2 main subgroups. One subgroup is Vδ1 T cells, which are abundant in thymus and mucosal epithelial tissues, produce a variety of cytokines such as TNF-α and IFN-γ and lyse infected or transformed target cells through cytotoxicity (213, 214). The other is Vδ2 T cells that are mainly distributed in peripheral blood and play a cytotoxic role in tumor immune regulation and virus infection (215).

γδ T cells regulate the immune function of body through the cell-to-cell contact or soluble factors such as cytokines (216). Numerous factors, such as IL-2, IL-15, IL-17, IL-21, TGF-β, and vitamin C, can regulate the differentiation of γδ T cells and their anti-tumor response (217–221). Besides, polyamines, as negative immune regulators, directly or indirectly affect the function of γδ T cells by regulating their secretion of cytokines and other mediators. eIF5A is a translation elongation factor that assists in the translation of specific transcripts, and spermidine is required for hypusination of eIF5A (44, 222). eIF5A is directly involved in the translation of IL-17, an inflammatory cytokine produced mainly by activated Th17 cells, while IL-17 produced by γδ T cells drives tumorigenesis and progression through several downstream effects on tumor cells, endothelial cells, and other immune cells (223–225). Therefore, spermidine may regulate the production of IL-17 in γδ T cells through eIF5A and participate in the immune regulation of a variety of cancers. Blocking intracellular polyamines with DFMO can significantly induce TGF-β mRNA expression and increase TGF-β content (226). TGF-β changes the adhesion characteristics of γδ T cells and plays an important role in promoting the migration ability and tissue homing of γδ T cells (227). Therefore, the occurrence and development of cancer is usually accompanied by an increase of polyamines, which may inhibit the toxic activity of γδ T cells. In recent years, researchers have discovered that γδ T cells can promote tumor promotion by regulating PD-1/PDL-1 (228). The immune checkpoint molecule PD-1 and its ligand PDL-1/2 are one of the main regulatory mechanisms that temper tumor immunity (229, 230). *In vitro* studies have shown that tumor-infiltrating γδ T cells inhibit αβ T cell activation *via* cell-to-cell contact by PD-1/PD-L1 (228), and polyamine blockade therapy has been reported to enhances the antitumor efficacy of PD-1 blockade (231), which indicates that polyamines may affect the immune function of γδT cells through PD-1/PD-L1, thereby inhibiting the activation of αβ T cells, and ultimately promote tumor progression.

## 4 Role of polyamines in the adaptive immune responses in TIME

Tumor infiltrated lymphocytes (TILs) play an important role in the establishment of a pro- or anti-tumorigenic TME (232). T lymphocytes are usually the major components of TILs, among which $CD4^+$ T helper cells (e.g., Th1), $CD4^+CD25^+$ regulatory T cells (Tregs), $CD8^+$ cytotoxic T cells are frequently observed in various cancers (233–235). Clinically, TILs can be separated,

screened and amplified *in vitro*, and then implanted into the patient's body to exert a specific killing effect on the tumor (236).

## 4.1 Polyamine for CD8+ tumor-infiltrating lymphocytes: TIME's "enemy"

$CD8^+$ tumor-infiltrating lymphocytes play a key role in the host's anti-tumor immune response by acting as cytotoxic cells through the release of granzyme B, perforin, and pro-inflammatory cytokines such as TNF-α, IFN-γ, and IL-12 (237, 238). However, many factors, such as indoleamine-2, 3-dioxygenase (IDO), PD-L1, cytokine milieu, and the state of protein kinases in TIME, can suppress the infiltration and cytotoxic activities of $CD8^+$ T cells and eventually lead to immune evasion by tumor cells (239–241).

T lymphocytes obtain energy for their survival, proliferation, and biological functions through various metabolic pathways, while dysregulated metabolism in TME contributes to aberrant functions of TILs, including $CD8^+$ cytotoxic T cells (242, 243). Alterations in different metabolic pathways in TME can lead to exhaustion, impaired effector functions and survival of $CD8^+$ cytotoxic T cells in various types of cancer (244–246). Previous studies have indicated that increased polyamine metabolism is also involved in regulation of the survival and effector function of $CD8^+$ TILs (68, 247). For example, polyamines and polyamine oxidation products may inhibit the activation and proliferation of $CD8^+$ TILs by down-regulating the production of IL-2 (248, 249). Increased polyamine production was associated not only with increased IL-10 levels, but also with decreased IL-12 levels, suggesting that polyamines may inhibit the cytotoxic function and cause deficiency of $CD8^+$ TILs (250–252). In addition, polyamines can also reduce the expression of chemokines, thus inhibiting the migration and recruitment of $CD8^+$ TILs, a key step for anti-tumor response (45, 253, 254). It has been reported that the expression of T cell co-inhibitory molecules (PD1, PD-L1 and CTLA-4) can induce exhaustion of effector T cells, while blockade of PD-1/PD-L1 T cell co-inhibitory axis can efficiently enhance the infiltration of $CD8^+$ T cells into TIME and restore the anti-tumor immune response (255, 256). Most recently, several lines of evidence have shown that polyamine blocking therapy (PBT) can improve the anti-tumor efficacy of PD-1 blockade along with an increase in tumor infiltration of granzyme $B^+$, IFN-$\gamma^+$ $CD8^+$ T-cells and a decrease in immunosuppressive tumor infiltrating cells including Gr-$1^+CD11b^+$ myeloid derived suppressor cells (MDSCs), $CD4^+CD25^+$ Tregs, and $CD206^+F4/80^+$ M2 macrophages (231, 257, 258). These findings suggest that polyamines are directly or indirectly involved in regulating the function of $CD8^+$ TILs. Adenosine is a mediator of TME immunosuppression, and its physiological activity is mediated by adenosine receptors (ARs). It may limit the success of immunotherapy, especially the adoptive cell transfer of TILs (259–261). Activation of adenylate cyclase by inhibiting ARs can induce the increase of cellular cAMP levels (262). Studies have shown that cAMP-elevating agents have excellent anti-tumor activity, and when used in combination with other anti-tumor agents, cAMP-elevating agents show enhanced anti-tumor activity (263, 264). Furthermore, ARs inhibitors have been shown to prevent Ado-mediated inhibition of $CD8^+$ TILs, probably by inhibiting ODC and even disrupting spermine synthesis, leading to a significant reduction in total polyamines (265, 266).

## 4.2 Polyamines are central determinants for the fidelity of Th1 cell subsets

T lymphocyte response is necessary for the host to defend against pathogens. According to the difference of antigen and cytokine microenvironment during activation, human $CD4^+$ effector T cells can differentiate into at least four main subtypes, including Th1, Th2, Th9, and Th17 (267–269). The main inducers of Th1 cells are IL-12 and IFN-γ. IL-12 is produced by antigen-presenting cells and interacts with its receptors to induce the expression STAT4 and T-bet, the main transcription factor of Th1 cells. T-bet directly binds to the promotor of various Th1 specific genes and promotes their expression (270). T-bet can also negatively regulate the expression of Th2 and Th17 specific genes to inhibit the differentiation of Th2 and Th17 cells. STAT4 can directly bind to the Ifng locus and stimulate IFN-γ production. The cooperation of STAT4 and T-bet will induce the greatest amount of IFN-γ. Therefore, in the absence of STAT4, T-bet alone cannot induce an optimal expression of IFN-γ (270–272).

Metabolic reprogramming is an important factor in the activation and differentiation of T cells (242). Recent studies have shown that polyamine metabolism is a major determinant of fidelity of helper T cell lineages (223). Ornithine decarboxylase is a key enzyme in polyamine synthesis. Lack of ornithine decarboxylase leads to the serious failure of $CD4^+$ T cells to adopt the correct subgroup specification, which is highlighted by the ectopic expression of a variety of cytokines and lineage-defining transcription factors across Th cell subsets (223). Even though spermidine does not inhibit the cell proliferation or cytokine production of Th1 cells, T-$bet^+$ T cells were slightly reduced when stimulated with higher doses of spermidine, indicating that spermidine may interfere with the Th1 cell differentiation process (273). The expression of inducible co-stimulator (ICOS) is an important indicator of the anti-tumor response of Th1 cells (274, 275), and serves as a new potential biomarker for T cell-mediated immunotherapy response (276–278). However, PD-1 down-regulates ICOS on $CD4^+$ T cells, which inhibits the differentiation of $CD4^+$ T cells into Th1 cells and affects the anti-tumor response of Th1 cells (256, 279).

Polyamines may affect the expression of ICOS in Th1 cells through PD-1 and then regulate the immune function of Th1 cells, while PBT (polyamine Blocking Therapy) has been shown to enhance the anti-tumor effect of PD-1 blockade. These data imply that polyamine and PD-1/PD-L1 may synergistically contribute to impaired functions of effector T cells and then tumor growth (231, 256, 279). Meanwhile, polyamines can also regulate the function of Th1 cells by regulating the production of cytokines. For instance, polyamines, especially spermidine, have been reported to inhibit the production of IL-12 in immune cells, thus resulting in a reduced expression of STAT4 and T-bet, and ultimately, a significant reduction in IFN-γ production (45, 123, 250, 270–272). Taken together, polyamines may play important roles in regulating the antitumor immunity of Th1 cells.

### 4.3 Polyamine-Treg cells: Inhibitory fuel for TIME

Tregs cells are a small subset of $CD4^+$ T lymphocytes (about 5%), which are composed of several cell subgroups with similar phenotypes and can inhibit the function of autologous conventional T cells (Tconv) (280, 281). There are two main subgroups of Treg cells: natural Treg cells and adaptive Treg cells. Natural Treg cells originate from the thymus and mediate inhibition through cells contact-dependent mechanism. Adaptive Treg cells, also called type 1 regulatory T cells (Tr1), are induced in the periphery in response to environmental signals, including antigens, IL-2, TGF-β, IL -10 and cAMP (282, 283). The homing of Treg cells is a key step in the initiation and spread of immunosuppressive TME (284). In TIME, Tregs cross-talk with other types of cells, including infiltrating effector T cells, stromal cells, and tumor cells. Treg cells contribute to the immunosuppressive TME through multiple mechanisms, such as inhibiting the maturation of antigen presenting cells (APC), the secretion of pro-inflammatory cytokines and the production of cytotoxic granzymes and perforin by Th1 and $CD8^+$ T cells (285). Studies also indicate that Tregs can also support tumor progression through some non-immune mechanisms, such as promoting angiogenesis, proliferation, and metastasis of tumor cells (286–288).

Several lines of evidence have implicated the important role of polyamines in regulating Tregs (289). A recent study has demonstrated that polyamine-related enzyme expression was significantly enhanced in pathogenic Th17 cell but suppressed in Treg cells, while pharmacological and genetic ablation of polyamine metabolism inhibited Th17 cytokine production and reprogrammed the transcriptome and epigenome of Th17 cells toward a Treg-like state as evidenced by enhanced Foxp3 expression (290). Spermidine can also regulate T cell development and enhance the differentiation of mouse and human naive T cells into Treg cells in an autophagy-related manner. The increased synthesis of polyamines in tumor cells may lead to increased secretion of spermidine, which in turn may damage anti-tumor immunity by promoting Treg cells (273). In the process of polyamine catabolism, a large amount of reactive oxygen species (ROS) is produced (77, 79). In TME, ROS can affect the function of immune cells, e. g. the inhibition or activation of Treg functions depending on its concentration (291, 292). In general, ROS at a low level suppresses the function of Treg cells. *In vitro*, neutrophil cytoplasmic factor 1-deficient mice have lower ROS levels than wild-type mice, and the Treg cells isolated from neutrophil cytoplasmic factor 1-deficient mice have weakened functions. In addition, thiol-bearing antioxidants or NADPH oxidase inhibitors reduce ROS levels and then can block or attenuate Treg-mediated inhibition of $CD4^+$ effector T cells (293). However, in psoriatic dermatitis, elevated ROS levels can induce hyperfunction of Treg cells (294). Moreover, Treg cells are hyperactive in the culture of 3-dimethoxy-1,4-naphthoquinone (DMNQ), which can induce an increase in ROS levels in a dose-dependent manner (295). It was reported that spermidine ameliorated Dextran Sulfate Sodium -induced inflammatory bowel disease (IBD) in mice by promoting M2 macrophage polarization by inducing mitochondrial reactive oxygen species (mtROS). ROS are key signaling molecules that play a critical role in tumor immunity. Whereas, how ROS production during polyamine catabolism could affect the immune function of Tregs cells, and to what extend would ROS contribute to polyamines's function in Treg cells regulation, remain to be further investigated.

## 5 Clinical studies of polyamine blockade therapy for cancer

Due to the general elevated level of polyamines in TIME and their wide spectrum effects on tumor and immune cells, polyamine blockade therapy (PBT) is emerging as a novel adjuvant therapy of both chemo- and immune-therapies for a variety of cancers (9, 67, 296). DFMO is a potent, highly specific enzyme-activated, irreversible inhibitor of ODC activity (297–299). DFMO has shown excellent promise in chemoprevention and/or treatment of cancer (9). However, a major disadvantage of DFMO as monotherapy is the compensatory increase in polyamine transport when polyamines are depleted. Therefore, the use of nontoxic polyamine transport inhibitors in combination with DFMO to deplete polyamine levels is a more promising area, which is PBT therapy (300). The most exciting finding is that PBT therapy not only depletes polyamines in tumor cells, but also promotes anti-tumor immune responses, resulting in greater anti-tumor effects than expected. In immunocompetent mouse models of lymphoma, melanoma, and colon cancer, treatment with DFMO in

combination with AMXT 1501 inhibited tumor growth by reducing tumor-infiltrating myelosuppressor cells and increasing $CD3^+$ T cells (68). In addition to AMXT1501, DFMO can also be used in combination with different polyamine transport inhibitors (Trimer PTIs) to increase granzase B and IFN-γ and activate effector T cells, ultimately inhibiting tumor-promoting microenvironment and increasing antitumor immune responses (67). To date, numerous inhibitors of polyamine metabolism-related enzymes or polyamine transport have been shown to possess potent antitumor effects both *in vitro* and in preclinical cancer models, and several of them have been moved into clinical trials for treating a variety of cancer (Table 1).

In addition to clinically tested inhibitors of enzymes involved in polyamine metabolism or polyamine transport, there are a number of newly discovered inhibitors that were not initially used to inhibit polyamine levels. Clofazimine (CLF) is a riminophenazine-based drug approved by the US FDA for the treatment of leprosy and tuberculosis (301, 302). CLF plays A role in tumor xenografts by inhibiting Kv1.3 potassium channels, interfering with Wnt signaling, or enhancing phospholipase A2 activity (303–307). Some of these effects of CLF can be explained by CLF-dependent inhibition of polyamines, as polyamines have previously been shown to inhibit phospholipase A2 and C activities (308). In addition, CLF was found to inhibit multiple myeloma through the Aryl hydrocarbon receptor/polyamine biosynthesis axis (309). The Aryl hydrocarbon receptor (AHR) is a direct transcriptional activator of ODC1 and AZIN1. CLF treatment reduced the binding of AHR to the promoters of AZIN1 and ODC1 in a dose-dependent manner, accompanied by a decrease in the levels of putrescine, spermidine and spermine. Not only this, but CLF can also induce secretion of acetylated polyamines (catalyzed by SSAT) as well as increased protein levels of SMOX, suggesting that CLF promotes polyamine catabolism (309). Therefore, it is not necessary to only use traditional polyamine

TABLE 1 Polyamine metabolism interventions in cancers: Clinical trials*.

| Inhibitor | Target | Cancer | Status | Phase | Interventions | Plus drugs | Immune cells that may be involved |
|---|---|---|---|---|---|---|---|
| DFMO | ODC | Prostate Cancer | Completed | 2 | DFMO in high-risk therapy | – | – |
| | | Prostate Cancer | Completed | 2 | DFMO to prevent recurrence | Bicalutamide | – |
| | | Non-melanoma Skin Cancer | Recruiting | 2 | DFMO for chemoprophylaxis | Solaraze | – |
| | | Non-melanomatous Skin Cancer | Completed | 3 | DFMO to prevent recurrence | – | – |
| | | Non-melanomatous Skin Cancer (Precancerous/ nonmalignant condition) | Completed | 2 | DFMO to prevent recurrence | Triamcinolone | – |
| | | Bladder Cancer | Completed | 3 | DFMO to prevent recurrence | – | – |
| | | Cervical Cancer (Precancerous condition) | Completed | 2 | DFMO to prevent recurrence | – | – |
| | | Esophageal Cancer | Completed | 2 | DFMO to prevent recurrence | – | – |
| | | Colorectal Cancer (with familial adenomatous polyposis) | Completed | 2 | DFMO in high-risk therapy | Celecoxib | – |
| | | Colorectal Cancer (Precancerous condition) | Completed | 3 | DFMO to prevent recurrence | Sulindac | – |
| | | Colorectal Neoplasms | Recruiting | 3 | DFMO to prevent recurrence | Sulindac | – |
| | | Adenomatous Polyp | Completed | 2 | DFMO in high-risk therapy | Aspirin | – |
| | | Gastric Cancer | Recruiting | 2 | DFMO in high-risk therapy | – | – |
| | | Anaplastic Astrocytoma | Recruiting | 3 | DFMO to prevent recurrence | Lomustine | – |
| | | Medulloblastoma | Recruiting | 2 | DFMO in high-risk therapy | – | – |

*(Continued)*

TABLE 1 Continued

| Inhibitor | Target | Cancer | Status | Phase | Interventions | Plus drugs | Immune cells that may be involved |
|---|---|---|---|---|---|---|---|
| | | Neuroblastoma | Recruiting | 2 | DFMO to prevent recurrence | Etoposide | – |
| | | Neuroblastoma | Active, not recruiting | 2 | DFMO to prevent recurrence | – | – |
| | | Neuroblastoma | Active, not recruiting | 2 | DFMO to prevent recurrence | – | – |
| | | Neuroblastoma | Active, not recruiting | 1 | DFMO to prevent recurrence | Celecoxib, Topotecan, Cyclophosphamide | – |
| | | Neuroblastoma | Active, not recruiting | 1/2 | DFMO to prevent recurrence | Bortezomib | – |
| | | Neuroblastoma | Recruiting | 2 | DFMO to prevent recurrence | – | – |
| | | Neuroblastoma | Completed | 1 | DFMO to prevent recurrence | Etoposide | – |
| | | Neuroblastoma | Recruiting | 2 | DFMO in high-risk therapy | Ceritinib, Dasatinib, Sorafenib, Vorinostat | – |
| | | Neuroblastoma | Suspended (Scheduled Interim Monitoring) | 2 | DFMO to prevent recurrence | Dinutuximab, Sargramostim, Temozolomide, Irinotecan Hydrochloride | – |
| BENSpm | SSAT, SMOX | Hepatocellular Carcinoma | Terminated | 1/2 | BENSpm in high-risk therapy | – | – |
| PG-11047 | ODC, AMD1, SRM, SMS, SSAT, SMOX | Solid Tumors | Completed | 1 | PG-11047 in advanced refractory therapy | – | – |
| | | Solid tumors and lymphoma | Completed | 1 | PG-11047 in advanced therapy | Gemcitabine, Docetaxel, Bevacizumab, Erlotinib, Cisplatin, Sunitinib 5-flurouracil/ leucovorin | Lymphocytes, Macrophages, NK cells |
| | | Lymphoma | Completed | 1 | PG-11047 to prevent recurrence | - | Macrophages, Lymphocytes, NK cells |
| AMXT 1501 | Polyamine transport | Solid Tumors | Recruiting | 1 | AMXT 1501 in advanced therapy | DFMO | – |

*All clinical trials on cancers intervention are based on polyamine level inhibition, as listed in the https://clinicaltrials.gov/, query date Mar. 4, 2022.

inhibitors to intervene polyamine metabolism, but also can be combined with other drugs to intervene polyamine metabolism, or combined with other immunotherapy modalities. However, these require further investigation to realize the full potential of this strategy.

## 6 Conclusions

Despite extensive research in the field of polyamines and cancer, the role of polyamines in immunomodulatory function in the complex TIME environment remains uncertain, especially the mechanism by which they promote tumor immune evasion. Various inhibitors utilizing polyamine depletion strategies are currently being tested in clinical trials. DFMO, a specific inhibitor of ODC, shows excellent promise in chemoprevention and/or treatment of cancer. Moreover, recent evidence suggests that PBT therapy can mediate the remodeling of the immune landscape of the tumor microenvironment, particularly to promote antitumor immune responses. Emerging evidence in preclinical models of inflammation demonstrates the critical regulatory role of polyamines in immune cell lineage specification, proliferation, and function (Figure 3).

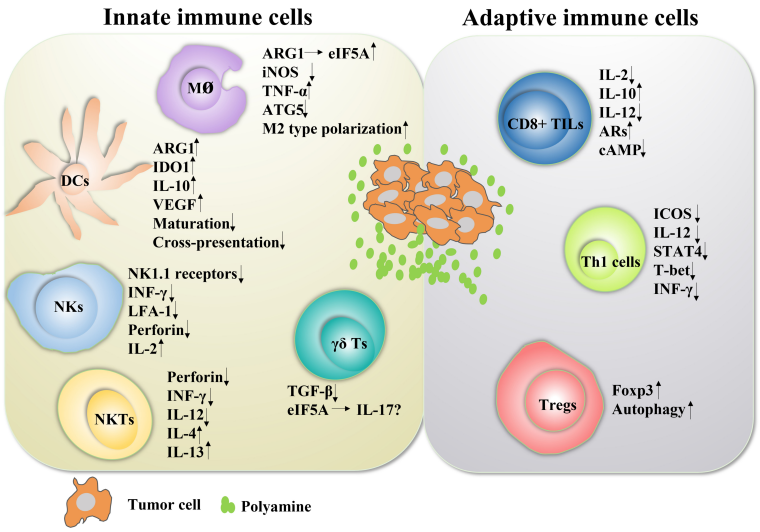


FIGURE 3
The role of polyamines in both innate and adaptive immune responses in cancer Polyamines and their key enzymes can reshape the tumor immune microenvironment through a variety of transcription factors or cytokines, even have dual roles. The polyamine-eIF5A-hypusine axis regulates macrophage polarization, especially polyamines tend to promote the polarization of M2-type macrophages. Polyamines also negatively regulated the functions of DC cells, NKT cells, CD8+ TILs and Th1 cells, and positively regulated the functions of Treg cells. For NK cells, polyamines are a double-edged sword. In fact, the tumor immune microenvironment is mutually influenced and restricted by a variety of factors. The regulation of polyamines in regulating the function of immune cells is not absolute, which will change according to the changes of tumor immune microenvironment.

Furthermore, the combination of polyamine blockade and checkpoint immunotherapy (anti-PD1 or anti-PDL1 immunotherapy) has yielded exciting results in multiple cancer models in mice. All these reports may provide a rationale for utilizing polyamine depletion strategies to promote antitumor immune responses. In fact, the effect of polyamines on immune function was discovered in 1977, and in this pioneering work, exogenous polyamine administration suppressed innate and adaptive immune responses in mouse splenocytes. After decades of intensive research and thousands of studies published, the effects of polyamines on immunity and cancer are surprising. However, the studies on these immune functions are not comprehensive, mainly focusing on macrophages and T lymphocytes, and there are significant differences between different cell types and different diseases. Therefore, it is necessary to further explore the role of polyamines in different tumor immune microenvironments.

## Author contributions

All authors contributed significantly to the drafting and editing of this manuscript. JZ, XQ, YL conceived the manuscript idea and wrote the manuscript. JL, HZ and JZ revised the manuscript content. ML, ZY, and BL created the manuscript tables and figures. All authors contributed to the article and approved the submitted version.

## Funding

This study was supported by grants from the Dongguan Social Science and Technology Development Project (20211800904532), Natural Science Foundation of Guangdong Province (2021A1515012054, 2021B1515140066, 2019A1515110042, 2019A1515011713), Characteristic Innovation Experimental Project of Ordinary Universities in Guangdong Province (2020KTSCX044), Research Foundation of Guangdong Medical University for Ph.D. Staff (GDMUB2020017), the Open Program of Guangdong Provincial Key Laboratory of Medical Molecular Diagnostics (GPKLMMD-OP202107), the Medical Science Foundation of Guangdong Province (A2021438, A2020331, A2020211).

## Conflict of interest

The authors declare that the research was conducted in the absence of any commercial or financial relationships that could be construed as a potential conflict of interest.

## Publisher's note



## References

1. Igarashi, K, and Kashiwagi, K. Modulation of cellular function by polyamines. *Int J Biochem Cell Biol* (2010) 42:39–51. doi: 10.1016/j.biocel.2009.07.009

2. Pegg, AE, and Casero, RAJr. Current status of the polyamine research field. *Methods Mol Biol* (2011) 720:3–35. doi: 10.1007/978-1-61779-034-8_1

3. Terui, Y, Yoshida, T, Sakamoto, A, Saito, D, Oshima, T, Kawazoe, M, et al. Polyamines protect nucleic acids against depurination. *Int J Biochem Cell Biol* (2018) 99:147–53. doi: 10.1016/j.biocel.2018.04.008

4. Kurata, HT, Akrouh, A, Li, JB, Marton, LJ, and Nichols, CG. Scanning the topography of polyamine blocker binding in an inwardly rectifying potassium channel. *J Biol Chem* (2013) 288:6591–601. doi: 10.1074/jbc.M112.383794

5. Rao, JN, Rathor, N, Zhuang, R, Zou, T, Liu, L, Xiao, L, et al. Polyamines regulate intestinal epithelial restitution through Trpc1-mediated Ca(2)+ signaling by differentially modulating Stim1 and Stim2. *Am J Physiol Cell Physiol* (2012) 303: C308–17. doi: 10.1152/ajpcell.00120.2012

6. Janne, J, Alhonen, L, Pietila, M, and Keinanen, TA. Genetic approaches to the cellular functions of polyamines in mammals. *Eur J Biochem* (2004) 271:877–94. doi: 10.1111/j.1432-1033.2004.04009.x

7. Pegg, AE. Mammalian polyamine metabolism and function. *IUBMB Life* (2009) 61:880–94. doi: 10.1002/iub.230

8. Murray-Stewart, TR, Woster, PM, and Casero, RAJr. Targeting polyamine metabolism for cancer therapy and prevention. *Biochem J* (2016) 473:2937–53. doi: 10.1042/BCJ20160383

9. Casero, RAJr., Murray Stewart, T, and Pegg, AE. Polyamine metabolism and cancer: Treatments, challenges and opportunities. *Nat Rev Cancer* (2018) 18:681–95. doi: 10.1038/s41568-018-0050-3

10. Nishimura, K, Shiina, R, Kashiwagi, K, and Igarashi, K. Decrease in polyamines with aging and their ingestion from food and drink. *J Biochem* (2006) 139:81–90. doi: 10.1093/jb/mvj003

11. Matsumoto, M, Kibe, R, Ooga, T, Aiba, Y, Kurihara, S, Sawaki, E, et al. Impact of intestinal microbiota on intestinal luminal metabolome. *Sci Rep* (2012) 2:233. doi: 10.1038/srep00233

12. Sugiyama, Y, Nara, M, Sakanaka, M, Gotoh, A, Kitakata, A, Okuda, S, et al. Comprehensive analysis of polyamine transport and biosynthesis in the dominant human gut bacteria: Potential presence of novel polyamine metabolism and transport genes. *Int J Biochem Cell Biol* (2017) 93:52–61. doi: 10.1016/j.biocel.2017.10.015

13. Munoz-Esparza, NC, Latorre-Moratalla, ML, Comas-Baste, O, Toro-Funes, N, Veciana-Nogues, MT, and Vidal-Carou, MC. Polyamines in food. *Front Nutr* (2019) 6:108. doi: 10.3389/fnut.2019.00108

14. Hirano, R, Shirasawa, H, and Kurihara, S. Health-promoting effects of dietary polyamines. *Med Sci (Basel)* (2021) 9:8. doi: 10.3390/medsci9010008

15. Madeo, F, Eisenberg, T, Pietrocola, F, and Kroemer, G. Spermidine in health and disease. *Science* (2018) 359:6374. doi: 10.1126/science.aan2788

16. Eisenberg, T, Abdellatif, M, Schroeder, S, Primessnig, U, Stekovic, S, Pendl, T, et al. Cardioprotection and lifespan extension by the natural polyamine spermidine. *Nat Med* (2016) 22:1428–38. doi: 10.1038/nm.4222

17. Pietrocola, F, Pol, J, Vacchelli, E, Rao, S, Enot, DP, Baracco, EE, et al. Caloric restriction mimetics enhance anticancer immunosurveillance. *Cancer Cell* (2016) 30:147–60. doi: 10.1016/j.ccell.2016.05.016

18. Gomez-Gallego, C, Garcia Romo, M, Frias, R, Periago, MJ, Ros, G, Salminen, S, et al. Mice exposed to infant formula enriched with polyamines: Impact on host transcriptome and microbiome. *Food Funct* (2017) 8:1622–26. doi: 10.1039/c7fo00073a

19. Matsumoto, M, and Benno, Y. The relationship between microbiota and polyamine concentration in the human intestine: A pilot study. *Microbiol Immunol* (2007) 51:25–35. doi: 10.1111/j.1348-0421.2007.tb03887.x

20. Tofalo, R, Cocchi, S, and Suzzi, G. Polyamines and gut microbiota. *Front Nutr* (2019) 6:16. doi: 10.3389/fnut.2019.00016

21. Ramos-Molina, B, Queipo-Ortuno, MI, Lambertos, A, Tinahones, FJ, and Penafiel, R. Dietary and gut microbiota polyamines in obesity- and age-related diseases. *Front Nutr* (2019) 6:24. doi: 10.3389/fnut.2019.00024

22. Matsumoto, M, Kurihara, S, Kibe, R, Ashida, H, and Benno, Y. Longevity in mice is promoted by probiotic-induced suppression of colonic senescence dependent on upregulation of gut bacterial polyamine production. *PLoS One* (2011) 6:e23652. doi: 10.1371/journal.pone.0023652

23. Kibe, R, Kurihara, S, Sakai, Y, Suzuki, H, Ooga, T, Sawaki, E, et al. Upregulation of colonic luminal polyamines produced by intestinal microbiota delays senescence in mice. *Sci Rep* (2014) 4:4548. doi: 10.1038/srep04548

24. O'Toole, PW, Marchesi, JR, and Hill, C. Next-generation probiotics: The spectrum from probiotics to live biotherapeutics. *Nat Microbiol* (2017) 2:17057. doi: 10.1038/nmicrobiol.2017.57

25. Matsumoto, M, Aranami, A, Ishige, A, Watanabe, K, and Benno, Y. Lkm512 yogurt consumption improves the intestinal environment and induces the T-helper type 1 cytokine in adult patients with intractable atopic dermatitis. *Clin Exp Allergy* (2007) 37:358–70. doi: 10.1111/j.1365-2222.2007.02642.x

26. Matsumoto, M, Kitada, Y, Shimomura, Y, and Naito, Y. Bifidobacterium animalis subsp. lactis Lkm512 reduces levels of intestinal trimethylamine produced by intestinal microbiota in healthy volunteers: A double-blind, placebo-controlled study. *J Funct Foods* (2017) 36:94–101. doi: 10.1016/J.JFF.2017.06.032

27. Matsumoto, M, Ohishi, H, and Benno, Y. Impact of Lkm512 yogurt on improvement of intestinal environment of the elderly. *FEMS Immunol Med Microbiol* (2001) 31:181–6. doi: 10.1111/j.1574-695X.2001.tb00518.x

28. Albini, A, and Sporn, MB. The tumour microenvironment as a target for chemoprevention. *Nat Rev Cancer* (2007) 7:139–47. doi: 10.1038/nrc2067

29. Hanahan, D, and Coussens, LM. Accessories to the crime: Functions of cells recruited to the tumor microenvironment. *Cancer Cell* (2012) 21:309–22. doi: 10.1016/j.ccr.2012.02.022

30. Gajewski, TF, Schreiber, H, and Fu, YX. Innate and adaptive immune cells in the tumor microenvironment. *Nat Immunol* (2013) 14:1014–22. doi: 10.1038/ni.2703

31. Hanahan, D, and Weinberg, RA. Hallmarks of cancer: The next generation. *Cell* (2011) 144:646–74. doi: 10.1016/j.cell.2011.02.013

32. Bates, JP, Derakhshandeh, R, Jones, L, and Webb, TJ. Mechanisms of immune evasion in breast cancer. *BMC Cancer* (2018) 18:556. doi: 10.1186/s12885-018-4441-3

33. Kim, R, Emi, M, and Tanabe, K. Cancer immunoediting from immune surveillance to immune escape. *Immunology* (2007) 121:1–14. doi: 10.1111/j.1365-2567.2007.02587.x

34. Heriot, AG, Marriott, JB, Cookson, S, Kumar, D, and Dalgleish, AG. Reduction in cytokine production in colorectal cancer patients: Association with stage and reversal by resection. *Br J Cancer* (2000) 82:1009–12. doi: 10.1054/bjoc.1999.1034

35. Rampone, B, Rampone, A, Tirabasso, S, Panariello, S, and Rampone, N. Immunological variations in women suffering from ovarian cancer. influence of radical surgical treatment. *Minerva Ginecol* (2001) 53:116–9.

36. Monson, JR, Ramsden, C, and Guillou, PJ. Decreased interleukin-2 production in patients with gastrointestinal cancer. *Br J Surg* (1986) 73:483–6. doi: 10.1002/bjs.1800730620

37. Lan, L, Hayes, CS, Laury-Kleintop, L, and Gilmour, SK. Suprabasal induction of ornithine decarboxylase in adult mouse skin is sufficient to activate keratinocytes. *J Invest Dermatol* (2005) 124:602–14. doi: 10.1111/j.0022-202X.2005.23620.x

38. Takigawa, M, Enomoto, M, Nishida, Y, Pan, HO, Kinoshita, A, and Suzuki, F. Tumor angiogenesis and polyamines: Alpha-difluoromethylornithine, an irreversible inhibitor of ornithine decarboxylase, inhibits B16 melanoma-induced angiogenesis in ovo and the proliferation of vascular endothelial cells *in vitro*. *Cancer Res* (1990) 50:4131–8.

39. Lan, L, Trempus, C, and Gilmour, SK. Inhibition of ornithine decarboxylase (Odc) decreases tumor vascularization and reverses spontaneous tumors in Odc/Ras transgenic mice. *Cancer Res* (2000) 60:5696–703.

40. Gilmour, SK. Polyamines and nonmelanoma skin cancer. *Toxicol Appl Pharmacol* (2007) 224:249–56. doi: 10.1016/j.taap.2006.11.023

41. Weiss, TS, Bernhardt, G, Buschauer, A, Thasler, WE, Dolgner, D, Zirngibl, H, et al. Polyamine levels of human colorectal adenocarcinomas are correlated with tumor stage and grade. *Int J Colorectal Dis* (2002) 17:381–7. doi: 10.1007/s00384-002-0394-7

42. Linsalata, M, Caruso, MG, Leo, S, Guerra, V, D'Attoma, B, and Di Leo, A. Prognostic value of tissue polyamine levels in human colorectal carcinoma. *Anticancer Res* (2002) 22:2465–9.

43. Wang, Q, Zhang, M, Ding, Y, Wang, Q, Zhang, W, Song, P, et al. Activation of Nad(P)H oxidase by tryptophan-derived 3-hydroxykynurenine accelerates endothelial apoptosis and dysfunction *in vivo*. *Circ Res* (2014) 114:480–92. doi: 10.1161/CIRCRESAHA.114.302113

44. Puleston, DJ, Buck, MD, Klein Geltink, RI, Kyle, RL, Caputa, G, O'Sullivan, D, et al. Polyamines and Eif5a hypusination modulate mitochondrial respiration and macrophage activation. *Cell Metab* (2019) 30:352–63.e8. doi: 10.1016/j.cmet.2019.05.003

45. Yang, Q, Zheng, C, Cao, J, Cao, G, Shou, P, Lin, L, et al. Spermidine alleviates experimental autoimmune encephalomyelitis through inducing inhibitory macrophages. *Cell Death Differ* (2016) 23:1850–61. doi: 10.1038/cdd.2016.71

46. Merkley, SD, Chock, CJ, Yang, XO, Harris, J, and Castillo, EF. Modulating T cell responses *via* autophagy: The intrinsic influence controlling the function of both antigen-presenting cells and T cells. *Front Immunol* (2018) 9:2914. doi: 10.3389/fimmu.2018.02914

47. Li, C, Capan, E, Zhao, Y, Zhao, J, Stolz, D, Watkins, SC, et al. Autophagy is induced in Cd4+ T cells and important for the growth factor-withdrawal cell death. *J Immunol* (2006) 177:5163–8. doi: 10.4049/jimmunol.177.8.5163

48. Mocholi, E, Dowling, SD, Botbol, Y, Gruber, RC, Ray, AK, Vastert, S, et al. Autophagy is a tolerance-avoidance mechanism that modulates tcr-mediated signaling and cell metabolism to prevent induction of T cell anergy. *Cell Rep* (2018) 24:1136–50. doi: 10.1016/j.celrep.2018.06.065

49. Pua, HH, Dzhagalov, I, Chuck, M, Mizushima, N, and He, YW. A critical role for the autophagy gene Atg5 in T cell survival and proliferation. *J Exp Med* (2007) 204:25–31. doi: 10.1084/jem.20061303

50. Kovacs, JR, Li, C, Yang, Q, Li, G, Garcia, IG, Ju, S, et al. Autophagy promotes T-cell survival through degradation of proteins of the cell death machinery. *Cell Death Differ* (2012) 19:144–52. doi: 10.1038/cdd.2011.78

51. Nagaraj, S, Youn, JI, and Gabrilovich, DI. Reciprocal relationship between myeloid-derived suppressor cells and T cells. *J Immunol* (2013) 191:17–23. doi: 10.4049/jimmunol.1300654

52. Sunderkotter, C, Nikolic, T, Dillon, MJ, Van Rooijen, N, Stehling, M, Drevets, DA, et al. Subpopulations of mouse blood monocytes differ in maturation stage and inflammatory response. *J Immunol* (2004) 172:4410–7. doi: 10.4049/jimmunol.172.7.4410

53. Voisin, MB, Buzoni-Gatel, D, Bout, D, and Velge-Roussel, F. Both expansion of regulatory Gr1+ Cd11b+ myeloid cells and anergy of T lymphocytes participate in hyporesponsiveness of the lung-associated immune system during acute toxoplasmosis. *Infect Immun* (2004) 72:5487–92. doi: 10.1128/IAI.72.9.5487-5492.2004

54. Mencacci, A, Montagnoli, C, Bacci, A, Cenci, E, Pitzurra, L, Spreca, A, et al. Cd80+Gr-1+ myeloid cells inhibit development of antifungal Th1 immunity in mice with candidiasis. *J Immunol* (2002) 169:3180–90. doi: 10.4049/jimmunol.169.6.3180

55. Garg, A, and Spector, SA. Hiv type 1 Gp120-induced expansion of myeloid derived suppressor cells is dependent on interleukin 6 and suppresses immunity. *J Infect Dis* (2014) 209:441–51. doi: 10.1093/infdis/jit469

56. Kumar, V, Patel, S, Tcyganov, E, and Gabrilovich, DI. The nature of myeloid-derived suppressor cells in the tumor microenvironment. *Trends Immunol* (2016) 37:208–20. doi: 10.1016/j.it.2016.01.004

57. Labib, RS, and Tomasi, TBJr. Enzymatic oxidation of polyamines. relationship to immunosuppressive properties. *Eur J Immunol* (1981) 11:266–9. doi: 10.1002/eji.1830110318

58. Ferrante, A, Maxwell, GM, Rencis, VO, Allison, AC, and Morgan, DM. Inhibition of the respiratory burst of human neutrophils by the polyamine oxidase-polyamine system. *Int J Immunopharmacol* (1986) 8:411–7. doi: 10.1016/0192-0561(86)90125-6

59. Chamaillard, L, Quemener, V, Havouis, R, and Moulinoux, JP. Polyamine deprivation stimulates natural killer cell activity in cancerous mice. *Anticancer Res* (1993) 13:1027–33.

60. Chamaillard, L, Catros-Quemener, V, Delcros, JG, Bansard, JY, Havouis, R, Desury, D, et al. Polyamine deprivation prevents the development of tumour-induced immune suppression. *Br J Cancer* (1997) 76:365–70. doi: 10.1038/bjc.1997.391

61. Soda, K. The mechanisms by which polyamines accelerate tumor spread. *J Exp Clin Cancer Res* (2011) 30:95. doi: 10.1186/1756-9966-30-95

62. Ganeshan, K, and Chawla, A. Metabolic regulation of immune responses. *Annu Rev Immunol* (2014) 32:609–34. doi: 10.1146/annurev-immunol-032713-120236

63. Bowlin, TL, McKown, BJ, and Sunkara, PS. The effect of alpha-difluoromethylornithine, an inhibitor of polyamine biosynthesis, on mitogen-induced interleukin 2 production. *Immunopharmacology* (1987) 13:143–7. doi: 10.1016/0162-3109(87)90051-8

64. Bronte, V, and Zanovello, P. Regulation of immune responses by l-arginine metabolism. *Nat Rev Immunol* (2005) 5:641–54. doi: 10.1038/nri1668

65. Ye, C, Geng, Z, Dominguez, D, Chen, S, Fan, J, Qin, L, et al. Targeting ornithine decarboxylase by alpha-difluoromethylornithine inhibits tumor growth by impairing myeloid-derived suppressor cells. *J Immunol* (2016) 196:915–23. doi: 10.4049/jimmunol.1500729

66. Bowlin, TL, Hoeper, BJ, Rosenberger, AL, Davis, GF, and Sunkara, PS. Effects of three irreversible inhibitors of ornithine decarboxylase on macrophage-mediated tumoricidal activity and antitumor activity in B16f1 tumor-bearing mice. *Cancer Res* (1990) 50:4510–4.

67. Alexander, ET, Minton, A, Peters, MC, Phanstiel, O, and Gilmour, SK. A novel polyamine blockade therapy activates an anti-tumor immune response. *Oncotarget* (2017) 8:84140–52. doi: 10.18632/oncotarget.20493

68. Hayes, CS, Shicora, AC, Keough, MP, Snook, AE, Burns, MR, and Gilmour, SK. Polyamine-blocking therapy reverses immunosuppression in the tumor microenvironment. *Cancer Immunol Res* (2014) 2:274–85. doi: 10.1158/2326-6066.CIR-13-0120-T

69. Casero, RAJr., and Marton, LJ. Targeting polyamine metabolism and function in cancer and other hyperproliferative diseases. *Nat Rev Drug Discovery* (2007) 6:373–90. doi: 10.1038/nrd2243

70. Wallace, HM. The physiological role of the polyamines. *Eur J Clin Invest* (2000) 30:1–3. doi: 10.1046/j.1365-2362.2000.00585.x

71. Pegg, AE. Regulation of ornithine decarboxylase. *J Biol Chem* (2006) 281:14529–32. doi: 10.1074/jbc.R500031200

72. Pegg, AE. S-adenosylmethionine decarboxylase. *Essays Biochem* (2009) 46:25–45. doi: 10.1042/bse0460003

73. Raina, A, and Janne, J. Biosynthesis of putrescine: Characterization of ornithine decarboxylase from regenerating rat liver. *Acta Chem Scand* (1968) 22:2375–8. doi: 10.3891/acta.chem.scand.22-2375

74. Chiang, PK, Gordon, RK, Tal, J, Zeng, GC, Doctor, BP, Pardhasaradhi, K, et al. S-adenosylmethionine and methylation. *FASEB J* (1996) 10:471–80. doi: 10.1096/fasebj.10.4.8647346

75. Morales-Nebreda, L, McLafferty, FS, and Singer, BD. DNA Methylation as a transcriptional regulator of the immune system. *Transl Res* (2019) 204:1–18. doi: 10.1016/j.trsl.2018.08.001

76. Ikeguchi, Y, Bewley, MC, and Pegg, AE. Aminopropyltransferases: Function, structure and genetics. *J Biochem* (2006) 139:1–9. doi: 10.1093/jb/mvj019

77. Casero, RA, and Pegg, AE. Polyamine catabolism and disease. *Biochem J* (2009) 421:323–38. doi: 10.1042/BJ20090598

78. Pegg, AE. Spermidine/Spermine-N(1)-Acetyltransferase: A key metabolic regulator. *Am J Physiol Endocrinol Metab* (2008) 294:E995–1010. doi: 10.1152/ajpendo.90217.2008

79. Pegg, AE. Toxicity of polyamines and their metabolic products. *Chem Res Toxicol* (2013) 26:1782–800. doi: 10.1021/tx400316s

80. Poulin, R, Casero, RA, and Soulet, D. Recent advances in the molecular biology of metazoan polyamine transport. *Amino Acids* (2012) 42:711–23. doi: 10.1007/s00726-011-0987-y

81. Soulet, D, Gagnon, B, Rivest, S, Audette, M, and Poulin, R. A fluorescent probe of polyamine transport accumulates into intracellular acidic vesicles *via* a two-step mechanism. *J Biol Chem* (2004) 279:49355–66. doi: 10.1074/jbc.M401287200

82. Belting, M, Mani, K, Jonsson, M, Cheng, F, Sandgren, S, Jonsson, S, et al. Glypican-1 is a vehicle for polyamine uptake in mammalian cells: A pivital role for nitrosothiol-derived nitric oxide. *J Biol Chem* (2003) 278:47181–9. doi: 10.1074/jbc.M308325200

83. Kahana, C. Protein degradation, the main hub in the regulation of cellular polyamines. *Biochem J* (2016) 473:4551–58. doi: 10.1042/BCJ20160519C

84. Kahana, C. Regulation of cellular polyamine levels and cellular proliferation by antizyme and antizyme inhibitor. *Essays Biochem* (2009) 46:47–61. doi: 10.1042/bse0460004

85. Ivanov, IP, Gesteland, RF, and Atkins, JF. Antizyme expression: A subversion of triplet decoding, which is remarkably conserved by evolution, is a

sensor for an autoregulatory circuit. *Nucleic Acids Res* (2000) 28:3185–96. doi: 10.1093/nar/28.17.3185

86. Ivanov, IP, Gesteland, RF, and Atkins, JF. A second mammalian antizyme: Conservation of programmed ribosomal frameshifting. *Genomics* (1998) 52:119–29. doi: 10.1006/geno.1998.5434

87. Zhu, C, Lang, DW, and Coffino, P. Antizyme2 is a negative regulator of ornithine decarboxylase and polyamine transport. *J Biol Chem* (1999) 274:26425–30. doi: 10.1074/jbc.274.37.26425

88. Ivanov, IP, Rohrwasser, A, Terreros, DA, Gesteland, RF, and Atkins, JF. Discovery of a spermatogenesis stage-specific ornithine decarboxylase antizyme: Antizyme 3. *Proc Natl Acad Sci USA* (2000) 97:4808–13. doi: 10.1073/pnas.070055897

89. Tosaka, Y, Tanaka, H, Yano, Y, Masai, K, Nozaki, M, Yomogida, K, et al. Identification and characterization of testis specific ornithine decarboxylase antizyme (Oaz-T) gene: Expression in haploid germ cells and polyamine-induced frameshifting. *Genes Cells* (2000) 5:265–76. doi: 10.1046/j.1365-2443.2000.00324.x

90. Kahana, C. Antizyme and antizyme inhibitor, a regulatory tango. *Cell Mol Life Sci* (2009) 66:2479–88. doi: 10.1007/s00018-009-0033-3

91. Wu, HY, Chen, SF, Hsieh, JY, Chou, F, Wang, YH, Lin, WT, et al. Structural basis of antizyme-mediated regulation of polyamine homeostasis. *Proc Natl Acad Sci USA* (2015) 112:11229–34. doi: 10.1073/pnas.1508187112

92. Fujita, K, Murakami, Y, and Hayashi, S. A macromolecular inhibitor of the antizyme to ornithine decarboxylase. *Biochem J* (1982) 204:647–52. doi: 10.1042/bj2040647

93. Murakami, Y, Ichiba, T, Matsufuji, S, and Hayashi, S. Cloning of antizyme inhibitor, a highly homologous protein to ornithine decarboxylase. *J Biol Chem* (1996) 271:3340–2. doi: 10.1074/jbc.271.7.3340

94. Bercovich, Z, and Kahana, C. Degradation of antizyme inhibitor, an ornithine decarboxylase homologous protein, is ubiquitin-dependent and is inhibited by antizyme. *J Biol Chem* (2004) 279:54097–102. doi: 10.1074/jbc.M410234200

95. Ramos-Molina, B, Lambertos, A, and Penafiel, R. Antizyme inhibitors in polyamine metabolism and beyond: Physiopathological implications. *Med Sci (Basel)* (2018) 6. doi: 10.3390/medsci6040089

96. Lopez-Contreras, AJ, Ramos-Molina, B, Cremades, A, and Penafiel, R. Antizyme inhibitor 2 (Azin2/Odcp) stimulates polyamine uptake in mammalian cells. *J Biol Chem* (2008) 283:20761–9. doi: 10.1074/jbc.M801024200

97. Snapir, Z, Keren-Paz, A, Bercovich, Z, and Kahana, C. Odcp, a brain- and testis-specific ornithine decarboxylase paralogue, functions as an antizyme inhibitor, although less efficiently than Azi1. *Biochem J* (2008) 410:613–9. doi: 10.1042/BJ20071423

98. Mitchell, JL, Thane, TK, Sequeira, JM, Marton, LJ, and Thokala, R. Antizyme and antizyme inhibitor activities influence cellular responses to polyamine analogs. *Amino Acids* (2007) 33:291–7. doi: 10.1007/s00726-007-0523-2

99. Keren-Paz, A, Bercovich, Z, Porat, Z, Erez, O, Brener, O, and Kahana, C. Overexpression of antizyme-inhibitor in Nih3t3 fibroblasts provides growth advantage through neutralization of antizyme functions. *Oncogene* (2006) 25:5163–72. doi: 10.1038/sj.onc.1209521

100. Olsen, RR, and Zetter, BR. Evidence of a role for antizyme and antizyme inhibitor as regulators of human cancer. *Mol Cancer Res* (2011) 9:1285–93. doi: 10.1158/1541-7786.MCR-11-0178

101. Jung, MH, Kim, SC, Jeon, GA, Kim, SH, Kim, Y, Choi, KS, et al. Identification of differentially expressed genes in normal and tumor human gastric tissue. *Genomics* (2000) 69:281–6. doi: 10.1006/geno.2000.6338

102. Schaner, ME, Ross, DT, Ciaravino, G, Sorlie, T, Troyanskaya, O, Diehn, M, et al. Gene expression patterns in ovarian carcinomas. *Mol Biol Cell* (2003) 14:4376–86. doi: 10.1091/mbc.e03-05-0279

103. van Duin, M, van Marion, R, Vissers, K, Watson, JE, van Weerden, WM, Schroder, FH, et al. High-resolution array comparative genomic hybridization of chromosome arm 8q: Evaluation of genetic progression markers for prostate cancer. *Genes Chromosomes Cancer* (2005) 44:438–49. doi: 10.1002/gcc.20259

104. Peng, L, Guo, J, Zhang, Z, Liu, L, Cao, Y, Shi, H, et al. A candidate gene study for the association of host single nucleotide polymorphisms with liver cirrhosis risk in Chinese hepatitis b patients. *Genet Test Mol Biomarkers* (2013) 17:681–6. doi: 10.1089/gtmb.2013.0058

105. Silva, TM, Cirenajwis, H, Wallace, HM, Oredsson, S, and Persson, L. A role for antizyme inhibitor in cell proliferation. *Amino Acids* (2015) 47:1341–52. doi: 10.1007/s00726-015-1957-6

106. Fong, LY, Feith, DJ, and Pegg, AE. Antizyme overexpression in transgenic mice reduces cell proliferation, increases apoptosis, and reduces n-Nitrosomethylbenzylamine-Induced forestomach carcinogenesis. *Cancer Res* (2003) 63:3945–54.

107. Wei, Y, Zhang, H, Feng, Q, Wang, S, Shao, Y, Wu, J, et al. A novel mechanism for a-to-I rna-edited Azin1 in promoting tumor angiogenesis in colorectal cancer. *Cell Death Dis* (2022) 13:294. doi: 10.1038/s41419-022-04734-8

108. Li, R, Chung, AC, Dong, Y, Yang, W, Zhong, X, and Lan, HY. The microrna mir-433 promotes renal fibrosis by amplifying the tgf-Beta/Smad3-Azin1 pathway. *Kidney Int* (2013) 84:1129–44. doi: 10.1038/ki.2013.272

109. Teijeira, A, Garasa, S, Ochoa, MC, Villalba, M, Olivera, I, Cirella, A, et al. Il8, neutrophils, and nets in a collusion against cancer immunity and immunotherapy. *Clin Cancer Res* (2021) 27:2383–93. doi: 10.1158/1078-0432.CCR-20-1319

110. Harik, SI, and Sutton, CH. Putrescine as a biochemical marker of malignant brain tumors. *Cancer Res* (1979) 39:5010–5.

111. Farriol, M, Segovia-Silvestre, T, Castellanos, JM, Venereo, Y, and Orta, X. Role of putrescine in cell proliferation in a colon carcinoma cell line. *Nutrition* (2001) 17:934–8. doi: 10.1016/s0899-9007(01)00670-0

112. Liu, B, Jiang, X, Cai, L, Zhao, X, Dai, Z, Wu, G, et al. Putrescine mitigates intestinal atrophy through suppressing inflammatory response in weanling piglets. *J Anim Sci Biotechnol* (2019) 10:69. doi: 10.1186/s40104-019-0379-9

113. Zhang, X, Chen, Y, Hao, L, Hou, A, Chen, X, Li, Y, et al. Macrophages induce resistance to 5-fluorouracil chemotherapy in colorectal cancer through the release of putrescine. *Cancer Lett* (2016) 381:305–13. doi: 10.1016/j.canlet.2016.08.004

114. Susskind, BM, and Chandrasekaran, J. Inhibition of cytolytic T lymphocyte maturation with ornithine, arginine, and putrescine. *J Immunol* (1987) 139:905–12.

115. Childs, AC, Mehta, DJ, and Gerner, EW. Polyamine-dependent gene expression. *Cell Mol Life Sci* (2003) 60:1394–406. doi: 10.1007/s00018-003-2332-4

116. Eisenberg, T, Knauer, H, Schauer, A, Buttner, S, Ruckenstuhl, C, Carmona-Gutierrez, D, et al. Induction of autophagy by spermidine promotes longevity. *Nat Cell Biol* (2009) 11:1305–14. doi: 10.1038/ncb1975

117. Fan, J, Feng, Z, and Chen, N. Spermidine as a target for cancer therapy. *Pharmacol Res* (2020) 159:104943. doi: 10.1016/j.phrs.2020.104943

118. Adibhatla, RM, Hatcher, JF, Sailor, K, and Dempsey, RJ. Polyamines and central nervous system injury: Spermine and spermidine decrease following transient focal cerebral ischemia in spontaneously hypertensive rats. *Brain Res* (2002) 938:81–6. doi: 10.1016/s0006-8993(02)02447-2

119. Rider, JE, Hacker, A, Mackintosh, CA, Pegg, AE, Woster, PM, and Casero, RAJr. Spermine and spermidine mediate protection against oxidative damage caused by hydrogen peroxide. *Amino Acids* (2007) 33:231–40. doi: 10.1007/s00726-007-0513-4

120. Perez-Cano, FJ, Gonzalez-Castro, A, Castellote, C, Franch, A, and Castell, M. Influence of breast milk polyamines on suckling rat immune system maturation. *Dev Comp Immunol* (2010) 34:210–8. doi: 10.1016/j.dci.2009.10.001

121. Xu, TT, Li, H, Dai, Z, Lau, GK, Li, BY, Zhu, WL, et al. Spermidine and spermine delay brain aging by inducing autophagy in Samp8 mice. *Aging (Albany NY)* (2020) 12:6401–14. doi: 10.18632/aging.103035

122. Fischer, M, Ruhnau, J, Schulze, J, Obst, D, Floel, A, and Vogelgesang, A. Spermine and spermidine modulate T-cell function in older adults with and without cognitive decline ex vivo. *Aging (Albany NY)* (2020) 12:13716–39. doi: 10.18632/aging.103527

123. Cao, W, Wu, X, Jia, G, Zhao, H, Chen, X, Wu, C, et al. New insights into the role of dietary spermine on inflammation, immune function and related-signalling molecules in the thymus and spleen of piglets. *Arch Anim Nutr* (2017) 71:175–91. doi: 10.1080/1745039X.2017.1314610

124. Murray, PJ, and Wynn, TA. Protective and pathogenic functions of macrophage subsets. *Nat Rev Immunol* (2011) 11:723–37. doi: 10.1038/nri3073

125. Shapouri-Moghaddam, A, Mohammadian, S, Vazini, H, Taghadosi, M, Esmaeili, SA, Mardani, F, et al. Macrophage plasticity, polarization, and function in health and disease. *J Cell Physiol* (2018) 233:6425–40. doi: 10.1002/jcp.26429

126. Najafi, M, Hashemi Goradel, N, Farhood, B, Salehi, E, Nashtaei, MS, Khanlarkhani, N, et al. Macrophage polarity in cancer: A review. *J Cell Biochem* (2019) 120:2756–65. doi: 10.1002/jcb.27646

127. Lin, Y, Xu, J, and Lan, H. Tumor-associated macrophages in tumor metastasis: Biological roles and clinical therapeutic applications. *J Hematol Oncol* (2019) 12:76. doi: 10.1186/s13045-019-0760-3

128. Laoui, D, Movahedi, K, Van Overmeire, E, Van den Bossche, J, Schouppe, E, Mommer, C, et al. Tumor-associated macrophages in breast cancer: Distinct subsets, distinct functions. *Int J Dev Biol* (2011) 55:861–7. doi: 10.1387/ijdb.113371dl

129. Mantovani, A, Sozzani, S, Locati, M, Allavena, P, and Sica, A. Macrophage polarization: Tumor-associated macrophages as a paradigm for polarized M2 mononuclear phagocytes. *Trends Immunol* (2002) 23:549–55. doi: 10.1016/s1471-4906(02)02302-5

130. Zhang, M, He, Y, Sun, X, Li, Q, Wang, W, Zhao, A, et al. A high M1/M2 ratio of tumor-associated macrophages is associated with extended survival in ovarian cancer patients. *J Ovarian Res* (2014) 7:19. doi: 10.1186/1757-2215-7-19

131. Henze, AT, and Mazzone, M. The impact of hypoxia on tumor-associated macrophages. *J Clin Invest* (2016) 126:3672–79. doi: 10.1172/JCI84427

132. Hagemann, T, Lawrence, T, McNeish, I, Charles, KA, Kulbe, H, Thompson, RG, et al. "Re-educating" tumor-associated macrophages by targeting nf-kappab. *J Exp Med* (2008) 205:1261–8. doi: 10.1084/jem.20080108

133. Rutschman, R, Lang, R, Hesse, M, Ihle, JN, Wynn, TA, and Murray, PJ. Cutting edge: Stat6-dependent substrate depletion regulates nitric oxide production. *J Immunol* (2001) 166:2173–7. doi: 10.4049/jimmunol.166.4.2173

134. Kawanishi, N, Yano, H, Yokogawa, Y, and Suzuki, K. Exercise training inhibits inflammation in adipose tissue *via* both suppression of macrophage infiltration and acceleration of phenotypic switching from M1 to M2 macrophages in high-Fat-Diet-Induced obese mice. *Exerc Immunol Rev* (2010) 16:105–18.

135. Mylonas, KJ, Nair, MG, Prieto-Lafuente, L, Paape, D, and Allen, JE. Alternatively activated macrophages elicited by helminth infection can be reprogrammed to enable microbial killing. *J Immunol* (2009) 182:3084–94. doi: 10.4049/jimmunol.0803463

136. Stout, RD, Jiang, C, Matta, B, Tietzel, I, Watkins, SK, and Suttles, J. Macrophages sequentially change their functional phenotype in response to changes in microenvironmental influences. *J Immunol* (2005) 175:342–9. doi: 10.4049/jimmunol.175.1.342

137. Stout, RD, and Suttles, J. Functional plasticity of macrophages: Reversible adaptation to changing microenvironments. *J Leukoc Biol* (2004) 76:509–13. doi: 10.1189/jlb.0504272

138. Latour, YL, Gobert, AP, and Wilson, KT. The role of polyamines in the regulation of macrophage polarization and function. *Amino Acids* (2020) 52:151–60. doi: 10.1007/s00726-019-02719-0

139. Liu, R, Li, X, Ma, H, Yang, Q, Shang, Q, Song, L, et al. Spermidine endows macrophages anti-inflammatory properties by inducing mitochondrial superoxide-dependent ampk activation, hif-1alpha upregulation and autophagy. *Free Radic Biol Med* (2020) 161:339–50. doi: 10.1016/j.freeradbiomed.2020.10.029

140. Bussiere, FI, Chaturvedi, R, Cheng, Y, Gobert, AP, Asim, M, Blumberg, DR, et al. Spermine causes loss of innate immune response to helicobacter pylori by inhibition of inducible nitric-oxide synthase translation. *J Biol Chem* (2005) 280:2409–12. doi: 10.1074/jbc.C400498200

141. Zhou, S, Gu, J, Liu, R, Wei, S, Wang, Q, Shen, H, et al. Spermine alleviates acute liver injury by inhibiting liver-resident macrophage pro-inflammatory response through Atg5-dependent autophagy. *Front Immunol* (2018) 9:948. doi: 10.3389/fimmu.2018.00948

142. Monin, L, Griffiths, KL, Lam, WY, Gopal, R, Kang, DD, Ahmed, M, et al. Helminth-induced arginase-1 exacerbates lung inflammation and disease severity in tuberculosis. *J Clin Invest* (2015) 125:4699–713. doi: 10.1172/JCI77378

143. Singh, K, Coburn, LA, Asim, M, Barry, DP, Allaman, MM, Shi, C, et al. Ornithine decarboxylase in macrophages exacerbates colitis and promotes colitis-associated colon carcinogenesis by impairing M1 immune responses. *Cancer Res* (2018) 78:4303–15. doi: 10.1158/0008-5472.CAN-18-0116

144. Mai, S, Liu, L, Jiang, J, Ren, P, Diao, D, Wang, H, et al. Oesophageal squamous cell carcinoma-associated il-33 rewires macrophage polarization towards M2 *via* activating ornithine decarboxylase. *Cell Prolif* (2021) 54:e12960. doi: 10.1111/cpr.12960

145. Keyel, PA, Romero, M, Wu, W, Kwak, DH, Zhu, Q, Liu, X, et al. Methylthioadenosine reprograms macrophage activation through adenosine receptor stimulation. *PLoS One* (2014) 9:e104210. doi: 10.1371/journal.pone.0104210

146. Banchereau, J, and Steinman, RM. Dendritic cells and the control of immunity. *Nature* (1998) 392:245–52. doi: 10.1038/32588

147. Steinman, RM, and Banchereau, J. Taking dendritic cells into medicine. *Nature* (2007) 449:419–26. doi: 10.1038/nature06175

148. Steinman, RM. Decisions about dendritic cells: Past, present, and future. *Annu Rev Immunol* (2012) 30:1–22. doi: 10.1146/annurev-immunol-100311-102839

149. Schlitzer, A, McGovern, N, and Ginhoux, F. Dendritic cells and monocyte-derived cells: Two complementary and integrated functional systems. *Semin Cell Dev Biol* (2015) 41:9–22. doi: 10.1016/j.semcdb.2015.03.011

150. Diamond, MS, Kinder, M, Matsushita, H, Mashayekhi, M, Dunn, GP, Archambault, JM, et al. Type I interferon is selectively required by dendritic cells for immune rejection of tumors. *J Exp Med* (2011) 208:1989–2003. doi: 10.1084/jem.20101158

151. Fuertes, MB, Kacha, AK, Kline, J, Woo, SR, Kranz, DM, Murphy, KM, et al. Host type I ifn signals are required for antitumor Cd8+ T cell responses through Cd8{Alpha}+ dendritic cells. *J Exp Med* (2011) 208:2005–16. doi: 10.1084/jem.20101159

152. Fiorentino, DF, Zlotnik, A, Vieira, P, Mosmann, TR, Howard, M, Moore, KW, et al. Il-10 acts on the antigen-presenting cell to inhibit cytokine production by Th1 cells. *J Immunol* (1991) 146:3444–51.

153. Steinbrink, K, Wolfl, M, Jonuleit, H, Knop, J, and Enk, AH. Induction of tolerance by il-10-Treated dendritic cells. *J Immunol* (1997) 159:4772–80.

154. Hiltbold, EM, Vlad, AM, Ciborowski, P, Watkins, SC, and Finn, OJ. The mechanism of unresponsiveness to circulating tumor antigen Muc1 is a block in intracellular sorting and processing by dendritic cells. *J Immunol* (2000) 165:3730–41. doi: 10.4049/jimmunol.165.7.3730

155. Gabrilovich, DI, Ostrand-Rosenberg, S, and Bronte, V. Coordinated regulation of myeloid cells by tumours. *Nat Rev Immunol* (2012) 12:253–68. doi: 10.1038/nri3175

156. Parker, KH, Beury, DW, and Ostrand-Rosenberg, S. Myeloid-derived suppressor cells: Critical cells driving immune suppression in the tumor microenvironment. *Adv Cancer Res* (2015) 128:95–139. doi: 10.1016/bs.acr.2015.04.002

157. Ruffell, B, and Coussens, LM. Macrophages and therapeutic resistance in cancer. *Cancer Cell* (2015) 27:462–72. doi: 10.1016/j.ccell.2015.02.015

158. Mondanelli, G, Ugel, S, Grohmann, U, and Bronte, V. The immune regulation in cancer by the amino acid metabolizing enzymes arg and ido. *Curr Opin Pharmacol* (2017) 35:30–9. doi: 10.1016/j.coph.2017.05.002

159. Bronte, V, Serafini, P, Mazzoni, A, Segal, DM, and Zanovello, P. L-arginine metabolism in myeloid cells controls T-lymphocyte functions. *Trends Immunol* (2003) 24:302–6. doi: 10.1016/s1471-4906(03)00132-7

160. Gabrilovich, DI, and Nagaraj, S. Myeloid-derived suppressor cells as regulators of the immune system. *Nat Rev Immunol* (2009) 9:162–74. doi: 10.1038/nri2506

161. Lou, F, Sun, Y, Xu, Z, Niu, L, Wang, Z, Deng, S, et al. Excessive polyamine generation in keratinocytes promotes self-rna sensing by dendritic cells in psoriasis. *Immunity* (2020) 53:204–16 e10. doi: 10.1016/j.immuni.2020.06.004

162. Gervais, A, Leveque, J, Bouet-Toussaint, F, Burtin, F, Lesimple, T, Sulpice, L, et al. Dendritic cells are defective in breast cancer patients: A potential role for polyamine in this immunodeficiency. *Breast Cancer Res* (2005) 7:R326–35. doi: 10.1186/bcr1001

163. Mondanelli, G, Bianchi, R, Pallotta, MT, Orabona, C, Albini, E, Iacono, A, et al. A relay pathway between arginine and tryptophan metabolism confers immunosuppressive properties on dendritic cells. *Immunity* (2017) 46:233–44. doi: 10.1016/j.immuni.2017.01.005

164. Hasko, G, Kuhel, DG, Marton, A, Nemeth, ZH, Deitch, EA, and Szabo, C. Spermine differentially regulates the production of interleukin-12 P40 and interleukin-10 and suppresses the release of the T helper 1 cytokine interferon-gamma. *Shock* (2000) 14:144–9. doi: 10.1097/00024382-200014020-00012

165. Yuan, H, Wu, SX, Zhou, YF, and Peng, F. Spermidine inhibits joints inflammation and macrophage activation in mice with collagen-induced arthritis. *J Inflammation Res* (2021) 14:2713–21. doi: 10.2147/JIR.S313179

166. Steinbrink, K, Jonuleit, H, Muller, G, Schuler, G, Knop, J, and Enk, AH. Interleukin-10-Treated human dendritic cells induce a melanoma-Antigen-Specific anergy in Cd8(+) T cells resulting in a failure to lyse tumor cells. *Blood* (1999) 93:1634–42. doi: 10.1182/blood.V93.5.1634

167. Nicoletti, R, Venza, I, Ceci, G, Visalli, M, Teti, D, and Reibaldi, A. Vitreous polyamines spermidine, putrescine, and spermine in human proliferative disorders of the retina. *Br J Ophthalmol* (2003) 87:1038–42. doi: 10.1136/bjo.87.8.1038

168. Gabrilovich, D, Ishida, T, Oyama, T, Ran, S, Kravtsov, V, Nadaf, S, et al. Vascular endothelial growth factor inhibits the development of dendritic cells and dramatically affects the differentiation of multiple hematopoietic lineages *in vivo*. *Blood* (1998) 92:4150–66. doi: 10.1182/blood.V92.11.4150

169. Shi, Y, Yu, P, Zeng, D, Qian, F, Lei, X, Zhao, Y, et al. Suppression of vascular endothelial growth factor abrogates the immunosuppressive capability of murine gastric cancer cells and elicits antitumor immunity. *FEBS J* (2014) 281:3882–93. doi: 10.1111/febs.12923

170. Paardekooper, LM, Vos, W, and van den Bogaart, G. Oxygen in the tumor microenvironment: Effects on dendritic cell function. *Oncotarget* (2019) 10:883–96. doi: 10.18632/oncotarget.26608

171. Chougnet, CA, Thacker, RI, Shehata, HM, Hennies, CM, Lehn, MA, Lages, CS, et al. Loss of phagocytic and antigen cross-presenting capacity in aging dendritic cells is associated with mitochondrial dysfunction. *J Immunol* (2015) 195:2624–32. doi: 10.4049/jimmunol.1501006

172. Cubillos-Ruiz, JR, Silberman, PC, Rutkowski, MR, Chopra, S, Perales-Puchalt, A, Song, M, et al. Er stress sensor Xbp1 controls anti-tumor immunity by disrupting dendritic cell homeostasis. *Cell* (2015) 161:1527–38. doi: 10.1016/j.cell.2015.05.025

173. Chiossone, L, Dumas, PY, Vienne, M, and Vivier, E. Natural killer cells and other innate lymphoid cells in cancer. *Nat Rev Immunol* (2018) 18:671–88. doi: 10.1038/s41577-018-0061-z

174. Brigl, M, Tatituri, RV, Watts, GF, Bhowruth, V, Leadbetter, EA, Barton, N, et al. Innate and cytokine-driven signals, rather than microbial antigens, dominate in natural killer T cell activation during microbial infection. *J Exp Med* (2011) 208:1163–77. doi: 10.1084/jem.20102555

175. Huntington, ND, Vosshenrich, CA, and Di Santo, JP. Developmental pathways that generate natural-Killer-Cell diversity in mice and humans. *Nat Rev Immunol* (2007) 7:703–14. doi: 10.1038/nri2154

176. Wu, SY, Fu, T, Jiang, YZ, and Shao, ZM. Natural killer cells in cancer biology and therapy. *Mol Cancer* (2020) 19:120. doi: 10.1186/s12943-020-01238-x

177. Vivier, E, Raulet, DH, Moretta, A, Caligiuri, MA, Zitvogel, L, Lanier, LL, et al. Innate or adaptive immunity? the example of natural killer cells. *Science* (2011) 331:44–9. doi: 10.1126/science.1198687

178. Sun, JC, Beilke, JN, and Lanier, LL. Adaptive immune features of natural killer cells. *Nature* (2009) 457:557–61. doi: 10.1038/nature07665

179. Karre, K. Nk cells, mhc class I molecules and the missing self. *Scand J Immunol* (2002) 55:221–8. doi: 10.1046/j.1365-3083.2002.01053.x

180. Vitale, M, Cantoni, C, Pietra, G, Mingari, MC, and Moretta, L. Effect of tumor cells and tumor microenvironment on nk-cell function. *Eur J Immunol* (2014) 44:1582–92. doi: 10.1002/eji.201344272

181. Pegg, AE, and Feith, DJ. Polyamines and neoplastic growth. *Biochem Soc Trans* (2007) 35:295–9. doi: 10.1042/BST0350295

182. Janakiram, NB, Mohammed, A, Bryant, T, Zhang, Y, Brewer, M, Duff, A, et al. Potentiating nk cell activity by combination of rosuvastatin and difluoromethylornithine for effective chemopreventive efficacy against colon cancer. *Sci Rep* (2016) 6:37046. doi: 10.1038/srep37046

183. Urlaub, D, Hofer, K, Muller, ML, and Watzl, C. Lfa-1 activation in nk cells and their subsets: Influence of receptors, maturation, and cytokine stimulation. *J Immunol* (2017) 198:1944–51. doi: 10.4049/jimmunol.1601004

184. Soda, K, Kano, Y, Nakamura, T, Kasono, K, Kawakami, M, and Konishi, F. Spermine, a natural polyamine, suppresses lfa-1 expression on human lymphocyte. *J Immunol* (2005) 175:237–45. doi: 10.4049/jimmunol.175.1.237

185. Levin, AM, Bates, DL, Ring, AM, Krieg, C, Lin, JT, Su, L, et al. Exploiting a natural conformational switch to engineer an interleukin-2 'Superkine'. *Nature* (2012) 484:529–33. doi: 10.1038/nature10975

186. Flescher, E, Bowlin, TL, and Talal, N. Polyamine oxidation down-regulates il-2 production by human peripheral blood mononuclear cells. *J Immunol* (1989) 142:907–12.

187. Zhang, H, and Simon, AK. Polyamines reverse immune senescence *via* the translational control of autophagy. *Autophagy* (2020) 16:181–82. doi: 10.1080/15548627.2019.1687967

188. Wang, S, Xia, P, Huang, G, Zhu, P, Liu, J, Ye, B, et al. Foxo1-mediated autophagy is required for nk cell development and innate immunity. *Nat Commun* (2016) 7:11023. doi: 10.1038/ncomms11023

189. O'Sullivan, TE, Geary, CD, Weizman, OE, Geiger, TL, Rapp, M, Dorn, GW2nd, et al. Atg5 is essential for the development and survival of innate lymphocytes. *Cell Rep* (2016) 15:1910–9. doi: 10.1016/j.celrep.2016.04.082

190. O'Sullivan, TE, Johnson, LR, Kang, HH, and Sun, JC. Bnip3- and Bnip3l-mediated mitophagy promotes the generation of natural killer cell memory. *Immunity* (2015) 43:331–42. doi: 10.1016/j.immuni.2015.07.012

191. McEwen-Smith, RM, Salio, M, and Cerundolo, V. The regulatory role of invariant nkt cells in tumor immunity. *Cancer Immunol Res* (2015) 3:425–35. doi: 10.1158/2326-6066.CIR-15-0062

192. Terabe, M, and Berzofsky, JA. The role of nkt cells in tumor immunity. *Adv Cancer Res* (2008) 101:277–348. doi: 10.1016/S0065-230X(08)00408-9

193. Robertson, FC, Berzofsky, JA, and Terabe, M. Nkt cell networks in the regulation of tumor immunity. *Front Immunol* (2014) 5:543. doi: 10.3389/fimmu.2014.00543

194. Bendelac, A, Savage, PB, and Teyton, L. The biology of nkt cells. *Annu Rev Immunol* (2007) 25:297–336. doi: 10.1146/annurev.immunol.25.022106.141711

195. Rhost, S, Lofbom, L, Rynmark, BM, Pei, B, Mansson, JE, Teneberg, S, et al. Identification of novel glycolipid ligands activating a sulfatide-reactive, Cd1d-restricted, type ii natural killer T lymphocyte. *Eur J Immunol* (2012) 42:2851–60. doi: 10.1002/eji.201142350

196. Gapin, L, Godfrey, DI, and Rossjohn, J. Natural killer T cell obsession with self-antigens. *Curr Opin Immunol* (2013) 25:168–73. doi: 10.1016/j.coi.2013.01.002

197. Terabe, M, and Berzofsky, JA. The immunoregulatory role of type I and type ii nkt cells in cancer and other diseases. *Cancer Immunol Immunother* (2014) 63:199–213. doi: 10.1007/s00262-013-1509-4

198. Ambrosino, E, Terabe, M, Halder, RC, Peng, J, Takaku, S, Miyake, S, et al. Cross-regulation between type I and type ii nkt cells in regulating tumor immunity: A new immunoregulatory axis. *J Immunol* (2007) 179:5126–36. doi: 10.4049/jimmunol.179.8.5126

199. Kawano, T, Nakayama, T, Kamada, N, Kaneko, Y, Harada, M, Ogura, N, et al. Antitumor cytotoxicity mediated by ligand-activated human V Alpha24 nkt cells. *Cancer Res* (1999) 59:5102–5.

200. Coquet, JM, Kyparissoudis, K, Pellicci, DG, Besra, G, Berzins, SP, Smyth, MJ, et al. Il-21 is produced by nkt cells and modulates nkt cell activation and cytokine production. *J Immunol* (2007) 178:2827–34. doi: 10.4049/jimmunol.178.5.2827

201. Kitamura, H, Iwakabe, K, Yahata, T, Nishimura, S, Ohta, A, Ohmi, Y, et al. (Nkt) cell ligand alpha-galactosylceramide demonstrates its immunopotentiating effect by inducing interleukin (Il)-12 production by dendritic cells and il-12 receptor expression on nkt cells. *J Exp Med* (1999) 189:1121–8. doi: 10.1084/jem.189.7.1121

202. Fujii, S, Shimizu, K, Smith, C, Bonifaz, L, and Steinman, RM. Activation of natural killer T cells by alpha-galactosylceramide rapidly induces the full maturation of dendritic cells *in vivo* and thereby acts as an adjuvant for combined Cd4 and Cd8 T cell immunity to a coadministered protein. *J Exp Med* (2003) 198:267–79. doi: 10.1084/jem.20030324

203. Smyth, MJ, Wallace, ME, Nutt, SL, Yagita, H, Godfrey, DI, and Hayakawa, Y. Sequential activation of nkt cells and nk cells provides effective innate immunotherapy of cancer. *J Exp Med* (2005) 201:1973–85. doi: 10.1084/jem.20042280

204. Terabe, M, Matsui, S, Noben-Trauth, N, Chen, H, Watson, C, Donaldson, DD, et al. Nkt cell-mediated repression of tumor immunosurveillance by il-13 and the il-4r-Stat6 pathway. *Nat Immunol* (2000) 1:515–20. doi: 10.1038/82771

205. Van den Bossche, J, Lamers, WH, Koehler, ES, Geuns, JM, Alhonen, L, Uimari, A, et al. Pivotal advance: Arginase-1-Independent polyamine production stimulates the expression of il-4-Induced alternatively activated macrophage markers while inhibiting lps-induced expression of inflammatory genes. *J Leukoc Biol* (2012) 91:685–99. doi: 10.1189/jlb.0911453

206. Kronenberg, M, and Rudensky, A. Regulation of immunity by self-reactive T cells. *Nature* (2005) 435:598–604. doi: 10.1038/nature03725

207. Chen, J, Rao, JN, Zou, T, Liu, L, Marasa, BS, Xiao, L, et al. Polyamines are required for expression of toll-like receptor 2 modulating intestinal epithelial barrier integrity. *Am J Physiol Gastrointest Liver Physiol* (2007) 293:G568–76. doi: 10.1152/ajpgi.00201.2007

208. Bottino, C, Tambussi, G, Ferrini, S, Ciccone, E, Varese, P, Mingari, MC, et al. Two subsets of human T lymphocytes expressing Gamma/Delta antigen receptor are identifiable by monoclonal antibodies directed to two distinct molecular forms of the receptor. *J Exp Med* (1988) 168:491–505. doi: 10.1084/jem.168.2.491

209. Poggi, A, and Zocchi, MR. Gammadelta T lymphocytes as a first line of immune defense: Old and new ways of antigen recognition and implications for cancer immunotherapy. *Front Immunol* (2014) 5:575. doi: 10.3389/fimmu.2014.00575

210. Sciammas, R, Tatsumi, Y, Sperling, AI, Arunan, K, and Bluestone, JA. Tcr gamma delta cells: Mysterious cells of the immune system. *Immunol Res* (1994) 13:268–79. doi: 10.1007/BF02935618

211. Kozbor, D, Trinchieri, G, Monos, DS, Isobe, M, Russo, G, Haney, JA, et al. Human tcr-Gamma+/Delta+, Cd8+ T lymphocytes recognize tetanus toxoid in an mhc-restricted fashion. *J Exp Med* (1989) 169:1847–51. doi: 10.1084/jem.169.5.1847

212. Rust, CJ, and Koning, F. Gamma delta T cell reactivity towards bacterial superantigens. *Semin Immunol* (1993) 5:41–6. doi: 10.1006/smim.1993.1006

213. Todaro, M, D'Asaro, M, Caccamo, N, Iovino, F, Francipane, MG, Meraviglia, S, et al. Efficient killing of human colon cancer stem cells by gammadelta T lymphocytes. *J Immunol* (2009) 182:7287–96. doi: 10.4049/jimmunol.0804288

214. Aotsuka, A, Matsumoto, Y, Arimoto, T, Kawata, A, Ogishima, J, Taguchi, A, et al. Interleukin-17 is associated with expression of programmed cell death 1 ligand 1 in ovarian carcinoma. *Cancer Sci* (2019) 110:3068–78. doi: 10.1111/cas.14174

215. Li, X, Lu, H, Gu, Y, Zhang, X, Zhang, G, Shi, T, et al. Tim-3 suppresses the killing effect of Vgamma9vdelta2t cells on colon cancer cells by reducing perforin and granzyme b expression. *Exp Cell Res* (2020) 386:111719. doi: 10.1016/j.yexcr.2019.111719

216. Bekiaris, V, Sedy, JR, and Ware, CF. Mixing signals: Molecular turn ons and turn offs for innate gammadelta T-cells. *Front Immunol* (2014) 5:654. doi: 10.3389/fimmu.2014.00654

217. Capietto, AH, Martinet, L, Cendron, D, Fruchon, S, Pont, F, and Fournie, JJ. Phosphoantigens overcome human Tcrvgamma9+ gammadelta cell

immunosuppression by tgf-beta: Relevance for cancer immunotherapy. *J Immunol* (2010) 184:6680–7. doi: 10.4049/jimmunol.1000681

218. Van Acker, HH, Anguille, S, Willemen, Y, Van den Bergh, JM, Berneman, ZN, Lion, E, et al. Interleukin-15 enhances the proliferation, stimulatory phenotype, and antitumor effector functions of human gamma delta T cells. *J Hematol Oncol* (2016) 9:101. doi: 10.1186/s13045-016-0329-3

219. Fabre, J, Giustiniani, J, Garbar, C, Antonicelli, F, Merrouche, Y, Bensussan, A, et al. Targeting the tumor microenvironment: The protumor effects of il-17 related to cancer type. *Int J Mol Sci* (2016) 17:1433. doi: 10.3390/ijms17091433

220. Thedrez, A, Harly, C, Morice, A, Salot, S, Bonneville, M, and Scotet, E. Il-21-Mediated potentiation of antitumor cytolytic and proinflammatory responses of human V gamma 9v delta 2 T cells for adoptive immunotherapy. *J Immunol* (2009) 182:3423–31. doi: 10.4049/jimmunol.0803068

221. Kouakanou, L, Xu, Y, Peters, C, He, J, Wu, Y, Yin, Z, et al. Vitamin c promotes the proliferation and effector functions of human gammadelta T cells. *Cell Mol Immunol* (2020) 17:462–73. doi: 10.1038/s41423-019-0247-8

222. Schuller, AP, Wu, CC, Dever, TE, Buskirk, AR, and Green, R. Eif5a functions globally in translation elongation and termination. *Mol Cell* (2017) 66:194–205 e5. doi: 10.1016/j.molcel.2017.03.003

223. Puleston, DJ, Baixauli, F, Sanin, DE, Edwards-Hicks, J, Villa, M, Kabat, AM, et al. Polyamine metabolism is a central determinant of helper T cell lineage fidelity. *Cell* (2021) 184:4186–202 e20. doi: 10.1016/j.cell.2021.06.007

224. Wakita, D, Sumida, K, Iwakura, Y, Nishikawa, H, Ohkuri, T, Chamoto, K, et al. Tumor-infiltrating il-17-Producing gammadelta T cells support the progression of tumor by promoting angiogenesis. *Eur J Immunol* (2010) 40:1927–37. doi: 10.1002/eji.200940157

225. Ma, R, Yuan, D, Guo, Y, Yan, R, and Li, K. Immune effects of gammadelta T cells in colorectal cancer: A review. *Front Immunol* (2020) 11:1600. doi: 10.3389/fimmu.2020.01600

226. Liu, L, Santora, R, Rao, JN, Guo, X, Zou, T, Zhang, HM, et al. Activation of tgf-Beta-Smad signaling pathway following polyamine depletion in intestinal epithelial cells. *Am J Physiol Gastrointest Liver Physiol* (2003) 285:G1056–67. doi: 10.1152/ajpgi.00151.2003

227. Peters, C, Meyer, A, Kouakanou, L, Feder, J, Schricker, T, Lettau, M, et al. Tgf-beta enhances the cytotoxic activity of Vdelta2 T cells. *Oncoimmunology* (2019) 8:e1522471. doi: 10.1080/2162402X.2018.1522471

228. Fleming, C, Morrissey, S, Cai, Y, and Yan, J. Gammadelta T cells: Unexpected regulators of cancer development and progression. *Trends Cancer* (2017) 3:561–70. doi: 10.1016/j.trecan.2017.06.003

229. Hodi, FS, O'Day, SJ, McDermott, DF, Weber, RW, Sosman, JA, Haanen, JB, et al. Improved survival with ipilimumab in patients with metastatic melanoma. *N Engl J Med* (2010) 363:711–23. doi: 10.1056/NEJMoa1003466

230. Pitt, JM, Vetizou, M, Daillere, R, Roberti, MP, Yamazaki, T, Routy, B, et al. Resistance mechanisms to immune-checkpoint blockade in cancer: Tumor-intrinsic and -extrinsic factors. *Immunity* (2016) 44:1255–69. doi: 10.1016/j.immuni.2016.06.001

231. Alexander, ET, Mariner, K, Donnelly, J, Phanstiel, O, and Gilmour, SK. Polyamine blocking therapy decreases survival of tumor-infiltrating immunosuppressive myeloid cells and enhances the antitumor efficacy of pd-1 blockade. *Mol Cancer Ther* (2020) 19:2012–22. doi: 10.1158/1535-7163.MCT-19-1116

232. Finotello, F, and Trajanoski, Z. Quantifying tumor-infiltrating immune cells from transcriptomics data. *Cancer Immunol Immunother* (2018) 67:1031–40. doi: 10.1007/s00262-018-2150-z

233. Shimokawara, I, Imamura, M, Yamanaka, N, Ishii, Y, and Kikuchi, K. Identification of lymphocyte subpopulations in human breast cancer tissue and its significance: An immunoperoxidase study with anti-human T- and b-cell sera. *Cancer* (1982) 49:1456–64. doi: 10.1002/1097-0142(19820401)49:7<1456::aid-cncr2820490724>3.0.co;2-#

234. Hiratsuka, H, Imamura, M, Ishii, Y, Kohama, G, and Kikuchi, K. Immunohistologic detection of lymphocyte subpopulations infiltrating in human oral cancer with special reference to its clinical significance. *Cancer* (1984) 53:2456–66. doi: 10.1002/1097-0142(19840601)53:11<2456::aid-cncr2820531116>3.0.co;2-6

235. Hiratsuka, H, Imamura, M, Kasai, K, Kamiya, H, Ishii, Y, Kohama, G, et al. Lymphocyte subpopulations and T-cell subsets in human oral cancer tissues: Immunohistologic analysis by monoclonal antibodies. *Am J Clin Pathol* (1984) 81:464–70. doi: 10.1093/ajcp/81.4.464

236. Weber, EW, Maus, MV, and Mackall, CL. The emerging landscape of immune cell therapies. *Cell* (2020) 181:46–62. doi: 10.1016/j.cell.2020.03.001

237. Zajac, AJ, Blattman, JN, Murali-Krishna, K, Sourdive, DJ, Suresh, M, Altman, JD, et al. Viral immune evasion due to persistence of activated T cells without effector function. *J Exp Med* (1998) 188:2205–13. doi: 10.1084/jem.188.12.2205

238. Wherry, EJ, Blattman, JN, Murali-Krishna, K, van der Most, R, and Ahmed, R. Viral persistence alters Cd8 T-cell immunodominance and tissue distribution and results in distinct stages of functional impairment. *J Virol* (2003) 77:4911–27. doi: 10.1128/jvi.77.8.4911-4927.2003

239. Spranger, S, Spaapen, RM, Zha, Y, Williams, J, Meng, Y, Ha, TT, et al. Up-regulation of pd-L1, ido, and T(Regs) in the melanoma tumor microenvironment is driven by Cd8(+) T cells. *Sci Transl Med* (2013) 5:200ra116. doi: 10.1126/scitranslmed.3006504

240. Santana Carrero, RM, Beceren-Braun, F, Rivas, SC, Hegde, SM, Gangadharan, A, Plote, D, et al. Il-15 is a component of the inflammatory milieu in the tumor microenvironment promoting antitumor responses. *Proc Natl Acad Sci USA* (2019) 116:599–608. doi: 10.1073/pnas.1814642116

241. Finlay, D, and Cantrell, D. The coordination of T-cell function by Serine/Threonine kinases. *Cold Spring Harb Perspect Biol* (2011) 3:a002261. doi: 10.1101/cshperspect.a002261

242. Buck, MD, O'Sullivan, D, and Pearce, EL. T Cell metabolism drives immunity. *J Exp Med* (2015) 212:1345–60. doi: 10.1084/jem.20151159

243. Maciolek, JA, Pasternak, JA, and Wilson, HL. Metabolism of activated T lymphocytes. *Curr Opin Immunol* (2014) 27:60–74. doi: 10.1016/j.coi.2014.01.006

244. Bengsch, B, Johnson, AL, Kurachi, M, Odorizzi, PM, Pauken, KE, Attanasio, J, et al. Bioenergetic insufficiencies due to metabolic alterations regulated by the inhibitory receptor pd-1 are an early driver of Cd8(+) T cell exhaustion. *Immunity* (2016) 45:358–73. doi: 10.1016/j.immuni.2016.07.008

245. Gemta, LF, Siska, PJ, Nelson, ME, Gao, X, Liu, X, Locasale, JW, et al. Impaired enolase 1 glycolytic activity restrains effector functions of tumor-infiltrating Cd8(+) T cells. *Sci Immunol* (2019) 4:9520. doi: 10.1126/sciimmunol.aap9520

246. Wang, JJ, Siu, MK, Jiang, YX, Leung, TH, Chan, DW, Cheng, RR, et al. Aberrant upregulation of Pdk1 in ovarian cancer cells impairs Cd8(+) T cell function and survival through elevation of pd-L1. *Oncoimmunology* (2019) 8:e1659092. doi: 10.1080/2162402X.2019.1659092

247. Gerner, EW, and Meyskens, FLJr. Polyamines and cancer: Old molecules, new understanding. *Nat Rev Cancer* (2004) 4:781–92. doi: 10.1038/nrc1454

248. Flescher, E, Bowlin, TL, Ballester, A, Houk, R, and Talal, N. Increased polyamines may downregulate interleukin 2 production in rheumatoid arthritis. *J Clin Invest* (1989) 83:1356–62. doi: 10.1172/JCI114023

249. Flescher, E, Bowlin, TL, and Talal, N. Regulation of il-2 production by mononuclear cells from rheumatoid arthritis synovial fluids. *Clin Exp Immunol* (1992) 87:435–7. doi: 10.1111/j.1365-2249.1992.tb03015.x

250. Mandal, A, Das, S, Kumar, A, Roy, S, Verma, S, Ghosh, AK, et al. L-arginine uptake by cationic amino acid transporter promotes intra-macrophage survival of leishmania donovani by enhancing arginase-mediated polyamine synthesis. *Front Immunol* (2017) 8:839. doi: 10.3389/fimmu.2017.00839

251. Sawant, DV, Yano, H, Chikina, M, Zhang, Q, Liao, M, Liu, C, et al. Adaptive plasticity of il-10(+) and il-35(+) treg cells cooperatively promotes tumor T cell exhaustion. *Nat Immunol* (2019) 20:724–35. doi: 10.1038/s41590-019-0346-9

252. Jackaman, C, Bundell, CS, Kinnear, BF, Smith, AM, Filion, P, van Hagen, D, et al. Il-2 intratumoral immunotherapy enhances Cd8+ T cells that mediate destruction of tumor cells and tumor-associated vasculature: A novel mechanism for il-2. *J Immunol* (2003) 171:5051–63. doi: 10.4049/jimmunol.171.10.5051

253. Okumura, S, Teratani, T, Fujimoto, Y, Zhao, X, Tsuruyama, T, Masano, Y, et al. Oral administration of polyamines ameliorates liver Ischemia/Reperfusion injury and promotes liver regeneration in rats. *Liver Transpl* (2016) 22:1231–44. doi: 10.1002/lt.24471

254. Stoll, G, Pol, J, Soumelis, V, Zitvogel, L, and Kroemer, G. Impact of chemotactic factors and receptors on the cancer immune infiltrate: A bioinformatics study revealing homogeneity and heterogeneity among patient cohorts. *Oncoimmunology* (2018) 7:e1484980. doi: 10.1080/2162402X.2018.1484980

255. Philip, M, Fairchild, L, Sun, L, Horste, EL, Camara, S, Shakiba, M, et al. Chromatin states define tumour-specific T cell dysfunction and reprogramming. *Nature* (2017) 545:452–56. doi: 10.1038/nature22367

256. Zhang, M, Xia, L, Yang, Y, Liu, S, Ji, P, Wang, S, et al. Pd-1 blockade augments humoral immunity through icos-mediated Cd4(+) T cell instruction. *Int Immunopharmacol* (2019) 66:127–38. doi: 10.1016/j.intimp.2018.10.045

257. Nakkina, SP, Gitto, SB, Beardsley, JM, Pandey, V, Rohr, MW, Parikh, JG, et al. Dfmo improves survival and increases immune cell infiltration in association

with myc downregulation in the pancreatic tumor microenvironment. *Int J Mol Sci* (2021) 22:13175. doi: 10.3390/ijms222413175

258. Dryja, P, Fisher, C, Woster, PM, and Bartee, E. Inhibition of polyamine biosynthesis using difluoromethylornithine acts as a potent immune modulator and displays therapeutic synergy with pd-1-Blockade. *J Immunother* (2021) 44:283–91. doi: 10.1097/cji.0000000000000379

259. Jacobson, KA, Tosh, DK, Jain, S, and Gao, ZG. Historical and current adenosine receptor agonists in preclinical and clinical development. *Front Cell Neurosci* (2019) 13:124. doi: 10.3389/fncel.2019.00124

260. Young, A, Ngiow, SF, Barkauskas, DS, Sult, E, Hay, C, Blake, SJ, et al. Co-Inhibition of Cd73 and A2ar adenosine signaling improves anti-tumor immune responses. *Cancer Cell* (2016) 30:391–403. doi: 10.1016/j.ccell.2016.06.025

261. Beavis, PA, Henderson, MA, Giuffrida, L, Mills, JK, Sek, K, Cross, RS, et al. Targeting the adenosine 2a receptor enhances chimeric antigen receptor T cell efficacy. *J Clin Invest* (2017) 127:929–41. doi: 10.1172/JCI89455

262. Draper-Joyce, CJ, Khoshouei, M, Thal, DM, Liang, YL, Nguyen, ATN, Furness, SGB, et al. Structure of the adenosine-bound human adenosine A1 receptor-gi complex. *Nature* (2018) 558:559–63. doi: 10.1038/s41586-018-0236-6

263. Yan, K, Gao, LN, Cui, YL, Zhang, Y, and Zhou, X. The cyclic amp signaling pathway: Exploring targets for successful drug discovery (Review). *Mol Med Rep* (2016) 13:3715–23. doi: 10.3892/mmr.2016.5005

264. Li, K, Zhang, H, Qiu, J, Lin, Y, Liang, J, Xiao, X, et al. Activation of cyclic adenosine monophosphate pathway increases the sensitivity of cancer cells to the oncolytic virus M1. *Mol Ther* (2016) 24:156–65. doi: 10.1038/mt.2015.172

265. Ma, H, Li, Q, Wang, J, Pan, J, Su, Z, and Liu, S. Dual inhibition of ornithine decarboxylase and A1 adenosine receptor efficiently suppresses breast tumor cells. *Front Oncol* (2021) 11:636373. doi: 10.3389/fonc.2021.636373

266. Mastelic-Gavillet, B, Navarro Rodrigo, B, Decombaz, L, Wang, H, Ercolano, G, Ahmed, R, et al. Adenosine mediates functional and metabolic suppression of peripheral and tumor-infiltrating Cd8(+) T cells. *J Immunother Cancer* (2019) 7:257. doi: 10.1186/s40425-019-0719-5

267. Mosmann, TR, Cherwinski, H, Bond, MW, Giedlin, MA, and Coffman, RL. Two types of murine helper T cell clone. i. definition according to profiles of lymphokine activities and secreted proteins. *J Immunol* (1986) 136:2348–57.

268. Veldhoen, M, Uyttenhove, C, van Snick, J, Helmby, H, Westendorf, A, Buer, J, et al. Transforming growth factor-beta 'Reprograms' the differentiation of T helper 2 cells and promotes an interleukin 9-producing subset. *Nat Immunol* (2008) 9:1341–6. doi: 10.1038/ni.1659

269. Harrington, LE, Hatton, RD, Mangan, PR, Turner, H, Murphy, TL, Murphy, KM, et al. Interleukin 17-producing Cd4+ effector T cells develop *via* a lineage distinct from the T helper type 1 and 2 lineages. *Nat Immunol* (2005) 6:1123–32. doi: 10.1038/ni1254

270. Zhu, J, Jankovic, D, Oler, AJ, Wei, G, Sharma, S, Hu, G, et al. The transcription factor T-bet is induced by multiple pathways and prevents an endogenous Th2 cell program during Th1 cell responses. *Immunity* (2012) 37:660–73. doi: 10.1016/j.immuni.2012.09.007

271. Zhu, J, Yamane, H, and Paul, WE. Differentiation of effector Cd4 T cell populations (*). *Annu Rev Immunol* (2010) 28:445–89. doi: 10.1146/annurev-immunol-030409-101212

272. Wei, L, Vahedi, G, Sun, HW, Watford, WT, Takatori, H, Ramos, HL, et al. Discrete roles of Stat4 and Stat6 transcription factors in tuning epigenetic modifications and transcription during T helper cell differentiation. *Immunity* (2010) 32:840–51. doi: 10.1016/j.immuni.2010.06.003

273. Carriche, GM, Almeida, L, Stuve, P, Velasquez, L, Dhillon-LaBrooy, A, Roy, U, et al. Regulating T-cell differentiation through the polyamine spermidine. *J Allergy Clin Immunol* (2021) 147:335–48 e11. doi: 10.1016/j.jaci.2020.04.037

274. Liakou, CI, Kamat, A, Tang, DN, Chen, H, Sun, J, Troncoso, P, et al. Ctla-4 blockade increases ifngamma-producing Cd4+Icoshi cells to shift the ratio of effector to regulatory T cells in cancer patients. *Proc Natl Acad Sci USA* (2008) 105:14987–92. doi: 10.1073/pnas.0806075105

275. Wei, SC, Sharma, R, Anang, NAS, Levine, JH, Zhao, Y, Mancuso, JJ, et al. Negative Co-stimulation constrains T cell differentiation by imposing boundaries on possible cell states. *Immunity* (2019) 50:1084–98.e10. doi: 10.1016/j.immuni.2019.03.004

276. Rudd, CE, and Schneider, H. Unifying concepts in Cd28, icos and Ctla4 Co-receptor signalling. *Nat Rev Immunol* (2003) 3:544–56. doi: 10.1038/nri1131

277. Hutloff, A, Dittrich, AM, Beier, KC, Eljaschewitsch, B, Kraft, R, Anagnostopoulos, I, et al. Icos is an inducible T-cell Co-stimulator structurally and functionally related to Cd28. *Nature* (1999) 397:263–6. doi: 10.1038/16717

278. Xiao, Z, Mayer, AT, Nobashi, TW, and Gambhir, SS. Icos is an indicator of T-Cell-Mediated response to cancer immunotherapy. *Cancer Res* (2020) 80:3023–32. doi: 10.1158/0008-5472.CAN-19-3265

279. Wei, SC, Anang, NAS, Sharma, R, Andrews, MC, Reuben, A, Levine, JH, et al. Combination anti-Ctla-4 plus anti-Pd-1 checkpoint blockade utilizes cellular mechanisms partially distinct from monotherapies. *Proc Natl Acad Sci USA* (2019) 116:22699–709. doi: 10.1073/pnas.1821218116

280. Nishikawa, H, and Sakaguchi, S. Regulatory T cells in tumor immunity. *Int J Cancer* (2010) 127:759–67. doi: 10.1002/ijc.25429

281. Shevach, EM. Mechanisms of Foxp3+ T regulatory cell-mediated suppression. *Immunity* (2009) 30:636–45. doi: 10.1016/j.immuni.2009.04.010

282. Raimondi, G, Turner, MS, Thomson, AW, and Morel, PA. Naturally occurring regulatory T cells: Recent insights in health and disease. *Crit Rev Immunol* (2007) 27:61–95. doi: 10.1615/critrevimmunol.v27.i1.50

283. Roncarolo, MG, Bacchetta, R, Bordignon, C, Narula, S, and Levings, MK. Type 1 T regulatory cells. *Immunol Rev* (2001) 182:68–79. doi: 10.1034/j.1600-065x.2001.1820105.x

284. Tan, MC, Goedegebuure, PS, Belt, BA, Flaherty, B, Sankpal, N, Gillanders, WE, et al. Disruption of Ccr5-dependent homing of regulatory T cells inhibits tumor growth in a murine model of pancreatic cancer. *J Immunol* (2009) 182:1746–55. doi: 10.4049/jimmunol.182.3.1746

285. Whiteside, TL. Clinical impact of regulatory T cells (Treg) in cancer and hiv. *Cancer Microenviron* (2015) 8:201–7. doi: 10.1007/s12307-014-0159-1

286. Facciabene, A, Motz, GT, and Coukos, G. T-Regulatory cells: Key players in tumor immune escape and angiogenesis. *Cancer Res* (2012) 72:2162–71. doi: 10.1158/0008-5472.CAN-11-3687

287. Facciabene, A, Peng, X, Hagemann, IS, Balint, K, Barchetti, A, Wang, LP, et al. Tumour hypoxia promotes tolerance and angiogenesis *via* Ccl28 and T(Reg) cells. *Nature* (2011) 475:226–30. doi: 10.1038/nature10169

288. Katsuno, Y, Lamouille, S, and Derynck, R. Tgf-beta signaling and epithelial-mesenchymal transition in cancer progression. *Curr Opin Oncol* (2013) 25:76–84. doi: 10.1097/CCO.0b013e32835b6371

289. Hesterberg, RS, Cleveland, JL, and Epling-Burnette, PK. Role of polyamines in immune cell functions. *Med Sci (Basel)* (2018) 6:22. doi: 10.3390/medsci6010022

290. Wagner, A, Wang, C, Fessler, J, DeTomaso, D, Avila-Pacheco, J, Kaminski, J, et al. Metabolic modeling of single Th17 cells reveals regulators of autoimmunity. *Cell* (2021) 184:4168–85.e21. doi: 10.1016/j.cell.2021.05.045

291. Yang, Y, Bazhin, AV, Werner, J, and Karakhanova, S. Reactive oxygen species in the immune system. *Int Rev Immunol* (2013) 32:249–70. doi: 10.3109/08830185.2012.755176

292. Yarosz, EL, and Chang, CH. The role of reactive oxygen species in regulating T cell-mediated immunity and disease. *Immune Netw* (2018) 18:e14. doi: 10.4110/in.2018.18.e14

293. Efimova, O, Szankasi, P, and Kelley, TW. Ncf1 (P47phox) is essential for direct regulatory T cell mediated suppression of Cd4+ effector T cells. *PLoS One* (2011) 6:e16013. doi: 10.1371/journal.pone.0016013

294. Kim, HR, Lee, A, Choi, EJ, Hong, MP, Kie, JH, Lim, W, et al. Reactive oxygen species prevent imiquimod-induced psoriatic dermatitis through enhancing regulatory T cell function. *PLoS One* (2014) 9:e91146. doi: 10.1371/journal.pone.0091146

295. Novo, E, Busletta, C, Bonzo, LV, Povero, D, Paternostro, C, Mareschi, K, et al. Intracellular reactive oxygen species are required for directional migration of resident and bone marrow-derived hepatic pro-fibrogenic cells. *J Hepatol* (2011) 54:964–74. doi: 10.1016/j.jhep.2010.09.022

296. Proietti, E, Rossini, S, Grohmann, U, and Mondanelli, G. Polyamines and kynurenines at the intersection of immune modulation. *Trends Immunol* (2020) 41:1037–50. doi: 10.1016/j.it.2020.09.007

297. Qu, N, Ignatenko, NA, Yamauchi, P, Stringer, DE, Levenson, C, Shannon, P, et al. Inhibition of human ornithine decarboxylase activity by enantiomers of difluoromethylornithine. *Biochem J* (2003) 375:465–70. doi: 10.1042/BJ20030382

298. Danzin, C, Casara, P, Claverie, N, Metcalf, BW, and Jung, MJ. (2r,5r)-6-Heptyne-2,5-Diamine, an extremely potent inhibitor of mammalian ornithine decarboxylase. *Biochem Biophys Res Commun* (1983) 116:237–43. doi: 10.1016/0006-291x(83)90406-0

299. Mamont, PS, Duchesne, MC, Grove, J, and Bey, P. Anti-proliferative properties of dl-Alpha-Difluoromethyl ornithine in cultured cells. a consequence of the irreversible inhibition of ornithine decarboxylase. *Biochem Biophys Res Commun* (1978) 81:58–66. doi: 10.1016/0006-291x(78)91630-3

300. Burns, MR, Graminski, GF, Weeks, RS, Chen, Y, and O'Brien, TG. Lipophilic lysine-spermine conjugates are potent polyamine transport inhibitors for use in combination with a polyamine biosynthesis inhibitor. *J Med Chem* (2009) 52:1983–93. doi: 10.1021/jm801580w

301. Gopal, M, Padayatchi, N, Metcalfe, JZ, and O'Donnell, MR. Systematic review of clofazimine for the treatment of drug-resistant tuberculosis. *Int J Tuberc Lung Dis* (2013) 17:1001–7. doi: 10.5588/ijtld.12.0144

302. Smith, CS, Aerts, A, Saunderson, P, Kawuma, J, Kita, E, and Virmond, M. Multidrug therapy for leprosy: A game changer on the path to elimination. *Lancet Infect Dis* (2017) 17:e293–e97. doi: 10.1016/S1473-3099(17)30418-8

303. Leanza, L, Henry, B, Sassi, N, Zoratti, M, Chandy, KG, Gulbins, E, et al. Inhibitors of mitochondrial Kv1.3 channels induce Bax/Bak-independent death of cancer cells. *EMBO Mol Med* (2012) 4:577–93. doi: 10.1002/emmm.201200235

304. Zaccagnino, A, Manago, A, Leanza, L, Gontarewitz, A, Linder, B, Azzolini, M, et al. Tumor-reducing effect of the clinically used drug clofazimine in a scid mouse model of pancreatic ductal adenocarcinoma. *Oncotarget* (2017) 8:38276–93. doi: 10.18632/oncotarget.11299

305. Durusu, IZ, Husnugil, HH, Atas, H, Biber, A, Gerekci, S, Gulec, EA, et al. Anti-cancer effect of clofazimine as a single agent and in combination with cisplatin on U266 multiple myeloma cell line. *Leuk Res* (2017) 55:33–40. doi: 10.1016/j.leukres.2017.01.019

306. Koval, AV, Vlasov, P, Shichkova, P, Khunderyakova, S, Markov, Y, Panchenko, J, et al. Anti-leprosy drug clofazimine inhibits growth of triple-negative breast cancer cells *via* inhibition of canonical wnt signaling. *Biochem Pharmacol* (2014) 87:571–8. doi: 10.1016/j.bcp.2013.12.007

307. Van Rensburg, CE, Van Staden, AM, and Anderson, R. The riminophenazine agents clofazimine and B669 inhibit the proliferation of cancer cell lines *in vitro* by phospholipase A2-mediated oxidative and nonoxidative mechanisms. *Cancer Res* (1993) 53:318–23.

308. Sechi, AM, Cabrini, L, Landi, L, Pasquali, P, and Lenaz, G. Inhibition of phospholipase A2 and phospholipase c by polyamines. *Arch Biochem Biophys* (1978) 186:248–54. doi: 10.1016/0003-9861(78)90433-2

309. Bianchi-Smiraglia, A, Bagati, A, Fink, EE, Affronti, HC, Lipchick, BC, Moparthy, S, et al. Inhibition of the aryl hydrocarbon Receptor/Polyamine biosynthesis axis suppresses multiple myeloma. *J Clin Invest* (2018) 128:4682–96. doi: 10.1172/JCI70712

frontiers | Frontiers in Immunology

TYPE Original Research
PUBLISHED 23 September 2022
DOI 10.3389/fimmu.2022.933241



OPEN ACCESS

EDITED BY
Yuyan Wang,
Beijing Cancer Hospital, China

REVIEWED BY
Di Yu,
Uppsala University, Sweden
Yona Keisari,
Tel Aviv University, Israel

*CORRESPONDENCE
Huihuang Li
lhhuang1994@163.com
Zhenghao Li
lizhenghao@csu.edu.cn

SPECIALTY SECTION
This article was submitted to Cancer Immunity and Immunotherapy, a section of the journal Frontiers in Immunology

RECEIVED 30 April 2022
ACCEPTED 22 August 2022
PUBLISHED 23 September 2022

CITATION
Cai Z, He Y', Yu Z, Hu J, Xiao Z, Zu X, Li Z and Li H (2022) Cuproptosis-related modification patterns depict the tumor microenvironment, precision immunotherapy, and prognosis of kidney renal clear cell carcinoma. *Front. Immunol.* 13:933241. doi: 10.3389/fimmu.2022.933241



# Cuproptosis-related modification patterns depict the tumor microenvironment, precision immunotherapy, and prognosis of kidney renal clear cell carcinoma

Zhiyong Cai[1], You'e He[2], Zhengzheng Yu[3], Jiao Hu[1], Zicheng Xiao[1], Xiongbing Zu[1], Zhenghao Li[4]* and Huihuang Li[1]*

[1]Department of Urology, Xiangya Hospital, Central South University, Changsha, China, [2]National Clinical Research Center for Geriatric Disorder, Xiangya Hospital, Central South University, Changsha, China, [3]Research Center of Carcinogenesis and Targeted Therapy, Xiangya Hospital, Central South University, Changsha, China, [4]Hunan Provincial Key Laboratory of Hepatobiliary Disease Research and Division of Hepato-Biliary-Pancreatic Surgery, Department of General Surgery, The Second Xiangya Hospital, Central South University, Changsha, China

**Background:** Due to the different infiltration abundance of immune cells in tumor, the efficacy of immunotherapy varies widely among individuals. Recently, growing evidence suggested that cuproptosis has impact on cancer immunity profoundly. However, the comprehensive roles of cuproptosis-related genes in tumor microenvironment (TME) and in response to immunotherapy are still unclear.

**Methods:** Based on 43 cuproptosis-related genes, we employed unsupervised clustering to identify cuproptosis-related patterns and single-sample gene set enrichment analysis algorithm to build a cuproptosis signature for individual patient's immune cell infiltration and efficacy of immune checkpoint blockade (ICB) evaluation. Then, the cuproptosis-related genes were narrowed down using univariate Cox regression model and least absolute shrinkage and selection operator algorithm. Finally, a cuproptosis risk score was built by random survival forest based on these narrowed-down genes.

**Results:** Two distinct cuproptosis-related patterns were developed, with cuproptosis cluster 1 showing better prognosis and higher enrichment of immune-related pathways and infiltration of immune cells. For individual evaluation, the cuproptosis signature that we built could be used not only for predicting immune cell infiltration in TME but also for evaluating an individual's sensitivity to ICBs. Patients with higher cuproptosis signature scores exhibited more activated cancer immune processes, higher immune cell infiltration, and better curative efficacy of ICBs. Furthermore, a robust cuproptosis risk score indicated that patients with higher risk scores showed worse survival

outcomes, which could be validated in internal and external validation cohorts. Ultimately, a nomogram which combined the risk score with the prognostic clinical factors was developed, and it showed excellent prediction accuracy for survival outcomes.

**Conclusion:** Distinct cuproptosis-related patterns have significant differences on prognosis and immune cell infiltration in kidney renal clear cell carcinoma (KIRC). Cuproptosis signature and risk score are able to provide guidance for precision therapy and accurate prognosis prediction for patients with KIRC.

KEYWORDS

cuproptosis, KIRC, tumor microenvironment, immunotherapy, prognosis

# Introduction

Kidney renal clear cell carcinoma (KIRC) is the most common malignant tumor in renal cell carcinoma (RCC) (1). It is estimated that over 75,000 cases occur and that 13,000 patients die each year (2). Although the prognosis of localized KIRC is favorable, the 5-year overall survival (OS) rate is lower than 10% in metastatic KIRC (mKIRC) (3). Recently, immunotherapy, especially immune checkpoint inhibitors (ICB), has achieved brilliant efficacy in mKIRC individuals (4). The CheckMate 214 clinical trial has reported that intermediate-risk and poor-risk patients can benefit more from ICB treatment than targeted therapy (5). However, only a proportion of patients can produce an anti-tumor response (6). Hence, it is urgent to find a predictor which can guide clinicians for ICB application.

The tumor microenvironment (TME) is a complicated tissue environment, which consists of various immune cells, stromal cells, and noncellular components (7). Hence, there is a large heterogeneity in the TME. According to the infiltration levels of tumor-fighting effector cells and inflammatory cytokines, the TME can be sorted into inflamed type and non-inflamed type in brief (8). Meanwhile, several large-scale studies have demonstrated that the abundance of pre-existing infiltrated immune cells determines the efficacy of ICB therapy (9–12).

Cuproptosis, a brand-new concept which is defined as copper-dependent cell death, is accompanied with elevated mitochondrial-dependent energy metabolism and accumulation of reactive oxygen species (ROS) (13). Intriguingly, several studies reported that cuproptosis-related genes, such as ATOX1 and CP, can affect the progression of cancer (14, 15). More importantly, Voli et al. found that the variation of copper transporter 1 has influence on the expression of programmed cell death 1 ligand 1 (PD-L1) and the infiltration quantity of $CD8^+$T cells and NK cells in the TME (16). However, all these studies merely focused on one or two cuproptosis-related genes and their roles in the TME. A comprehensive analysis of multiple cuproptosis-related genes and their roles in assessing the TME, efficacy of ICB, and prognosis in KIRC is lacking. So, we systematically correlated cuproptosis-related genes with the TME as well as their sensitivity to immunotherapy in KIRC for the first time.

# Methods

## Data collection and processing

The high-throughput sequencing data of mRNA, clinically associated data, and survival data of The Cancer Genome Atlas (TCGA)-KIRC (526 samples) were downloaded from UCSC Xena (http://xena.ucsc.edu/) (17). The expression matrix of mRNA was transformed from fragments per kilobase per million mapped fragments to transcripts per kilobase million. As an external validation set, the E-MTAB-1980 KIRC cohort (101 samples) was downloaded from ArrayExpress (https://www.ebi.ac.uk/arrayexpress/). Furthermore, as our previous study has reported (18), 46 renal cell carcinoma samples were collected from our hospital and named the Xiangya-RCC cohort.

Immunotherapy cohorts were downloaded from the study of Gide et al. (PMID30753825 cohort, anti-PD-1 or combined anti-PD-1 with anti-CTLA-4) (19), the study of Kim et al. (PMID30013197, anti-PD-1/PD-L1) (20), the study of Allen et al. (PMID26359337, anti-CTLA-4) (21), GSE35640 (MAGE-A3 immunotherapy), GSE111636 (anti-PD-1 immunotherapy), GSE126044 (anti-PD-1 treatment), GSE173839 (anti-PD-L1 treatment), and GSE135222 (anti-PD-1/PD-L1 treatment).

## Unsupervised clustering for cuproptosis-related patterns

Forty-three cuproptosis-related genes were selected from the review of Chang et al. (13) (Supplementary Table S1). Consensus clustering algorithm (maxK = 5, reps = 1,000, pItem = 0.8, distance = "manhattan", clusterAIg = "pam") was employed to judge the quantity and stability of clusters based on these genes (ConsensuClusterPlus R package) (22).

## Differentially expressed genes and functional analysis

Limma R package was used to screen differentially expressed genes (DEGs) between cuproptosis-related patterns, and the screen criteria were set as |log fold change| >1 and adjusted *p*-value <0.05.

Gene Ontology (GO) and Kyoto Encyclopedia of Genes and Genomes (KEGG) analysis were conducted using Gene Set Enrichment Analysis (GSEA) algorithm in GSVA R package. The gmt files "c2.cp.kegg.v6.2.symbols.gmt" and "h.all.v7.2.symbols.gmt" were downloaded from the molecular signature database (http://www.gsea-msigdb.org/gsea/msigdb). |Normalized enrichment score| >1 and adjusted *p*-value <0.05 were used as criteria for significant enrichment.

## Description of the tumor immune characteristics of KIRC and construction of the cuproptosis signature

We described the TME of KIRC in five aspects: Firstly, seven steps of cancer immunity cycle were analyzed by using the Tracking Tumor Immunophenotype website (http://biocc.hrbmu.edu.cn/TIP/) (23). Secondly, cell markers of tumor-infiltrating leukocytes (TILs) were downloaded from the study of Charoentong (24), and infiltration of TILs was calculated using single-sample gene set enrichment analysis (ssGSEA) algorithm. A cuproptosis signature was also generated using ssGSEA based on 43 cuproptosis-related genes. In order to eliminate the effects of different algorithms, another three algorithms for immune cell calculation, including MCP, Quantiseq, and TIMER, were also applied. Thirdly, the effector genes of immune cells were gathered from our previous study (25). Fourthly, 22 inhibitory immune checkpoints were assembled from the study of Auslander et al. (26). Finally, T cell inflamed score (TIS) was employed to evaluate the potential response probability to ICB (25).

## Analysis of scRNA-seq cohort

Seven single-cell RNA sequencing (scRNA-seq) count matrixes of KIRC were downloaded from the supplemental material of GSE159115 (27). We then converted the seven matrixes into Seurat objects using the CreateSeuratObject function (Seurat R package, version 4.1.1). Single cells with less than 1,000 UMIs or less than 200 genes or with a value of $\log_{10}$ genes per UMI less than 0.70 or more than 20% mitochondrion-derived UMI counts were regarded as low-quality cells and filtered out for further analysis. Based on the top 3,000 variable genes, we then integrated seven samples into one Seurat object using the IntegrateData function in Seurat to eliminate batch effects. We then identified the main cell clusters using the FindClusters function in Seurat (resolution = 0.4) and visualized these cell clusters using uniform manifold approximation and projection. The cell clusters were first recognized using SingleR R package, and then the cell types were confirmed based on the markers obtained from previous studies (27, 28).

## Construction and validation of the cuproptosis risk score

A total of 43 cuproptosis-related genes were used to screen genes possessing univariate prognostic values by univariate Cox analysis. These prognostic genes were further narrowed down by least absolute shrinkage and selection operator (LASSO) regression with minimal lambda (0.05). Subsequently, a cuproptosis risk score was constructed using the "rfsrc" function in "randomForestSRC" R package based on the expression of these genes.

Individuals in the TCGA-KIRC cohort were randomly divided into training and internal validation cohorts in a 7:3 ratio, while the E-MTAB-1980 KIRC cohort was set as the external validation cohort. According to the median value of risk score, we classified individuals into high-risk group and low-risk group. Kaplan–Meier (K–M) survival curve and log-rank test were employed to compare the prognosis difference between two groups by survminer R package. In additional, tROC R package was used to estimate the prediction reliability of risk score.

## Establishment of a nomogram

Univariate Cox analyses, along with multivariate Cox analyses, were employed to filter the independent impact factor in cohorts. Then, rms R package was applied to establish the nomogram. Subsequently, calibration curves and

time-dependent receiver operating characteristic curves were used to estimate the clinical relevance and prediction accuracy, respectively.

## Statistical analysis

*T*-test or Mann–Whitney *U*-test was employed to compare the continuous variables between two groups. Chi-square test or fisher exact test was used to compare differences between groups with dichotomous variables. Pearson or Spearman correlation analysis was conducted to assess the relation between different factors. $P$ <0.05 was set as criterion for judging a significant difference. Two-side statistical tests were used. R software (version 4.1.3) was applied throughout the analysis.

# Results

## Development of cuproptosis-related patterns

On the basis of the 43 cuproptosis-related genes, their mRNA expression levels were compared between tumor tissues and adjacent normal tissues in the TCGA-KIRC cohort (Figure 1A). We found that 32 genes showed significant differences on RNA expression, containing ATOX1, ATP7B, CCS, CD274, CP, LOXL2, MAP2K2, PDK1, SCO2, SLC31A2, TYR, UBE2D2, ULK1, VEGFA, and so on. Next, a univariate Cox analysis was employed to filter cuproptosis-related genes with prognostic value and found 21 genes with a significant prognostic value (Figure 1B, Supplementary Figure S1, Supplementary Table S2), including SCO2, MT2A, DBH, CCL8, MT1G, MT1X, MT-CO2, MT1F and so on. To explore the interaction probability among cuproptosis-related genes, a comprehensive correlation analysis was implemented and found intimate interactions among them (Figure 1C). Therefore, an unsupervised clustering analysis was conducted based on cuproptosis-related genes and found two distinct clusters (Supplementary Figure S2), which were named as cuproptosis-related patterns. Furthermore, 362 individuals and 164 individuals were divided into cluster 1 and cluster 2, respectively. As shown in Figure 1D, cluster 1 has a better survival outcome than cluster 2 ($p$ = 0.019). The distribution of clinical features (age, gender, tumor grade, and tumor stage) and the distinct expression modes between two patterns were displayed in a heat map (Figure 1E).

## Expression patterns of cuproptosis-related genes on the single-cell level

Seven samples from seven KIRC patients were involved in this analysis. After quality control, a total of 20,900 single cells were included for further analysis. As shown in Figure 2A, these cells could be classified into 15 main cell clusters. Then, these cell clusters were recognized based on the cell markers reported in previous studies: cancer cells ("NDUFA4L2", "CA9", "SLC17A3", and "NNMT") (Supplementary Figure S3A), endothelial cells ("KDR", "PECAM1", "ESM1", and "PLVAP") (Supplementary Figure S3B), vascular smooth muscle (VSM) cells ("ACTA2", "PDGFRB", "CNN1", and "MYH11") (Supplementary Figure S3C), macrophage cells ("LYZ", "CD68", "CD163", and "HLA-DRA") (Supplementary Figure S3D), T cells ("CD3D", "CD3E", and "CD3G") (Supplementary Figure S3E), B cells ("CD79A") (Supplementary Figure S3F), and mast cells ("TPSAB1", "CPA3", and "MS4A2") (Supplementary Figure S3G) (27, 28). In addition to cancer cells, two kinds of normal cell types, including endothelial and VSM cells, and four kinds of immune cell types, including macrophage, T cells, B cells, and mast cells, were identified (Figure 2B). We divided these cell types into cancer cells and non-cancer cells and compared the expression patterns of cuproptosis-related genes (Supplementary Figure S4A, Supplementary Table S3). A majority of cuproptosis-related genes like CP, MT1E, MT1F, MT1X, VEGFA, and PDK1 were expressed significantly higher on cancer cells (Figures 2C–H), indicating that cuproptosis might occur mainly on cancer cells. However, the detailed mechanism needs to be further explored *in vivo* and *in vitro*.

## Functional enrichment analysis and cancer immunity assessment of cuproptosis-based patterns

On account of significant difference in prognosis between two patterns, we intended to explore the underlying mechanism. DEGs were displayed in a heat map and a volcano plot (Supplementary Figures S4B, C, Supplementary Table S4). Surprisingly, there were several immune-related genes, such as ST8SIA6, CNTN1, KCNK2, F13A1, MTRNR2L12, PVALB, MT-ATP8, and KLK3. Friedman et al. reported that the overexpression of ST8SIA6 can change tumor growth by suppressing the immune response (29). Lin et al. demonstrated that a varied expression of KCNK2 can affect the infiltration of immune cells (30). Consequently, these findings inferred that cuproptosis-related patterns link with immune-related pathways.

According to the fold change value of all genes in TCGA-KIRC between two patterns, GSEA algorithm was employed to ascertain the detailed enrichment pathways. GO analysis indicated that the pathways of chemokine activity, chemokine production, response to chemokine, and positive regulation of chemokine production were significantly activated in cluster 1 (Figure 3A, Supplementary Table S5). Furthermore, GO analysis also revealed that the activity of pathways of T cell migration, T cell activation, T cell differentiation, regulation of T cell activation, and T cell differentiation in thymus were enhanced

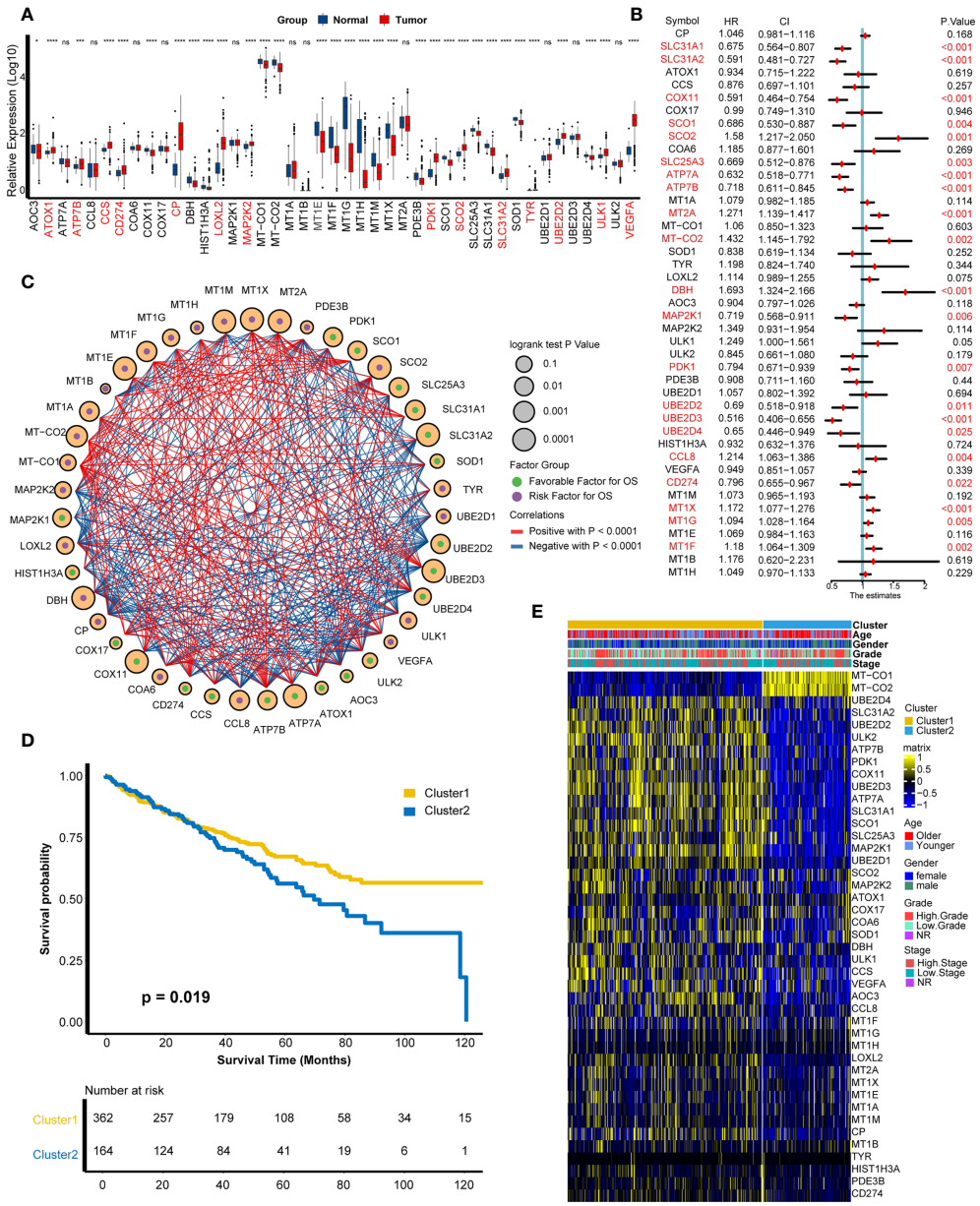


FIGURE 1
Development of cuproptosis-related patterns. **(A)** Expression of cuproptosis-related genes in tumors and adjacent normal tissues. **(B)** Prognostic analysis of cuproptosis-related genes using univariate Cox regression. **(C)** Correlation analysis among cuproptosis-related genes. The size of the circle represented the *p*-value of overall survival, the green and purple dots in the circle meant favorable and risk factor in prognosis, and the red and blue lines that connected two circles meant positive and negative regulating relationships, respectively. **(D)** Survival outcome between two patterns. **(E)** Distribution of clinical features (age, gender, grade, and stage) and expression matrix of cuproptosis-related patterns. *p < 0.05, ***p < 0.001, ****p < 0.0001; ns, not statistically significant.

in cluster 1 (Figure 3B, Supplementary Table S5). KEGG analysis exhibited that the activities of chemokine signaling pathways and cytokine–cytokine receptor interaction signaling pathways were significantly upregulated in cluster 1 (Figure 3C, Supplementary Table S6). These findings indicated that individuals in cluster 1 had a more vibrant tumor-fighting process than those in cluster 2.

The cancer immunity cycle, containing the initiation of tumor immunity to killing cancer cells by infiltrated T cells (31, 32), acts a critical part in the TME. It was of great interest to us

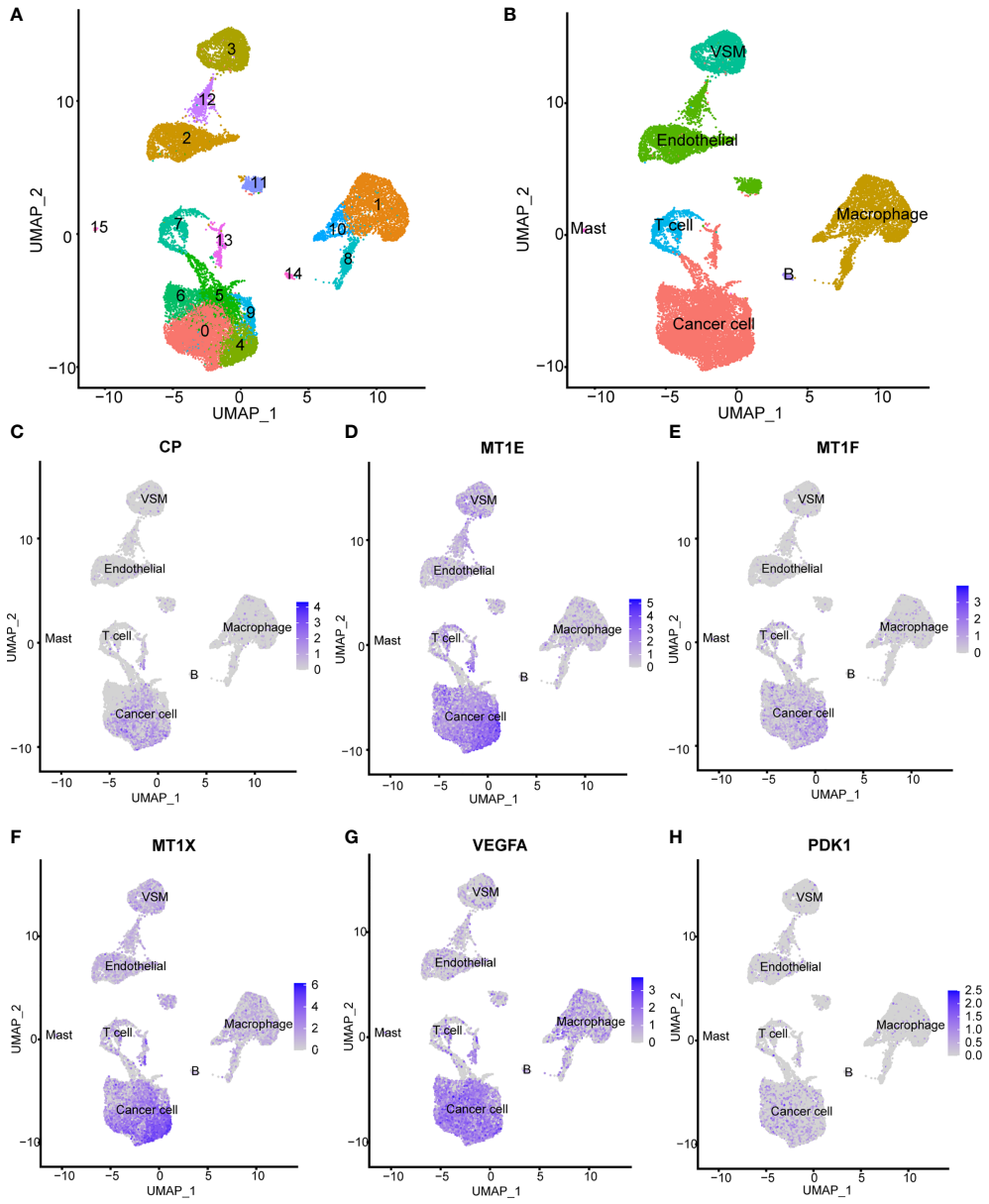


FIGURE 2
Expression patterns of cuproptosis-related genes on the single-cell level. **(A)** Fifteen main cell clusters in the scRNA KIRC cohort. **(B)** Six recognized cell types based on previous cell markers: cancer cells, endothelial cells, vascular smooth muscle cells, T cells, B cells, and macrophage cells. **(C–H)** Selected cuproptosis-related genes were expressed significantly higher in cancer cells: CP, MT1E, MT1F, MT1X, VEGFA, and PDK1.

whether there are differences in cancer immunity steps between two patterns. As expected, cluster 1 showed a more active process than cluster 2, including recognition of cancer antigen, initiating response of immune cells, T cell recruiting, and killing cancer cell by TILs (Figure 3D). The outcome can infer that cluster 1 probably represents an inflamed type of the TME and produces a better response to immunotherapy (33, 34). Hence, the infiltration levels of various immune cells in the TME were compared between two patterns through four independent algorithms (ssGSEA, MCP, Quantiseq, and TIMER). Consistently, cluster 1 had a higher infiltration level of TILs than cluster 2, containing $CD4^+$T cells, $CD8^+$T cells, myeloid dendritic cells, macrophage cells, monocytes, B cells, and neutrophils (Figure 3D). The result demonstrated that two cuproptosis-related patterns represent two types of the TME: inflamed TME and non-inflamed type.

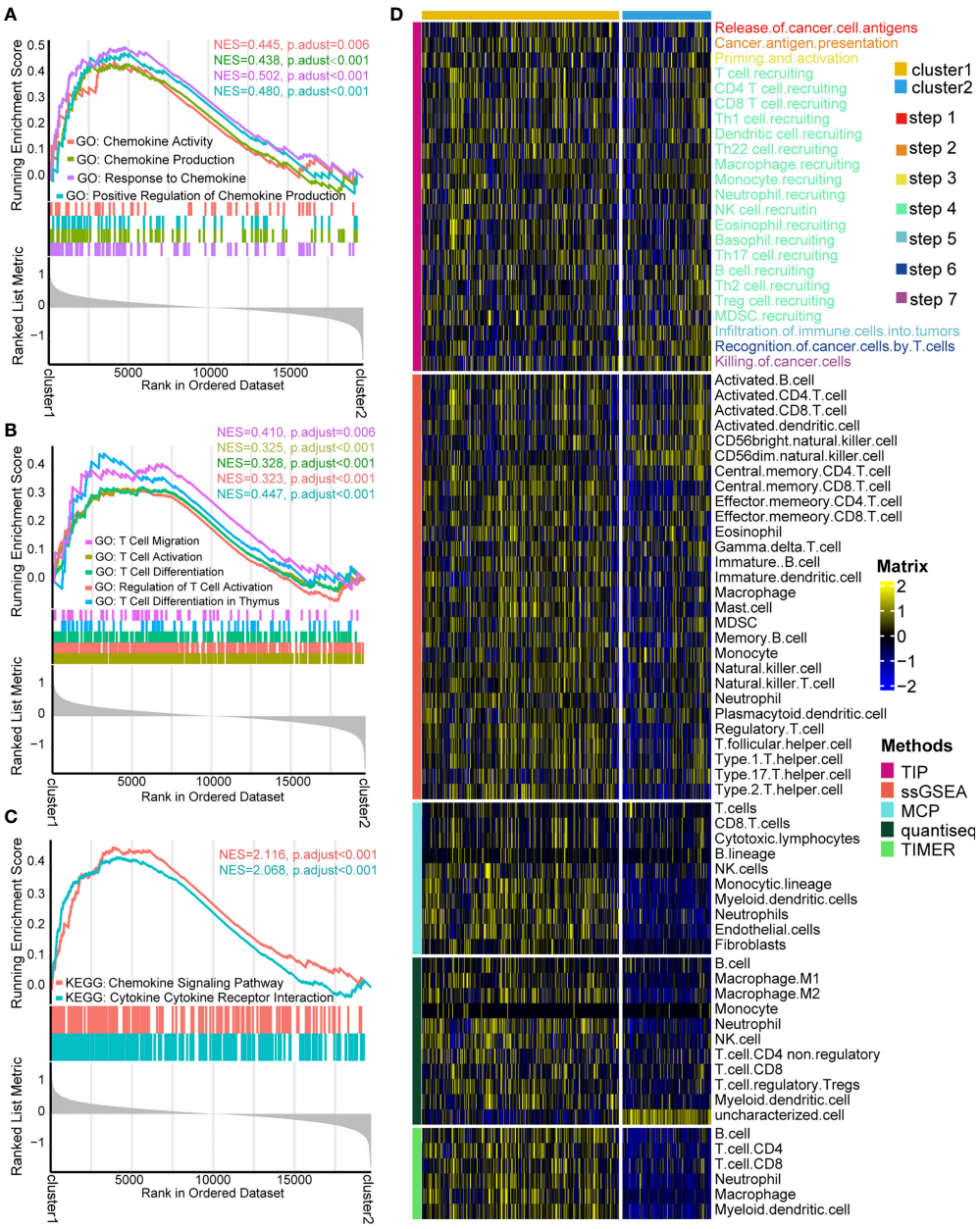


FIGURE 3
Functional enrichment analysis and cancer immunity assessment of cuproptosis-based patterns. **(A)** Gene Ontology (GO) functional enrichment analysis of chemokine-related pathways. **(B)** GO functional enrichment analysis of T cell-related pathways. **(C)** Kyoto Encyclopedia of Genes and Genomes functional enrichment analysis of cytokine/chemokine-related signaling pathways. **(D)** Expression matrix of cancer immunity cycles and tumor-infiltrating leukocytes between two patterns.

## Estimating the infiltration level of TILs and the efficacy of ICB on individuals by cuproptosis signature

Although cuproptosis-related patterns played an essential role on distinguishing the infiltration level of TILs in the whole cohort, the patterns lacked the ability to evaluate an individual patient's TME status. Consequently, we constructed a cuproptosis signature based on these 43 cuproptosis-related genes by ssGSEA algorithm to estimate the abundance of TILs and the efficacy of ICB for individual patients.

Interestingly, the cuproptosis signature was significantly positively related to major steps of the cancer immunity cycle both in the TCGA-KIRC cohort and the Xiangya-RCC cohort

(Figure 4A, Supplementary Tables S7, S8), including release of tumor antigen, recognition of tumor cell by T cell, and recruitment of diverse immune cells (T cell, macrophage, neutrophil, and Th17). To validate this finding, the cuproptosis signature was directly associated with infiltration of TILs in the TCGA-KIRC cohort and the Xiangya-RCC cohort.

In line with a previous outcome, the cuproptosis signature showed a significantly positive connection to infiltration of TILs (Figures 4B, C, Supplementary Tables S9, S10), containing gamma delta T cell, activated $CD8^+$ T cell, activated dendritic cell, activated B cell, natural killer T cell, type 1 T helper cell (Th1 cell), type 2 T helper cell (Th2 cell), and

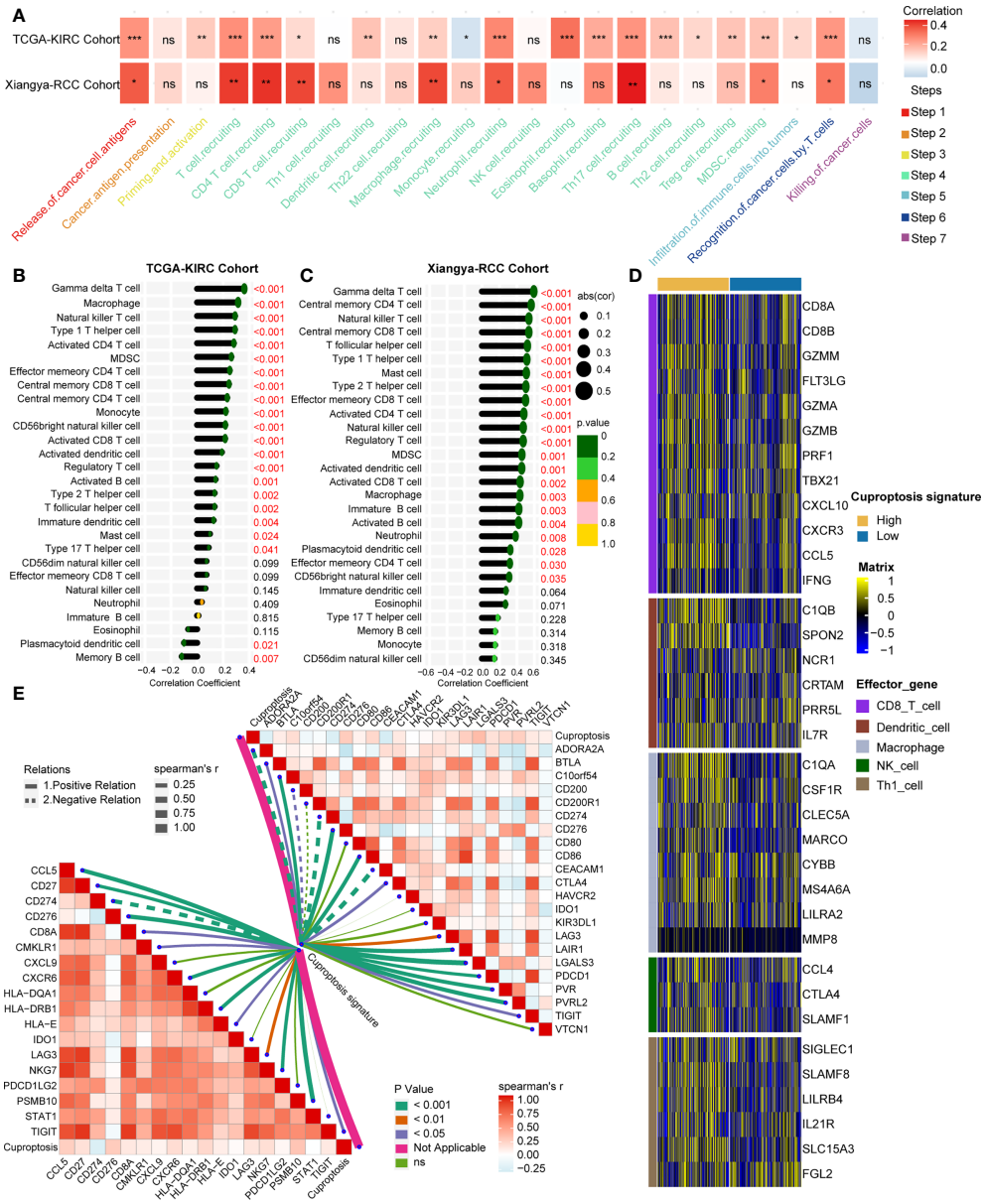


FIGURE 4
Estimated infiltration level of tumor-infiltrating leukocytes (TILs) and efficacy of immune checkpoint blockade on individuals by cuproptosis signature. **(A)** Correlation analysis on cuproptosis signature and cancer immunity steps in the TCGA-KIRC and Xiangya-RCC cohorts. *$p < 0.05$, **$p < 0.01$, ***$p < 0.001$; ns, not statistically significant. **(B, C)** Correlation analysis on cuproptosis signature and TILs in the TCGA-KIRC and Xiangya-RCC cohorts. **(D)** Expression matrix of TILs ($CD8^+$T cell, dendritic cell, macrophage cell, NK cell, and Th1 cell in the high- and low-score signature groups. **(E)** Correlation analysis on cuproptosis signature and T cell inflamed score (left) and inhibitory immune checkpoints (right). The solid and dotted lines represent positive and negative connections, respectively; the thickness of the lines represents the coefficient of the relations; and the diverse colors of the lines represent the *p*-values of the relations.

so on. Meanwhile, we compared the effector genes of main TILs ($CD8^+$T cell, dendritic cell, macrophage cell, NK cell, and Th1 cell) between high- and low-cuproptosis-signature groups. As anticipated, the effector genes of TILs were expressed higher in the high-score signature group (Figure 4D). These findings demonstrated that cuproptosis signature is capable of assessing the level of infiltrated immune cells on individuals.

It is widely thought that inflamed TME is the foundation of producing a response to immunotherapy (35, 36). Therefore, TIS, which can predict the efficacy of immunotherapy (37, 38) along with inhibitory immune checkpoints, was further studied. A total of 18 TLS-related genes and 22 ICB-associated genes were collected and were used to correlate with the cuproptosis signature. Collectively, the signature showed significant positive relations with TIS and inhibitory immune checkpoints (Figure 4E, Supplementary Tables S11, S12), from which it can be inferred that the cuproptosis signature has the capacity to predict the efficacy of immunotherapy.

## Direct comparison of ICBs' efficacy in multiple immunotherapy cohorts

Despite the fact that we evaluated an individual's efficacy of ICB by cuproptosis signature, it is necessary to directly compare the curative effect of ICB cohorts in the high- and low-score-signature group. Hence, eight immunotherapy cohorts were included in our study. In the PMID30753825 cohort, a 93.75% response rate occurred in the high-score group compared to 37.5% in the low-score group ($p < 0.001$) (Figure 5A). In the GSE35640 cohort, the response rate ratio was 50 *versus* 12.5% between two groups ($p = 0.029$) (Figure 5B). Although there were no significant differences between the two groups in the other six cohorts (GSE124044, GSE111636, GSE173839, GSE135222, PMID30013197, and PMID26359337), patients with a high score showed a better curative effect (Figures 5C–H). These findings further demonstrated that cuproptosis signature is qualified to forecast the efficacy of ICB and provide guidance for the precise application of immunotherapy.

## Assessing the prognosis of individuals using cuproptosis risk score

Then, we developed and validated a robust cuproptosis risk score for predicting the survival outcome of an individual. LASSO algorithm was used to select the optimal candidate genes. As a result, seven candidate genes (SLC31A2, SCO2, MT2A, DBH, UBE2D3, CCL8, and MT1X) with minimal lambda (0.05) were chosen from the 43 cuproptosis-associated genes (Figures 6A, B). Subsequently, the cuproptosis risk score was built using the "rfsrc" function in "randomForestSRC" R package, and the risk score was significantly positively correlated with cuproptosis signature (Supplementary Figure S5A).

On the basis of the median value of the risk score, individuals were divided into a high-risk group and a low-risk group. In the TCGA training cohort, the high-risk group comprised more death cases and worse survival probability ($p < 0.0001$) than the low-risk group (Figures 6C, D). Moreover, the prediction accuracy of the survival outcomes at 12, 36, and 60 months were 0.84, 0.82, and 0.80, respectively (Figure 6E). In the TCGA internal validation cohort, the survival status and the survival probability ($p = 0.00027$) between the two groups were in accordance with the outcomes of the TCGA training cohort (Figures 6F, G). The area under the curve (AUC) of the survival outcomes at 12, 36, and 60 months were 0.66, 0.60, and 0.67, respectively (Figure 6H). Importantly, in the external validation cohort (E-MTAB-1980), individuals in the low-risk group manifested better survival status and survival probability ($p = 0.0019$) in comparison with the high-risk group (Figures 6I, J). The prediction accuracy of prognosis at 12, 36, and 60 months were 0.82, 0.75, and 0.74, respectively (Figure 6K). In line with the outcome that patients with a high cuproptosis risk score exhibited a worse OS, patients with higher tumor grade and stage had a significantly higher risk score (Supplementary Figures S5B, C). However, there were no differences on risk score between different ages and genders (Supplementary Figures S5D, E). All these results demonstrated that cuproptosis risk score can precisely foretell the prognosis of a KIRC individual.

## Development of a nomogram for better forecasting survival outcome in clinical practice

In order to improve the prediction accuracy of OS in clinical practice, we developed a nomogram incorporating the cuproptosis risk score and the essential clinical characteristics. In the TCGA-KIRC cohort, univariate Cox regression was used to select the prognostic factors. Except for gender ($p = 0.73$), other indicators had a significant prognostic value ($p < 0.001$) (Figure 7A). Then, multivariate Cox regression was applied to identify the independent prognostic factors. Cuproptosis risk score ($p < 0.001$), age ($p = 0.002$), and tumor stage ($p < 0.001$) were eligible (Figure 7B) and incorporated into a nomogram (Figure 7C). By means of calibration curves, the predicted probability values of OS at 1 year (Figure 7D), 3 years (Figure 7E), and 5 years (Figure 7F) were similar with the actual probability OS, which demonstrated that the nomogram has a crucial clinical value. Additionally, we compared the prediction accuracy between nomogram, cuproptosis risk score, age, and stage, respectively. The outcome indicated that the nomogram is the most precise tool to predict OS at 1 year (AUC = 0.87), 3 years (AUC = 0.84), and 5 years (AUC = 0.82) (Figures 7G–I).

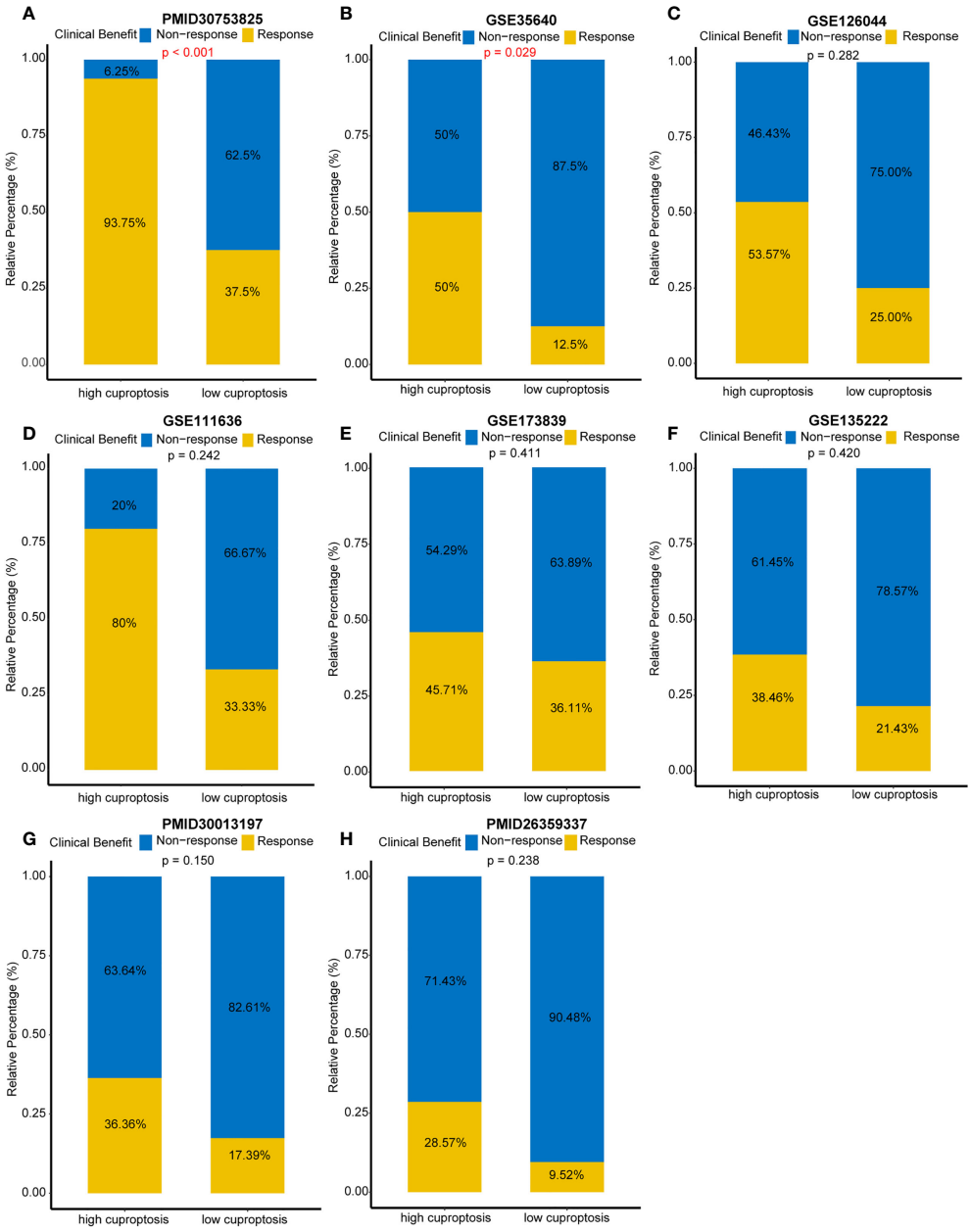


FIGURE 5
Direct comparison of immune checkpoint blockades' efficacy in multiple immunotherapy cohorts. **(A)** Response rates between different cuproptosis signature groups in the PMID30753825 cohort. **(B)** Response rates between different cuproptosis signature groups in the GSE35640 cohort. **(C–H)** Response rates between different cuproptosis signature groups in the GSE126044, GSE111636, GSE173839, GSE135222, PMID30013197, and PMID26359337 cohorts, respectively.

# Discussion

Copper is the essential element for cell proliferation and cell death. Meanwhile, it is also the necessary cofactor for enzymes and transporters (39). Dysfunction of copper metabolism will cause a cytotoxic effect and an oxidative stress response in various types of cells (40, 41). Hence, we defined copper-dependent cell proliferation as cuproplasia. In contrast, copper-dependent cell death is defined as cuproptosis, whose mechanism probably is to increase the energy metabolism of the

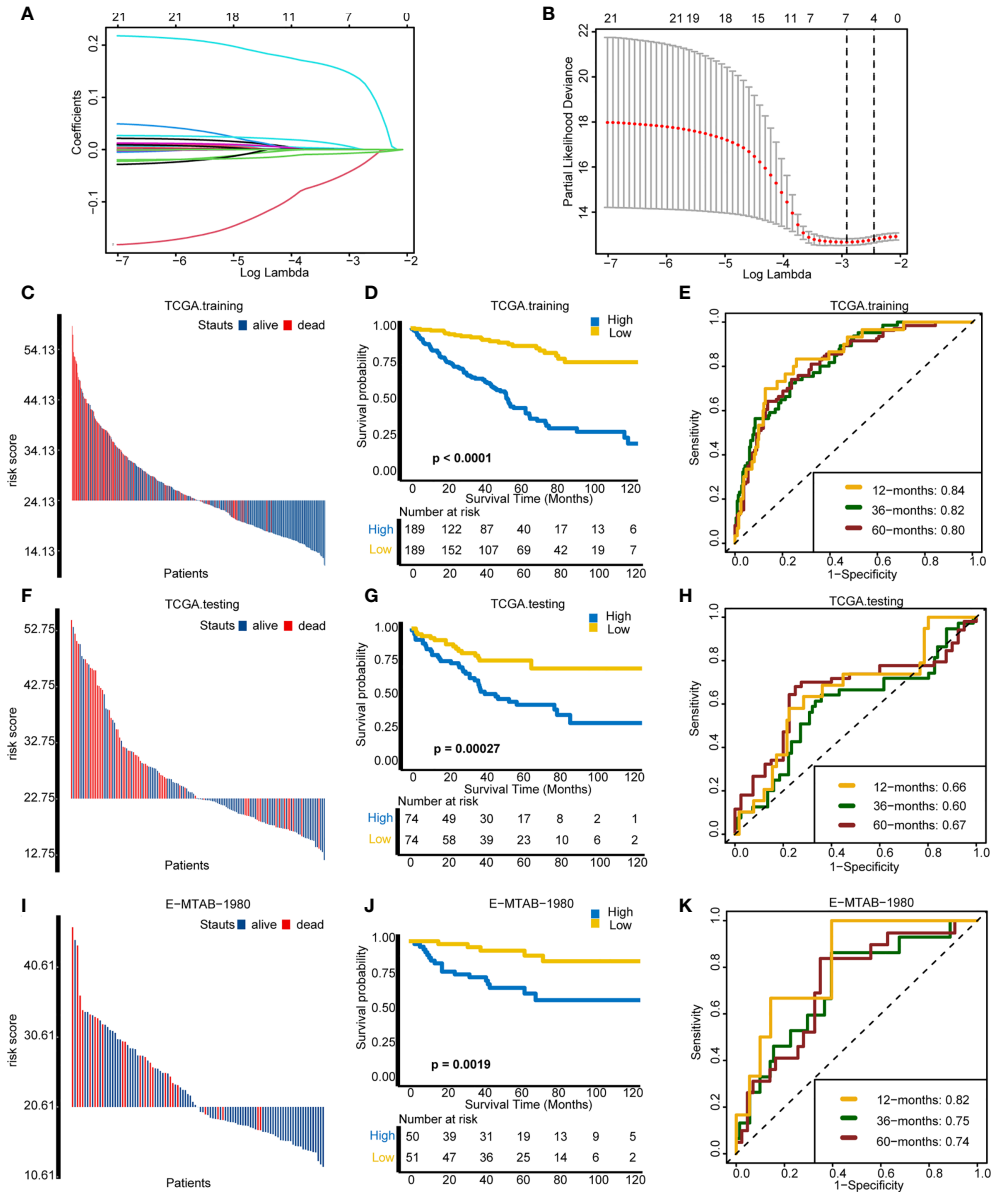


FIGURE 6
Assessing the prognosis of individuals using the cuproptosis risk score. **(A)** Coefficients of 21 cuproptosis-related genes with prognostic value. **(B)** Cross-validation of parameter selection based on the minimum criteria of LASSO regression model. **(C–E)** Comparisons of survival events, Kaplan–Meier (K–M) survival curves, and time-dependent receiver operating characteristic (ROC) curves between different risk score groups in TCGA training cohort. **(F–H)** Comparisons of survival events, (K–M) survival curves, and time-dependent ROC curves between different risk score groups in The Cancer Genome Atlas testing cohort. **(I–K)** Comparisons of survival events, (K–M) survival curves, and time-dependent ROC curves between different risk score groups in the external validation cohort (E-MTAB-1980).

mitochondria and the accumulation of ROS (42). More importantly, recently, cuproptosis was found to have a close connection with tumorigenesis, progression, and metastasis. Li et al. demonstrated that the activated cuproptosis-associated axis (IL-17-STEAP4-XIAP) can turn colon inflammation into cancer (43). Petris et al. revealed that silenced ATP7A can inhibit the progression and metastasis of lung cancer *via* altering the activity of LOX family's enzymes (44). Furthermore, a close correlation between cuproptosis and infiltration of immune cells has been found in several studies. Paredes et al. reported that the mutation of MAP2K1 can change the abundance of macrophage, mature dendritic cell, regulatory T cell, and cytotoxic

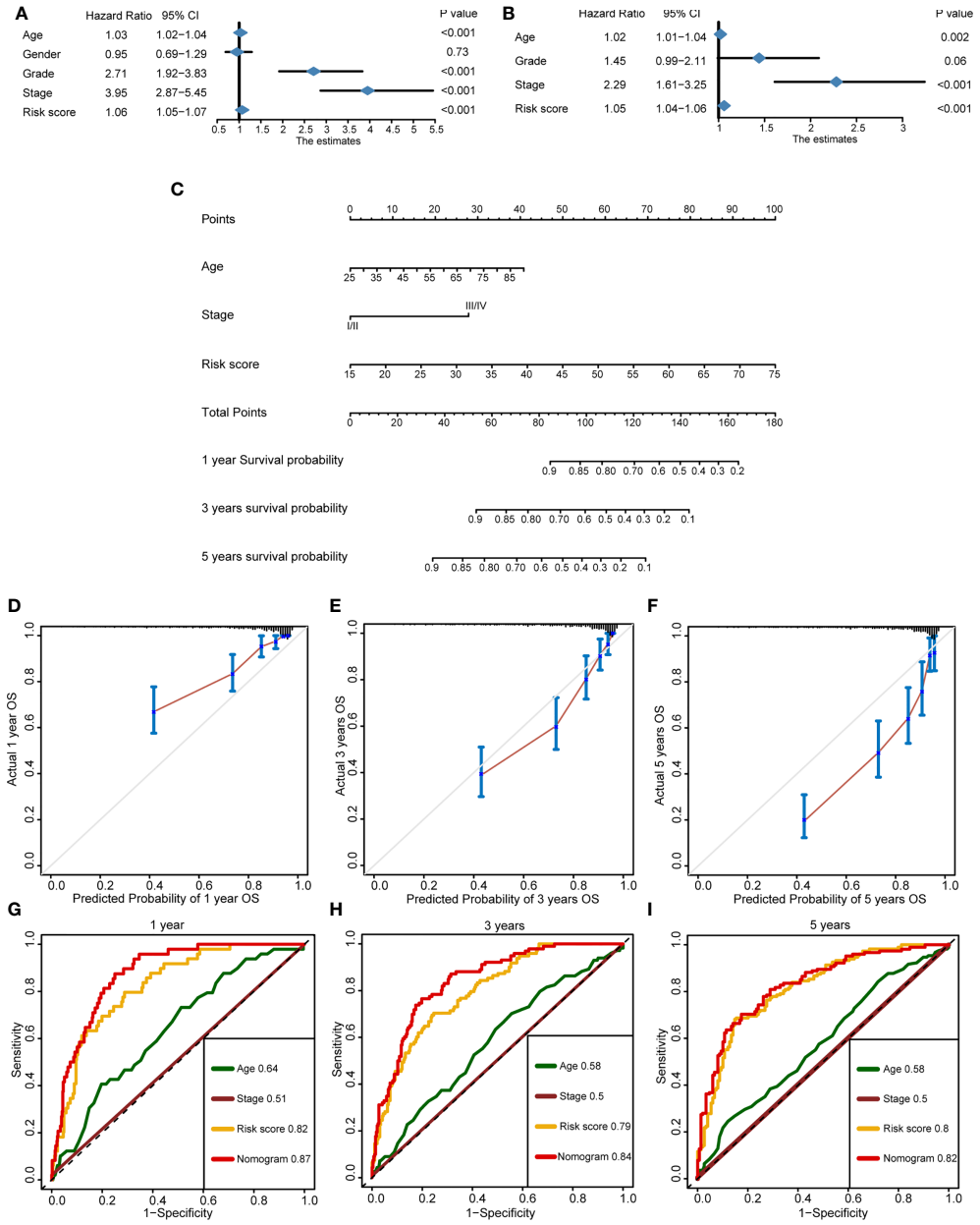


FIGURE 7
Development of a nomogram for better forecasting survival outcome in clinical practice. **(A)** Prognostic factors selected by univariate Cox regression. **(B)** Independent prognostic factors selected by multivariate Cox regression. **(C)** The nomogram-predicted overall survival at 1, 3, and 5 years by incorporating independent prognostic factors. **(D–F)** The calibration curves exhibited the clinical relevance of a nomogram at 1, 3, and 5 years. **(G–I)** Time-dependent receiver operating characteristics showed the prediction accuracy of a nomogram, risk score, age, and stage at 1, 3, and 5 years.

lymphocyte (45). Tan et al. revealed that ceruloplasmin plays an important role in the immune infiltration of breast cancer (46).

Based on the abundance and location of cytotoxic lymphocytes in tumor tissue and invasive margin, the TME can be sorted into inflamed (hot) type and non-inflamed (cold) types (47). It is generally thought that the type of the TME has an important influence on the efficacy of immunotherapy (48, 49)—for example, van der Burg et al. found that a higher infiltration level of $CD4^+$T cells and $CD8^+$T cells shows longer overall survival and recurrence-free survival in patients who accepted anti-PD-1/

PD-L1 immunotherapy (50). Rabadan et al. found that converting the non-inflamed TME of glioblastoma into inflamed TME can significantly improve the response rate to anti-PD-1 therapy (51). On the foundation of a set of vital genes and unsupervised clustering, there are many studies that correlated gene patterns with prognosis and the TME phenotypes. According to the expression of 21 m6A regulators, Zhang et al. correlated the m6A modification patterns with prognosis and the characteristics of the TME cell infiltration in gastric cancer (52). Chen et al. depicted the leukocyte infiltration level in pancreatic ductal adenocarcinoma using hypoxia- and immune-related patterns (53). Liu et al. made use of three m5C modified patterns for assessing the TME and prognosis of patients with lung adenocarcinoma (54). Based on 46 TNF-related genes, two distinct clusters were identified and employed to evaluate the immune characteristics of head and neck squamous cell carcinoma (55). For KIRC, two m6A-related patterns were found and used to predict the immune phenotypes and the efficacy of immunotherapy in our previous study (56). However, as far as we are concerned, this is the first study that systematically correlates cuproptosis-related genes with the immune infiltration level and prognosis in KIRC. We found that cuproptosis-related patterns are able to distinguish the subtypes of TME and survival outcome well. In addition, for evaluating the immune infiltration characteristic on an individual, ssGSEA algorithm was used to construct a cuproptosis signature, which is qualified to predict the inflamed level of the TME on an individual. Furthermore, multiple immunotherapy cohorts were employed to directly compare the response rate between high- and low-cuproptosis-signature groups. These findings are crucial indicators for supplying the precise therapy in KIRC.

More importantly, to predict the survival performance on an individual, cuproptosis risk score was built and showed accurate prediction in testing and multiple validating cohorts. Han et al. developed a cuproptosis-associated lncRNA risk score for prognosis and TME phenotype prediction in soft tissue sarcoma (57). However, their risk score was only validated in the TCGA internal cohort. For KIRC, Xu et al. developed a glycolysis-related risk score and correlated it with prognosis and the TME characteristics. Although they found that their risk score was an independent risk factor, its predictive accuracy in the validation cohort was unclear (58). Similar to Xu's study, Chen et al. and Xing et al. developed and validated a necroptosis and an autophagy-related risk score on the basis of the 11 related genes (59, 60). Our risk score built based on seven cuproptosis-related genes was more convenient for clinical application than Xing's 11 autophagy-related genes. While for Chen's study, though their risk score was successfully validated in the TCGA internal validation cohort, the predictive accuracy still needs further study. Different from most of the risk scores developed using Cox proportional hazard regression analysis, random survival forest (RSF) was used to construct a cuproptosis risk score, with satisfied reliability and extrapolation. In our previous study, precision and robustness of cox proportional hazard regression and RSF have been compared. The outcome indicated that RSF shows a better performance (61). Similarly, Yang et al. built prediction model by six different algorithms and found that RSF was optimal solution with best accuracy (62). It is considered that the excellent multi-process control property of RSF is the key. To sum up, cuproptosis risk scores were constructed by LASSO regression and RSF and validated in multiple cohorts for the first time. It is valuable for predicting the prognosis and conducting a precision treatment for a patient.

Inevitably, there are some limitations in the study. First of all, the follow-up time of the Xiangya-RCC cohort was not enough, which led to it being unqualified as an external validation cohort for prognosis. Secondly, both the training cohort and the validation cohort were retrospective cohorts; it is necessary to further validate the risk score in prospective cohorts. Thirdly, the underlying mechanism of cuproptosis in the TME still needs to be explored *in vitro* and *in vivo*.

## Conclusion

Distinct cuproptosis-related patterns have significant differences on prognosis and immune cell infiltration in KIRC. Cuproptosis signature and risk score are able to provide guidance for precision therapy and accurate prognosis prediction for patients with KIRC.

## Data availability statement

The datasets presented in this study can be found in online repositories. The names of the repository/repositories and accession number(s) can be found in the article/ Supplementary Material.

## Ethics statement

This study was reviewed and approved by Medical Ethics Committee of Xiangya Hospital Central South University (approval number:202104145). Written informed consent was obtained from all participants for their participation in this study.

## Author contributions

Conception and design: ZC, HL, ZL, and XZ. Collection and assembly of data: ZC and ZY. Statistical analyses: HL, JH, and ZX. Manuscript writing: ZC, HL, and YH. All authors contributed to the article and approved the submitted version.

## Funding

This study was supported by the National Natural Science Foundation of China (81873626, and 82070785) and Hunan Province Key R&D Program (2019SK2202).

## Acknowledgments

We sincerely thank all participants in the study.

## Conflict of interest

The authors declare that the research was conducted in the absence of any commercial or financial relationships that could be construed as a potential conflict of interest.

## Publisher's note

All claims expressed in this article are solely those of the authors and do not necessarily represent those of their affiliated organizations, or those of the publisher, the editors and the reviewers. Any product that may be evaluated in this article, or claim that may be made by its manufacturer, is not guaranteed or endorsed by the publisher.

## Supplementary material

The Supplementary Material for this article can be found online at: https://www.frontiersin.org/articles/10.3389/fimmu.2022.933241/full#supplementary-material

SUPPLEMENTARY FIGURE 1
Kaplan–Meier survival curves of 21 cuproptosis-related genes with prognostic value.

SUPPLEMENTARY FIGURE 2
Consensus score matrix of the TCGA-KIRC samples when set *k* was 2, 3, 4, and 5 separately.

SUPPLEMENTARY FIGURE 3
Detailed cell markers in recognized cell types. **(A)** Cancer cell. **(B)** Endothelial cells. **(C)** Vascular smooth muscle cell. **(D)** Macrophage cell. **(E)** T cell. **(F)** B cell. **(G)** Mast cell.

SUPPLEMENTARY FIGURE 4
**(A)** Expression patterns of cuproptosis-related genes in cancer cells and non-cancer cells. **(B)** Heat map of differentially expressed genes (DEGs) between cuproptosis-related patterns. **(C)** Volcano plot of DEGs between two patterns; several immune-related genes were marked. $*p < 0.05$, $**p < 0.01$, $***p < 0.001$; ns, not statistically significant.

SUPPLEMENTARY FIGURE 5
**(A)** Correlation between cuproptosis signature and risk score. **(B, C)** Cuproptosis risk score between different tumor grades and stages. **(D, E)** Cuproptosis risk score between different ages and genders.

SUPPLEMENTARY TABLE 5
Gene Ontology enrichment pathway analysis based on differentially expressed genes between two patterns.

SUPPLEMENTARY TABLE 6
Kyoto Encyclopedia of Genes and Genomes enrichment pathway analysis based on differentially expressed genes between two patterns.

## References

1. Ljungberg B, Albiges L, Abu-Ghanem Y, Bensalah K, Dabestani S, Fernández-Pello S, et al. European Association of urology guidelines on renal cell carcinoma: The 2019 update. *Eur Urol* (2019) 75(5):799–810. doi: 10.1016/j.eururo.2019.02.011

2. Siegel RL, Miller KD, Fuchs HE, Jemal A. Cancer statistics, 2021. *CA: Cancer J Clin* (2021) 71(1):7–33. doi: 10.3322/caac.21654

3. Simonaggio A, Epaillard N, Pobel C, Moreira M, Oudard S, Vano YA. Tumor microenvironment features as predictive biomarkers of response to immune checkpoint inhibitors (ICI) in metastatic clear cell renal cell carcinoma (mccRCC). *Cancers* (2021) 13(2):231–53. doi: 10.3390/cancers13020231

4. Larroquette M, Peyraud F, Domblides C, Lefort F, Bernhard JC, Ravaud A, et al. Adjuvant therapy in renal cell carcinoma: Current knowledges and future perspectives. *Cancer Treat Rev* (2021) 97:102207. doi: 10.1016/j.ctrv.2021.102207

5. Motzer RJ, Tannir NM, McDermott DF, Arén Frontera O, Melichar B, Choueiri TK, et al. Nivolumab plus ipilimumab versus sunitinib in advanced renal-cell carcinoma. *N Engl J Med* (2018) 378(14):1277–90. doi: 10.1056/NEJMoa1712126

6. Braun DA, Bakouny Z, Hirsch L, Flippot R, Van Allen EM, Wu CJ, et al. Beyond conventional immune-checkpoint inhibition - novel immunotherapies for renal cell carcinoma. *Nat Rev Clin Oncol* (2021) 18(4):199–214. doi: 10.1038/s41571-020-00455-z

7. Duan Q, Zhang H, Zheng J, Zhang L. Turning cold into hot: Firing up the tumor microenvironment. *Trends Cancer* (2020) 6(7):605–18. doi: 10.1016/j.trecan.2020.02.022

8. Gajewski TF. The next hurdle in cancer immunotherapy: Overcoming the non-T-Cell-Inflamed tumor microenvironment. *Semin Oncol* (2015) 42(4):663–71. doi: 10.1053/j.seminoncol.2015.05.011

9. Havel JJ, Chowell D, Chan TA. The evolving landscape of biomarkers for checkpoint inhibitor immunotherapy. *Nat Rev Cancer* (2019) 19(3):133–50. doi: 10.1038/s41568-019-0116-x

10. Riaz N, Havel JJ, Makarov V, Desrichard A, Urba WJ, Sims JS, et al. Tumor and microenvironment evolution during immunotherapy with nivolumab. *Cell* (2017) 171(4):934–49.e16. doi: 10.1016/j.cell.2017.09.028

11. Topalian SL, Drake CG, Pardoll DM. Immune checkpoint blockade: a common denominator approach to cancer therapy. *Cancer Cell* (2015) 27(4):450–61. doi: 10.1016/j.ccell.2015.03.001

12. Tumeh PC, Harview CL, Yearley JH, Shintaku IP, Taylor EJ, Robert L, et al. PD-1 blockade induces responses by inhibiting adaptive immune resistance. *Nature* (2014) 515(7528):568–71. doi: 10.1038/nature13954

13. Ge EJ, Bush AI, Casini A, Cobine PA, Cross JR, DeNicola GM, et al. Connecting copper and cancer: From transition metal signalling to metalloplasia. *Nat Rev Cancer* (2022) 22(2):102–13. doi: 10.1038/s41568-021-00417-2

14. Blockhuys S, Wittung-Stafshede P. Roles of copper-binding proteins in breast cancer. *Int J Mol Sci* (2017) 18:871–81. doi: 10.3390/ijms18040871

15. Kardos J, Héja L, Simon Á, Jablonkai I, Kovács R, Jemnitz K. Copper signalling: causes and consequences. *Cell Commun Signaling CCS* (2018) 16(1):71. doi: 10.1186/s12964-018-0277-3

16. Voli F, Valli E, Lerra L, Kimpton K, Saletta F, Giorgi FM, et al. Intratumoral copper modulates PD-L1 expression and influences tumor immune evasion. *Cancer Res* (2020) 80(19):4129–44. doi: 10.1158/0008-5472.Can-20-0471

17. Goldman MJ, Craft B, Hastie M, Repečka K, McDade F, Kamath A, et al. Visualizing and interpreting cancer genomics data *via* the xena platform. *Nat Biotechnol* (2020) 38(6):675–8. doi: 10.1038/s41587-020-0546-8

18. Guo T, Duan H, Chen J, Liu J, Othmane B, Hu J, et al. N6-methyladenosine writer gene ZC3H13 predicts immune phenotype and therapeutic opportunities in kidney renal clear cell carcinoma. *Front Oncol* (2021) 11:718644. doi: 10.3389/fonc.2021.718644

19. Gide TN, Quek C, Menzies AM, Tasker AT, Shang P, Holst J, et al. Distinct immune cell populations define response to anti-PD-1 monotherapy and anti-PD-1/Anti-CTLA-4 combined therapy. *Cancer Cell* (2019) 35(2):238–55.e6. doi: 10.1016/j.ccell.2019.01.003

20. Kim ST, Cristescu R, Bass AJ, Kim KM, Odegaard JI, Kim K, et al. Comprehensive molecular characterization of clinical responses to PD-1 inhibition in metastatic gastric cancer. *Nat Med* (2018) 24(9):1449–58. doi: 10.1038/s41591-018-0101-z

21. Van Allen EM, Miao D, Schilling B, Shukla SA, Blank C, Zimmer L, et al. Genomic correlates of response to CTLA-4 blockade in metastatic melanoma. *Sci (New York NY)* (2015) 350(6257):207–11. doi: 10.1126/science.aad0095

22. Wilkerson MD, Hayes DN. ConsensusClusterPlus: A class discovery tool with confidence assessments and item tracking. *Bioinf (Oxford England)* (2010) 26 (12):1572–3. doi: 10.1093/bioinformatics/btq170

23. Xu L, Deng C, Pang B, Zhang X, Liu W, Liao G, et al. TIP: A web server for resolving tumor immunophenotype profiling. *Cancer Res* (2018) 78(23):6575–80. doi: 10.1158/0008-5472.Can-18-0689

24. Charoentong P, Finotello F, Angelova M, Mayer C, Efremova M, Rieder D, et al. Pan-cancer immunogenomic analyses reveal genotype-immunophenotype relationships and predictors of response to checkpoint blockade. *Cell Rep* (2017) 18 (1):248–62. doi: 10.1016/j.celrep.2016.12.019

25. Hu J, Yu A, Othmane B, Qiu D, Li H, Li C, et al. Siglec15 shapes a non-inflamed tumor microenvironment and predicts the molecular subtype in bladder cancer. *Theranostics* (2021) 11(7):3089–108. doi: 10.7150/thno.53649

26. Auslander N, Zhang G, Lee JS, Frederick DT, Miao B, Moll T, et al. Robust prediction of response to immune checkpoint blockade therapy in metastatic melanoma. *Nat Med* (2018) 24(10):1545–9. doi: 10.1038/s41591-018-0157-9

27. Zhang Y, Narayanan SP, Mannan R, Raskind G, Wang X, Vats P, et al. Single-cell analyses of renal cell cancers reveal insights into tumor microenvironment, cell of origin, and therapy response. *Proc Natl Acad Sci USA* (2021) 118(24):e2103240118. doi: 10.1073/pnas.2103240118

28. Hu J, Chen Z, Bao L, Zhou L, Hou Y, Liu L, et al. Single-cell transcriptome analysis reveals intratumoral heterogeneity in ccRCC, which results in different clinical outcomes. *Mol Ther J Am Soc Gene Ther* (2020) 28(7):1658–72. doi: 10.1016/j.ymthe.2020.04.023

29. Friedman DJ, Crotts SB, Shapiro MJ, Rajcula M, McCue S, Liu X, et al. ST8Sia6 promotes tumor growth in mice by inhibiting immune responses. *Cancer Immunol Res* (2021) 9(8):952–66. doi: 10.1158/2326-6066.Cir-20-0834

30. Lin X, Wu JF, Wang DM, Zhang J, Zhang WJ, Xue G. The correlation and role analysis of KCNK2/4/5/15 in human papillary thyroid carcinoma microenvironment. *J Cancer* (2020) 11(17):5162–76. doi: 10.7150/jca.45604

31. Chen DS, Mellman I. Oncology meets immunology: The cancer-immunity cycle. *Immunity* (2013) 39(1):1–10. doi: 10.1016/j.immuni.2013.07.012

32. Chen DS, Mellman I. Elements of cancer immunity and the cancer-immune set point. *Nature* (2017) 541(7637):321–30. doi: 10.1038/nature21349

33. Giraldo NA, Becht E, Remark R, Damotte D, Sautès-Fridman C, Fridman WH. The immune contexture of primary and metastatic human tumours. *Curr Opin Immunol* (2014) 27:8–15. doi: 10.1016/j.coi.2014.01.001

34. Liu Z, Han C, Fu YX. Targeting innate sensing in the tumor microenvironment to improve immunotherapy. *Cell Mol Immunol* (2020) 17 (1):13–26. doi: 10.1038/s41423-019-0341-y

35. Gajewski TF, Corrales L, Williams J, Horton B, Sivan A, Spranger S. Cancer immunotherapy targets based on understanding the T cell-inflamed versus non-T cell-inflamed tumor microenvironment. *Adv Exp Med Biol* (2017) 1036:19–31. doi: 10.1007/978-3-319-67577-0_2

36. Ji RR, Chasalow SD, Wang L, Hamid O, Schmidt H, Cogswell J, et al. An immune-active tumor microenvironment favors clinical response to ipilimumab. *Cancer Immunol Immunother CII* (2012) 61(7):1019–31. doi: 10.1007/s00262-011-1172-6

37. Owonikoko TK, Dwivedi B, Chen Z, Zhang C, Barwick B, Ernani V, et al. YAP1 expression in SCLC defines a distinct subtype with T-cell-Inflamed phenotype. *J Thorac Oncol Off Publ Int Assoc Study Lung Cancer* (2021) 16 (3):464–76. doi: 10.1016/j.jtho.2020.11.006

38. Romero JM, Grünwald B, Jang GH, Bavi PP, Jhaveri A, Masoomian M, et al. A four-chemokine signature is associated with a T-cell-Inflamed phenotype in primary and metastatic pancreatic cancer. *Clin Cancer Res Off J Am Assoc Cancer Res* (2020) 26(8):1997–2010. doi: 10.1158/1078-0432.Ccr-19-2803

39. Michalczyk K, Cymbaluk-Płoska A. The role of zinc and copper in gynecological malignancies. *Nutrients* (2020) 12(12):3732–53. doi: 10.3390/nu12123732

40. Que EL, Domaille DW, Chang CJ. Metals in neurobiology: Probing their chemistry and biology with molecular imaging. *Chem Rev* (2008) 108(5):1517–49. doi: 10.1021/cr078203u

41. Shanbhag VC, Gudekar N, Jasmer K, Papageorgiou C, Singh K, Petris MJ. Copper metabolism as a unique vulnerability in cancer. *Biochim Biophys Acta Mol Cell Res* (2021) 1868(2):118893. doi: 10.1016/j.bbamcr.2020.118893

42. Tsvetkov P, Coy S, Petrova B, Dreishpoon M, Verma A, Abdusamad M, et al. Copper induces cell death by targeting lipoylated TCA cycle proteins. *Sci (New York NY)* (2022) 375(6586):1254–61. doi: 10.1126/science.abf0529

43. Liao Y, Zhao J, Bulek K, Tang F, Chen X, Cai G, et al. Inflammation mobilizes copper metabolism to promote colon tumorigenesis *via* an IL-17-STEAP4-XIAP axis. *Nat Commun* (2020) 11(1):900. doi: 10.1038/s41467-020-14698-y

44. Shanbhag V, Jasmer-McDonald K, Zhu S, Martin AL, Gudekar N, Khan A, et al. ATP7A delivers copper to the lysyl oxidase family of enzymes and promotes tumorigenesis and metastasis. *Proc Natl Acad Sci United States America* (2019) 116 (14):6836–41. doi: 10.1073/pnas.1817473116

45. Paredes SEY, Almeida LY, Trevisan GL, Polanco XBJ, Silveira HA, Vilela Silva E, et al. Immunohistochemical characterization of immune cell infiltration in paediatric and adult langerhans cell histiocytosis. *Scandinavian J Immunol* (2020) 92(6):e12950. doi: 10.1111/sji.12950

46. Chen F, Han B, Meng Y, Han Y, Liu B, Zhang B, et al. Ceruloplasmin correlates with immune infiltration and serves as a prognostic biomarker in breast cancer. *Aging* (2021) 13(16):20438–67. doi: 10.18632/aging.203427

47. Galon J, Bruni D. Approaches to treat immune hot, altered and cold tumours with combination immunotherapies. *Nat Rev Drug Discovery* (2019) 18 (3):197–218. doi: 10.1038/s41573-018-0007-y

48. Meurette O, Mehlen P. Notch signaling in the tumor microenvironment. *Cancer Cell* (2018) 34(4):536–48. doi: 10.1016/j.ccell.2018.07.009

49. Zemek RM, De Jong E, Chin WL, Schuster IS, Fear VS, Casey TH, et al. Sensitization to immune checkpoint blockade through activation of a STAT1/NK axis in the tumor microenvironment. *Sci Trans Med* (2019) 11(501):14–27. doi: 10.1126/scitranslmed.aav7816

50. Kortekaas KE, Santegoets SJ, Tas L, Ehsan I, Charoentong P, van Doorn HC, et al. Primary vulvar squamous cell carcinomas with high T cell infiltration and active immune signaling are potential candidates for neoadjuvant PD-1/PD-L1 immunotherapy. *J Immunother Cancer* (2021) 9:e003671. doi: 10.1136/jitc-2021-003671

51. Zhao J, Chen AX, Gartrell RD, Silverman AM, Aparicio L, Chu T, et al. Immune and genomic correlates of response to anti-PD-1 immunotherapy in glioblastoma. *Nat Med* (2019) 25(3):462–9. doi: 10.1038/s41591-019-0349-y

52. Zhang B, Wu Q, Li B, Wang D, Wang L, Zhou YL. m(6)A regulator-mediated methylation modification patterns and tumor microenvironment infiltration characterization in gastric cancer. *Mol Cancer* (2020) 19(1):53. doi: 10.1186/s12943-020-01170-0

53. Chen D, Huang H, Zang L, Gao W, Zhu H, Yu X. Development and verification of the hypoxia- and immune-associated prognostic signature for pancreatic ductal adenocarcinoma. *Front Immunol* (2021) 12:728062. doi: 10.3389/fimmu.2021.728062

54. Liu T, Hu X, Lin C, Shi X, He Y, Zhang J, et al. 5-methylcytosine RNA methylation regulators affect prognosis and tumor microenvironment in lung adenocarcinoma. *Ann Trans Med* (2022) 10(5):259. doi: 10.21037/atm-22-500

55. Long Q, Huang C, Meng Q, Peng J, Yao F, Du D, et al. TNF patterns and tumor microenvironment characterization in head and neck squamous cell carcinoma. *Front Immunol* (2021) 12:754818. doi: 10.3389/fimmu.2021.754818

56. Li H, Hu J, Yu A, Othmane B, Guo T, Liu J, et al. RNA Modification of N6-methyladenosine predicts immune phenotypes and therapeutic opportunities in kidney renal clear cell carcinoma. *Front Oncol* (2021) 11:642159. doi: 10.3389/fonc.2021.642159

57. Han J, Hu Y, Liu S, Jiang J, Wang H. A newly established cuproptosis-associated long non-coding RNA signature for predicting prognosis and indicating immune microenvironment features in soft tissue sarcoma. *J Oncol* (2022) 2022:8489387. doi: 10.1155/2022/8489387

58. Xu F, Guan Y, Xue L, Huang S, Gao K, Yang Z, et al. The effect of a novel glycolysis-related gene signature on progression, prognosis and immune microenvironment of renal cell carcinoma. *BMC Cancer* (2020) 20(1):1207. doi: 10.1186/s12885-020-07702-7

59. Xing Q, Ji C, Zhu B, Cong R, Wang Y. Identification of small molecule drugs and development of a novel autophagy-related prognostic signature for kidney renal clear cell carcinoma. *Cancer Med* (2020) 9(19):7034–51. doi: 10.1002/cam4.3367

60. Chen W, Lin W, Wu L, Xu A, Liu C, Huang P. A novel prognostic predictor of immune microenvironment and therapeutic response in kidney renal clear cell carcinoma based on necroptosis-related gene signature. *Int J Med Sci* (2022) 19 (2):377–92. doi: 10.7150/ijms.69060

61. Li H, Liu S, Li C, Xiao Z, Hu J, Zhao C. TNF family-based signature predicts prognosis, tumor microenvironment, and molecular subtypes in bladder carcinoma. *Front Cell Dev Biol* (2021) 9:800967. doi: 10.3389/fcell.2021.800967

62. Yang L, Wu H, Jin X, Zheng P, Hu S, Xu X, et al. Study of cardiovascular disease prediction model based on random forest in eastern China. *Sci Rep* (2020) 10(1):5245. doi: 10.1038/s41598-020-62133-5

# Glossary

| | |
|---|---|
| KIRC | kidney renal clear cell carcinoma |
| TME | tumor microenvironment |
| ICB | immune checkpoint inhibitors |
| OS | overall survival |
| RCC | renal cell carcinoma |
| ROS | reactive oxygen species |
| CTR-1 | copper transporter 1 |
| PD-1 | programmed cell death 1 |
| PD-L1 | programmed cell death 1 ligand 1 |
| CTLA-4 | cytotoxic T lymphocyte-associated antigen-4 |
| MAGE-A3 | Melanoma antigen family A-3 |
| TCGA | The Cancer Genome Atlas |
| DEGs | differentially expressed genes |
| FC | fold change |
| GSEA | gene set enrichment analysis |
| NES | normalized enrichment score |
| GO | Gene Ontology |
| KEGG | Kyoto Encyclopedia of Genes and Genomes |
| TIP | Tracking Tumor Immunophenotype |
| ssGSEA | single-sample gene set enrichment analysis |
| TIS | T cell inflamed score |
| LASSO | least absolute shrinkage and selection operator |
| K–M | Kaplan–Meier |
| ROC | receiver operating characteristic |
| AUC | area under curve |
| TILs | tumor infiltrating leukocytes |
| MCP | microenvironment cell populations |
| Quantiseq | quantification of the tumor immune contexture from human RNA-seq data |
| TIMER | tumor immune estimation resource |
| NK cell | nature killer |
| Th1 cell | type 1 T helper cell |
| scRNA-seq | single-cell RNA sequencing |
| VSM | vascular smooth muscle |
| m6A | N6-methyladenosine |
| TNF | tumor necrosis factor |
| RSF | random survival forest |

frontiers | Frontiers in Immunology

TYPE Review
PUBLISHED 26 September 2022
DOI 10.3389/fimmu.2022.983581



OPEN ACCESS

EDITED BY
Xiaoran Yin,
Second Affiliated Hospital of Xi'an Jiaotong University, China

REVIEWED BY
Lin Wu,
Hunan Cancer Hospital, Central South University, China
Jianguo Sun,
Xinqiao Hospital, China
Chunxia Su,
Shanghai Pulmonary Hospital, China

*CORRESPONDENCE
Bicheng Zhang
bichengzhang@hotmail.com

†These authors have contributed equally to this work and share first authorship

SPECIALTY SECTION
This article was submitted to Cancer Immunity and Immunotherapy, a section of the journal Frontiers in Immunology

RECEIVED 01 July 2022
ACCEPTED 12 September 2022
PUBLISHED 26 September 2022

CITATION
Yin J, Song Y, Tang J and Zhang B (2022) What is the optimal duration of immune checkpoint inhibitors in malignant tumors?
*Front. Immunol.* 13:983581.
doi: 10.3389/fimmu.2022.983581



# What is the optimal duration of immune checkpoint inhibitors in malignant tumors?

Jiaxin Yin†, Yuxiao Song†, Jiazhuo Tang and Bicheng Zhang*

Cancer Center, Renmin Hospital of Wuhan University, Wuhan, China

Immunotherapy, represented by immune checkpoint inhibitors (ICIs), has made a revolutionary difference in the treatment of malignant tumors, and considerably extended patients' overall survival (OS). In the world medical profession, however, there still reaches no clear consensus on the optimal duration of ICIs therapy. As reported, immunotherapy response patterns, immune-related adverse events (irAEs) and tumor stages are all related to the diversity of ICIs duration in previous researches. Besides, there lacks clear clinical guidance on the intermittent or continuous use of ICIs. This review aims to discuss the optimal duration of ICIs, hoping to help guide clinical work based on the literature.

KEYWORDS

duration, immune checkpoint inhibitors, immunotherapy, malignant tumor, optimization

## Introduction

In recent years, immune checkpoint inhibitors (ICIs), represented by programmed cell death protein-1 (PD-1)/programmed cell death ligand 1 (PD-L1) and cytotoxic T lymphocyte-associated protein 4 (CTLA-4) monoclonal antibodies, have revolutionized the treatment of malignant tumors. Consequently, patients are accessible to more treatment options and acquire longer overall survival (OS). Despite the significant efficacy, ICIs simultaneously trigger off a growing number of issues, such as the management of immune-related adverse events (irAEs), the mechanism and the management strategies of immunotherapy resistance, valid predictive biomarkers of ICIs treatment, the optimization of ICIs-based combination therapies and using ICIs in special populations, all of which not only puzzle both oncologists and patients but remain further exploration. Moreover, there exists no clear consensus on the optimal duration of ICIs therapy (1–4), about which an up-to-date review of the current cognition is presented here.

## Response patterns determine the duration of ICIs

With the widespread clinical application of ICIs, it has been gradually found that only a fraction of patients treated with ICIs can achieve durable responses, which means significant and long-lasting curative effect. During ICIs treatment, a considerable percentage of patients exhibits alternative response patterns including pseudoprogression, hyperprogression and dissociated response (5, 6). The prognosis of patients significantly varies from different response patterns, and the duration of ICIs treatment needs to be adjusted accordingly (Figure 1).

### Durable response

Currently, the definition of durable response remains controversial. In a randomized phase III trial, the durable response was defined as follows: Progression-free survival (PFS) of a patient exceeded three times longer than the median PFS of the same group (7). Durable responses can persist for months or years in patients treated with ICIs, some of them even have improved responses to ICIs over time, usually bringing a longer OS (8).

According to published clinical consensus, patients with advanced malignant melanoma who have achieved both complete response (CR) and ICIs treatment for at least six months can consider ceasing ICIs. If the efficacy is assessed as partial response (PR) or stable disease (SD) after two years of ICIs treatment, cessation may be taken into account (1, 9, 10). PET-CT, liquid biopsy (e.g., ctDNA) or tissue biopsy are recommended options for determining efficacy evaluation during ICIs treatment. This consensus on ICIs duration is worth applying to the immunotherapy of other malignant tumors. However, a small number of trials have found that one year of nivolumab treatment for advanced non-small cell lung cancer (NSCLC) may be insufficient. More studies are exploring the feasibility of early discontinuing ICIs treatment, which aims to achieve less treatment-related toxicities and longer OS (11). Some researchers put forward that limited ICIs rather than continuous ICIs might be adequate to induce a durable response (12).

In addition, if there remains a durable response after ICIs cessation (including programmed cessation and cessation for reasons such as economic conditions), restarting ICIs treatment may be considered in the situation of relapse or progressive disease (PD). Clinical studies researching the efficacy of re-challenging ICIs after early discontinuation exist as well. In conclusion, the optimal duration of ICIs is still debatable for patients with a durable response and needs to be further explored with prospective studies.

### Pseudoprogression

The tumors can present a transient increase in volume or number of lesions (temporary progression) after ICIs treatment, followed by PR or SD, which is defined as pseudoprogression (13). Pseudoprogression was first identified in patients with metastatic melanoma treated with ipilimumab (14). Up to 10% of melanoma patients experience pseudoprogression after starting ICIs treatment. Pseudoprogression is discovered with no tumor progression and is often associated with better long-

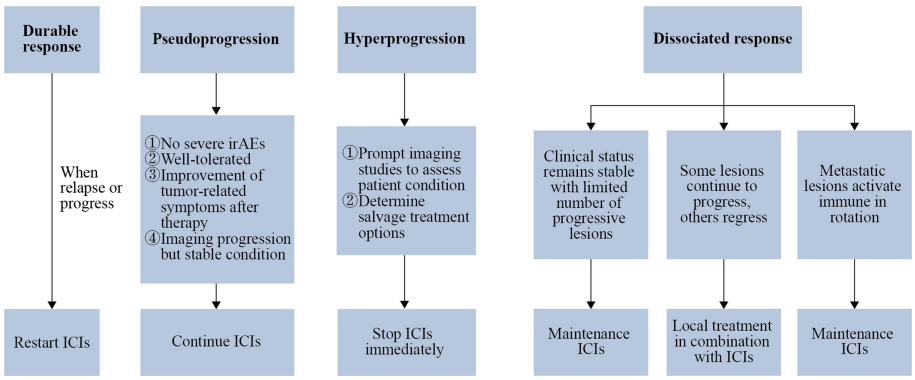


FIGURE 1
Response patterns determine the duration of ICIs. If there remains a durable response after ICIs cessation, restarting ICIs treatment may be considered in the situation of relapse or progression. Patients who match the exhibiting criteria can be considered for continuation of ICIs after being diagnosed with pseudoprogression. When hyperprogression is confirmed, ICIs treatment should be stopped as soon as possible, followed by radiologic examination to assess the patient's condition and decide the treatment alternatives. As for patients with a dissociated response, when the clinical condition remains stable and the number of progressive lesions is limited, maintenance ICIs may be an option; when a minority of metastatic lesions continue to progress while the rest of the metastatic lesions are in remission, local treatment can be chosen in conjunction with ICIs treatment; when metastatic lesions activate immune in rotation, ICIs should be maintained without local treatment.

term survival (15). The increased tumor volume shown by imaging examination probably owes to the recruitment of activated T cells at the tumor site during ICIs treatment. Before these cells exert their anti-tumor functions, they lead to inflammation and developed tumor volume as well as immune infiltration, edema, and necrosis. The incidence of pseudoprogression varies among tumor types but is rarely >10% (16–19). Pseudoprogression often occurs after initial ICIs treatment. It is not specific to ICIs but is more common in ICIs treatment (17).

Pseudoprogression, as an unusual but beneficial response pattern of ICIs treatment, should be emphasized and carefully recognized in clinical trials. To assist oncologists screen out patients more likely to experience pseudoprogression rather than real progression, auxiliary examinations including radiological evidence, biomarker predictors and biopsies are very useful. Only with correct diagnosis can we avoid incorrect discontinuation of effective ICIs treatment (20). Patients diagnosed as pseudoprogression can be considered for continuation of ICIs when matching all the exhibiting criteria: no severe irAEs, well-tolerated, improvement of tumor-related symptoms and imaging progression but stable condition, etc.

## Hyperprogression

Some patients can be discovered with accelerated disease progression after the initiation of ICIs therapy, thus the concept of hyperprogression was proposed (21). There is no standardized definition of hyperprogression, and the definitions varies in different studies. In the research of Champiat et al. (22), hyperprogression was defined as a Response Evaluation Criteria in Solid Tumors (RECIST) progression at the first evaluation and at least a two-fold increase of the tumor growth rate (TGR) upon prior anti-PD-1/PD-L1 therapy. A retrospective study indicated that patients who developed hyperprogression upon ICIs treatment within six weeks had worse median OS compared to patients with typical progression (23).

In the perspective of hyperprogression, both the patient's survival and access to other alternative treatments are limited. A case report revealed that a lung cancer patient's rib metastasis progressed rapidly after receiving ICIs-based combination therapy, and the diagnosis of hyperprogression was then set with early imaging and pathological examinations. Significant shrinkage of the metastatic lesion occurred after one month timely salvage treatment (24). For patients receiving ICIs-based combination therapy, it is necessary to make a rigorous follow-up regimen. To achieve symptom relief and longer OS in cancer patients, early detection and intervention of hyperprogression are crucial. More researches are indispensable to explore the molecular and immunological mechanisms of hyperprogression, favoring predicting and avoiding hyperprogression induced by ICIs treatment (17).

Given the perspective of clinical practice, it is necessary to figure out whether a rapid progression is hyperprogression or not. Once progression occurs, patients should be reassessed immediately and prepared to transfer to the salvage therapeutic strategy. When hyperprogression is confirmed, ICIs treatment should be stopped as soon as possible, followed by a radiologic examination to assess the patient's condition and decide the treatment alternatives. Chemotherapy could allow a rapid tumoral response before the timepoint of the anti-tumor immune response, or even counterbalance the deleterious effect of ICIs treatment (25). As a result, combining ICIs with chemotherapy may be a helpful strategy for preventing and reversing hyperprogression.

## Dissociated response

The dissociated response is characterized by some portion of tumor lesions progressed while the other portion shrank after ICIs treatment. This kind of response pattern is similar to mixed responses seen with chemotherapy and targeted therapy (26). The dissociated response is mainly due to the tumor cells in the individual undergoing multiple divisions and proliferation during the growth process, leading to molecular biological or genetic changes in daughter cells, which consequently contributes to variances in drug sensitivity (27). The standard definition of a dissociated response needs to be further clarified. According to the RECIST version 1.1, a dissociated response is defined as an increase of some tumor lesions >20% and a shrinkage of other tumor lesions >30% (28).

The dissociated response is discovered a relatively common and unique response pattern during ICIs treatment. It is regarded as a preferable treatment response and a signal of better clinical prognosis which brings longer OS than typical progression (29). When dissociated response occurs during ICIs treatment, continuous ICIs can often evolve into a durable response (30). A specific classification for tumor lesions with the dissociated response is necessary to guide the ICIs treatment (28): As for patients with a dissociated response (1), When the clinical condition remains stable and the number of progressive lesions is limited, maintenance ICIs is recommended (2); When a minority of metastatic lesions continues to progress on CT or PET/CT, suggesting persistent immunotherapy resistance, but the rest of the metastatic lesions are in remission, local treatment in conjunction with systemic ICIs treatment can be considered (3); When different metastatic lesions activate immune in rotation (similar to a pseudoprogression pattern), ICIs are recommended maintained without local treatment.

# IrAEs determine the duration of ICIs

While achieving good efficacy, ICIs treatment may lead to some irAEs. The longer patients are on ICIs treatment, the more likely they are to develop irAEs. In most cases, irAEs emerge

within 1-6 months after the initiation of ICIs treatment. Favara et al. (31) put forward that 91 days is the median onset time of irAEs at any grade. In a retrospective study, 75.8% of patients with advanced melanoma treated with ICIs experienced irAEs of any grade. The majority of irAEs appeared during the first treatment cycle, but only a small percentage (11.2%) occurred after ICIs treatment. Mild grade 1-2 irAEs tended to appear within the first two months of ICIs treatment, while grade 3-4 irAEs appeared later. There is no significant correlation between ICIs duration and irAEs severity (32). Late-onset irAEs are irAEs that occur after ICIs have been stopped (33). Previous oncological drug administration before ICIs treatment is a significant risk factor for late-onset irAEs over two years after beginning ICIs treatment (34). Therefore, it is reasonable to discontinue ICIs to avoid irAEs after achieving CR.

IrAEs often result in the discontinuation of ICIs treatment and the administration of immunosuppressant therapies. The best strategy to manage irAEs is to identify them early and stop ICIs as soon as possible, which helps to avoid or minimize the risk of rare fatal outcomes (33). The 2021 Chinese Society of Clinical Oncology (CSCO) immune checkpoint inhibitor-related toxicity management guideline (35) clearly states that when different doses and dosage forms of glucocorticoids and other immunosuppressive agents are properly combined, irAEs can usually be well managed. However, long-term use of drugs such as glucocorticoids has a risk of toxicity and may be associated with poorer survival outcomes.

Management of irAEs and ICIs treatment are not completely contradictory. When G1 irAEs appear, ICIs treatment can usually be continued while treating the toxic side effects. When G2 irAEs appear, ICIs treatment generally needs to be suspended while managing toxic side effects. In addition to certain cases, when the G2 irAEs reduce to ≤ G1, the resumption of ICIs is worth considering. After G3-G4 irAEs are properly treated, especially for G3-G4 cardiotoxicity, pulmonary toxicity, and neurotoxicity, it is generally recommended that ICIs should never be restarted. According to retrospective research, 68 (14%) of NSCLC patients treated with anti-PD-L1 therapy discontinued due to irAEs and 38 (56%) of these patients restarted ICIs after treating irAEs (36). Since the optimal duration of ICIs is unknown, the retreatment of ICIs following irAEs remission remains controversial.

## Tumor stage determines the duration of ICIs

Current clinical trials show that the duration of ICIs varies depending on the tumor stage. A brief summary is as follows (37) (Table 1).

First or second-line treatment for patients with advanced tumors. Most clinical studies in advanced tumors are currently set up for two years of ICIs treatment. Taking advanced NSCLC as an example, based on available clinical studies, it is recommended to use ICIs for two years among first-line monotherapy, second-line monotherapy, first-line immunotherapy combined with chemotherapy, and dual immunotherapy (38). The National Comprehensive Cancer Network (NCCN) guidelines recommend that patients with NSCLC should receive maintenance ICIs therapy for 2 years if they received first-line immunotherapy (39). For advanced liver cancer and renal cancer, a two-year combination of ICIs and anti-angiogenic therapy is the main first-line treatment option. In addition, dual immunotherapy has been approved as a first-line treatment for various cancers, including advanced renal cancer, NSCLC, pleural mesothelioma, malignant melanoma and colorectal cancer, with the same recommendation of two years duration. After two years of ICIs treatment, drug withdrawal can be considered; if the patient desires to continue ICIs treatment, consent can be provided in principle.

Consolidation immunotherapy for patients with locally advanced tumors. The duration is usually 1-2 years. The PACIFIC study aims to evaluate the efficacy of consolidation therapy with durvalumab in patients with locally advanced NSCLC who have not experienced disease progression after concurrent chemoradiotherapy with platinum-containing

TABLE 1 Duration of ICIs for different tumors and stages.

| Tumor stages | Treatment |
|---|---|
| Advanced NSCLC | Two years ICIs treatment |
| Advanced hepatocellular carcinoma and renal carcinoma | Two-year ICIs in combination with anti-angiogenic therapy |
| Advanced pleural mesothelioma, malignant melanoma, and colorectal cancer | Two years of dual immunotherapy |
| Locally advanced tumors | Two years of consolidation immunotherapy after concurrent chemoradiotherapy or sequential chemoradiotherapy |
| Early and middle stage tumors | Preoperative neoadjuvant therapy: 2-4 cycles of ICIs combined with chemotherapy followed by surgery, as well as one year of adjuvant ICIs after surgery |
| Early and middle stage tumors | Post-operative adjuvant therapy: one year of ICIs treatment |

NSCLC, non-small cell lung cancer; ICIs, immune checkpoint inhibitors.

regimens. In 2017, the study published the first results that PFS was significantly longer in the one-year group on durvalumab consolidation after concurrent chemoradiotherapy than in the placebo group, which quickly changed the clinical practice. Recently, the study reported a 42.9% five-year survival rate, with 1/3 of patients still alive after five years of PFS (40). However, there is no sufficient evidence of other tumor types. The newly published GEMSTONE-301 study recommended two years of consolidation immunotherapy after concurrent chemoradiotherapy or sequential chemoradiotherapy (41). For NSCLC, the existing guidelines recommend 2 years of ICIs therapy, with an overall fair safety profile and infrequent occurrence of irAEs. Therefore, a 2-year duration of consolidation immunotherapy is strongly recommended.

Preoperative neoadjuvant therapy for patients with early and middle stage tumors. In recent years, neoadjuvant therapy with ICIs alone or in combination with chemotherapy or dual immunotherapy has been used to treat tumors like NSCLC, triple-negative breast cancer, and esophageal cancer in several clinical studies. The major pathological remission (MPR) of patients who underwent surgery was twice that of neoadjuvant chemotherapy, and the safety was good. In 2021, a Phase III clinical trial CheckMate 816 reported that nivolumab combined with chemotherapy neoadjuvant therapy showed a significant improvement in pathological CR rates (42). The FDA approved nivolumab in combination with platinum-containing dual chemotherapy for the neoadjuvant treatment of adult patients with resectable NSCLC on March 4, 2022, based on the Phase II clinical trial NADIM. Surgery is currently recommended after 2-4 cycles of ICIs combined with chemotherapy for NSCLC, triple-negative breast cancer and esophageal cancer. One year of adjuvant ICIs treatment is recommended following surgery. In addition, there are also other alternative options.

Postoperative adjuvant therapy for patients with early and middle stage tumors. The duration is usually one year. The therapy is applied in various tumors such as esophageal cancer, breast cancer, malignant melanoma, uroepithelial cancer, renal cancer, etc. Taking NSCLC as an example, based on the IMpower 010 study, on March 16, 2022, the National Medical Products Administration (NMPA) approved atezolizumab as adjuvant therapy for patients with stage II-IIIA NSCLC with ≥ 1% tumor cell PD-L1 expression, surgically removed and platinum-based chemotherapy (43). Recently, the KEYNOTE-091 study also demonstrated that pembrolizumab in combination with or without adjuvant chemotherapy significantly improved disease-free survival in patients with stage IB-IIIA NSCLC after surgical resection, regardless of PD-L1 expression level.

## Debate for limited or continuous ICIs

In the medical community, there exists a pair of opposite perspectives on the optimal duration of ICIs. On the one hand, ICIs treatment induces a durable response in the body, allowing the previously activated immune system to regress tumor growth. In addition, short-term ICIs treatment can also avoid the toxic side effects attributed to long-term use. Therefore, some experts advocated discontinuing ICIs after a period of treatment. On the other hand, insufficient ICIs treatment duration may result in disease progression or relapse following remission. Therefore, other experts advocated continuing ICIs treatment to improve patients' long-term PFS and OS. Numerous clinical trials and other studies have set the duration of ICIs, thus we can determine the optimal duration of ICIs more properly based on the results of these trials. The results of these clinical trials are shown in Table 2. During the European Lung Cancer Congress 2022, a session was allocated to this topic for debate and voting by the conference committee.

### Limited ICIs treatment

At present, more studies are standing for this view. Jansen et al. (44) found that in 185 patients with advanced melanoma who had accepted one year of pembrolizumab treatment, the risk of disease recurrence was low when treatment is stopped after achieving CR, and the risk of progression was reduced in patients who had CR for more than six months. But patients who achieved PR or SD were more likely to relapse after discontinuation. Patients who discontinued pembrolizumab after achieving SD had a high risk of disease progression, thus effective ICIs treatment should not be discontinued unless there occurred fatal irAEs (45). Similarly in NSCLC, a real-world study noted that duration of disease control after ICIs discontinuation was correlated with tumor response situation when treatment discontinued, and these results called for caution in discontinuing treatment in patients with SD as the best response (46). In the KEYNOTE-001 study, patients who stopped taking pembrolizumab after achieving CR had an 89.9% disease-free survival rate after 24 months (9). A real-world study showed that patients who responded early to ICIs had a longer OS and a lower risk of disease progression when they discontinued ICIs after achieving CR (47). A multicenter retrospective study (KCSG LU20-11) reported the long-term follow-up results in patients with advanced and/or metastatic NSCLC. It was found that a significantly high proportion of patients who completed 2 years of ICIs therapy continued to experience long-term PFS. Even if ICIs were discontinued in patients without disease progression after 6 months administration, they might achieve a durable response and facilitate long-term survival (48). In an observational cohort study, 52 patients with metastatic melanoma who discontinued anti-PD-1 therapy after one year remained free of disease progression in the long-term follow-up, and the risk of disease progression was low even in patients with remnant lesions by imaging (49). It has been shown that when the active disease is

TABLE 2 Clinical trials investigating the duration of ICIs.

| Trials | Cancer | Phase/Size | ICIs | Duration | Results |
|---|---|---|---|---|---|
| The Safe Stop trial (NL7293) (3) | Melanoma | N=200 | Anti-PD-1 | 1 year<br>Until CR or PR | NR<br>NR |
| CheckMate153 (NCT02066636) (11) | NSCLC | III (N=1434) | Nivolumab | Until progression, unacceptable toxicity, or withdrawal of informed consent<br>1-year-fixed duration | PFS: 24.7m<br>OS: NR<br>PFS: 9.4m<br>OS: 32.5m |
| CheckMate067 (NCT01844505) (12) | Melanoma | III (N=1296) | Nivolumab and Ipilimumab<br>Nivolumab<br>Ipilimumab | Until progression, unacceptable toxicity, or withdrawal of informed consent | OS: NR<br>3-year OS: 58%<br>OS: 37.6m<br>3-year OS: 52%<br>OS:19.9m<br>3-year OS: 34% |
| KEYNOTE-024 (NCT02142738) (38) | NSCLC | III (N=305) | Pembrolizumab | 2 years | PFS:10.3m<br>OS:26.3m<br>5-year OS: 31.9% |
| KEYNOTE-042 (NCT03850444) (38) | NSCLC | III (N=262) | Pembrolizumab | 2 years | PFS: 5.4m<br>OS: 16.7m |
| KEYNOTE-189 (NCT03950674) (38) | NSCLC | III (N=40) | Pembrolizumab | 2 years | PFS: 9.0m<br>OS: 22m<br>ORR: 85.7% |
| KEYNOTE-407 (NCT03875092) (38) | NSCLC | III (N=125) | Pembrolizumab | 2 years | PFS: 6.4m<br>OS: 15.9m |
| IMpower110 (NCT02409342) (38) | NSCLC | III (N=572) | Atezolizumab | Until progression, unacceptable toxicity, or death (maximum up to approximately 58 months) | PFS: 5.7m<br>OS: 20.2m |
| IMpower130 (NCT02367781) (38) | NSCLC | III (N=723) | Atezolizumab | Until progression | PFS: 7.0m<br>OS: 18.6m |
| IMpower150 (NCT02366143) (38) | NSCLC | III (N=1202) | Atezolizumab | Until progression | PFS: 8.3m<br>OS: 19.8m |
| CheckMate227 (NCT02477826) (38) | NSCLC | III (N=2748) | Nivolumab and Ipilimumab | Until progression, unacceptable toxicity, or for 2 years | PFS: 5.1m<br>OS: 17.1m |
| CheckMate9LA (NCT03215706) (38) | NSCLC | III (N=719) | Nivolumab and Ipilimumab | Until progression, unacceptable toxicity, or for 2 years | OS: 15.6m |
| PACIFIC (NCT04230408) (40) | NSCLC | III (N=48) | Durvalumab | 1 year | PFS: 16.9m<br>OS: 47.5m |
| GEMSTONE-301 (41) | NSCLC | III (N=381) | Sugemalimab | 2 years | PFS: 9.0m |
| CheckMate816 (NCT02998528) (42) | NSCLC | III (N=505) | Neoadjuvant Nivolumab | Until surgery | EFS: 31.6m |
| IMpower010 (NCT02486718) (43) | NSCLC | III (N=1280) | Atezolizumab | 1 year | HR for DFS: 0.81 (0·67-0·99; p=0·040) |
| NCT0267397 (44) | Melanoma | N=200 | Pembrolizumab or Nivolumab | 1 year | ORR: 96% |
| The DANTE trial (ISRCTN15837212) (45) | Melanoma | III (N=1208) | Anti-PD-1 | Until progression, unacceptable toxicity, or for 2 years | NR |
| KEYNOTE-001 (NCT01295827) (46) | NSCLC | I (N=550) | Pembrolizumab | Until progression, unacceptable toxicity, or for 2 years | OS: 22.3m<br>5-year OS: 29.6% |
| CA209-003 (NCT00730639) (47) | NSCLC | I (N=395) | Nivolumab | Until progression, unacceptable toxicity, confirmed CR, or for 2 years | 5-year OS: 16% |
| Mäkelä et al. (48) | Melanoma | N=40 | Anti-PD-1 | 6 months | PFS: 12m<br>OS: NR |
| KEYNOTE-006 (NCT01866319) (49) | Melanoma | III (N=834) | Pembrolizumab<br>Ipilimumab | 2 years | PFS: 8.4m<br>OS: 32.7m<br>PFS: 3.4m<br>OS: 15.9m |
| KEYNOTE-010 (NCT01905657) (50) | NSCLC | II/III (N=1034) | Pembrolizumab | 2 years | 3-year OS: 83.0%<br>5-year OS: 25.0% |
| NCT01693562 (51) | Various | I/II (N=1022) | Durvalumab | Retreatment after 1 year | PFS: 5.9m<br>OS: 23.8m |

ICIs, immune checkpoint inhibitors; m, months; NSCLC, non-small cell lung cancer; NR, not reached; N, number; PFS, progression-free survival; OS, overall survival; ORR, overall response rate; EFS, event-free survival; DFS, disease-free survival; HR, hazard ratio.

not detected on CT or PET/CT scans or biopsies, discontinuing anti-PD-1 therapy after 12 months may result in a lower rate of disease recurrence in patients with advanced melanoma (50). In a retrospective study by Valentin et al., patients with advanced melanoma who discontinued anti-PD-1 therapy for reasons other than disease progression were shown to have durable responses with a disease recurrence rate of only 18.5% (51). A real-world multicentric observational study including 1011 patients in India showed that short-course ICIs therapy had comparable efficacy/safety to standard ICIs therapy (52). Oulu University Hospital retrospectively collected all patients who had been treated with anti-PD-1 therapy for metastatic disease in lung and genitourinary (renal and bladder) cancers as well as melanoma, with maximal anti-PD-1 therapy length restricted to 6 months, turning out 11 of 17 responders who discontinued anti-PD-1 therapy after 6 months therapy remained SD after 1 year (53). The above studies all suggest that discontinuation of anti-PD-1 therapy may be attempted in specific populations.

To verify the above, there are at least two prospective investigations currently in progress. The DANTE trial was designed to determine whether time-limited therapy could improve clinical outcomes by reducing toxicities while maintaining treatment benefits. The results supported time-limited therapy for patients with metastatic melanoma continuously remaining progression-free after two years of ICIs (54). The Dutch Safe Stop trial will confirm the feasibility of early discontinuation of ICIs by assessing sustaining response rates after discontinuing first-line nivolumab or pembrolizumab monotherapy in patients with advanced melanoma who achieve CR or PR (3).

Therefore, there is a premature suggestion for melanoma-early discontinuation of ICIs can be considered in CR patients ready to receive additional treatment for 6 months after achieving CR (55). However, unlike melanoma, CR as a sign for treatment cessation has not been widely adopted in advanced NSCLC due to the low CR rates (< 5%) (56). In the CA209-003 study, more than 75% of NSCLC patients treated with 96 weeks of time-limited nivolumab showed a five-year PFS (57). For patients with advanced NSCLC, a treatment regimen of up to two years of ICIs is still widely recommended.

## Continuous ICIs treatment

Despite the perspective of limited ICIs treatment, other studies have suggested that stopping ICIs after two years of treatment may result in disease progression. In the KEYNOTE-189 study, half of the 56 patients who completed 35 cycles (approximately two years) of pembrolizumab progressed after stopping ICIs treatment (58). In the KEYNOTE-010 study, 25 patients (32%) experienced disease progression after stopping treatment with 35 cycles of pembrolizumab (59). Similarly, 54% of 39 patients treated with 35 cycles of pembrolizumab had disease progression two years after stopping ICIs treatment (60).

Arbitrary discontinuation may result in disease relapse in the absence of reliable response markers and predictors of long-term benefit. In a prospective trial, 17 patients dropped out after six months of anti-PD-1 treatment, and 14 (82%) of those experienced relapse (61). In the phase I clinical trial, patients with solid tumors who were treated with ICIs for < 12 months had a higher rate of disease recurrence than those who were treated for > 12 months, and disease recurrence often occurred during the early post-treatment discontinuation period (62). According to a study on advanced melanoma, patients with advanced tumors and those whose best response is not CR should receive ICIs for a longer duration and should not discontinue ICIs before 18 months (63).

So, is two years of ICIs really the best option for patients with advanced tumors? Data from patients in the CheckMate 153 trial, in which patients with NSCLC responding to anti-PD-1 therapy were randomly assigned to one year versus continuous nivolumab, suggested that the median PFS and OS were longer for continuous ICIs treatment group (11). This study also supported the administration of nivolumab for more than one year in previously treated patients with advanced NSCLC. According to a long-term analysis of KEYNOTE-010, 91.0% (72/79) of the 79 patients who completed two years of pembrolizumab therapy survived, with an estimated 24-month OS rate of 86.3% (59). In existing clinical protocols, anti-PD-1 monoclonal antibodies are generally administered for two years or longer (64). A study showed that continuous ICIs treatment for more than two years resulted in higher 3-year OS rates (85.7% *vs*. 100%, 2-year group *vs*. > 2-year group) and the lower 3-year OS rate in the < 2-year group (49%), suggesting that the clinical benefit is likely to be seen in patients who had been on continuous treatment for more than two years (65). However, longer ICIs treatment also contributes to more severe irAEs. Clinical practitioners must weigh the benefits of therapy duration against the risks of toxicities.

Dual immunotherapy causes more severe irAEs than immune monotherapy or immunotherapy combined with chemotherapy. Hence, the optimal duration of dual immunotherapy also needs to be clarified. Prospective studies are currently being conducted to determine the appropriate duration of combination immunotherapy. In the phase III DISCIPLE (NCT03469960) study to determine the optimal duration of dual immunotherapy of ipilimumab and nivolumab in patients with advanced NSCLC, patients who do not progress after six months of dual immunotherapy will be randomly assigned to a group to continue ICIs treatment until disease progression, or to the other group to stop ICIs treatment (1). A figure displaying the optimal duration of ICIs based on tumor types was composed for consultation (Figure 2).

## ICIs re-challenge

The problems associated with long-term continuous ICIs treatment include the potential risk of late toxicity, the financial burden of the high cost and the poor life quality of patients due to irAEs, etc. There emerge growing interests in two aspects: predicting the long-term prognosis of discontinuing ICIs, and re-challenging anti-PD-1 therapy when the disease progresses.

Restarting ICIs when disease progresses in patients who initially benefited from ICIs treatment is considered safe and effective and can achieve disease control during ICIs treatment. In the phase III KEYNOTE-006 study, 12 of 27 patients who progressed after completing two years of pembrolizumab treatment were re-treated with pembrolizumab, and the best overall response was 3 CR, 3 PR, 3 SD, 1 PD, and 2 with evaluation pending (66). In the KEYNOTE-010 trial, 21 patients who progressed after completing two years of pembrolizumab restarted ICIs treatment, reporting that 11 (52.4%) had objective responses and 15 (71.4%) were alive at the time of data cutoff (67). In a trial of patients treated with durvalumab for one year and then discontinued, 71 patients experienced disease progression during that time and restarted durvalumab treatment, with more than 70% of patients experiencing clinical benefit (68). In the study by Warner et al., 15% of patients responded to re-treatment with anti-PD-1 therapy and 25% responded to re-treatment with the combination of ipilimumab and nivolumab (69). In addition, patients who have suspended ICIs because of irAEs need to be aware of the following four points before restarting ICIs treatment (70–72) (1): Population selection. If patients have responded to ICIs (CR or PR) before the appearance of irAEs, there is no need to restart once the irAEs have been resolved. Conversely, ICIs treatment should be restarted if there is no tumor response. It is conceivable that patients who develop irAEs while receiving ICIs treatment have a high immune response (2). Informed consent. Restarting ICIs treatment increases the likelihood of irAE recurrence by roughly 50%. Recurring irAEs can manifest as either familiar or unexpected symptoms. If hospitalization is required when irAEs occur for the first time, irAEs are more likely to occur when ICIs are used again. As a result, obtaining informed consent from the patient is critical before cautiously beginning. If irAEs recur after a restart, the treatment protocol is the same as before, but this type of ICIs should be stopped permanently (3). Treatment principles for restarting ICIs varies when previous irAEs organs are diverse. Taking into account irAEs in different organs, restarting ICIs requires distinct considerations, including the indication for restart. Therefore, a specialist consultation should be invited before restarting ICIs treatment. For further information, see the 2021 CSCO immune checkpoint inhibitor-related toxicity management guideline (35) (4). When restarting, try to choose ICIs distinct from previous treatment. For example, if a patient has developed grade 3 or 4 toxicity with an ipilimumab-containing regimen, further treatment may include PD-1 or PD-L1 inhibitor monotherapy after the early toxicity is eliminated.

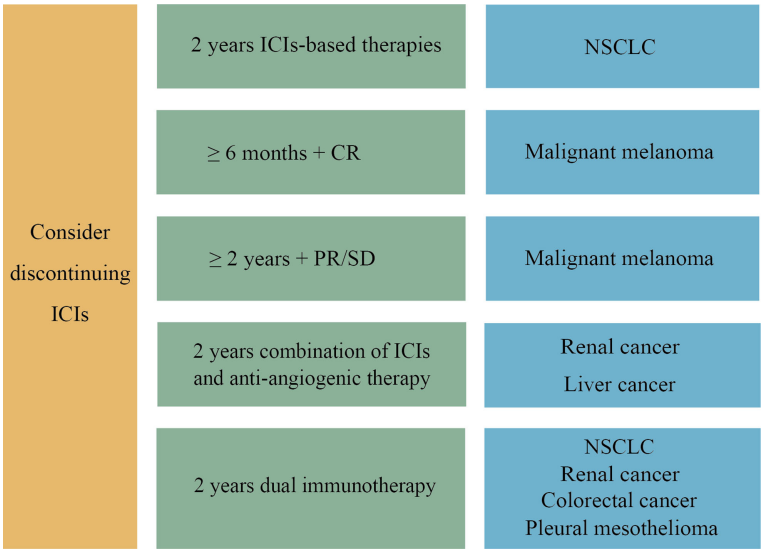


FIGURE 2
The optimal duration of ICIs in different tumor types. For NSCLC, we recommend that discontinuation be considered when 2 years of ICIs-based therapy are completed. For advanced malignant melanoma, early discontinuation of ICIs can be considered in CR patients ready to receive additional treatment for 6 months after achieving CR. If the efficacy is assessed as PR or SD after two years of ICIs treatment, cessation may be taken into account. A two-year combination of ICIs and anti-angiogenic therapy is the main first-line treatment option for advanced liver cancer and renal cancer. In addition, dual immunotherapy has been approved as a first-line treatment for various cancers, including NSCLC, advanced renal cancer, colorectal cancer and pleural mesothelioma, with the same recommendation of two years duration. After two years of ICIs treatment, drug withdrawal can be considered.

## Conclusion and perspectives

According to existing studies, there is no conclusive evidence regarding the optimal duration of ICIs. A growing number of studies have explored the timing of discontinuing and restarting ICIs in malignant melanoma and NSCLC based on efficacy and irAEs, but there is not yet sufficient evidence to answer this question. For melanoma, the recommended optimal duration of ICIs is an additional 6 months of ICIs treatment after the patient achieving CR. The existing consensus suggests that the optimal duration of ICIs should be considered based on the response pattern, irAEs, and tumor stages. Meanwhile, combining some necessary examinations such as PET-CT, liquid biopsy (e.g., ctDNA) or tissue biopsy can help determine when to discontinue ICIs. As more and more prospective studies are completed and published, the optimal duration of ICIs will be found.

## Author contributions

JY, YS and JT collected and analyzed the literatures. JY and YS drafted the manuscript. JT revised the manuscript. BZ came up with the origin idea and supervised the work. All authors contributed to the article and approved the final version.

## Funding

This research was funded by National Natural Science Foundation of China (Grant No. 82272928), CSCO-BMS Cancer Immunotherapy Research Foundation (Grant No. Y-BMS2019-003) and Wuhan Municipal Science and Technology Bureau Knowledge Innovation Special Project (Grant No. 2022020801010475).

## Conflict of interest

The authors declare that the research was conducted in the absence of any commercial or financial relationships that could be construed as a potential conflict of interest.

## Publisher's note



## References

1. Robert C, Marabelle A, Herrscher H, Caramella C, Rouby P, Fizazi K, et al. Immunotherapy discontinuation–how, and when? data from melanoma as a paradigm. *Nat Rev Clin Oncol* (2020) 17(11):707–15. doi: 10.1038/s41571-020-0399-6

2. Marron TU, Ryan AE, Reddy SM, Kaczanowska S, Younis RH, Thakkar D, et al. Considerations for treatment duration in responders to immune checkpoint inhibitors. *J Immunotherapy Cancer* (2021) 9(3):e001901. doi: 10.1136/jitc-2020-001901

3. Mulder E, de Joode K, Litière S, Ten Tije A, Suijkerbuijk K, Boers-Sonderen M, et al. Early discontinuation of pd-1 blockade upon achieving a complete or partial response in patients with advanced melanoma: The multicentre prospective safe stop trial. *BMC Cancer* (2021) 21(1):1–9. doi: 10.1186/s12885-021-08018-w

4. Jansen Y, van der Veldt A, Awada G, Neyns B. Anti-PD-1: When to stop treatment. *Curr Oncol Reports* (2022) 24:905–15. doi: 10.1007/s11912-022-01264-6

5. Tang J, Song Y, Zhang B. Response patterns of tumor immunotherapy. *Herald of Medicine* (2022) 41(3):297–302. doi: 10.3870/j.issn.1004-0781.2022.03.004

6. Borcoman E, Kanjanapan Y, Champiat S, Kato S, Servois V, Kurzrock R, et al. Novel patterns of response under immunotherapy. *Ann Oncol* (2019) 30(3):385–96. doi: 10.1093/annonc/mdz003

7. Pons-Tostivint E, Latouche A, Vaflard P, Ricci F, Loirat D, Hescot S, et al. Comparative analysis of durable responses on immune checkpoint inhibitors versus other systemic therapies: A pooled analysis of phase iii trials. *JCO Precis Oncol* (2019) 3:1–10. doi: 10.1200/PO.18.00114

8. Tan A, Emmett L, Lo S, Liu V, Kapoor R, Carlino M, et al. Fdg-pet response and outcome from anti-Pd-1 therapy in metastatic melanoma. *Ann Oncol* (2018) 29(10):2115–20. doi: 10.1093/annonc/mdy330

9. Robert C, Ribas A, Hamid O, Daud A, Wolchok JD, Joshua AM, et al. Durable complete response after discontinuation of pembrolizumab in patients with metastatic melanoma. *J Clin Oncol* (2018) 36(17):1668–74. doi: 10.1200/JCO.2017.75.6270

10. Michielin O, Van Akkooi A, Ascierto P, Dummer R, Keilholz U. Cutaneous melanoma: Esmo clinical practice guidelines for diagnosis, treatment and follow-up. *Ann Oncol* (2019) 30(12):1884–901. doi: 10.1093/annonc/mdz411

11. Waterhouse DM, Garon EB, Chandler J, McCleod M, Hussein M, Jotte R, et al. Continuous versus 1-year fixed-duration nivolumab in previously treated advanced non–Small-Cell lung cancer: Checkmate 153. *J Clin Oncol* (2020) 38 (33):3863. doi: 10.1200/JCO.20.00131

12. Wolchok JD, Chiarion-Sileni V, Gonzalez R, Rutkowski P, Grob J-J, Cowey CL, et al. Overall survival with combined nivolumab and ipilimumab in advanced melanoma. *N Engl J Med* (2017) 377(14):1345–56. doi: 10.1056/NEJMoa1709684

13. Chiou VL, Burotto M. Pseudoprogression and immune-related response in solid tumors. *J Clin Oncol* (2015) 33(31):3541. doi: 10.1200/JCO.2015.61.6870

14. Di Giacomo AM, Danielli R, Guidoboni M, Calabrò L, Carlucci D, Miracco C, et al. Therapeutic efficacy of ipilimumab, an anti-Ctla-4 monoclonal antibody, in patients with metastatic melanoma unresponsive to prior systemic treatments: Clinical and immunological evidence from three patient cases. *Cancer Immunol Immunotheraphy* (2009) 58(8):1297–306. doi: 10.1007/s00262-008-0642-y

15. Hodi FS, Ribas A, Daud A, Hamid O, Robert C, Kefford R, et al. Patterns of response in patients with advanced melanoma treated with pembrolizumab (Mk-3475) and evaluation of immune-related response criteria (Irrc). *J Immuno Therapy Cancer* (2014) 2(3):1–2. doi: 10.1186/2051-1426-2-S3-P103

16. Manitz J, D'Angelo SP, Apolo AB, Eggleton SP, Bajars M, Bohnsack O, et al. Comparison of tumor assessments using recist 1.1 and irrecist, and association with overall survival. *J Immunotherapy Cancer* (2022) 10(2):e003302. doi: 10.1136/jitc-2021-003302

17. Wang Q, Gao J, Wu X. Pseudoprogression and hyperprogression after checkpoint blockade. *Int Immunopharmacol* (2018) 58:125–35. doi: 10.1016/j.intimp.2018.03.018

18. Borcoman E, Nandikolla A, Long G, Goel S, Le Tourneau C. Patterns of response and progression to immunotherapy. *Am Soc Clin Oncol Educ book* (2018) 38:169–78. doi: 10.1200/EDBK_200643

19. Tanizaki J, Hayashi H, Kimura M, Tanaka K, Takeda M, Shimizu S, et al. Report of two cases of pseudoprogression in patients with non–small cell lung cancer treated with nivolumab–including histological analysis of one case after tumor regression. *Lung Cancer* (2016) 102:44–8. doi: 10.1016/j.lungcan.2016.10.014

20. Failing JJ, Dudek OA, Marin Acevedo JA, Chirila RM, Dong H, Markovic SN, et al. Biomarkers of hyperprogression and pseudoprogression with immune checkpoint inhibitor therapy. *Future Oncol* (2019) 15(22):2645–56. doi: 10.2217/fon-2019-0183

21. Chubachi S, Yasuda H, Irie H, Fukunaga K, Naoki K, Soejima K, et al. A case of non-small cell lung cancer with possible "Disease flare" on nivolumab treatment. *Case Rep Oncological Med* (2016) 2016:1075641. doi: 10.1155/2016/1075641

22. Champiat S, Ferrara R, Massard C, Besse B, Marabelle A, Soria JC, et al. Hyperprogressive disease: Recognizing a novel pattern to improve patient management. *Nat Rev Clin Oncol* (2018) 15(12):748–62. doi: 10.1038/s41571-018-0111-2

23. Ferrara R, Mezquita L, Texier M, Lahmar J, Audigier-Valette C, Tessonnier L, et al. Hyperprogressive disease in patients with advanced non–small cell lung cancer treated with pd-1/Pd-L1 inhibitors or with single-agent chemotherapy. *JAMA Oncol* (2018) 4(11):1543–52. doi: 10.1001/jamaoncol.2018.3676

24. Yang N, Zhang P-L, Liu Z-J. Iodine-125 radioactive particles antagonize hyperprogressive disease following immunotherapy: A case report. *Medicine* (2020) 99(44):e22933. doi: 10.1097/md.0000000000022933

25. Frelaut M, du Rusquec P, de Moura A, Le Tourneau C, Borcoman E. Pseudoprogression and hyperprogression as new forms of response to immunotherapy. *BioDrugs* (2020) 34(4):463–76. doi: 10.1007/s40259-020-00425-y

26. Tabatabai R, Natale R. Immunotherapy and mixed radiographic response in non-small cell lung cancer. *J Cancer Clin* (2018) 1(1):1005.

27. Tazdait M, Mezquita L, Lahmar J, Ferrara R, Bidault F, Ammari S, et al. Patterns of responses in metastatic nsclc during pd-1 or pdl-1 inhibitor therapy: Comparison of recist 1.1, irrecist and irecist criteria. *Eur J Cancer* (2018) 88:38–47. doi: 10.1016/j.ejca.2017.10.017

28. Humbert O, Chardin D. Dissociated response in metastatic cancer: An atypical pattern brought into the spotlight with immunotherapy. *Front Oncol* (2020) 10:566297. doi: 10.3389/fonc.2020.566297

29. Tozuka T, Kitazono S, Sakamoto H, Yoshida H, Amino Y, Uematsu S, et al. Dissociated responses at initial computed tomography evaluation is a good prognostic factor in non-small cell lung cancer patients treated with anti-programmed cell death-1/Ligand 1 inhibitors. *BMC Cancer* (2020) 20(1):1–8. doi: 10.1186/s12885-020-6704-z

30. Humbert O, Cadour N, Paquet M, Schiappa R, Poudenx M, Chardin D, et al. (18)Fdg Pet/Ct in the early assessment of non-small cell lung cancer response to immunotherapy: Frequency and clinical significance of atypical evolutive patterns. *Eur J Nucl Med Mol Imaging* (2020) 47(5):1158–67. doi: 10.1007/s00259-019-04573-4

31. Favara DM, Spain L, Au L, Clark J, Daniels E, Diem S, et al. Five-year review of corticosteroid duration and complications in the management of immune checkpoint inhibitor-related diarrhoea and colitis in advanced melanoma. *ESMO Open* (2020) 5(4):e000585. doi: 10.1136/esmoopen-2019-000585

32. Villa-Crespo L, Podlipnik S, Anglada N, Izquierdo C, Giavedoni P, Iglesias P, et al. Timeline of adverse events during immune checkpoint inhibitors for advanced melanoma and their impacts on survival. *Cancers (Basel)* (2022) 14 (5):1237. doi: 10.3390/cancers14051237

33. Martins F, Sofiya L, Sykiotis GP, Lamine F, Maillard M, Fraga M, et al. Adverse effects of immune-checkpoint inhibitors: Epidemiology, management and surveillance. *Nat Rev Clin Oncol* (2019) 16(9):563–80. doi: 10.1038/s41571-019-0218-0

34. L'Orphelin JM, Varey E, Khammari A, Dreno B, Dompmartin A. Severe late-onset grade iii-iv adverse events under immunotherapy: A retrospective study of 79 cases. *Cancers (Basel)* (2021) 13(19):4928. doi: 10.3390/cancers13194928

35. Committee CSoCOGW. *Guidelines of Chinese society of clinical oncology (Csco) management of immune checkpoint inhibitor-related toxicity*. Beijing: People's Health Publishing House (2021).

36. Santini FC, Rizvi H, Plodkowski AJ, Ni A, Lacouture ME, Gambarin-Gelwan M, et al. Safety and efficacy of re-treating with immunotherapy after immune-related adverse events in patients with nsclc. *Cancer Immunol Res* (2018) 6(9):1093–9. doi: 10.1158/2326-6066.Cir-17-0755

37. Committee CSoCOGW. *Guidelines of Chinese society of clinical oncology (Csco) immune checkpoint inhibitor clinical practice*. Beijing: People's Health Publishing House (2022).

38. Nasser NJ, Gorenberg M, Agbarya A. First line immunotherapy for non-small cell lung cancer. *Pharmaceuticals (Basel)* (2020) 13(11):373. doi: 10.3390/ph13110373

39. Ettinger DS, Wood DE, Aisner DL, Akerley W, Bauman JR, Bharat A, et al. Non-small cell lung cancer, version 3.2022, nccn clinical practice guidelines in oncology. *J Natl Compr Canc Netw* (2022) 20(5):497–530. doi: 10.6004/jnccn.2022.0025

40. Spigel DR, Faivre-Finn C, Gray JE, Vicente D, Planchard D, Paz-Ares L, et al. Five-year survival outcomes from the pacific trial: Durvalumab after chemoradiotherapy in stage iii non-Small-Cell lung cancer. *J Clin Oncol* (2022) 40(12):1301–11. doi: 10.1200/jco.21.01308

41. Zhou Q, Chen M, Jiang O, Pan Y, Hu D, Lin Q, et al. Sugemalimab versus placebo after concurrent or sequential chemoradiotherapy in patients with locally advanced, unresectable, stage iii non-Small-Cell lung cancer in China (Gemstone-301): Interim results of a randomised, double-blind, multicentre, phase 3 trial. *Lancet Oncol* (2022) 23(2):209–19. doi: 10.1016/s1470-2045(21)00630-6

42. Forde PM, Spicer J, Lu S, Provencio M, Mitsudomi T, Awad MM, et al. Neoadjuvant nivolumab plus chemotherapy in resectable lung cancer. *N Engl J Med* (2022) 386(21):1973–85. doi: 10.1056/NEJMoa2202170

43. Felip E, Altorki N, Zhou C, Csőszi T, Vynnychenko I, Goloborodko O, et al. Adjuvant atezolizumab after adjuvant chemotherapy in resected stage ib-iiia non-Small-Cell lung cancer (Impower010): A randomised, multicentre, open-label, phase 3 trial. *Lancet* (2021) 398(10308):1344–57. doi: 10.1016/s0140-6736(21)02098-5

44. Jansen YJL, Rozeman EA, Mason R, Goldinger SM, Geukes Foppen MH, Hoejberg L, et al. Discontinuation of anti-Pd-1 antibody therapy in the absence of disease progression or treatment limiting toxicity: Clinical outcomes in advanced melanoma. *Ann Oncol* (2019) 30(7):1154–61. doi: 10.1093/annonc/mdz110

45. Hamid O, Robert C, Daud A, Carlino MS, Mitchell TC, Hersey P, et al. Long-term outcomes in patients with advanced melanoma who had initial stable disease with pembrolizumab in keynote-001 and keynote-006. *Eur J Cancer* (2021) 157:391–402. doi: 10.1016/j.ejca.2021.08.013

46. Bilger G, Girard N, Doubre H, Levra MG, Giroux-Leprieur E, Giraud F, et al. Discontinuation of immune checkpoint inhibitor (Ici) above 18 months of treatment in real-life patients with advanced non-small cell lung cancer (Nsclc): Intepi, a multicentric retrospective study. *Cancer Immunol Immunother* (2022) 71 (7):1719–31. doi: 10.1007/s00262-021-03114-z

47. van Zeijl MCT, van den Eertwegh AJM, Wouters M, de Wreede LC, Aarts MJB, van den Berkmortel F, et al. Discontinuation of anti-Pd-1 monotherapy in advanced melanoma-outcomes of daily clinical practice. *Int J Cancer* (2022) 150 (2):317–26. doi: 10.1002/ijc.33800

48. Kim H, Kim DW, Kim M, Lee Y, Ahn HK, Cho JH, et al. Long-term outcomes in patients with advanced and/or metastatic non-small cell lung cancer who completed 2 years of immune checkpoint inhibitors or achieved a durable response after discontinuation without disease progression: Multicenter, real-world data (Kcsg Lu20-11). *Cancer* (2022) 128(4):778–87. doi: 10.1002/cncr.33984

49. Pokorny R, McPherson JP, Haaland B, Grossmann KF, Luckett C, Voorhies BN, et al. Real-world experience with elective discontinuation of pd-1 inhibitors at 1 year in patients with metastatic melanoma. *J Immunother Cancer* (2021) 9(1): e001781. doi: 10.1136/jitc-2020-001781

50. Gibney GT, Zaemes J, Shand S, Shah NJ, Swoboda D, Gardner K, et al. Pet/Ct scan and biopsy-driven approach for safe anti-Pd-1 therapy discontinuation in patients with advanced melanoma. *J Immunother Cancer* (2021) 9(10):e002955. doi: 10.1136/jitc-2021-002955

51. Valentin J, Ferté T, Dorizy-Vuong V, Dousset L, Prey S, Dutriaux C, et al. Real-world survival in patients with metastatic melanoma after discontinuation of anti-Pd-1 immunotherapy for objective response or adverse effects: A retrospective study. *J Oncol* (2021) 2021:5524685. doi: 10.1155/2021/5524685

52. Abraham G, Noronha V, Rajappa S, Agarwal A, Batra U, Somani N, et al. The clinical utility and safety of short-course immune checkpoint inhibitors in multiple tumours-a real-world multicentric study from India. *Int J Cancer* (2022) 150(6):1045–52. doi: 10.1002/ijc.33868

53. Iivanainen S, Koivunen JP. Early pd-1 therapy discontinuation in responding metastatic cancer patients. *Oncology* (2019) 96(3):125–31. doi: 10.1159/000493193

54. Coen O, Corrie P, Marshall H, Plummer R, Ottensmeier C, Hook J, et al. The Dante trial protocol: A randomised phase iii trial to evaluate the duration of anti-Pd-1 monoclonal antibody treatment in patients with metastatic melanoma. *BMC Cancer* (2021) 21(1):761. doi: 10.1186/s12885-021-08509-w

55. Jiang M, Hu Y, Lin G, Chen C. Dosing regimens of immune checkpoint inhibitors: Attempts at lower dose, less frequency, shorter course. *Front Oncol* (2022) 12:906251. doi: 10.3389/fonc.2022.906251

56. Garon EB, Hellmann MD, Rizvi NA, Carcereny E, Leighl NB, Ahn MJ, et al. Five-year overall survival for patients with advanced Non–Small-cell lung cancer treated with pembrolizumab: Results from the phase I keynote-001 study. *J Clin Oncol* (2019) 37(28):2518–27. doi: 10.1200/jco.19.00934

57. Gettinger S, Horn L, Jackman D, Spigel D, Antonia S, Hellmann M, et al. Five-year follow-up of nivolumab in previously treated advanced non-Small-Cell lung cancer: Results from the Ca209-003 study. *J Clin Oncol* (2018) 36(17):1675–84. doi: 10.1200/jco.2017.77.0412

58. Rodríguez-Abreu D, Powell SF, Hochmair MJ, Gadgeel S, Esteban E, Felip E, et al. Pemetrexed plus platinum with or without pembrolizumab in patients with previously untreated metastatic nonsquamous nsclc: Protocol-specified final analysis from keynote-189. *Ann Oncol* (2021) 32(7):881–95. doi: 10.1016/j.annonc.2021.04.008

59. Herbst RS, Garon EB, Kim DW, Cho BC, Perez-Gracia JL, Han JY, et al. Long-term outcomes and retreatment among patients with previously treated, programmed death-ligand 1–Positive, advanced Non–Small-cell lung cancer in the keynote-010 study. *J Clin Oncol* (2020) 38(14):1580–90. doi: 10.1200/jco.19.02446

60. Reck M, Rodriguez-Abreu D, Robinson AG, Hui R, Csőszi T, Fülöp A, et al. Five-year outcomes with pembrolizumab versus chemotherapy for metastatic non-Small-Cell lung cancer with pd-L1 tumor proportion score ≥ 50. *J Clin Oncol* (2021) 39(21):2339–49. doi: 10.1200/jco.21.00174

61. Mäkelä S, Kohtamäki L, Laukka M, Juteau S, Hernberg M. Limited-duration anti-Pd-1 therapy for patients with metastatic melanoma. *Acta Oncol* (2020) 59 (4):438–43. doi: 10.1080/0284186x.2020.1716388

62. Gauci ML, Lanoy E, Champiat S, Caramella C, Ammari S, Aspeslagh S, et al. Long-term survival in patients responding to anti-Pd-1/Pd-L1 therapy and disease outcome upon treatment discontinuation. *Clin Cancer Res* (2019) 25(3):946–56. doi: 10.1158/1078-0432.Ccr-18-0793

63. Asher N, Israeli-Weller N, Shapira-Frommer R, Ben-Betzalel G, Schachter J, Meirson T, et al. Immunotherapy discontinuation in metastatic melanoma: Lessons from real-life clinical experience. *Cancers (Basel)* (2021) 13(12):3074. doi: 10.3390/cancers13123074

64. Davies MA. Is it safe to stop anti-Pd-1 immunotherapy in patients with metastatic melanoma who achieve a complete response? *J Clin Oncol* (2020) 38 (15):1645–7. doi: 10.1200/jco.20.00136

65. Geier M, Descourt R, Corre R, Léveiller G, Lamy R , Goarant É, et al. Duration of nivolumab for pretreated, advanced non-Small-Cell lung cancer. *Cancer Med* (2020) 9(19):6923–32. doi: 10.1002/cam4.3120

66. Robert C, Ribas A, Schachter J, Arance A, Grob JJ, Mortier L, et al. Pembrolizumab versus ipilimumab in advanced melanoma (Keynote-006): Post-hoc 5-year results from an open-label, multicentre, randomised, controlled, phase 3 study. *Lancet Oncol* (2019) 20(9):1239–51. doi: 10.1016/s1470-2045(19)30388-2

67. Herbst RS, Garon EB, Kim DW, Cho BC, Gervais R, Perez-Gracia JL, et al. Five year survival update from keynote-010: Pembrolizumab versus docetaxel for previously treated, programmed death-ligand 1-positive advanced nsclc. *J Thorac Oncol* (2021) 16(10):1718–32. doi: 10.1016/j.jtho.2021.05.001

68. Sheth S, Gao C, Mueller N, Angra N, Gupta A, Germa C, et al. Durvalumab activity in previously treated patients who stopped durvalumab without disease progression. *J Immunother Cancer* (2020) 8(2):e000650. doi: 10.1136/jitc-2020-000650

69. Betof Warner A, Palmer JS, Shoushtari AN, Goldman DA, Panageas KS, Hayes SA, et al. Long-term outcomes and responses to retreatment in patients with melanoma treated with pd-1 blockade. *J Clin Oncol* (2020) 38(15):1655–63. doi: 10.1200/jco.19.01464

70. Schadendorf D, Wolchok JD, Hodi FS, Chiarion-Sileni V, Gonzalez R, Rutkowski P, et al. Efficacy and safety outcomes in patients with advanced melanoma who discontinued treatment with nivolumab and ipilimumab because of adverse events: A pooled analysis of randomized phase ii and iii trials. *J Clin Oncol* (2017) 35(34):3807–14. doi: 10.1200/jco.2017.73.2289

71. Horiguchi M, Uno H, Wei LJ. Patients with advanced melanoma who discontinued treatment with nivolumab and ipilimumab as a result of adverse events lived significantly longer than patients who continued treatment. *J Clin Oncol* (2018) 36(7):720–1. doi: 10.1200/jco.2017.76.0983

72. Dick J, Enk A, Hassel JC. Long-lasting responses under treatment with ipilimumab: An argument against maintenance therapy? *Dermatology* (2015) 230 (1):8–10. doi: 10.1159/000365078

frontiers | Frontiers in Immunology

TYPE Original Research
PUBLISHED 27 September 2022
DOI 10.3389/fimmu.2022.1011498



OPEN ACCESS

EDITED BY
Xiaoran Yin,
Second Affiliated Hospital of Xi'an Jiaotong University, China

REVIEWED BY
Xianbin Kong,
Tianjin University of Traditional Chinese Medicine, China
Marzieh Rezaei,
Isfahan University of Medical Sciences, Iran

*CORRESPONDENCE
Cristina Graham Martínez
cristina.grahammartinez@radboudumc.nl

SPECIALTY SECTION
This article was submitted to Cancer Immunity and Immunotherapy, a section of the journal Frontiers in Immunology

RECEIVED 04 August 2022
ACCEPTED 29 August 2022
PUBLISHED 27 September 2022

CITATION
Graham Martínez C, Barella Y, Kus Öztürk S, Ansems M, Gorris MAJ, van Vliet S, Marijnen CAM and Nagtegaal ID (2022) The immune microenvironment landscape shows treatment-specific differences in rectal cancer patients.
*Front. Immunol.* 13:1011498.
doi: 10.3389/fimmu.2022.1011498



# The immune microenvironment landscape shows treatment-specific differences in rectal cancer patients

Cristina Graham Martínez[1]*, Yari Barella[1], Sonay Kus Öztürk[1], Marleen Ansems[2], Mark A.J Gorris[3,4], Shannon van Vliet[1], Corrie A.M Marijnen[5,6] and Iris D Nagtegaal[1]

[1]Department of Pathology, Radboud University Medical Centre, Nijmegen, Netherlands, [2]Radiotherapy & OncoImmunology Laboratory, Department of Radiation Oncology, Radboud University Medical Centre, Nijmegen, Netherlands, [3]Department of Tumor Immunology, Radboud University Medical Centre, Nijmegen, Netherlands, [4]Oncode Institute, Utrecht, Netherlands, [5]Department of Radiotherapy, Netherlands Cancer Institute, Amsterdam, Netherlands, [6]Department of Medical Oncology, Leiden University Medical Centre, Leiden, Netherlands

Neoadjuvant therapy is the cornerstone of modern rectal cancer treatment. Insights into the biology of tumor responses are essential for the successful implementation of organ-preserving strategies, as different treatments may lead to specific tumor responses. In this study, we aim to explore treatment-specific responses of the tumor microenvironment. Patients with locally advanced adenocarcinoma of the rectum who had received neo-adjuvant chemotherapy (CT), neo-adjuvant radiochemotherapy (RCT), neo-adjuvant radiotherapy with a long-interval (LRT) or short-interval (SRT) or no neoadjuvant therapy (NT) as control were included. Multiplex-immunofluorescence was performed to determine the presence of cytotoxic T-cells (T-cyt; CD3+CD8+), regulatory T-cells (T-reg; CD3+FOXP3+), T-helper cells (T-helper; CD3+CD8-FOXP3-), B cells (CD20+), dendritic cells (CD11c+) and tumor cells (panCK+). A total of 80 rectal cancer patients were included. Treatment groups were matched for gender, tumor location, response to therapy, and TNM stage. The pattern of response (shrinkage *vs.* fragmentation) was, however, different between treatment groups. Our analyses reveal that RCT-treated patients exhibited lower stromal T-helper, T-reg, and T-cyt cells compared to other treatment regimens. In conclusion, we demonstrated treatment-specific differences in the immune microenvironment landscape of rectal cancer patients. Understanding the underlying mechanisms of this landscape after a specific therapy will benefit future treatment decisions.

KEYWORDS

**immune microenvironment, response, rectal cancer, neoadjuvant treatment, immune landscape**

# 1 Introduction

In recent times, the prognosis of patients with rectal cancer (RC) has improved immensely (1). Neoadjuvant therapy is the cornerstone of RC treatment, allowing for easier resections and better clinical outcomes (2, 3). The presence of various degrees of tumor response demonstrates organ-preserving treatments are possible in selected patients (4, 5). To fully exploit the organ-preserving potential, we need to fully understand this response and the role of the tumor microenvironment in this process.

Different types of treatments have different clinical effects. A simple comparison of pathological complete response (pCR) rates already illustrates this. Neoadjuvant radiochemotherapy (RCT) has increased pCR rates, with an incidence of approximately 14% of patients (6). Lower pCR rates are present in patients treated with 5x5Gy radiotherapy (RT), depending on the treatment interval; either short (SRT) (reported pCR of 0.3% but increasing after 4 week waiting period) or long wait (LRT) (pCR range 9.3%-10.4%) (7, 8). New clinical trials with different combinations of chemotherapy and, especially, wait intervals provide promising results, in some cases reaching 28% pCR rates (6). In general, longer waiting time after initial treatment and more intense local therapy are considered to improve pCR and several oncological outcomes (9).

Previous studies have shown the potential role of immune infiltrates in the prediction of radio-responsiveness to neoadjuvant RCT in rectal cancer (10). These improved outcomes might also be induced by changes in the immune cell and cytokine composition as a response to therapy, and may, therefore, be therapy-specific. The immune microenvironment of RC is complex, different from colon cancer, with variable prognostic impact of individual types of immune cells, such as tumor-infiltrating T-regs (11–17). The well-established role of CD3+ and CD8+ cells in colorectal cancer (i.e., the immunoscore (18)) has paved the road to investigate the impact of other immune cell subsets. CD11c+ (dendritic cells (DCs)) (19, 20), CD20+ (B cells) (21, 22), CD3+CD8-FOXP3- (T-helper cells) (10), CD3+FOXP3+[T-regulatory cells (T-regs)]] (23, 24) and CD3+CD8+[cytotoxic T cells (T-cyt)] cells (25, 26) have been some of the major targets of immune-profiling in recent years. In newly diagnosed rectal cancers, several studies have elegantly shown an increased presence of T-helper and cytotoxic T cells prior to RCT correlates with better response (27, 28) and better recurrence-free survival (29).

Since local treatment interferes with this microenvironment, investigating the repopulation of the immune infiltrate after each type of therapy is crucial to understanding the biology of the tumor response. Some studies have shown differences in the circulating subpopulations of immune cells throughout therapy or after it (30, 31), but, to the best of our knowledge, little is known about specific changes in the tumor and tumor microenvironment locally, in relation to tumor response. We have recently described a biology-based classification of tumor response (32) that allows us to integrate the tumor response and the microenvironment. According to this, a partial response can be classified into a fragmented (disintegration of the tumor mass in different sized and shaped fragments) or shrinkage (downsizing of tumor mass) pattern of response which has prognostic implications for the patient. Our integrative approach allows us to compare the effects of specific therapeutic strategies in order to elucidate relevant differences in the microenvironment.

Here, we explore the effects and interactions of the different types of treatment on tumor cells and microenvironment and correlate this with a biologically meaningful and clinically relevant response scoring method.

# 2 Methods

## 2.1 Patient cohort and material used

From an original in-house cohort of 728 rectal cancer (RC) patients from the Radboud University Medical Center Nijmegen, a total of 80 patients with adenocarcinoma NOS (not otherwise specified) of the rectum were selected to be included in this study. Patients with known hereditary colorectal cancer were excluded. An opt-out system for ethical approval was in place. Patient material was obtained from the pathology archives of the Radboud University Medical Centre, Nijmegen, The Netherlands. Selected patients received one of four different treatment regimens between 2015 and 2019; neo-adjuvant chemotherapy (CT), neo-adjuvant radiochemotherapy (RCT), neo-adjuvant radiotherapy with a long interval (LRT), or neo-adjuvant radiotherapy with a short interval (SRT), with no neo-adjuvant therapy (NT) serving as control. Per group, 16 patients matched (as much as possible) for gender, tumor location, and cTNM stage were included (details are shown in Table 1).

For each patient, two consecutive slides were cut from the most representative block of the primary tumor and were stained for H&E and an immunofluorescence (IF)-multiplex panel (33) (Figure 1).

## 2.2 Mutation analysis and MSI status

Sufficient material was present for 64 out of the 80 patients for molecular analysis. A targeted mutational panel (PATHv3) used in routine diagnostics was used to determine any mutations that could clearly influence the immune phenotype of patients (exact panel targets can be found in Supplementary Table 2).

10.3389/fimmu.2022.1011498

TABLE 1 Relevant patient information.

| Variable | NT n(%) | CT n(%) | RCT n(%) | LRT n(%) | SRT n(%) | P |
|---|---|---|---|---|---|---|
| **Age, median (IQR)** | 65 (39-84) | 60 (29-78) | 64 (46-80) | 67 (49-79) | 74 (40-87) | 0.02 |
| **Gender** | | | | | | 0.44 |
| Male | 9 (56%) | 9 (56%) | 8 (50%) | 12 (75%) | 12 (75%) | |
| Female | 7 (44%) | 7 (44%) | 8 (50%) | 4 (25%) | 4 (25%) | |
| **Tumor location** | | | | | | 0.02 |
| Rectum | 7 (47%) | 12 (75%) | 14 (88%) | 15 (94%) | 14 (88%) | |
| Rectosigmoid | 7 (47%) | 4 (25%) | 0 (0%) | 0 (0%) | 2 (12%) | |
| LAR (low anterior res) | 1 (6%) | 0 (0%) | 2 (12%) | 1 (6%) | 0 (0%) | |
| **Differentiation grade** | | | | | | 0.17 |
| Good | 16 (100%) | 16 (100%) | 15 (94%) | 15 (94%) | 13 (81%) | |
| Poor | 0 (0%) | 0 (0%) | 1(6%) | 1(6%) | 3 (19%) | |
| **(c)LN involvement** | 10 (100%) | 14 (100%) | 14 (100%) | 13 (100%) | 13 (100%) | <0.001 |
| Yes | 2 (20%) | 13 (93%) | 13 (93%) | 11 (85%) | 10 (77%) | |
| No | 8 (80%) | 1 (7%) | 1 (7%) | 2 (15%) | 3 (23%) | |
| **Angioinvasion** | | | | | | 0.13 |
| Yes | 10 (62%) | 6 (38%) | 6 (38%) | 7 (44%) | 12 (75%) | |
| No | 6 (38%) | 10 (62%) | 10 (62%) | 9 (56%) | 4 (25%) | |
| **(y*)pT category** | | | | | | <0.001 |
| 1 | 0 (0%) | 0 (0%) | 0 (0%) | 0 (0%) | 2 (13%) | |
| 2 | 8 (50%) | 3 (18%) | 7 (44%) | 5 (31%) | 1 (6%) | |
| 3 | 7 (44%) | 7 (44%) | 9 (56%) | 10 (63%) | 13 (81%) | |
| 4 | 1 (6%) | 6 (38%) | 0 (0%) | 1 (6%) | 0 (0%) | |
| **(y*)pN category** | | | | | | 0.07 |
| 0 | 14 (88%) | 4 (25%) | 10 (63%) | 7 (44%) | 9 (57%) | |
| 1 | 1 (6%) | 7 (44%) | 4 (25%) | 6 (38%) | 5 (31%) | |
| 2 | 1 (6%) | 5 (31%) | 2 (12%) | 3 (18%) | 2 (12%) | |
| **(y*)pM category** | | | | | | 0.11 |
| 0 | 15 (94%) | 12 (75%) | 16 (100%) | 16 (100%) | 16 (100%) | |
| 1 | 1 (6%) | 4 (25%) | 0 (0%) | 0 (0%) | 0 (0%) | |
| **Downstaging** | | | | | | 0.97 |
| Progression | * | 1 (6%) | 0 (0%) | 1 (6%) | 1 (6%) | |
| No change | * | 6 (38%) | 6 (38%) | 7 (44%) | 6 (38%) | |
| Downstage | * | 7 (44%) | 9 (56%) | 6 (38%) | 6 (38%) | |
| Unknown | * | 2 (12%) | 1 (6%) | 2 (12%) | 3 (18%) | |
| **Regression** | | | | | | 0.04 |
| Partial | * | 13 (81%) | 16 (100%) | 12 (75%) | 16 (100%) | |
| No | * | 3 (19%) | 0 (0%) | 4 (25%) | 0 (0%) | |
| **Pattern of response** | | | | | | 0.02 |
| Shrinkage | 8 (62%)* | 0 (0%) | 6 (37%) | 7 (64%) | 7 (50%) | |
| Fragmentation** | 5 (38%)* | 12 (100%) | 10 (63%) | 4 (36%) | 7 (50%) | |

This table shows the clinical variables of our cohort. Distribution of patients per treatment group with data as n/(%).
*Cannot be assessed because no therapy was given. **14 cases with No response were excluded.

## 2.3 Immunoflourescence stains

The multiplex IF staining protocol Opal™ 7 Tumor Infiltrating Lymphocyte (TIL) Kit (OP7TL3001KT, Akoya Biosciences, MA, USA), was modified and optimized for rectal 4µm thick FFPE tissue sections (34). In short, slides were sequentially stained using antibodies against CD8, CD20, CD3, Foxp3, CD11c, and pan-Cytokeratin AE 1/3 using the BOND RX automated research stainer (Leica Biosystems, Wetzlar, Germany). The anti-CD45RO used in a previous study (35) was exchanged for CD11c (ab52632, Abcam, Cambridge, UK, RRID: AB_2129793). Concentrations of antibodies, retrieval steps, and corresponding Opal dyes were adjusted (details available in Supplementary Table 1) to ensure the best signal

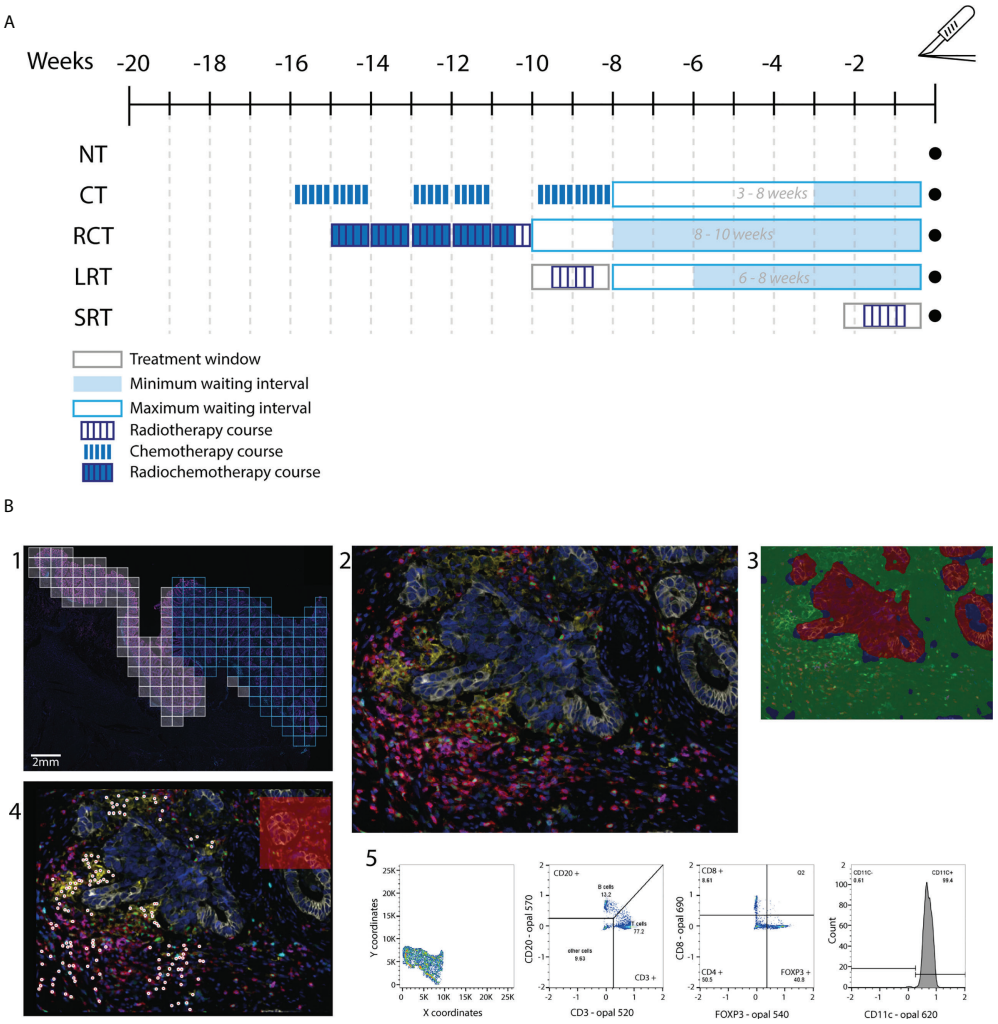


FIGURE 1
Flow diagram of the study. **(A)** Treatment schedule for included patients. Patients received one in 4 neoadjuvant therapy regimens. Treatment window, waiting period between therapy and surgery, and dose fractions are indicated. **(B)** Workflow followed for the immunophenotype quantification. In 1, the whole slide image is selected and regions of interest (ROIs) are drawn to scan at 20x. In blue we see an example of included ROIs, as the white ROIs on the left of the image are excluded as they contain normal rectal epithelium. 2, An example of a ROI output. 3, Tissue segmentation training leads to a quite accurate region classification. Red=tumor, green=stroma, blue=background. 4, Example of the cell phenotyping output from the in-house AI pipeline used. 5, Example of the gating used to discern immune cell populations. NT, No therapy; CT, Chemotherapy; RCT, Radiochemotherapy; LRT, Radiotherapy long course; SRT, Radiotherapy short course; BT, brachytherapy.

intensity for each marker that would allow exposure times of 15-100 ms on multispectral regions. Slides were manually stained with DAPI and mounted using Fluoromount-G® (0100-01, Southern Biotech, ALA, USA, RRID: SCR_015961).

## 2.4 Immunofluorescence imaging and data processing

Imaging was performed using the VECTRA 3 Quantitative Pathology Imaging System (PerkinElmer) and Vectra V3.0.4 software (PerkinElmer®, Hopkinton, MA, USA). All standard epi-fluorescent filters were used; DAPI, FITC, CY3, Texas Red, and CY5. Whole slide scans were acquired using x4 magnification and subsequently scanned at x20 magnification for the multispectral regions of interest (Figure 1B). Images were first processed using the inForm software (V.2.4.8, Akoya Biosciences, MA, USA, RRID: SCR_019155) for cell and tissue segmentation and then processed through an in-house AI pipeline to phenotype immune cells, which were thereafter analyzed in FlowJo™ (Ashland, OR, USA, RRID: SCR_008520) as previously described (35, 36).

## 2.5 Patterns of regression

Slides were visualized and annotated by two independent researchers (C.G.M & S.K.O.) and unclear slides were resolved by consensus with an expert gastrointestinal pathologist (I.D.N.). Each sample was scored blindly following an externally validated classification diagram that we developed for patterns of tumor response in esophageal cancer (32) and rectal cancer (unpublished data). Tumor patterns of regression were divided into fragmentation (disintegration of the tumor mass in different sized and shaped fragments) or shrinkage (the tumor mass downsizes) (Supplementary Figure 1A). The pattern of response was assessed blindly for all patients, regardless if they had had neoadjuvant therapy or not.

## 2.6 Statistical analysis

Statistical analysis was carried out using RStudio version 3.6.2 (Boston, MA, USA, RRID: SCR_000432). One-way ANOVA was done for comparisons between more than two groups in a parametric setting, while Kruskal Wallis one-way ANOVA was used in the non-parametric setting. Student's T-test was done for comparisons between two groups. Correlations between non-parametric variables were analyzed using Spearman´s rank order correlation test. When comparing categorical variables, a chi-square test was used. A principal component analysis was conducted using singular value decomposition. A P-value lower than 0.05 was considered statistically significant.

# 3 Results

## 3.1 Patient characteristics and treatment schedules

A total of 80 RC patients were included; despite matching, selection bias based on treatment indications remained between the groups (Table 1). Gender, differentiation grade, angioinvasion, pN, and pM stage were similar across therapy groups. However, median patient age, tumor location, regression to therapy, lymph node involvement, and pathological T stage were significantly different. Treatment schedule specifics can be found in Figure 1A.

## 3.2 Tumor response

An excellent interobserver agreement was reached ($\kappa$=0.84). Upon histological evaluation, 14 patients were categorized as "non-responders", as there was extensive tumor present and no evidence of regression such as fibrosis or mucin. Prevalence of shrinkage and fragmentation was significantly different across therapy groups (Table 1, p=0.02, Supplementary Figure 1B). Shrinkage was not present in any of the 16 patients treated with CT while being present in 6/16 patients, treated with RCT (Supplementary Figure 1B). When analyzing the immune spatial contexture of these patterns of response we did not observe any single or combinations of immune cells that could explain these patterns. However, we observed a tendency towards higher stromal T-cyt, T-reg, and T-helper cells in patients exhibiting a shrinkage pattern of response compared to those with a fragmented pattern (Supplementary Figure 2).

## 3.3 Tumor characteristics

Targeted sequencing for microsatellite instable (MSI) markers and 47 cancer-related genes identified pathogenic mutations in 61 of the 64 patients (88%) and MSI in 3 of the 69 patients (4%). The percentages of TP53, KRAS, PIK3CA, and NRAS mutated cases were respectively 74%, 56%, 11%, and 7%. These percentages are in the range of other cohorts (37). The samples with mutations were equally distributed over the different therapies. We then analyzed the relation between the molecular and the immune phenotype, we observed that MSI patients have higher immune cell densities compared to MSS, especially significant are T-cytotoxic cells ($p<0.0005$), and B cells ($p<0.0005$)(Supplementary Figures 3A, 3B). TP53-mutated tumors have lower immune cell densities compared to TP53-wild type tumors. The most affected immune cells seem to be T-helper cells ($p<0.005$) and dendritic cells ($p<0.005$) (Supplementary Figures 3C, 3D, respectively). Patients with PIK3CA-mutated tumors had higher tumoral dendritic cell infiltration compared to wild-type tumors ($p<0.05$, Supplementary Figure 3E).

## 3.4 Treatment analysis

The relative distribution of stromal immune cells showed T-helper cells as the predominant immune cell populations across therapies (Figure 2A). Moreover, a significantly higher density of absolute distribution of immune cells was observed in the stroma compared to the tumor infiltration (Supplementary Figure 4A). Immune infiltration in the tumor region did not show significant differences among therapies (Supplementary Figures 4B-F).

Differences in the immunophenotype per treatment could be observed (Figure 2B, Supplementary Figure 4A). T-helper cells were the most predominant population in the stroma of CT, NT, RTL, and RTS treated patients. RCT-treated patients had lower stromal T-helper cells and, had a higher population of T-cyt cells compared to all other treatments. Furthermore, differences could be observed between the stroma and the tumor region, as DCs were one of the predominant types in the tumor region after T-

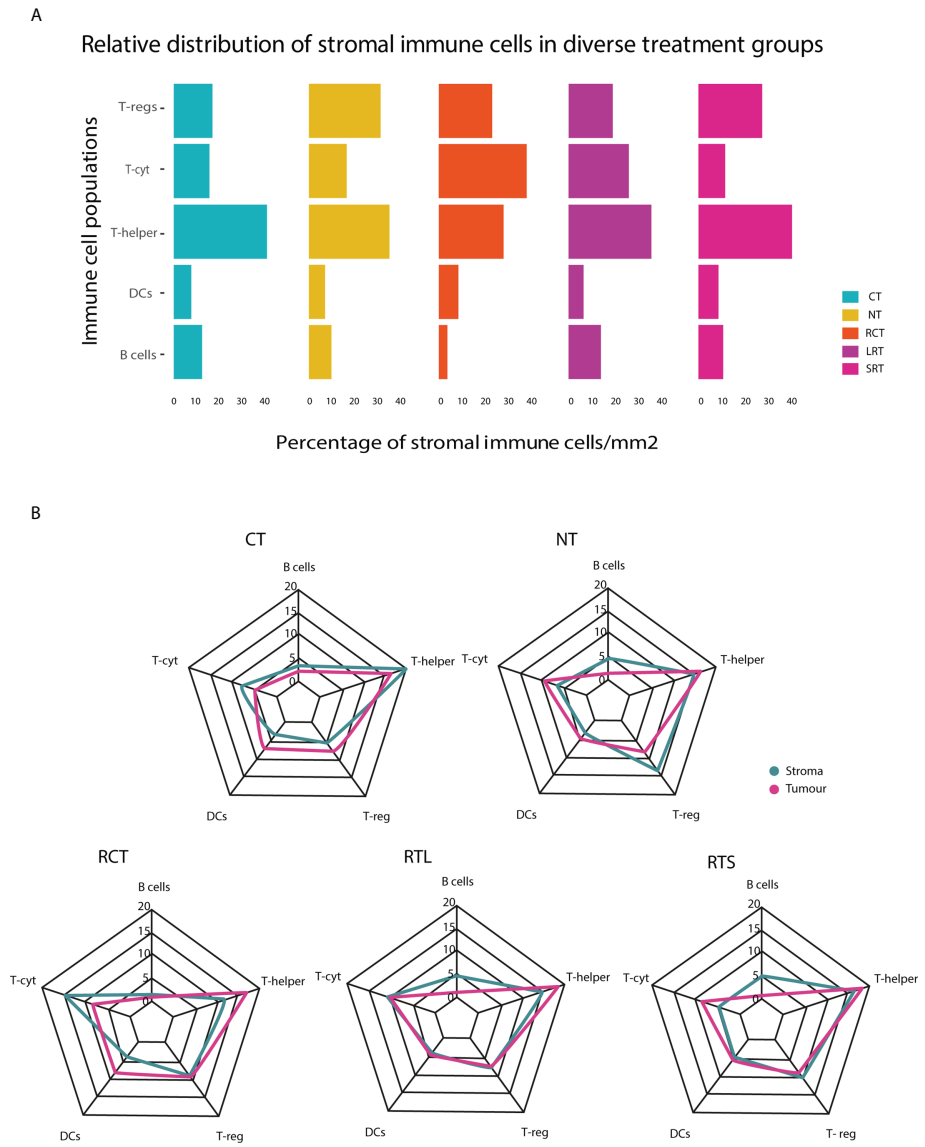


FIGURE 2
Relative immune cell population in tumor and stroma in diverse treatment settings. **(A)** This stacked bar graph represents the relative distribution of immune cells in the stroma surrounding the tumor. **(B)** Relative distribution of immune cells in the tumor and stroma regions for different treatment settings. NT, No therapy; CT, Chemotherapy; RCT, Radiochemotherapy; LRT, Radiotherapy long course; SRT, Radiotherapy short course.

helper cells, something that was not observed in the stromal region.

The stromal T-reg population was less present after any form of neoadjuvant therapy compared to NT, regardless of the waiting time (LRT vs. SRT) (Figure 3A, $p<0.001$). Acute radiotherapy effects were evaluated by comparing the SRT-treated group with the LRT-treated group. The presence of stromal T-cyt cells was significantly lower in SRT-treated patients (Figure 3B, $p<0.01$), especially compared to LRT-treated patients ($p=0.001$). A tendency toward lower T-helper cell density in SRT-treated patients compared to non-treated patients was also found (Figure 3C, $p=0.05$).

The impact of CT was evaluated in two ways, first by comparison with the NT group and secondly, by comparison of the RCT group with the LRT-treated group. The CT-treated group was then compared with the RCT-treated group to determine a potential synergistic effect of CT. Compared to NT, CT showed a decrease in T-regs in the tumor and the stroma, ($p=0.05$ and $p<0.01$, respectively Supplementary Figure 4D and Figure 3A). Differences in the presence of T-

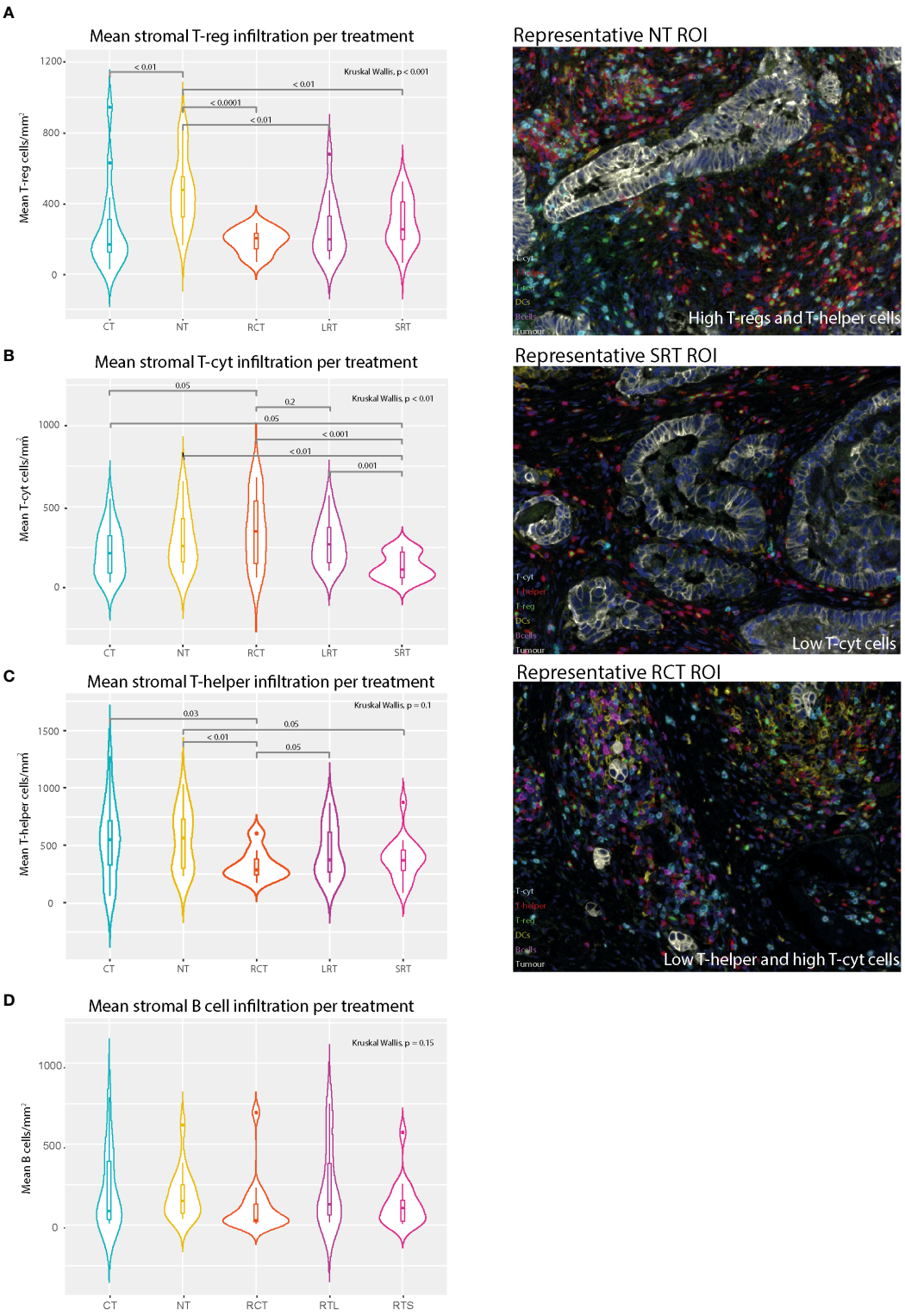


FIGURE 3
Mean stromal immune cell populations and representative immunofluorescence multiplex images. **(A)** Mean stromal T-reg density in different treatment settings. **(B)** Mean Stromal T-cytotoxic cell density in different treatment settings. **(C)** Mean stromal T-helper density per treatment regimen. **(D)** Mean stromal B cells. NT, No therapy; CT, Chemotherapy; RCT, Radiochemotherapy; LRT, Radiotherapy long course; SRT, Radiotherapy short course.

regs were observed when comparing LRT with RCT. Additionally, the tumor microenvironment showed higher stromal T-helper cells in LRT compared to RCT treated patients (p=0.045, Figure 3C). There was also a trend towards lower stromal B cells (p=0.1, Figure 3D) and T-regs (p=0.1, Figure 3A) in RCT-treated patients, as well as higher tumoral DCs (p=0.1, Supplementary Figure 4F) compared to LRT-treated patients. Moreover, when comparing RCT and CT-treated patients significantly higher stromal T-cyt cells (p=0.05) and significantly lower stromal T-helper cells (p=0.03) were found in RCT-treated patients.

## 3.5 Heterogeneity of the immune response according to therapy

When conducting a principal component analysis (PCA) to reduce the dimensions of the high-plex data, different-sized ellipses of the different treatment groups could be observed (Figures 4A, B). Local treatment including RT led to a more homogeneous overall immune response (smaller ellipse) compared to that of patients receiving no treatment or CT (large ellipse) only. Combining dimensions one and two we can explain around 56% of the variance. By analyzing the contribution of each variable to this overall variance we observed that the key players were T-helper cells.

## 3.6 Interaction between the network of immune cells

By grouping all treatment groups together we were able to analyze the overall immune spatial contexture and interplay between immune populations. There was a consistent correlation between the presence of immune cell subsets in different regions, where immune cell populations were positively correlated in stroma and tumor (Figure 5). Moderate correlations were present between the stromal populations of DCs, T-helper, T-reg cells, and T-cyt cells, with the strongest correlation being between stromal T-helper cells and T-regs (rs=0.65). Weaker correlations were observed in the tumor infiltrate, where the main correlations were found between T-regs, T-helper, and T-cyt cells. For more complex interactions, we demonstrated that the presence of T-helper cells positively correlated with all other immune cell populations in all compartments except for tumor-infiltrating DCs, suggesting that these cells behave differently from the rest of immune cell types, with, in many cases, weak negative correlations (Figure 5).

## 3.7 Exploratory analysis

### 3.7.1 Sub-analysis including brachytherapy treatment

A small exploratory cohort of five patients treated with brachytherapy (endoluminal radiotherapy) was also studied to investigate the immunophenotype as a result of this intense local form of therapy. Since three out of the five patients achieved a complete pathological response, we were only able to compare the tumor microenvironment in these five patients to those of the differently-treated patients, as a sample size of two for the tumor region would be biased and, therefore, not a reliable comparison. Strikingly, stromal T-helper, T-cyt, and T-regs showed very low immune densities compared to patients with other treatment regimens (Supplementary Figures 5A-C).

# 4 Discussion

Many studies have attempted to study the tumor microenvironment in RC (4, 10, 21, 24, 30, 38–41). One study (17) even compared the tumor immune microenvironment

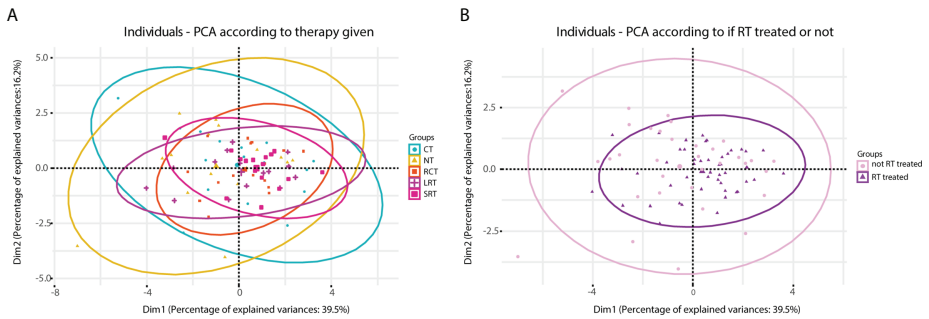


FIGURE 4
Principal component analysis (PCA) carried out according to therapy given. **(A)**, diagram obtained according to five treatment regimens. **(B)**, diagram obtained when stratified according to treated with RT or no RT. NT, No therapy; CT, Chemotherapy; RCT, Radiochemotherapy; LRT, Radiotherapy long course; SRT, Radiotherapy short course; RT, radiotherapy; noRT, no radiotherapy.

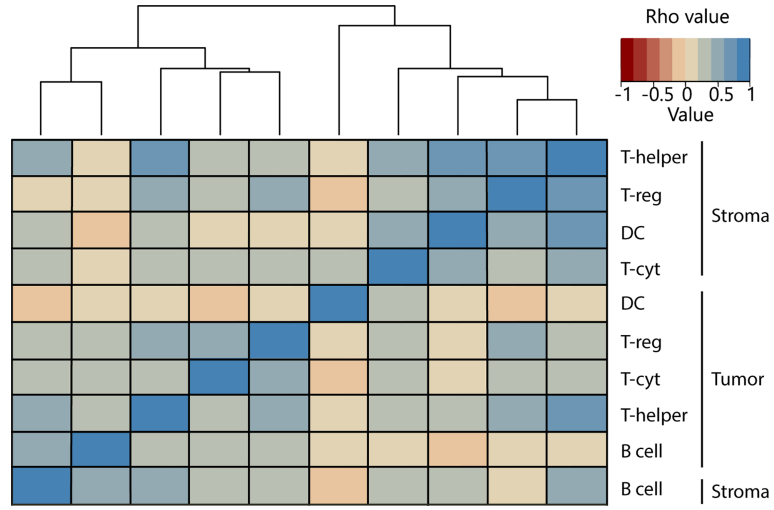


FIGURE 5
Correlation matrix explains the interaction between the network of immune cells.

between RC and CRC, where RC patients seem to have lower levels of immune activation. To the best of our knowledge, this is the first attempt to discover the particularities of the immune contexture in relation to treatment strategy and subsequent tumor response. By comparing different treatment groups, we are able to contribute specific effects to treatment modalities and timing. We have shown that T-regs are less present after any form of therapy, regardless of the treatment interval, suggesting a long and maybe permanent effect on the tumor microenvironment.

Furthermore, we have shown that acute RT (SRT) affects the presence of T-cyt and T-helper cell populations the most. Strikingly, this is less evident with LRT, suggesting repopulation takes place in the interval that distinguishes SRT and LRT, which is in line with previous models (4, 24, 30). Previously, Mezheyeuski (17) has shown that memory T-helper, memory T-cyt cells, and macrophage counts decreased immediately after radiotherapy and were increased after longer treatment intervals. Following this idea, the sub-analysis including BT-treated patients evidenced that a higher dose of radiation depletes the T-cyt and T-helper cell populations further than other therapies. This is especially striking given that the waiting period from end of therapy to surgery is equal to that of LRT, so either this interval is not enough to repopulate the tumor microenvironment after such an intense dose, or the mechanisms that control the repopulation process have been damaged.

Moreover, considerably fewer T-helper and T-regs were found in the RT-treated group when it was compared to non-RT-treated (Supplementary Figures 5D, E). This occurrence had been previously reported (42) and stated that T cell levels begin to decrease after RT is given and do not reach unirradiated levels until approximately two weeks after completion of treatment. Perhaps due to this somewhat coordinated response after the refractory period following RT, the immune response in RT-treated patients seems to be more homogeneous compared to that of non-RT-treated patients (as can be observed in Figure 4). Thus, taking into account these results and given that RT is a more localized treatment compared to CT, we hypothesize that the local microenvironment is more affected by RT and less affected by CT.

Finally, the synergistic effect of radiotherapy in combination with chemotherapy seems to increase the presence of T-cyt cells in the stroma and to decrease the presence of T-helper cells when compared to CT-only treated patients. Furthermore, differences in several immune cell populations were found when comparing LRT and RCT, despite the similar interval and RT regimen. Tumor-infiltrating DCs were found to be higher in RCT-treated patients compared to LRT-treated patients. RCT-treated patients also showed lower stromal T-helper, B cells, and T-regs compared to LRT-treated patients. This suggests that the synergistic effect of combination therapy induces proliferation of T-cyt cells but depletion of other immune cells in the stroma and induces DC tumor infiltration compared to LRT-treated patients.

To study spatial neighborhood relationships, we used multiplex immunohistochemistry, which allowed us to look at cell population interactions. High stromal densities result in more immune cells in the vicinity of the primary tumor, allowing infiltration. In addition, the study of multiple types of cells allows for the analysis of complex interactions. Indeed, as expected (43, 44), the presence of T-helper cells was associated with all other immune cell populations (Figure 5). Recent studies have found many correlations between specific immune cell types in

different regions (tumor and/or stroma) and prognosis in RC patients (21, 22). When we examined the interregional interactions, we confirmed the general premise that higher stromal cells correlate with higher immune infiltrate and we also found correlations between stromal DCs and T-cyt cells (Figure 5). It seems plausible that the reason for this correlation could be cross-priming, where DCs present in the tumor microenvironment activate T-cyt cells by cross-presenting antigens, generating anti-tumor immunity. Further research to confirm this is needed.

Further, we analyzed the spatial contexture of response in a broader sense, linking the histological classification of response with the immune microenvironment. We found that patterns of response could not be explained by a single or combination of multiple immune cell populations across different therapies. Nevertheless, a tendency towards higher stromal T-cyt, T-reg, and T-helper cells in patients exhibiting a shrinkage pattern of response compared to those with a fragmented pattern (Supplementary Figure 2) was observed. A plausible explanation could be that the coordinated presence of several types of immune cell lineages is necessary for a more effective cancer cell elimination, which seems to be the shrinkage pattern of response compared to the fragmented pattern.

Since our study included a heterogeneous group of patients (due to the different therapies given), outcome was not the main aim of our study and therefore we could not analyze immune populations for prognostic value. Nevertheless, a few studies had described a correlation between T-regs and improved survival (23, 24), which we could also observe in our cohort, regardless of treatment (data not shown).

There were several limitations to this study. Firstly, it was a retrospective study with relatively small patient groups from one single institution. Since RCT is the standard therapy for locally advanced RC, we could not expand the other treatment groups without introducing significant selection bias for patient and tumor characteristics. No outcome data could be reported since there was no randomization between the different treatment arms. Similarly, outcomes such as downstaging could not be compared since the different treatment groups did not have the same interval between therapy and surgery. The objective of this study was to explore the spatial and immune contexture after neoadjuvant therapy in rectal cancer to provide insight into their interplay as we move towards local and tailored treatments. Our goal was to unveil the unique immune infiltrate of the tumor and tumor microenvironment of differentially treated rectal cancer patients.

Further research should focus on unraveling the link between different patterns of response and the immune cell infiltrate. Potential therapeutic applications may arise as stimulating certain immune cell lineages could influence the pattern of response to treatment, which can be used to favor a shrinkage pattern environment instead of a fragmented or no response pattern. Moreover, the prognostic relevance of T-regs needs to be investigated in different regions of the primary tumor as its role in the stromal and tumor regions could be different.

In conclusion, we believe that this study is the first to report the differential effects of specific neoadjuvant therapies on the immune contexture of advanced rectal cancer. We have shown that many immune populations (including T-helper, T-cyt, and T-reg cells) are affected mainly by radiotherapy treatment. The re-emergence (or lack) of specific immune cell populations after treatment over time might be linked to tumor regression. Therefore, a better understanding of the reorganization of the immune contexture after therapy is important for the appropriate management of locally advanced RC patients.

## Data availability statement

The original contributions presented in the study are included in the article/Supplementary Material. Further inquiries can be directed to the corresponding authors.

## Ethics statement

Ethical review and approval was not required for the study on human participants in accordance with the local legislation and institutional requirements. Written informed consent for participation was not required for this study in accordance with the national legislation and the institutional requirements.

## Author contributions

The following detailed Credit author statement is added by the corresponding author, who is responsible for ensuring that the descriptions are accurate and agreed by all authors:

CG: methodology, formal analysis, data curation, writing - original draft preparation, visualization, and writing - review and editing. YB: methodology, formal analysis, data curation, and writing - original draft preparation. SKÖ: methodology, validation, and writing - review and editing. MA: interpretation of data, original draft preparation, and writing - review and editing. MG: methodology, data collection, interpretation of data, and writing - review and editing. SV: methodology and writing - review and editing. CM: conceptualization, data curation, writing - review and editing, and supervision. IN: conceptualization, methodology, validation, data curation,

writing - review and editing, and supervision. All authors contributed to the article and approved the submitted version.

## Funding

This work received funding from the Dutch Cancer Society in two grants; Alpe d'HuZes/KWF program grant (KWF UL 2013-6311) and a KWF grant (10602/2016-2).

## Conflict of interest

The authors declare that the research was conducted in the absence of any commercial or financial relationships that could be construed as a potential conflict of interest.

## Publisher's note



## Supplementary material

The Supplementary Material for this article can be found online at: https://www.frontiersin.org/articles/10.3389/fimmu.2022.1011498/full#supplementary-material

## References

1. Brouwer NPM, Bos A, Lemmens V, Tanis P.J, Hugen N, Nagtegaal ID, et al. An overview of 25 years of incidence, treatment and outcome of colorectal cancer patients. *Int J Cancer* (2018) 143(11):2758–66. doi: 10.1002/ijc.31785

2. Gijn van W, Marijnen CAM, Nagtegaal ID, Kranenbarg EM-K, Putter H, Wiggers T, et al. Preoperative radiotherapy combined with total mesorectal excision for resectable rectal cancer: 12-year follow-up of the multicentre, randomised controlled TME trial. *Lancet Oncol* (2011) 12(6):575–82. doi: 10.1016/S1470-2045(11)70097-3

3. Kapiteijn E, Marijnen CA, Nagtegaal ID, Putter H, Steup WH, Wiggers T, et al. Preoperative radiotherapy combined with total mesorectal excision for resectable rectal cancer. *N Engl J Med* (2001) 345(9):638–46. doi: 10.1056/NEJMoa010580

4. Glynne-Jones R, Hall M, Nagtegaal ID. The optimal timing for the interval to surgery after short course preoperative radiotherapy (5 x5 gy) in rectal cancer - are we too eager for surgery? *Cancer Treat Rev* (2020) 90:102104. doi: 10.1016/j.ctrv.2020.102104

5. Fischer J, Eglinton TW, Richards SJ, Frizelle FA. Predicting pathological response to chemoradiotherapy for rectal cancer: a systematic review. *Expert Rev Anticancer Ther* (2021) 21(5):489–500. doi: 10.1080/14737140.2021.1868992

6. Bahadoer RR, Dijkstra EA, Etten van B, Marijnen CAM, Putter H, Kranenbarg EM-K, et al. Short-course radiotherapy followed by chemotherapy before total mesorectal excision (TME) versus preoperative chemoradiotherapy, TME, and optional adjuvant chemotherapy in locally advanced rectal cancer (RAPIDO): a randomised, open-label, phase 3 trial. *Lancet Oncol* (2021) 22 (1):29–42. doi: 10.1016/S1470-2045(20)30555-6

7. Erlandsson J, Lorinc E, Ahlberg M, Pettersson D, Holm T, Glimelius B, et al. Tumour regression after radiotherapy for rectal cancer - results from the randomised Stockholm III trial. *Radiother Oncol* (2019) 135:178–86. doi: 10.1016/j.radonc.2019.03.016

8. Rombouts AJM, Hugen N, Verhoeven RHA, Elferink MAG, Poortmans PMP, Nagtegaal ID, et al. Tumor response after long interval comparing 5x5Gy radiation therapy with chemoradiation therapy in rectal cancer patients. *Eur J Surg Oncol* (2018) 44(7):1018–24. doi: 10.1016/j.ejso.2018.03.017

9. Suwanthanma W, Kitudomrat S, Euanorasetr C. Clinical outcome of neoadjuvant chemoradiation in rectal cancer treatment. *Med (Baltimore)* (2021) 100(38):e27366. doi: 10.1097/MD.0000000000027366

10. Park IJ, An S, Kim SY, Lim HM, Hong SM, Kim MJ, et al. Prediction of radio-responsiveness with immune-profiling in patients with rectal cancer. *Oncotarget* (2017) 8(45):79793–802. doi: 10.18632/oncotarget.19558

11. Nagtegaal ID, Marijnen CA, Kranenbarg EK, Mulder-Stapel A, Hermans J, Velde van CJ, et al. Local and distant recurrences in rectal cancer patients are predicted by the nonspecific immune response; specific immune response has only a systemic effect–a histopathological and immunohistochemical study. *BMC Cancer* (2001) 1:7. doi: 10.1186/1471-2407-1-7

12. Perez-Ruiz E, Berraondo P. Immunological landscape and clinical management of rectal cancer. *Front Immunol* (2016) 7:61. doi: 10.3389/fimmu.2016.00061

13. Reimers MS, Engels CC, Putter H, Morreau H, Liefers GJ, Velde van CJ, et al. Prognostic value of HLA class I, HLA-e, HLA-G and tregs in rectal cancer: a retrospective cohort study. *BMC Cancer* (2014) 14:486. doi: 10.1186/1471-2407-14-486

14. McMullen TP, Lai R, Dabbagh L, Wallace TM, Gara CJ. Survival in rectal cancer is predicted by T cell infiltration of tumour-associated lymphoid nodules. *Clin Exp Immunol* (2010) 161(1):81–8. doi: 10.1111/j.1365-2249.2010.04147.x

15. Iseas S, Sendoya JM, Robbio J, Coraglio M, Kujaruk M, Mikolaitis V, et al. Prognostic impact of an integrative landscape of clinical, immune, and molecular features in non-metastatic rectal cancer. *Front Oncol* (2021) 11:801880. doi: 10.3389/fonc.2021.801880

16. Zhang L, Zhao Y, Dai Y, Cheng JN, Gong Z, Feng Y, et al. Immune landscape of colorectal cancer tumor microenvironment from different primary tumor location. *Front Immunol* (2018) 9:1578. doi: 10.3389/fimmu.2018.01578

17. Mezheyeuski A, Micke P, Martin-Bernabe A, Backman M, Hrynchyk I, Hammarstrom K, et al. The immune landscape of colorectal cancer. *Cancers (Basel)* (2021) 13(21). doi: 10.3390/cancers13215545

18. Galon J, Pages F, Marincola FM, Angell H.K, Thurin M, Lugli A, et al. Cancer classification using the immunoscore: a worldwide task force. *J Transl Med* (2012) 10:205. doi: 10.1186/1479-5876-10-205

19. Nagorsen D, Voigt S, Berg E, Stein H, Thiel E, Loddenkemper C, et al. Tumor-infiltrating macrophages and dendritic cells in human colorectal cancer: relation to local regulatory T cells, systemic T-cell response against tumor-associated antigens and survival. *J Transl Med* (2007) 5:62. doi: 10.1186/1479-5876-5-62

20. Janco Tran JM, Lamichhane P, Karyampudi L, Knutson KL. Tumor-infiltrating dendritic cells in cancer pathogenesis. *J Immunol* (2015) 194 (7):2985–91. doi: 10.4049/jimmunol.1403134

21. Edin S, Kaprio T, Hagstrom J, Larsson P, Mustonen H, Bockelman C, et al. The prognostic importance of CD20(+) b lymphocytes in colorectal cancer and the relation to other immune cell subsets. *Sci Rep* (2019) 9(1):19997. doi: 10.1038/s41598-019-56441-8

22. Mlecnik B, Eynde den Van M, Bindea G, Church SE, Vasaturo A, Fredriksen T, et al. Comprehensive intrametastatic immune quantification and major impact of immunoscore on survival. *J Natl Cancer Inst* (2018) 110(1):97–108. doi: 10.1093/jnci/djx123

23. Kuwahara T, Hazama S, Suzuki N, Yoshida S, Tomochika S, Nakagami Y, et al. Intratumoural-infiltrating CD4 + and FOXP3 + T cells as strong positive predictive markers for the prognosis of resectable colorectal cancer. *Br J Cancer* (2019) 121(8):659–65. doi: 10.1038/s41416-019-0559-6

24. Yasui K, Kondou R, Iizuka A, Miyata H, Tanaka E, Ashizawa T, et al. Effect of preoperative chemoradiotherapy on the immunological status of rectal cancer patients. *J Radiat Res* (2020) 61(5):766–75. doi: 10.1093/jrr/rraa041

25. Schnellhardt S, Hirneth J, Buttner-Herold M, Daniel C, Haderlein M, Hartmann A, et al. The prognostic value of FoxP3+ tumour-infiltrating lymphocytes in rectal

cancer depends on immune phenotypes defined by CD8+ cytotoxic T cell density. *Front Immunol* (2022) 13:781222. doi: 10.3389/fimmu.2022.781222

26. Georges NDF, Oberli B, Rau TT, Galvan JA, Nagtegaal ID, Dawson H, et al. Tumour budding and CD8(+) T cells: 'attackers' and 'defenders' in rectal cancer with and without neoadjuvant chemoradiotherapy. *Histopathology* (2021) 78 (7):1009–18. doi: 10.1111/his.14319

27. Yasuda K, Nirei T, Sunami E, Nagawa H, Kitayama J. Density of CD4(+) and CD8(+) T lymphocytes in biopsy samples can be a predictor of pathological response to chemoradiotherapy (CRT) for rectal cancer. *Radiat Oncol* (2011) 6 (1):49–55. doi: 10.1186/1748-717X-6-49

28. Pages F, Berger A, Camus M, Sanchez-Cabo F, Costes A, Molidor R, et al. Effector memory T cells, early metastasis, and survival in colorectal cancer. *N Engl J Med* (2005) 353(25):2654–66. doi: 10.1056/NEJMoa051424

29. Szynglarewicz B MR, Suder E, Sydor D, Forgacz J, Pudełko M, Grzebieniak Z. Predictive value of lymphocytic infiltration and character of invasive margin following total mesorectal excision with sphincter preservation for the high-risk carcinoma of the rectum. *Adv Med Sci* (2007) 52:159–63.

30. Lee YJ, Lee SB, Beak SK, Han YD, Cho MS, Hur H, et al. Temporal changes in immune cell composition and cytokines in response to chemoradiation in rectal cancer. *Sci Rep* (2018) 8(1):7565. doi: 10.1038/s41598-018-25970-z

31. Wu Z, Zhang J, Cai Y, Deng R, Yang L, Li J, et al. Reduction of circulating lymphocyte count is a predictor of good tumor response after neoadjuvant treatment for rectal cancer. *Med (Baltimore)* (2018) 97(38):e11435. doi: 10.1097/MD.0000000000011435

32. Martinez Graham C, Ozturk Kus S, Al-Kaabi A, Valkema MJ, Bokhorst JM, Rosman C, et al. Shrinkage versus fragmentation response in neoadjuvantly treated oesophageal adenocarcinoma: significant prognostic relevance. *Histopathology* (2022) 80(6):982–94. doi: 10.1111/his.14644

33. Akoya Biosciences I. *Opal multiplex IHC assay development guide and image acquisition information phenoptics research solutions*. Akoya Biosciences, Inc. (2019) Available at: https://www.akoyabio.com/phenoptics/opal-kits-reagents/opal-7-tumor-infiltrating-lymphocyte-kit/.

34. Gorris MAJ, Halilovic A, Rabold K, Duffelen van A, Wickramasinghe IN, Verweij D, et al. Eight-color multiplex immunohistochemistry for simultaneous detection of multiple immune checkpoint molecules within the tumor microenvironment. *J Immunol* (2018) 200(1):347–54. doi: 10.4049/jimmunol.1701262

35. Gorris MAJ, Woude der van LL, Kroeze LI, Bol K, Verrijp K, Amir AL, et al. Paired primary and metastatic lesions of patients with ipilimumab-treated melanoma: high variation in lymphocyte infiltration and HLA-ABC expression whereas tumor mutational load is similar and correlates with clinical outcome. *J Immunother Cancer* (2022) 10(5). doi: 10.1136/jitc-2021-004329

36. Sultan S, Gorris MAJ, Woude der van LL, Buytenhuijs F, Martynova E, Wilpe van S, et al. A segmentation-free machine learning architecture for immune land-scape phenotyping in solid tumors by multichannel imaging. *bioRxiv* (2021), 2021. doi: 10.1101/2021.10.22.464548

37. Cancer Genome Atlas N. Comprehensive molecular characterization of human colon and rectal cancer. *Nature* (2012) 487(7407):330–7. doi: 10.1038/nature11252

38. Shinto E, Hase K, Hashiguchi Y, Sekizawa A, Ueno H, Shikina A, et al. CD8 + and FOXP3+ tumor-infiltrating T cells before and after chemoradiotherapy for rectal cancer. *Ann Surg Oncol* (2014) . 21 Suppl 3:S414–21. doi: 10.1245/s10434-014-3584-y

39. Anitei MG, Zeitoun G, Mlecnik B, Marliot F, Haicheur N, Todosi AM, et al. Prognostic and predictive values of the immunoscore in patients with rectal cancer. *Clin Cancer Res* (2014) 20(7):1891–9. doi: 10.1158/1078-0432.CCR-13-2830

40. Angell HK, Bruni D, Barrett JC, Herbst R, Galon J. The immunoscore: Colon cancer and beyond. *Clin Cancer Res* (2020) 26(2):332–9. doi: 10.1158/1078-0432.CCR-18-1851

41. Mlecnik B, Bifulco C, Bindea G, Marliot F, Lugli A, Lee JJ, et al. Multicenter international society for immunotherapy of cancer study of the consensus immunoscore for the prediction of survival and response to chemotherapy in stage III colon cancer. *J Clin Oncol* (2020), JCO1903205. doi: 10.1200/JCO.19.03205

42. Nagtegaal ID, Marijnen CA, Kranenbarg EK, Mulder-Stapel A, Hermans J, Velde van CJ, et al. Short-term preoperative radiotherapy interferes with the determination of pathological parameters in rectal cancer. *J Pathol* (2002) 197 (1):20–7. doi: 10.1002/path.1098

43. Alberts B JA, Lewis J. T Cells and MHC proteins. In: *Molecular biology of the cell, g. science*. New York: Science Garland (2002).

44. Bennett SR, Carbone FR, Karamalis F, Miller JF, Heath WR. Induction of a CD8+ cytotoxic T lymphocyte response by cross-priming requires cognate CD4+ T cell help. *J Exp Med* (1997) 186(1):65–70. doi: 10.1084/jem.186.1.65

frontiers | Frontiers in Immunology

TYPE Original Research
PUBLISHED 29 September 2022
DOI 10.3389/fimmu.2022.945516



OPEN ACCESS

EDITED BY
Xiaoran Yin,
Second Affiliated Hospital of Xi'an Jiaotong University, China

REVIEWED BY
Yi Ba,
Tianjin Medical University, China
Tian Yang,
Eastern Hepatobiliary Surgery Hospital, China
Weijian Guo,
Fudan University, China

*CORRESPONDENCE
Wensheng Qiu
wsqiuqd@163.com
Shasha Wang
wss_0528@qdu.edu.cn

†These authors have contributed equally to this work

SPECIALTY SECTION
This article was submitted to Cancer Immunity and Immunotherapy, a section of the journal Frontiers in Immunology

RECEIVED 16 May 2022
ACCEPTED 14 September 2022
PUBLISHED 29 September 2022

CITATION
Wang G, Xiao R, Zhao S, Sun L, Guo J, Li W, Zhang Y, Bian X, Qiu W and Wang S (2022) Cuproptosis regulator-mediated patterns associated with immune infiltration features and construction of cuproptosis-related signatures to guide immunotherapy. *Front. Immunol.* 13:945516. doi: 10.3389/fimmu.2022.945516



# Cuproptosis regulator-mediated patterns associated with immune infiltration features and construction of cuproptosis-related signatures to guide immunotherapy

Gongjun Wang[1,2†], Ruoxi Xiao[1†], Shufen Zhao[1], Libin Sun[1], Jing Guo[1], Wenqian Li[1], Yuqi Zhang[1], Xiaoqian Bian[1], Wensheng Qiu[1*] and Shasha Wang[1*]

[1]Department of Oncology, Affiliated Hospital of Qingdao University, Qingdao, China, [2]Shandong Cancer Hospital and Institute, Shandong First Medical University and Shandong Academy of Medical Sciences, Jinan, China

**Background:** Liver hepatocellular carcinoma (HCC) is a prevalent cancer that lacks a sufficiently efficient approach to guide immunotherapy. Additionally, cuproptosis is a recently identified regulated cell death program that is triggered by copper ionophores. However, its possible significance in tumor immune cell infiltration is still unclear.

**Methods:** Cuproptosis subtypes in HCC were identified using unsupervised consensus cluster analysis based on 10 cuproptosis regulators expressions, and a cuproptosis-related risk signature was generated using univariate and LASSO Cox regression and validated using the ICGC data. Moreover, the relationship between signature and tumor immune microenvironment (TME) was studied through tumor immunotherapy responsiveness, immune cell infiltration, and tumor stem cell analysis. Finally, clinical specimens were analyzed using immunohistochemistry to verify the expression of the three genes in the signature.

**Results:** Two subtypes of cuproptosis regulation were observed in HCC, with different immune cell infiltration features. Genes expressed differentially between the two cuproptosis clusters in the TCGA were determined and used to construct a risk signature that was validated using the ICGC cohort. Greater immune and stromal cell infiltration were observed in the high-risk group and were associated with unfavorable prognosis. Elevated risk scores were linked with higher RNA stemness scores (RNAss) and tumor mutational burden (TMB), together with a greater likelihood of benefitting from immunotherapy.

**Conclusion:** It was found that cuproptosis regulatory patterns may play important roles in the heterogeneity of immune cell infiltration. The risk

signature associated with cuproptosis can assess each patient's risk score, leading to more individualized and effective immunotherapy.

KEYWORDS

liver hepatocellular carcinoma, cuproptosis, risk signature, immunotherapy, prognosis

# Introduction

Liver cancer is an aggressive tumor with poor outcomes (1). Liver hepatocellular carcinoma (HCC) accounts for more than 80% of all primary liver malignancies for which surgical resection is currently the most effective treatment (2). Unfortunately, diagnosis of HCC is frequently delayed leading to unfavorable outcomes (3). Despite recent significant progress in immunotherapy and targeted therapy, the five-year survival rate remains low, at approximately 15% (4). An important reason for this is that patients with HCC vary in their response to immunotherapy, and the factors that influence and predict the response to immunotherapy in HCC remain unclear (5).

Recent research has shown that copper toxicity-mediated cell death differs from other forms of regulated cell death; this novel mechanism is termed cuproptosis (6). Copper is both necessary and potentially toxic for cells. It is an essential cofactor required by all living organisms to function properly (7–9); however, high levels of copper accumulation or improper distribution in the cell can lead to cell death. Imbalances in copper homeostasis in cells can lead to severe disease in humans, including tumor development (10, 11). Excess copper has been linked with various types of cancer, including breast (12–14), prostate (15–17), colon (18), lung (19), brain (20), and liver (21) cancer. However, the reasons underlying elevated copper levels in tumors are unclear. Recent studies revealed the mechanism associated with copper-mediated cell death. A study by Tsvetkov et al. showed that cuproptosis is associated with copper binding to fatty acylated moieties of tricarboxylic acid, resulting in the abnormal aggregation of fatty acylated proteins and the loss of iron-sulfur cluster proteins, leading to proteotoxic stress and cell death (6). These findings suggest a starting point for investigating the application of cuproptosis in disease treatment, especially, for tumor therapy.

Copper, as a key trace element, is necessary for the functioning of the immune system. Copper deficiency adversely affects immune function and exposes the organism to microbial infection (22). The immune system requires copper for a variety of functions. The metal can modulate the activation of cells associated with innate immunity such as macrophages and neutrophils during bacterial infection and leukocyte differentiation, maturation, and migration (23, 24). Copper deficiency may also affect immune cell distribution in tissues or the maturation pattern of leukocyte populations (25). In addition, intratumoral copper can regulate PD-L1 expression and affect tumor immune escape (26). These reports suggest an association between copper and the modulation of the immune response.

Here, we used data from the TCGA to investigate cuproptosis subtypes and correlate these subtypes with immune-infiltration features. Signature genes associated with cuproptosis were identified by differential and prognostic analysis, and a risk signature using these genes was generated. This cuproptosis-related risk signature identifies specific features of immune infiltration, permitting the development of individualized immunotherapy.

# Methods

## Collection of data

Data on gene expression (fragments per kilobase, FPKM), mutations, and clinical data were obtained from the Cancer Genome Atlas (TCGA) database (https://portal.gdc.cancer.gov/). Patients lacking survival information were not enrolled. Xena (http://xena.ucsc.edu/) was utilized to obtain copy number variation (CNV) data and RNA stemness scores (RNAss) for TCGA samples. Validation was performed using data available from the International Cancer Genome Consortium (ICGC) (https://dcc.ICGC.org/projects/LIRI-JP) for 229 HCC patients with complete information. The 10 cuproptosis regulators identified by Tsvetkov et al. (6) were used (Table S1). Since TCGA and ICGC data are publicly available, permission from an ethics committee was not necessary for this work. Despite this, the investigation was performed in conformity with the procedure specifications established by the TCGA and the ICGC.

## Profiling of cuproptosis regulators

Principal component analysis (PCA) using the expression of cuproptosis regulators was performed on both HCC and normal

samples with the package "scatterplot3d" in R, with relationships between the regulators examined using "corrplot", and the CNVs of 10 regulators on human chromosomes using "Rcircos".

## Consensus cluster analysis of cuproptosis regulators

The "ConsensusClusterPlus" package in R was employed for unsupervised consensus cluster analysis (27). The criteria for clustering were an initial gradual increase in the cumulative distribution function (CDF) curve, strong intraclass relationships and weak interclass relationships, and no unacceptably small sample sizes in any of the groups. The R packages "ggplot2" and "Rtsne" were used for PCA and t-distributed random neighbor embedding (t-SNE) analysis, respectively. Overall survival (OS) in the different clusters was analyzed with Kaplan-Meier (K-M) curves. Enrichment analysis of genes was conducted with gene set enrichment analysis (GSEA, v4.2.1; https://www.gsea-msigdb.org/gsea/downloads.jsp) (28) and Gene Ontology (GO) using the R package "clusterProfiler" (29).

## Immune infiltration profiles in the different groups

The relative abundance levels of immune cell types in the HCC microenvironment were examined by single-sample GSEA (ssGSEA) (30, 31). Immune cell genomes obtained from Charoentong et al. (32) were used as markers for the various cell types. Tumor immune dysfunction and rejection (TIDE; http://tide.dfci.harvard.edu/) was also used as a marker for examining immune escape mechanisms and predicting the response to immunotherapy (33). Higher TIDE scores indicate a greater likelihood of immune escape, leading to the probability of reduced treatment efficacy. The degree of infiltration of six immune cell types associated with the expression of three differentially expressed genes (DEGs) was determined with the Tumor Immune Estimation Resource (TIMER) database (https://cistrome.shinyapps.io/timer/) (34, 35). The "SCNA" module was utilized to compare infiltration levels between tumors with different CNVs for specific genes.

## Comparison of responsiveness to immunotherapy

The IMvigor 210 cohort comprising cancer patients treated with programmed death ligand 1 (PD-L1) inhibitors was used for the prediction of immunotherapy response (36). These samples were categorized based on the patient's response, namely partial response (PR), complete response (CR), progressive disease (PD), and stable disease (SD), with PR and CR representing immunotherapy response and PD and SD representing a lack of response. The R package "pRRophetic" was utilized to compute the half-maximal inhibitory concentration (IC50) of the drugs with low IC50 values indicating greater drug sensitivity.

## Construction and validation of the HCC risk signature

Two patient clusters were formed based on the expression of the 10 cuproptosis-related regulatory genes. Genes expressed differentially between the clusters were determined with the empirical Bayesian method in the "limma" package with significance set as an adjusted P-value < 0.0001. Further DEGs between HCC samples and adjacent normal tissue were analyzed to narrow down candidate signature genes (P<0.0001). Finally, univariate Cox regression as well as least absolute shrinkage and selection operator (LASSO) analysis (37) were employed to detect DEGs in the final signature. Risk scores were calculated for all HCC samples and groups with low-risk and high-risk were identified in the TCGA cohort based on median risk scores. The risk score was calculated as:

$$\text{Risk Score} = \sum_{i=0}^{n} \beta i * Gi$$

where $\beta i$ denotes the gene coefficient; $i$ and $n$ are the number of genes in the signature; $Gi$ denotes the gene expression value.

The risk scores for samples in the ICGC set were then determined using the risk coefficients of the signature DEGs in the TCGA, and the ICGC samples were allocated two groups (low risk and high risk) using the risk thresholds observed in the TCGA. K-M survival curves were utilized to evaluate OS between the groups. Risk signature sensitivity and specificity were calculated using receiver operating characteristic (ROC) curves.

## Nomogram construction and verification

In both the TCGA and ICGC cohorts, hazard ratio models were developed using univariate and multivariate Cox regression to detect independent prognostic variables. A nomogram including risk scores and other clinicopathological features was then constructed in the TCGA cohort and one-, three-, and five-year calibration curves for constructed for accuracy validation. The area under the ROC curve (AUC) and decision curve analysis (DCA) were used to evaluate the nomogram's discriminative power.

## Determination of the relationships between tumor mutation and risk signature

The R package "maftools" was used to generate the waterfall charts for the low- and high-risk groups respectively. Somatic mutation analysis was used to determine the tumor mutational burden (TMB) score of each TCGA-HCC patient. Subsequently, the Pearson correlation analysis was studied to determine the link between risk score and TMB. The data was further expressed in scatterplots and boxplots. In addition, boxplots were generated to demonstrate the differences in immune cell infiltration between the low- and high-TMB groups, respectively. The overall survival (OS) rate among these groups were determined through K-M survival curves.

## Comparison of immunohistochemistry in normal and HCC samples

Immunohistochemical staining was performed with antibodies against human G6PD (25413-1-AP; proteintech), CDCA8 (bs-7834R; Boaosen), and Cyclin B1 (bs-0572R; Boaosen), followed by a pathologist based on the percentage of positive cells and staining intensity to score sections. Staining intensity was scored as 0 (negative), 1 (weak), 2 (moderate), or 3 (strong), and the proportion of positive cells expressed was scored as 1 (0-25%), 2 (26-50%), 3 (51– 75%) or 4 (76–100%). The final score was obtained by multiplying the expression ratio and the signal intensity.

## Expression and prognostic analysis of three DEGs

The expression of three genes differentially expressed between normal tissues and HCC was analyzed using the "limma" R package, and the "surv cutpoint" function in "survminer" was employed to examine the optimal cut-off expression values for survival. Groups with high and low expression were established and OS was compared between groups using K-M analysis.

## Statistical analysis

All statistical analysis was conducted using R version 4.1.2 (http://www.R-project.org) and its accompanying packages. The Kruskal-Wallis test and one-way ANOVA were used to examine differences between three or more groups. OS comparisons were conducted using K-M analysis and the log-rank test. Univariate and multivariate Cox regression analyses were used to calculate hazard ratios and identify independent risk factors. The diagnostic value of risk scores and nomogram models was assessed using ROC curves. $P<0.05$ was considered to be the criterion for significant statistical difference.

# Results

## The landscape of cuproptosis regulators in HCC

Based on the study by Tsvetkov et al. (6),10 cuproptosis regulators (7 positive regulators and 3 negative regulators) were included in this study. The expression of these regulators differed significantly between normal and HCC tissues. Apart from the critical regulator FDX1, which was down-regulated in HCC, all other regulators were up-regulated in tumor tissue in comparison with controls (Figure 1A). PCA analysis indicated that the expression of all 10 regulatory genes clearly distinguished between HCC and normal tissue (Figure 1B). After the division of the genes into high and low expression groups using "survminer", it was observed that low levels of FDX1 were linked with poor HCC prognosis, while the remaining genes exhibited an opposite trend ($P>0.05$ for DLD due to insufficient sample) (Figure S1). Analysis of co-expression of the regulators indicated that all had positive regulatory relationships apart from FDX1 where a negative relationship was observed (Figure 1C). The highest correlation (0.47) was seen between DLD and PHAR1. The regulatory network demonstrated both the interactions between the genes and their potential prognostic significance for HCC (Figure 1D). The inconsistent findings for FDX1 suggest that it may be more critical in the regulation of cuproptosis (6). Further analysis of the genetic basis of cuproptosis using the TMBs and CNVs of the 10 regulators showed alterations in 5.85% of the 364 samples (16 mutations). The highest number of mutations was seen in CDKN2 followed by DLD and MTF1 (Figure 1E). CNVs were common in the 10 genes, with LOSS occurring more frequently than GAIN. LIAS and GLS showed higher CNV gains, while CDKN2 exhibited higher loss (Figure 1F). Figure 1G shows the chromosomal location of the regulators' CNVs. These findings marked different levels of these regulatory factors in tumor and normal tissues, implicating disturbances in cuproptosis regulator expression in HCC.

## Correlations between cuproptosis clusters and TME features

Patterns of cuproptosis were determined by unsupervised consensus cluster analysis of cuproptosis regulator expression in HCC and the results of the consensus clustering (k2–9) were visualized with a CDF plot (Figures 2A; S2). Examination of the

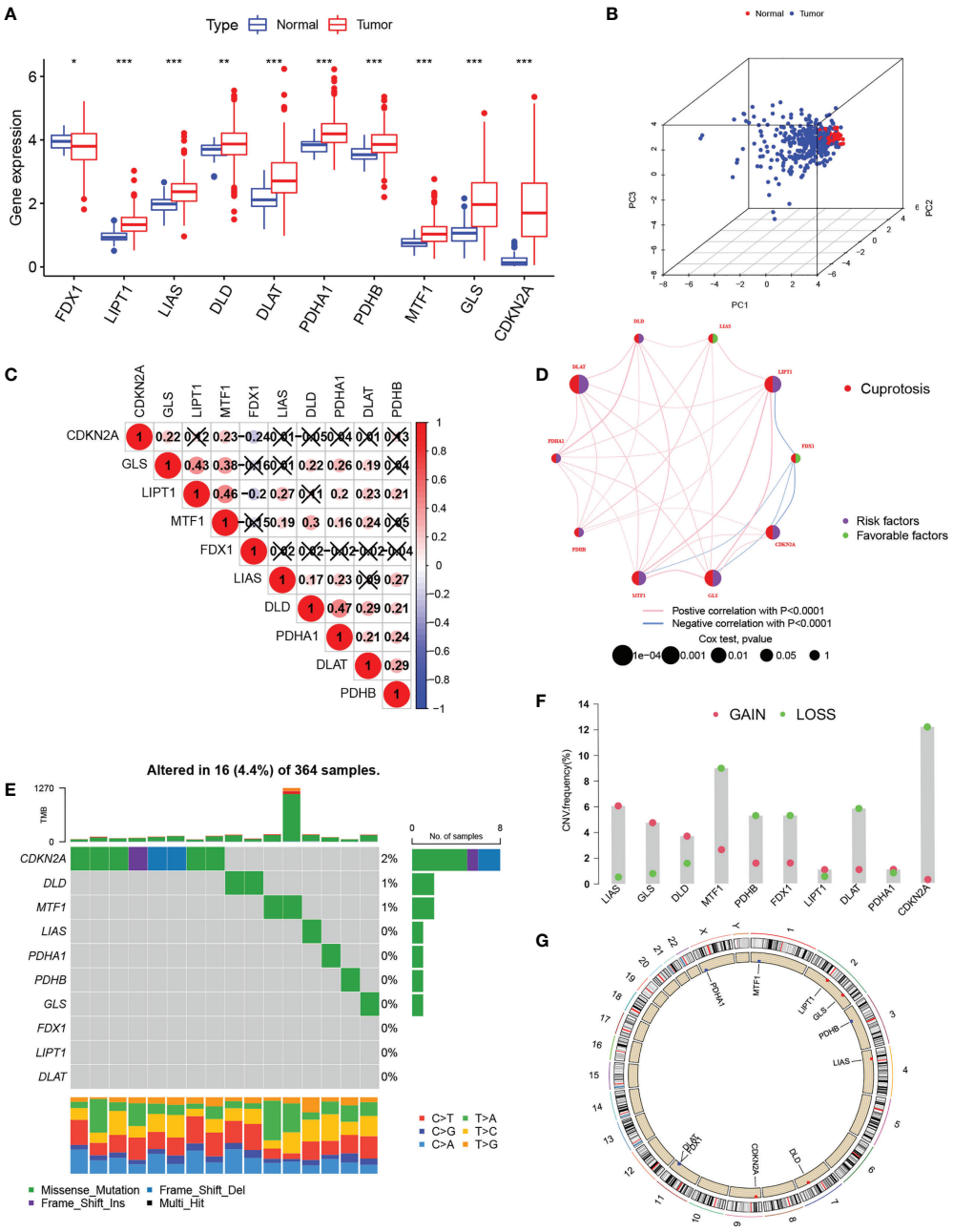


FIGURE 1
Expression of cuproptosis-regulatory genes in HCC. **(A)** Comparison of expression between normal and tumor tissues **(B)** PCA of the expression of the 10 genes. **(C)** Spearman correlations between genes. The color blue represents negative regulation; the color red represents positive regulation. **(D)** Comprehensive network map combining cuproptosis regulator interactions and prognosis. **(E)** Mutation frequencies of the 10 regulatory genes in 364 HCC s specimens. **(F)** CNV values for cuproptosis regulators in HCC specimens. **(G)** Chromosomal locations of CNV alterations in cuproptosis regulators. *P < 0.05; **P < 0.01; ***P < 0.001. HCC, hepatocellular carcinoma; PCA, principal component analysis; CNV, copy number variation.

consensus matrix showed that k=2 was the best option, and that each sample in the cluster exhibited a strong correlation (Figure 2A). The HCC patients were, therefore, assigned to one of two clusters (A or B). The clustering results are shown in Table S2. PCA (Figure 2B) and t-SNE (Figure 2C) analysis showed that there were two discrete directions within the clusters. Furthermore, we found that the prognosis of these patients was significantly different, with patients in cluster A showing better OS (Figure 2D). Multi-GSEA enrichment analysis indicated significant differences in biological processes between the clusters, specifically, in

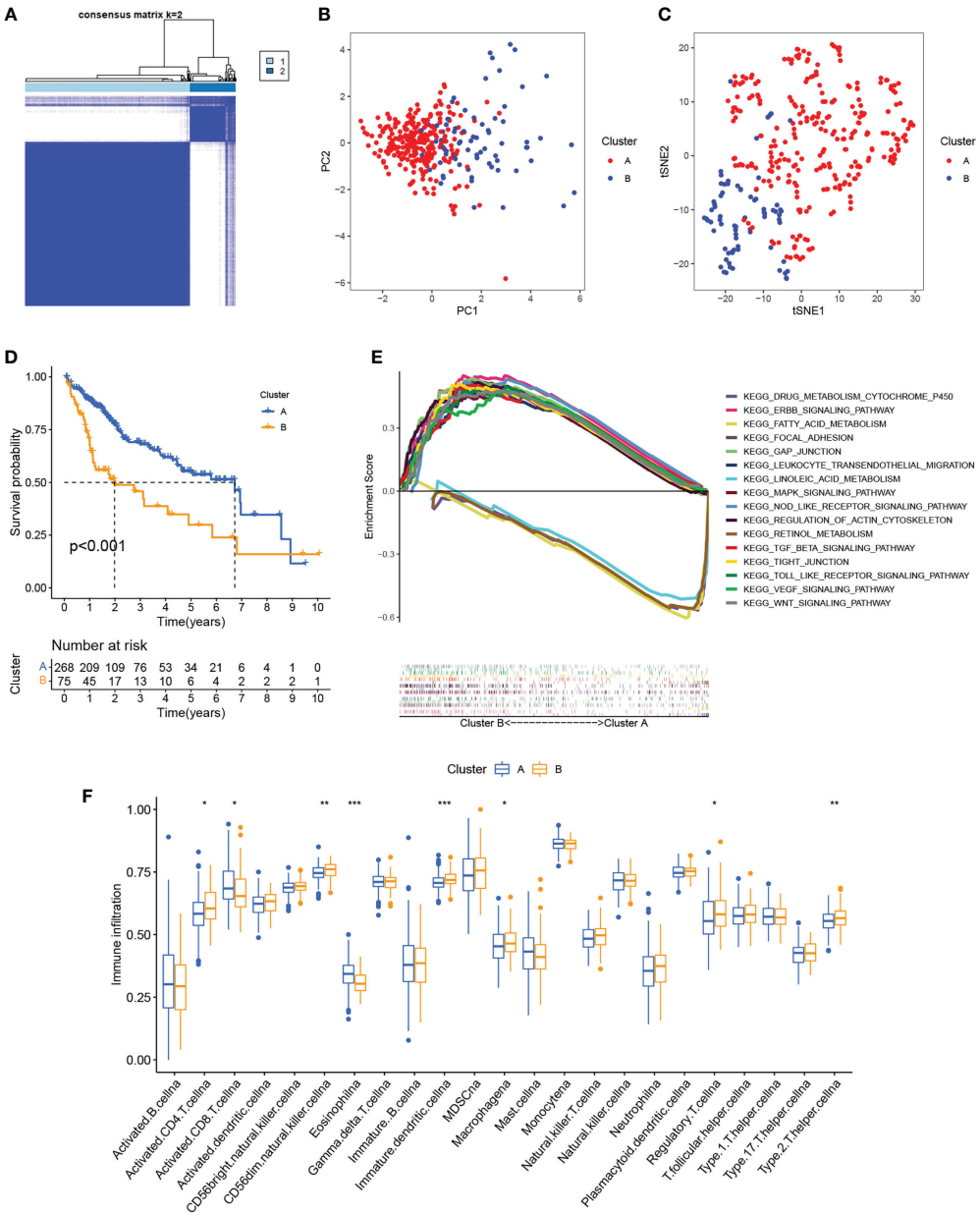


FIGURE 2
Identification of cuproptosis clusters. **(A)** Consensus matrix based on cuproptosis regulator expression in the HCC cohort at k = 2. **(B)** PCA of consensus matrix when k = 2. **(C)** T-SNE analysis of consensus matrix when k = 2. **(D)** K-M survival analysis between the two cuproptosis clusters. **(E)** Multiple GSEA analysis between the two cuproptosis clusters. **(F)** Infiltration of immune cells between the two cuproptosis clusters. *P < 0.05; **P < 0.01; ***P < 0.001. HCC, hepatocellular carcinoma; PCA, principal component analysis; T-SNE, t-distributed random neighbor embedding; K-M, Kaplan-Meier; GSEA, gene set enrichment analysis.

metabolism, tumor signaling pathways, and immune- and matrix-related pathways (Figure 2E). The enriched metabolic processes included those associated with fatty acid, linoleic acid, retinol, and drug metabolism cytochrome P450 showing greater enrichment in cluster A. Cluster B showed greater enrichment in the tumor-associated ERBB, MAPK, TGFβ, VEGF, and Wnt signaling pathways. Pathways related to immune activation were associated mostly with cluster B; these included leukocyte transendothelial migration, Toll-like receptor signaling, and NOD-like receptor signaling. We then investigated infiltrating immune cells in the clusters (Figure 2F), finding that the majority of immune cells were strongly associated with cluster B. At the same time, we also found that matrix-activated pathways such as focal adhesions, gap junctions, and tight junctions were enriched in cluster B

(Figure 2E). It has been reported that tumor stromal cells are involved in immune regulation (38). Stromal cells are able to block immune cell entry into the tumor parenchyma and can also block T-cell killing of tumor cells (39). Tumor cells and stromal cells can induce angiogenesis, thereby promoting tumor metastasis (40).. In addition, regulatory T cells and CD 56bright NK cells highly expressed in cluster B can act as immunosuppressive cells to promote tumorigenic immune escape (41, 42). The results of the immune microenvironment analysis described above validate the poor prognosis of cluster B patients. Taken together, we found that the expression of cuproptosis regulatory proteins in HCC defines two patient clusters with significantly different immune infiltration features. Cluster A is an immune-desert phenotype with reduced immune activity and immune cell numbers while cluster B is an immune-exclusion phenotype with infiltration restricted to the peripheral matrix of tumor cells.

## Characterization of cuproptosis-related phenotypes

We next identified 629 cuproptosis-associated DEGs using the R package "limma". GO analysis showed enrichment of the DEGs in immune- and stromal-associated pathways (including neutrophil mediated immunity, neutrophil activation involved in immune response, focal adhesion, and cell–substrate junctions), confirming that cuproptosis is closely associated with the regulation of the immune microenvironment of the tumor (Figure 3A). We then further narrowed the range by comparing gene expression between the normal and HCC groups to obtain 30 DEGs. Univariate Cox regression yielded 27 prognosis-associated DEGs with HCC patients again divided into two clusters according to the unsupervised consensus cluster analysis of the expression of these genes (Figures 3B; S3). The gene clustering results are presented in Table S3. Differential expression of most of the cuproptosis regulators was visible between the clusters (Figure 3C). Additionally, RNAss values were significantly increased in gene cluster B compared with gene cluster A (Figure 3D), demonstrating the adverse effects of high RNAss values on HCC prognosis (Figure 3E). Oncogenic and immune- and matrix-activated pathways were enriched in cluster B, while cluster A showed enrichment in metabolic pathways (Figure 3F). These findings suggest the presence of two cuproptosis-associated regulatory patterns in HCC.

## Development of the cuproptosis-associated risk signature

The above analysis was performed on a patient population. We then investigated the precise quantification of cuproptosis patterns in individual patients. Using the 27 genes identified in the univariate analysis (Figure 4A), we performed LASSO to prevent signature overfitting (Figures 4B, C). The risk signature was finally constructed using three signature genes (CDCA8, CCNB1, and G6PD). The risk score assigned to each sample was determined as: Risk Score = (0.066092028117448) × the CDCA8 expression + (0.00250484775117196) × the CCNB1 expression + (0.00581254249797367) × the G6PD expression. This enabled the HCC patients to be entirely separated into groups with low and high risk according to the median risk score. The risk score results are provided in Table S4. PCA showed the clear separation of the 343 HCC patients and 279 DEGs in two independent clusters, trending in two different directions (Figures 4D, E). The scatter plots of risk scores and patient survival statistics are presented in Figures 4F, G. As depicted in the figure, a higher risk score was related to both decreased survival and greater mortality. The heatmap (Figure 4H) shows the expression of the three DEGs in the signature in the TCGA cohort (Figure 4H). K-M curves indicated higher OS rates in the low-risk group (Figure 4I). To examine the performance of signature, ROC curves for one-, two-, and three-year OS were generated, with AUCs of 0.783, 0.725, and 0.686, respectively (Figure 4J). The risk signature's superiority was further established by comparing the one-year ROC curves with other clinicopathological features (Figure 4K). Univariate Cox regression was employed to examine associations, finding that stage (HR = 1.804, 95% CI = 1.456–2.234, $p < 0.001$) and risk score (HR = 3.935, 95% CI =2.740–5.649, $p < 0.001$) were related to OS in the TCGA set (Figure 4L). Multivariate regression verified that stage (HR = 1.609, 95% CI = 1.274–2.031, $p < 0.001$) and risk score (HR = 3.236, 95% CI = 2.176–4.811, $p < 0.001$) were independent prognostic factors for OS (Figure 4M).

## Validation of the risk signature

The test group samples from the ICGC were divided into low- (n = 104) and high- (n = 125) risk score groups using the cutoff values determined in the TCGA cohort. Figures 5A, B show the risk curves and scatterplots while the heatmap in Figure 5C illustrates the expression patterns of the three signature DEGs in the ICGC set. The high-risk group, as determined in the TCGA cohort, had a worse overall prognosis (Figure 5D). The AUCs of the ROC curves for one, two, and three years were 0.757, 0.760, and 0.785, respectively (Figure 5E), and the AUC of the risk score at one year was larger than those for other clinical parameters (Figure 5F). Both univariate and multivariate regression analyses found that the P-values for both risk score and sex were below 0.05, demonstrating that signature functioned as an independent predictor of HCC prognosis in the ICGC set, and further confirming its reliability in the TCGA set (Figures 5G, H).

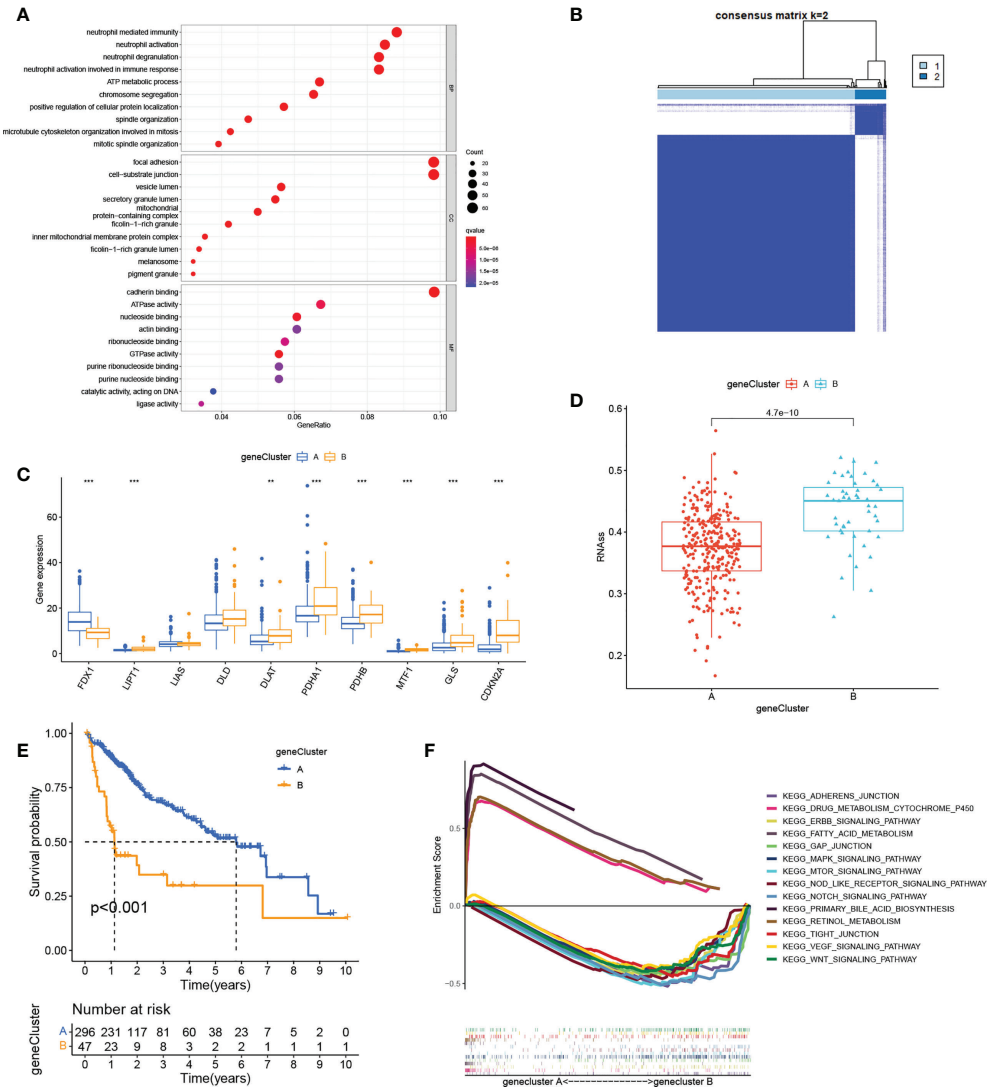


FIGURE 3
Gene cluster determination. **(A)** GO enrichment analysis of cuproptosis-related DEGs. **(B)** Consensus matrix based on cuproptosis-related gene expression in the HCC cohort at k = 2. **(C)** Differential expression of cuproptosis regulators in the two clusters. **(D)** RNAss values of cuproptosis regulators in the two clusters. **(E)** K-M survival analysis of cuproptosis regulators in the two clusters. **(F)** Multiple GSEA analysis between the two clusters. **P < 0.01; ***P < 0.001. GO, Gene Ontology; DEGs, differentially expressed genes; HCC, liver hepatocellular carcinoma; RNAss, RNA stemness scores; K-M, Kaplan-Meier; GSEA, gene set enrichment analysis.

## Nomogram creation and validation

To further improve the clinical utility of risk signature, the identified independent prognostic risk factors, namely, risk score and stage, were utilized to develop a nomogram for predicting OS in the TCGA cohort (Figure 5I). The calibration curves at one, three, and five years showed that the nomogram accurately predicted the outcomes of HCC patients (Figure 5J). In addition, the DCA curve showed that the nomogram had specific advantages over other clinical parameters (Figure 5K). The AUCs for the ROC curves suggested that the nomogram, with an AUC of 0.804, was superior to age (AUC=0.493), sex (AUC=0.508), pathological grade (AUC=0.490), TNM stage (AUC=0.713), and risk signature (AUC=0.788) for predicting prognosis in HCC patients (Figure 5L).

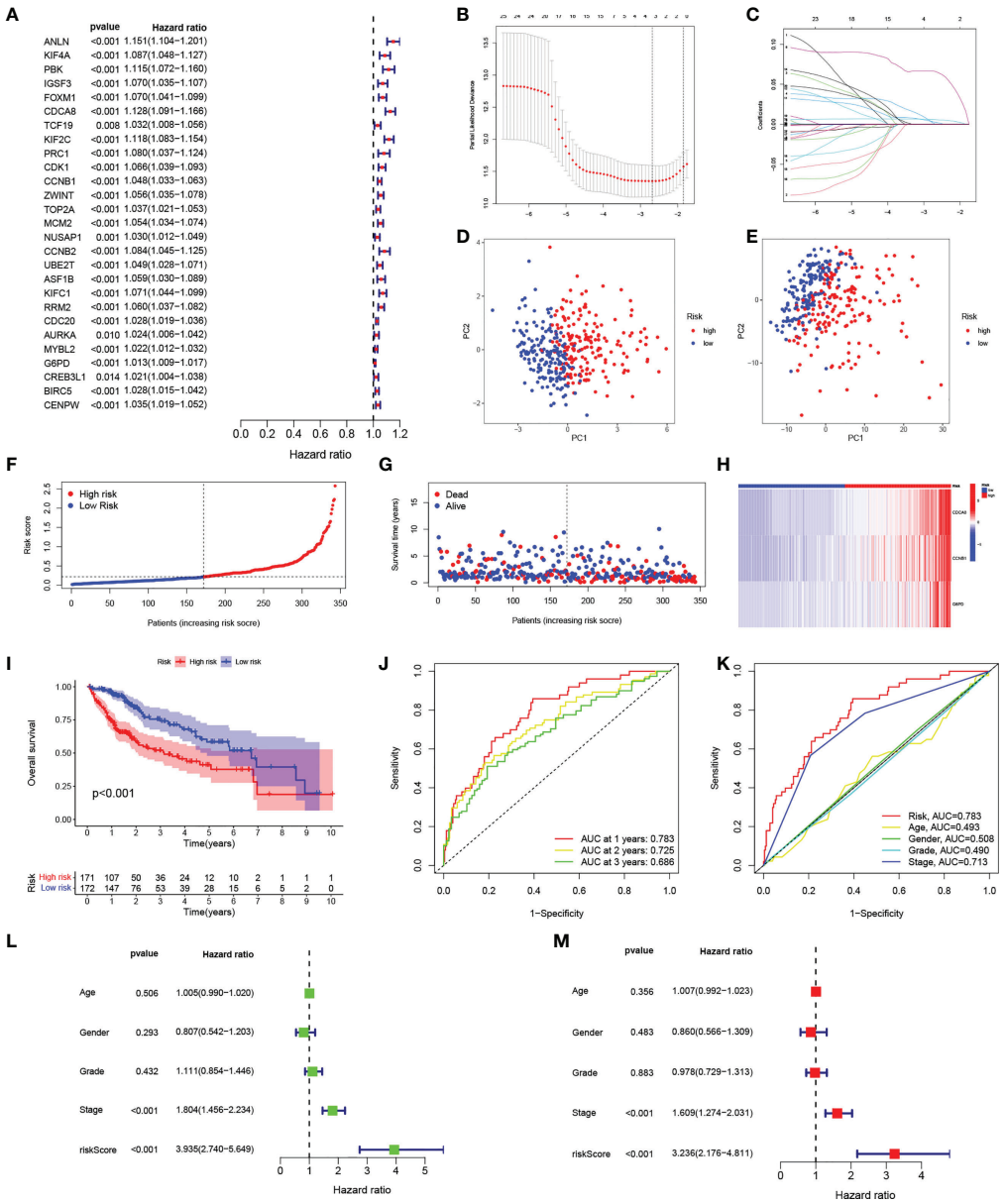


FIGURE 4
Construction of the risk signature. **(A)** Forest plot of univariate Cox regression results for the 27 DEGs. **(B)** Cross-validation for selection of tuning parameters in LASSO regression. **(C)** LASSO coefficient profiles of candidate DEGs. **(D)** PCA of samples from high- and low-risk groups. **(E)** PCA of DEGs in the high- and low-risk groups. **(F)** Risk score distribution of HCC patients in the TCGA cohort. **(G)** Scatter plot of survival status of HCC patients in the TCGA cohort. **(H)** Heatmap of the expression of the three signature genes in high- and low-risk populations in the TCGA cohort. **(I)** K-M curves of OS in HCC patients in the risk score-based TCGA cohort. **(J)** ROC curves of prognostic signatures for one, two, and three years in the TCGA cohort. **(K)** ROC curves of prognostic signatures and other clinicopathological features for one year in the TCGA cohort. **(L, M)** Forest plots of univariate and multivariate Cox regression analyses of prognostic signatures and clinical features in the TCGA cohort. DEGs, differentially expressed genes; LASSO, least absolute shrinkage and selection operator; PCA, principal component analysis; HCC, hepatocellular carcinoma; TCGA, the Cancer Genome Atlas; K-M, Kaplan-Meier; OS, overall survival; ROC, receiver operating characteristic.

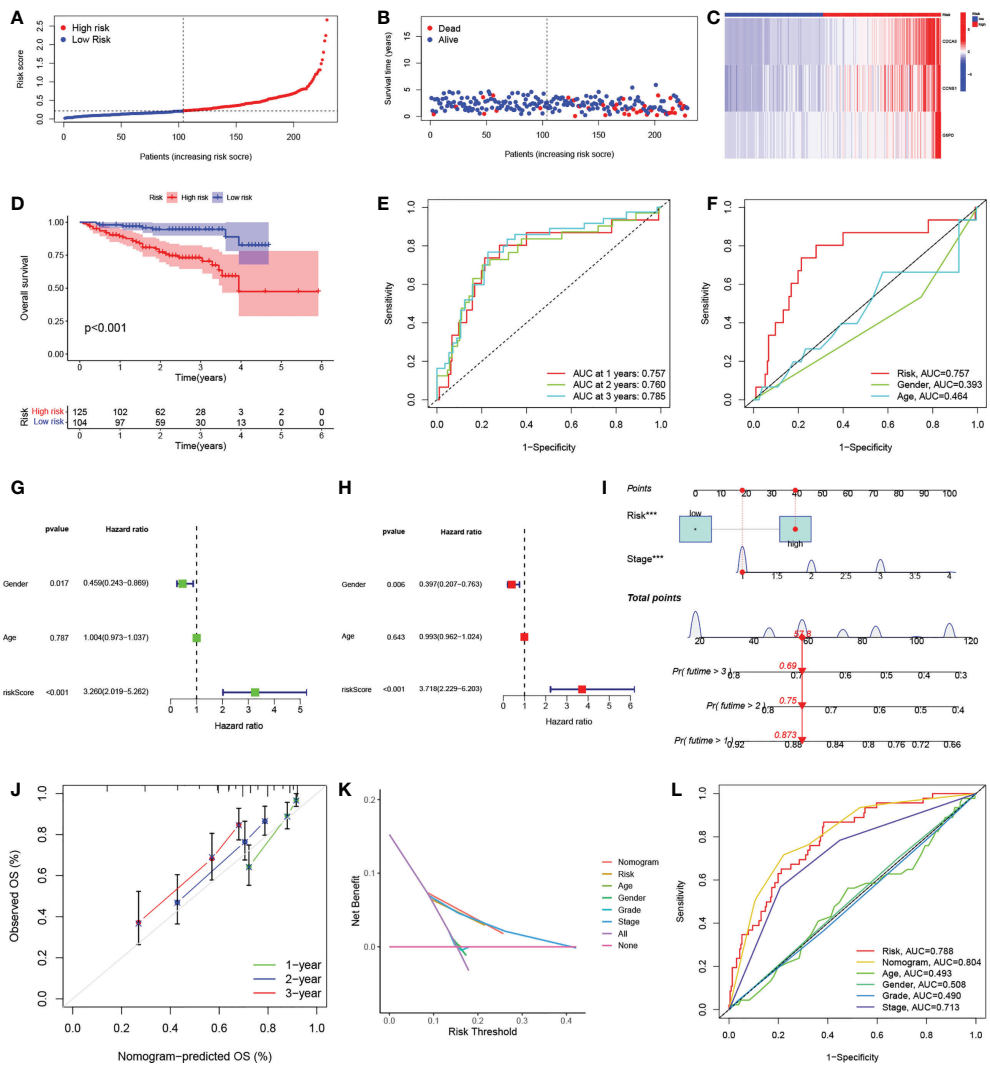


FIGURE 5
Independent verification of risk signatures and construction of nomograms. **(A)** Distribution of HCC patient risk scores in the ICGC cohort. **(B)** Scatterplot showing HCC patient OS in the ICGC cohort. **(C)** Heatmap of the expression of the three signature genes in high- and low-risk groups in the ICGC cohort. **(D)** K-M curves for HCC patient OS in the risk score-based ICGC cohort. **(E)** ROC curves of one-, two, and three-year prognostic signatures in the ICGC cohort. **(F)** ROC curves of one-year prognostic signatures with other clinicopathological characteristics in the ICGC cohort. **(G-H)** Forest plots of univariate and multivariate Cox regression analyses of prognostic signatures and other clinicopathological features in the ICGC cohort. **(I)** Nomogram combining risk signatures and clinical stages for OS prediction in the TCGA cohort. **(J)** Calibration plots for nomograms at one, three, and five years. **(K)** DCA of the nomogram, risk signature, and other clinicopathological features. **(L)** ROC curves of the nomogram, risk signature, and clinicopathological characteristics at one year. HCC, hepatocellular carcinoma; ICGC, International Cancer Genome Consortium; K-M, Kaplan-Meier; OS, overall survival; ROC, receiver operating characteristic; DCA, decision curve analysis.

## Relationships between the risk signature and immune characteristics, clinical parameters

A GSEA analysis was next used to investigate physiology-related differences between the groups (Figure 6A). The results were consistent with those of the clustering analysis, showing that many metabolism-related pathways, including those associated with fatty acid, cytochrome P450, and retinol metabolism were enriched in the low-risk group. Tumor-associated pathways (including the MAPK, NOTCH, and VEGF pathways) and immune- and matrix-related pathways (including the Toll-like receptor, B cell receptor, T cell receptor, chemotaxis factor pathways, and attachment junctions) were associated with high risk. To confirm the immune characteristics of the signature, we examined associations between immune

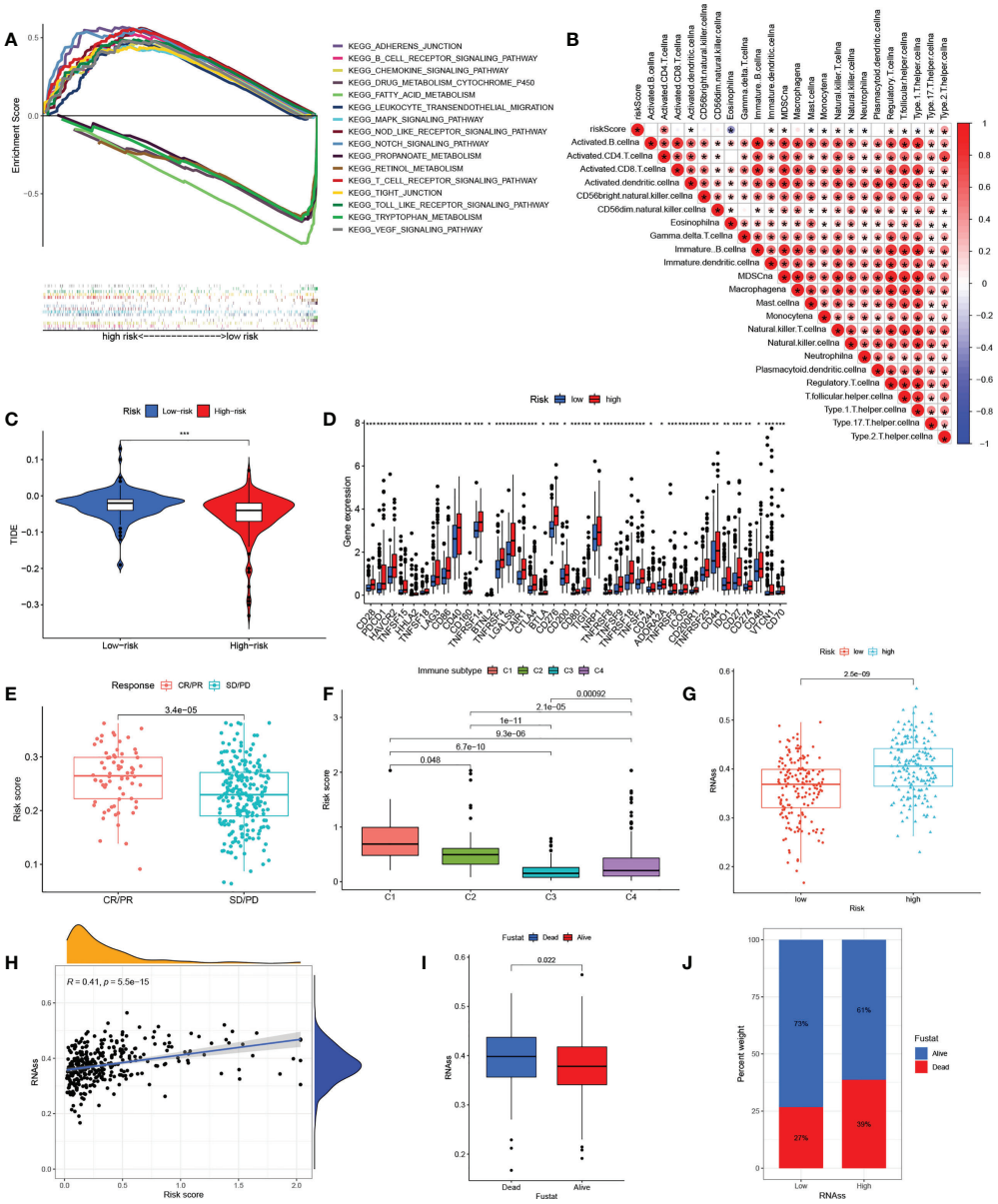


FIGURE 6
The correlation between the immunity and risk signature. **(A)** Multiplex GSEA analysis between groups with high and low risk **(B)** Correlations between infiltration of immune cell levels and risk scores. The color blue implies a negative association; the color red denotes a positive association. **(C)** TIDE scores in the groups with high and low risk. **(D)** Expression of immune checkpoints in the groups with high and low risk. **(E)** Risk scores in anti-PD1/PD-L1-treated CR/PR samples and SD/PD samples in the IMvigor210 cohort. **(F)** Risk scores in relation to immune cell subtypes. **(G)** RNAss values in the groups with high and low risk. **(H)** Relationships between risk scores and RNAss values. **(I)** RNAss values in deceased and surviving patients. **(J)** Proportions of deceased and surviving patients in the groups with high and low RNAss. GSEA, gene set enrichment analysis; TIDE, tumor immune dysfunction and rejection; PR, partial response; CR, complete response; PD, progressive disease; SD, stable disease; RNAss, RNA stemness scores. The asterisks represented the statistical p value (*P < 0.05; **P < 0.01; ***P < 0.001.)

cells and risk scores. This indicated a positive relationship between risk scores and most immune cells (Figure 6B). Taken together, it appears that high-risk scores are indeed associated with increased stromal activity and immune infiltration. Interestingly, the TIDE analysis indicated that immune escape was likely to be reduced in the high-risk group after immunotherapy (Figure 6C). It was also found that immune checkpoint levels, including those of PDCD1 and CTLA4, were raised in the high-risk group, which thus had a greater chance of benefitting from immunotherapy (Figure 6D). Calculation of the risk scores of patients in the IMvigor210 set using the TCGA set risk signature indicated that patients responding (CR/PR) to

anti-PD1/PD-L1 therapy showed significantly raised risk scores (Figure 6E). We then compared HCC samples for differences in risk scores based on tumor immunophenotyping established by Thorsson et al. (43). The immunophenotyping of the HCC samples is presented in Table S5. The Wound Healing (immune C1) risk score was found to be higher than others, suggesting that high-risk scores were associated with matrix activation (Figure 6F). In addition, analysis of tumor stemness indicated that RNAss was raised in the high-risk group (Figure 6G) with a positive association between the risk scores and RNAss (Figure 6H). The RNAss values of the HCC samples are presented in Table S6. Deceased HCC patients had higher RNAss values than surviving patients (Figure 6I). The OS values in the high- and low-RNAss groups were 61% and 73%, respectively (Figure 6J), indicating both the prognostic significance of RNAss and the reliability of the risk score measure. Furthermore, the associations between clinical features and risk scores are shown in Figures S4A–F. Risk scores were found to increase significantly with TNM stage from I to III, T stage from I to III, grade from G1 to G4, and AFP expression from low to high. The risk scores did not change significantly in response to age or sex. In addition, boxplots were used to show the results for 12 drug sensitivities by estimating IC50 values between the groups. Patient groups at low risk were significantly more sensitive to Gefitinib, Sorafenib, Nilotinib, Dasatinib, Erlotinib, and Metformin (Figure S5A–F), in contrast to high-risk patients who responded to Bleomycin, Doxorubicin, Gemcitabine, Tipifarnib, Imatinib, and Mitomycin.C (Figure S5G–K). This has reference significance for guiding the clinical medication of HCC treatment.

## Crosstalk among cuproptosis clusters, gene clusters, risk signature, and clinicopathological features

The alluvial map shown in Figure 7A illustrated the crosstalk among cuproptosis clusters, gene clusters, and risk scores. Higher risk scores were associated with gene cluster B rather than gene cluster A (Figure 7B) and the cuproptosis cluster B also had higher risk scores than cluster A (Figure 7C). The prognosis was significantly enhanced in both cluster A and gene cluster A in comparison with their respective B clusters, again confirming the reliability and consistency of the analysis. Figure 7D shows a comprehensive heatmap of risk scores in relation to clinical features (including age, sex, grade, and TNM, T, N, and M stages), cuproptosis clustering, gene clustering, and cuproptosis regulator expression. A strong association between cuproptosis clusters, gene clusters, and risk signatures can be observed.

## An examination of the correlation between the risk signature and genetic mutations

Differences in somatic mutation distribution between low- and high-risk scores in the TCGA set were investigated with the "maftools" package. As Figures 8A, B show, the TMB was greater in the group with the high-risk scores, together with an 88.89% mutation rate (altered in 144 of 162 samples) versus 80.72% for the low-scoring group (altered in 134 of 166 samples). Quantitative analysis confirmed that tumors with high scores were correlated with higher TMB values (Figure 8C) and that risk scores and TMB values were significantly positively correlated (Figure 8D). It has been reported that high TMB is related to long-term clinical sensitivity to anti-PD1/PD-L1 therapy (44), confirmed by the findings shown in Figures 6C–E. This suggests that curoptosis-associated variations in tumors may be critical for the anti-PD-1/PD-L1 therapeutic response. High TMB values were also linked to reduced immune cell infiltration in HCC (Figure 8E) while K-M survival curves showed an association between elevated TMB and worse OS (Figure 8F), indirectly confirming the effectiveness of the risk score in the prediction of immunotherapy outcome.

## Three DEGs in the risk signature

Finally, we analyzed the three DEGs in the risk signature. The expression of these genes was found to significantly raised in TCGA-HCC samples in comparison with normal tissue (Figures 9A–C). These results were confirmed by IHC analysis (Figures 9D–F). On the basis of gene expression, patients in the TCGA were classified into one of two groups. Low levels of expression were linked to a better prognosis, thus confirming the results in Figure 5, and all three genes represented prognostic risk factors for HCC in the risk signature (Figures 9G–I). Moreover, the DEGs expression was revealed to be positively associated with immune cell infiltration using TIMER (Figures S6A–C). Boxplots were used to compare the immune cell subset distribution with CNVs, and it can be seen that the greatest differences in arm-level gain in relation to immune infiltration were with CCNB1 and G6PD, whereas the level of immune infiltration with arm-level deletion was most significantly different in CDCA8 (Figures S6D–F).

# Discussion

Recent research has shown that the homeostasis of copper is rigorously regulated and that any imbalance reduces the organism's fitness (45). Disruptions to copper homeostasis have

10.3389/fimmu.2022.945516

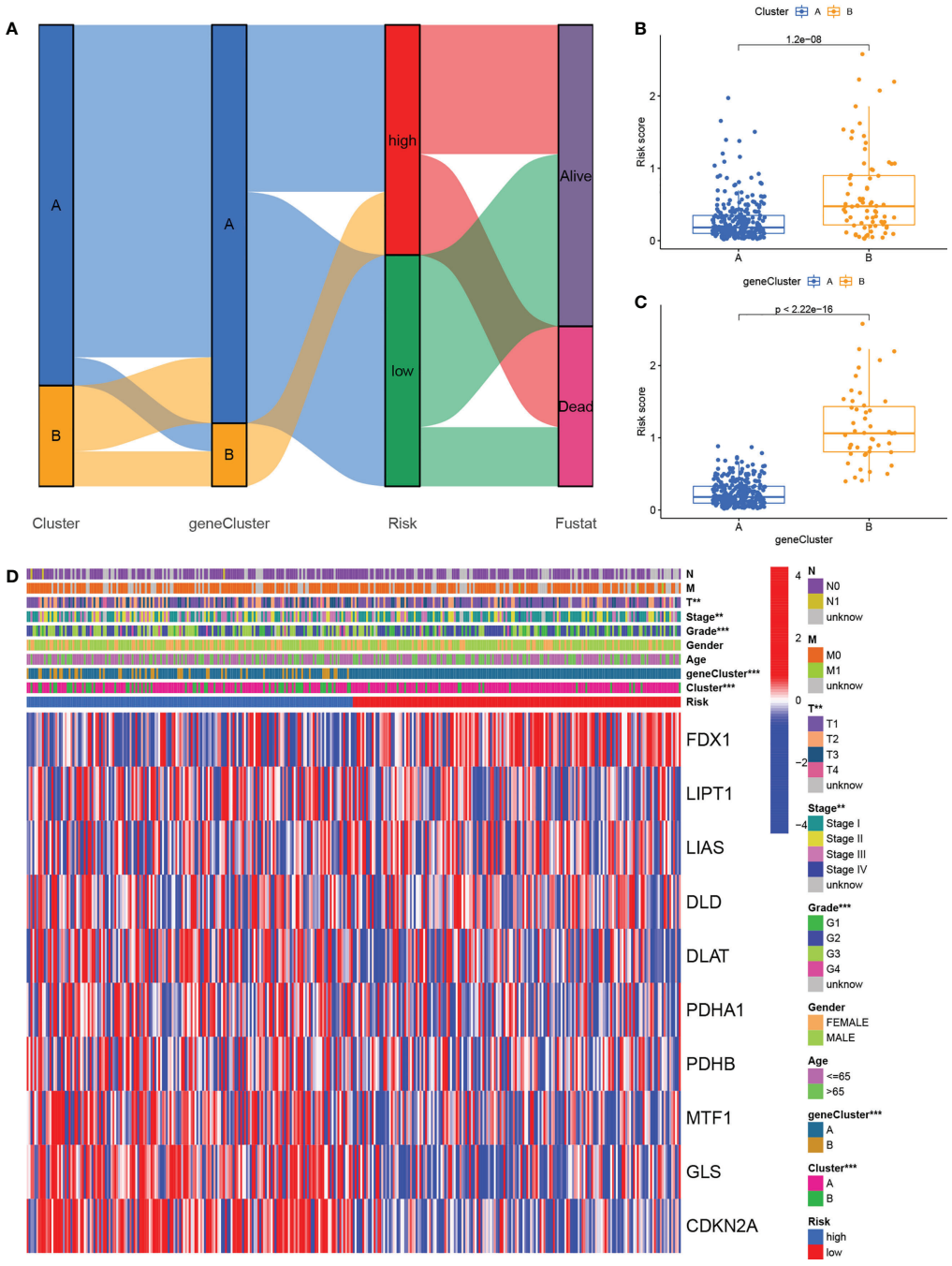


FIGURE 7
Relationship cross-links of cuproptosis clusters, gene clusters, risk signatures, and clinical features. **(A)** Alluvial diagram showing cuproptosis clusters, gene clusters, risk grouping, and survival status. **(B)** Risk scores in the cuproptosis clusters. **(C)** Risk scores in the gene clusters. **(D)** Heatmaps showing the integration of cuproptosis clusters, gene clusters, clinicopathological characteristics, and cuproptosis regulators' expression in relation to risk groups.

also been linked with tumor growth and irreversible damage (46). Thus, the role of copper *in vivo* has attracted much attention, specifically in the field of tumor therapy. Cuproptosis is a form of programmed cell death; the regulation of cuproptosis is complex, involving numerous regulatory factors. The role of cuproptosis in tumor development and its relationship to immunity has not been fully evaluated. Here, we systematically characterized immune cell infiltration mediated by cuproptosis, as well as the corresponding

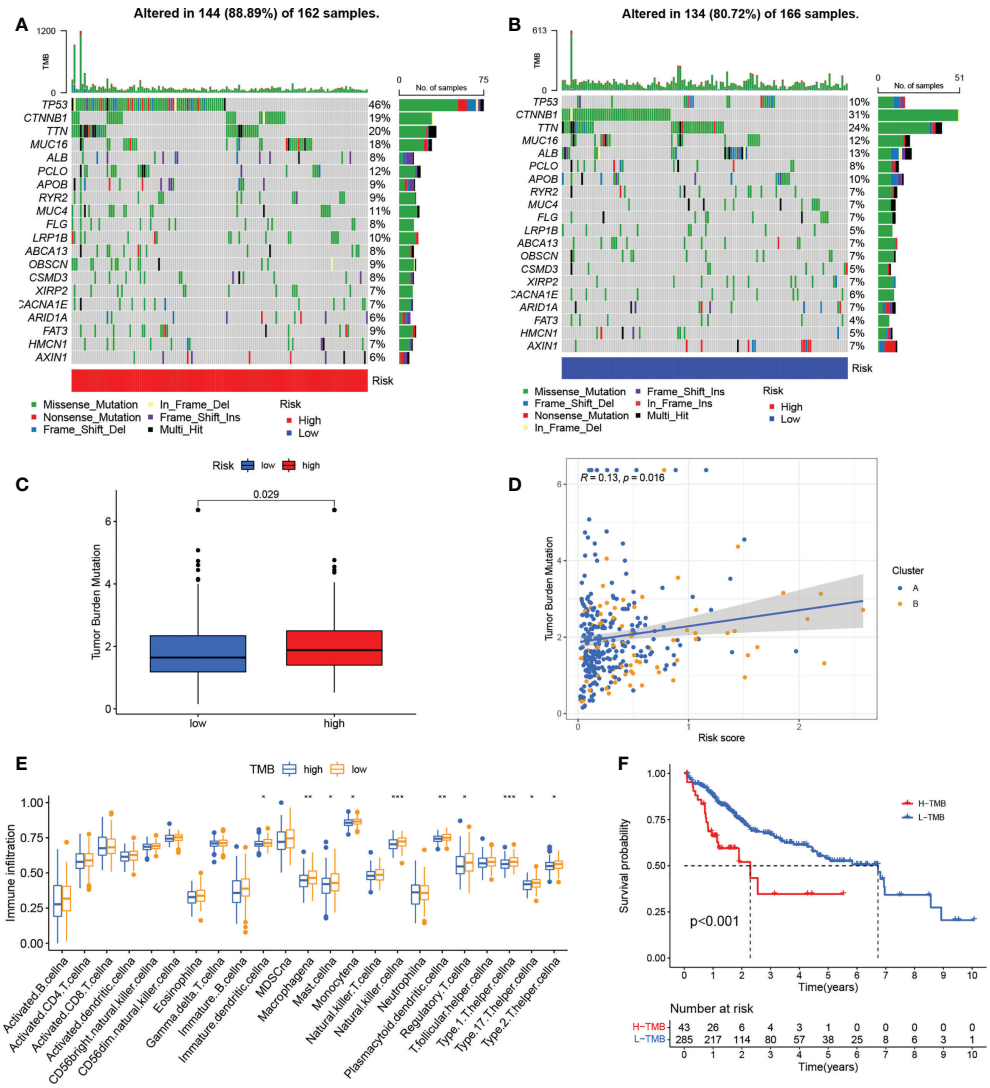


FIGURE 8
Associations between risk signatures and gene mutations. **(A, B)** Mutation frequencies in the groups with high and low risk **(C)** TMB values in the groups with high and low risk **(D)** Association between risk scores and TMB. **(E)** Infiltration of immune cell in the groups with high and low TMB. **(G)** K-M curves for OS in the groups with high and low TMB. *P < 0.05; **P < 0.01; ***P < 0.001. TMB, tumor mutational burden; K-M, Kaplan-Meier.

cuproptosis regulatory subtypes. In addition, a cuproptosis-related risk signature was developed to correlate individual cuproptosis subtypes with the patient's sensitivity to immunotherapy, suggesting the potential usefulness of the signature for personalized therapy.

The study initially evaluated the expression levels, somatic mutations, and CNVs of 10 cuproptosis regulators, observing that all of the regulatory genes were shown to be expressed differently in tumor and control tissues. The highest mutation frequency was seen in CDKN2A. In addition, the copy numbers of most of the cuproptosis regulators were altered. This suggests that dysfunctional expression of these regulator genes may play an essential role in HCC. Unsupervised consensus cluster analysis of the regulators identified two distinct subtypes in HCC, termed cuproptosis clusters A and B. Surprisingly, GSEA enrichment analysis found that cluster A was mainly related to metabolic processes, while cluster B was enriched in various oncogenic and immune- and stromal-related signaling pathways. Stromal cells are documented to play immunomodulatory roles in tumors (47, 48), are able to prevent the entry of immune cells into the tumor parenchyma (49) and, even if T cells do enter the tumor microenvironment, stromal cells can surround them and prevent an effective immune response (50). Further analysis showed that cuproptosis cluster B was correlated with significant infiltration of

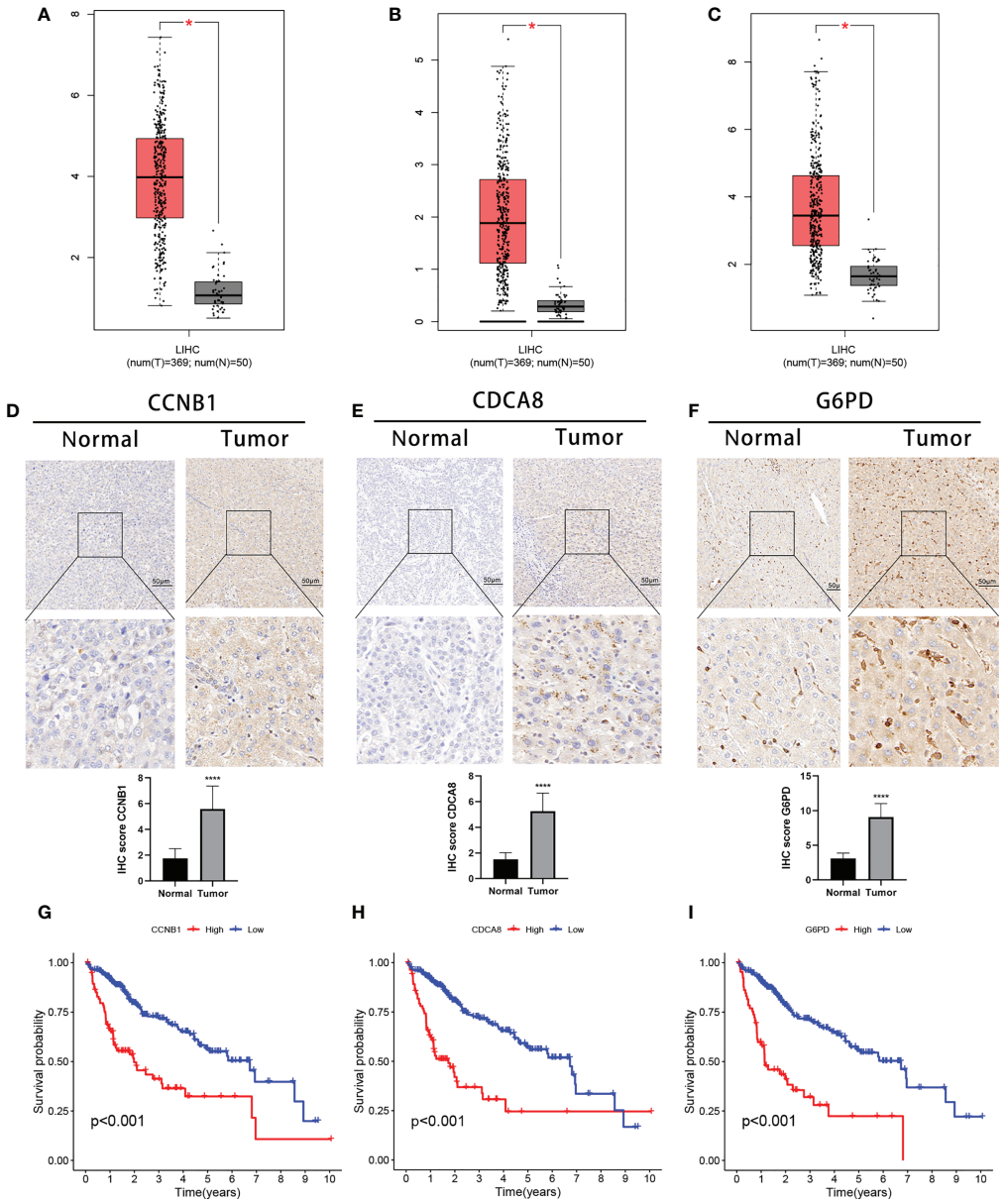


FIGURE 9
Expression of the three signature DEGs and their impact on prognosis. Expression of CCNB1 **(A)**, CDCA8 **(B)**, and G6PD **(C)** in tumor and normal samples (GEPIA). IHC analysis of CCNB1 **(D)**, CDCA8 **(E)**, and G6PD **(F)** expression in tumor and normal samples. K-M survival analysis between high- and low-expression groups of CCNB1 **(G)**, CDCA8 **(H)**, and G6PD **(I)**.*P < 0.05;****P < 0.0001. DEGs, differentially expressed genes.

immune cells, including regulatory cells such as regulatory T cells and CD 56bright NK cells. These findings suggest that cuproptosis cluster B contains a large number of immune cells, but activity may be suppressed by stromal and immune regulatory cells. K-M survival analysis showed that cluster B was linked with a poorer prognosis, possibly due to tumor escape resulting from immunosuppression.

To quantify the cuproptosis regulatory subtypes in individual tumors, a risk signature based on three DEGs was developed as a scoring system for individual HCC patients in the TCGA cohort. Both K-M survival and ROC curve evaluations verified the signature's accuracy and reliability for predicting patient prognosis. In addition, we independently verified the signature using gene expression and clinical data from the ICGC database. The signature served as an independent prognostic variable in both the TCGA and ICGC cohorts, as demonstrated by multivariate Cox regression. A nomogram using a

combination of the risk signature and clinical features was found to be more effective than other clinical features, greatly improving the clinical utility of the signature.

In our study, three DEGs were identified as cuproptosis-related signature genes. Glucose-6-phosphate dehydrogenase (G6PD) is a rate-limiting enzyme in the pentose phosphate pathway and is involved in energy generation through the maintenance of reduced NADPH co-enzyme levels (51). Because of its key metabolic role, G6PD is also involved in tumor pathogenesis where it has been reported to modulate proliferation (52, 53), metastasis (54), chemoresistance (55, 56), immune activation (57, 58), and tumor ferroptosis (59). Cell division cycle-associated 8 (CDCA8) forms part of the chromosomal passenger complex (CPC) and is necessary for the stabilization of the mitotic spindle. Disruption of cell cycle regulation is a hallmark of tumor development (60). CDCA8 levels are elevated in a variety of tumor types where it has been implicated in the growth and tumor progression (61–64). Cyclin B1 (CCNB1) belongs to the cyclin family and is the regulatory component of cyclin-dependent kinase 1 (65, 66). It has important functions in cell cycle regulation and dysfunctional expression promotes the development of various cancer types, including colon (67–69), cervical cancer (70), and kidney cancer (71). CCNB1 overexpression leads to unplanned entry into the cell cycle, uncontrolled cell proliferation, and tumorigenesis (69, 72–74). Studies have also shown that copper can affect the expression of G6PD and CCNB1, confirming a possible link between DEGs and cuproptosis (75, 76).

Although immunotherapy is effective for HCC (77), its efficacy has not proved consistent due to an incomplete understanding of the immune microenvironment and its variations in individual patients. It is thus necessary to determine which patients are most likely to react to immunotherapy. Here, it was found that the two risk-score subgroups had distinct immune infiltration characteristics with greater infiltration and matrix activity seen in patients with higher risk score. These patients also had lower TIDE scores, suggesting that they were more likely to be sensitive to immunotherapy and less likely to show immune escape (78). Another important result was that there was higher expression of immune checkpoints in this group. And these genes may be targeted by immunotherapy to determine the clinical response of patients (79). The accuracy of the cuproptosis-related risk signature for predicting the response to immunotherapy was confirmed by analysis in the IMvigor210 cohort. In addition, we found differences in TMB values between the groups and demonstrated an association between the risk and TMB scores. It has been reported that higher non-synonymous mutational burdens in tumors result in the formation of greater numbers of neoantigens, leading to greater immunogenicity and enhancing the immunotherapy response (80). This was an additional confirmation of the likelihood that high-risk patients will respond to immunotherapy. These findings indicate that the risk score is both reliable and effective for evaluating cuproptosis-modulating subtypes in individual patients and can also be applied effectively to determining the degree of immune cell infiltration and providing guidance for immunotherapy.

## Conclusion

In conclusion, our study identified two patterns of cuproptosis regulation based on the expression of 10 cuproptosis regulators that are important contributors to the heterogeneity of immune cell infiltration. The cuproptosis-related risk signature, which is closely associated with the prognosis, immune cell infiltration characteristics, and sensitivity to immunotherapy in HCC patients, can quantify the risk of individual patients, providing new directions for individualized anti-tumor immunotherapy for HCC patients.

## Data availability statement

The original contributions presented in the study are included in the article/Supplementary Material. Further inquiries can be directed to the corresponding authors.

## Ethics statement

The affiliated hospital of Qingdao University approved the collection of clinical data for research purposes. (Approval No. QYFYWZLL26947). The patients/participants provided their written informed consent to participate in this study.

## Author contributions

GW, RX, and SZ analyzed the data. GW, RX, LS, and JG wrote the manuscript. WL, YZ, and XB reviewed and comprehensively revised the manuscript. WQ and SW contributed to the design of the study. All authors contributed to the article and approved the submitted version.

## Funding

This study was supported by four grants: 1. Beijing Xisike Clinical Oncology Research Foundation (Y-XD2019-11) 2. Qingdao traditional Chinese medicine science and technology project (2021-zyym29) 3. Shandong medical and health science and technology development plan project (202103030554) 4. State Key Laboratory of Ultrasound in Medicine and Engineering (2021KFKT029).

## Acknowledgments

The authors gratefully acknowledge the data provided by patients and researchers participating in TCGA and ICGC.

## Conflict of interest

The authors declare that the research was conducted in the absence of any commercial or financial relationships that could be construed as a potential conflict of interest.

## Publisher's note

All claims expressed in this article are solely those of the authors and do not necessarily represent those of their affiliated organizations, or those of the publisher, the editors and the reviewers. Any product that may be evaluated in this article, or claim that may be made by its manufacturer, is not guaranteed or endorsed by the publisher.

## Supplementary material

The Supplementary Material for this article can be found online at: https://www.frontiersin.org/articles/10.3389/fimmu.2022.945516/full#supplementary-material

SUPPLEMENTARY FIGURE 1
Curves of K-M for OS in the groups with high and low expression of 10 cuproptosis regulators. **(A)** FDX1; **(B)** LITP1; **(C)** LIAS; **(D)** DLD; **(E)** DLAT; **(F)** PDHA1; **(G)** PDHB; **(H)** MTF1; **(I)** GLS; **(J)** CDKN2A. K-M Kaplan-Meier, OS overall survival

SUPPLEMENTARY FIGURE 2
Cuproptosis clustering. **(A–G)** Consensus matrix based on cuproptosis regulator expression in the HCC cohort at k = 2 - 9. **(H)** Consensus CDF plots for cuproptosis clustering. **(I)** The area under the CDF curve relative changes for cuproptosis clustering

SUPPLEMENTARY FIGURE 3
Gene clustering **(A–G)** Consensus matrix based on cuproptosis-related gene expression in the HCC cohort at k= 2-9. **(H)** Consensus CDF plots for gene clustering. **(I)** The area under the CDF curve relative changes for gene clustering. HCC hepatocellular carcinoma, CDF cumulative distribution function

SUPPLEMENTARY FIGURE 4
Comparison of risk scores within different grades or between different classifications of clinicopathological features. **(A)** Stage; **(B)**T; **(C)** Grade; **(D)** AFP expression; **(E)** Sex; **(F)** Age.

SUPPLEMENTARY FIGURE 5
Comparison of drug sensitivity between groups with high and low risk. **(A)** Gefitinib; **(B)** Sorafenib; **(C)** Nilotinib; **(D)** Dasatinib; **(E)** Erlotinib; **(F)** Metformin; **(G)** Bleomycin; **(H)** Doxorubicin; **(I)** Gemcitabine; **(J)** Tipifarnib; **(K)** Imatinib; **(L)** Mitomycin.C.

SUPPLEMENTARY FIGURE 6
The relationship between the three DEGs in the signature and immunity and copy number. **(A–C)** Correlation between expression of gene and infiltration of immune cell. **(D–F)** Association of gene copy number alterations with infiltration of immune cells. *P < 0.05; **P < 0.01; ***P < 0.001. DEGs differentially expressed genes

## References

1. Sung H, Ferlay J, Siegel RL, Laversanne M, Soerjomataram I, Jemal A, et al. Global cancer statistics 2020: GLOBOCAN estimates of incidence and mortality worldwide for 36 cancers in 185 countries. *CA: Cancer J Clin* (2021) 71(3):209–49. doi: 10.3322/caac.21660

2. Mehta N. Hepatocellular carcinoma-how to determine therapeutic options. *Hepatol Commun* (2020) 4(3):342–54. doi: 10.1002/hep4.1481

3. Fattovich G, Stroffolini T, Zagni I, Donato F. Hepatocellular carcinoma in cirrhosis: incidence and risk factors. *Gastroenterology.* (2004) 127(5 Suppl 1):S35–50. doi: 10.1053/j.gastro.2004.09.014

4. Yin JM, Sun LB, Zheng JS, Wang XX, Chen DX, Li N. Copper chelation by trientine dihydrochloride inhibits liver RFA-induced inflammatory responses *in vivo*. *Inflammation Res Off J Eur Histamine Res Soc [et al]* (2016) 65(12):1009–20. doi: 10.1007/s00011-016-0986-2

5. Zheng Y, Wang T, Tu X, Huang Y, Zhang H, Tan D, et al. Gut microbiome affects the response to anti-PD-1 immunotherapy in patients with hepatocellular carcinoma. *J immunother cancer.* (2019) 7(1):193. doi: 10.1186/s40425-019-0650-9

6. Tsvetkov P, Coy S, Petrova B, Dreishpoon M, Verma A, Abdusamad M, et al. Copper induces cell death by targeting lipoylated TCA cycle proteins. *Sci (New York NY)* (2022) 375(6586):1254–61. doi: 10.1126/science.abf0529

7. Tapiero H, Townsend DM, Tew KD. Trace elements in human physiology and pathology. *Copper Biomedicine pharmacotherapy = Biomedecine pharmacotherapie.* (2003) 57(9):386–98. doi: 10.1016/S0753-3322(03)00012-X

8. Vassiliev V, Harris ZL, Zatta P. Ceruloplasmin in neurodegenerative diseases. *Brain Res Brain Res Rev* (2005) 49(3):633–40. doi: 10.1016/j.brainresrev.2005.03.003

9. Fraga CG. Relevance, essentiality and toxicity of trace elements in human health. *Mol aspects Med* (2005) 26(4-5):235–44. doi: 10.1016/j.mam.2005.07.013

10. Squitti R, Polimanti R. Copper hypothesis in the missing hereditability of sporadic alzheimer's disease: ATP7B gene as potential harbor of rare variants. *J Alzheimer's Dis JAD.* (2012) 29(3):493–501. doi: 10.3233/JAD-2011-111991

11. Squitti R, Barbati G, Rossi L, Ventriglia M, Dal Forno G, Cesaretti S, et al. Excess of nonceruloplasmin serum copper in AD correlates with MMSE, CSF [beta]-amyloid, and h-tau. *Neurology.* (2006) 67(1):76–82. doi: 10.1212/01.wnl.0000223343.82809.cf

12. Huang YL, Sheu JY, Lin TH. Association between oxidative stress and changes of trace elements in patients with breast cancer. *Clin Biochem* (1999) 32(2):131–6. doi: 10.1016/S0009-9120(98)00096-4

13. Kuo HW, Chen SF, Wu CC, Chen DR, Lee JH. Serum and tissue trace elements in patients with breast cancer in Taiwan. *Biol Trace element Res* (2002) 89(1):1–11. doi: 10.1385/BTER:89:1:1

14. Rizk SL, Sky-Peck HH. Comparison between concentrations of trace elements in normal and neoplastic human breast tissue. *Cancer Res* (1984) 44(11):5390–4.

15. Habib FK, Dembinski TC, Stitch SR. The zinc and copper content of blood leucocytes and plasma from patients with benign and malignant prostates. *Clinica chimica acta; Int J Clin Chem* (1980) 104(3):329–35. doi: 10.1016/0009-8981(80)90390-3

16. Nayak SB, Bhat VR, Upadhyay D, Udupa SL. Copper and ceruloplasmin status in serum of prostate and colon cancer patients. *Indian J Physiol Pharmacol* (2003) 47(1):108–10.

17. Chen D, Dou QP. New uses for old copper-binding drugs: Converting the pro-angiogenic copper to a specific cancer cell death inducer. *Expert Opin Ther targets* (2008) 12(6):739–48. doi: 10.1517/14728222.12.6.739

18. Majumder S, Chatterjee S, Pal S, Biswas J, Efferth T, Choudhuri SK. The role of copper in drug-resistant murine and human tumors. *Biometals an Int J role*

*metal ions biology biochemistry Med* (2009) 22(2):377–84. doi: 10.1007/s10534-008-9174-3

19. Zhang X, Yang Q. Association between serum copper levels and lung cancer risk: A meta-analysis. *J Int Med Res* (2018) 46(12):4863–73. doi: 10.1177/0300060518798507

20. Turecký L, Kalina P, Uhlíková E, Námerová S, Krizko J. Serum ceruloplasmin and copper levels in patients with primary brain tumors. *Klinische Wochenschrift.* (1984) 62(4):187–9. doi: 10.1007/BF01731643

21. Moffett JR, Puthillathu N, Vengilote R, Jaworski DM, Namboodiri AM. Acetate revisited: A key biomolecule at the nexus of metabolism, epigenetics and oncogenesis-part 1: Acetyl-CoA, acetogenesis and acyl-CoA short-chain synthetases. *Front Physiol* (2020) 11:580167. doi: 10.3389/fphys.2020.580167

22. Muñoz C, Rios E, Olivos J, Brunser O, Olivares M. Iron, copper and immunocompetence. *Br J Nutr* (2007) 98 Suppl 1:S24–8. doi: 10.1017/S0007114507833046

23. Djoko KY, Ong CL, Walker MJ, McEwan AG. The role of copper and zinc toxicity in innate immune defense against bacterial pathogens. *J Biol Chem* (2015) 290(31):18954–61. doi: 10.1074/jbc.R115.647099

24. Festa RA, Thiele DJ. Copper at the front line of the host-pathogen battle. *Plos pathogens* (2012) 8(9):e1002887. doi: 10.1371/journal.ppat.1002887

25. Percival SS.Copper and immunity. *Am J Clin Nutr* (1998) 67 (5 Suppl):1064s–8s. doi: 10.1093/ajcn/67.5.1064S

26. Voli F, Valli E, Lerra L, Kimpton K, Saletta F, Giorgi FM, et al. Intratumoral copper modulates PD-L1 expression and influences tumor immune evasion. *Cancer Res* (2020) 80(19):4129–44. doi: 10.1158/0008-5472.CAN-20-0471

27. Wilkerson MD, Hayes DN. ConsensusClusterPlus: A class discovery tool with confidence assessments and item tracking. *Bioinf (Oxford England)* (2010) 26 (12):1572–3. doi: 10.1093/bioinformatics/btq170

28. Subramanian A, Tamayo P, Mootha VK, Mukherjee S, Ebert BL, Gillette MA, et al. Gene set enrichment analysis: A knowledge-based approach for interpreting genome-wide expression profiles. *Proc Natl Acad Sci USA* (2005) 102(43):15545–50. doi: 10.1073/pnas.0506580102

29. Yu G, Wang LG, Han Y, He QY. clusterProfiler: An r package for comparing biological themes among gene clusters. *Omics: J Integr Biol* (2012) 16(5):284–7. doi: 10.1089/omi.2011.0118

30. Bindea G, Mlecnik B, Tosolini M, Kirilovsky A, Waldner M, Obenauf AC, et al. Spatiotemporal dynamics of intratumoral immune cells reveal the immune landscape in human cancer. *Immunity* (2013) 39(4):782–95. doi: 10.1016/j.immuni.2013.10.003

31. Finotello F, Trajanoski Z. Quantifying tumor-infiltrating immune cells from transcriptomics data. *Cancer immunology immunother: CII* (2018) 67(7):1031–40. doi: 10.1007/s00262-018-2150-z

32. Charoentong P, Finotello F, Angelova M, Mayer C, Efremova M, Rieder D, et al. Pan-cancer immunogenomic analyses reveal genotype-immunophenotype relationships and predictors of response to checkpoint blockade. *Cell Rep* (2017) 18 (1):248–62. doi: 10.1016/j.celrep.2016.12.019

33. Jiang P, Gu S, Pan D, Fu J, Sahu A, Hu X, et al. Signatures of T cell dysfunction and exclusion predict cancer immunotherapy response. *Nat Med* (2018) 24(10):1550–8. doi: 10.1038/s41591-018-0136-1

34. Li B, Severson E, Pignon JC, Zhao H, Li T, Novak J, et al. Comprehensive analyses of tumor immunity: Implications for cancer immunotherapy. *Genome Biol* (2016) 17(1):174. doi: 10.1186/s13059-016-1028-7

35. Li T, Fan J, Wang B, Traugh N, Chen Q, Liu JS, et al. TIMER: A web server for comprehensive analysis of tumor-infiltrating immune cells. *Cancer Res* (2017) 77(21):e108–e10. doi: 10.1158/0008-5472.CAN-17-0307

36. Bell D, Berchuck A, Birrer M, Chien J, Cramer DW, Dao F. Integrated genomic analyses of ovarian carcinoma. *Nature.* (2011) 474(7353):609–15. doi: 10.1038/nature10166

37. Crown WH. Potential application of machine learning in health outcomes research and some statistical cautions. *Value Health J Int Soc Pharmacoeconomics Outcomes Res* (2015) 18(2):137–40. doi: 10.1016/j.jval.2014.12.005

38. Chen DS, Mellman I. Elements of cancer immunity and the cancer-immune set point. *Nature.* (2017) 541(7637):321–30. doi: 10.1038/nature21349

39. Zhang B, Wu Q, Li B, Wang D, Wang L, Zhou YL. m6A regulator-mediated methylation modification patterns and tumor microenvironment infiltration characterization in gastric cancer. *Mol cancer.* (2020) 19(1):53. doi: 10.1186/s12943-020-01170-0

40. Moserle L, Casanovas O. Anti-angiogenesis and metastasis: a tumour and stromal cell alliance. *J Internal Med* (2013) 273(2):128–37. doi: 10.1111/joim.12018

41. Groth C, Hu X, Weber R, Fleming V, Altevogt P, Utikal J, et al. Immunosuppression mediated by myeloid-derived suppressor cells (MDSCs) during tumour progression. *Br J cancer.* (2019) 120(1):16–25. doi: 10.1038/s41416-018-0333-1

42. Tian Z, Gershwin ME, Zhang C. Regulatory NK cells in autoimmune disease. *J autoimmunity* (2012) 39(3):206–15. doi: 10.1016/j.jaut.2012.05.006

43. Thorsson V, Gibbs DL, Brown SD, Wolf D, Bortone DS, Ou Yang TH, et al. The immune landscape of cancer. *Immunity.* (2018) 48(4):812–30.e14. doi: 10.1016/j.immuni.2018.03.023

44. Barroso-Sousa R, Keenan TE, Pernas S, Exman P, Jain E, Garrido-Castro AC, et al. Tumor mutational burden and PTEN alterations as molecular correlates of response to PD-1/L1 blockade in metastatic triple-negative breast cancer. *Clin Cancer research: an Off J Am Assoc Cancer Res* (2020) 26(11):2565–72. doi: 10.1158/1078-0432.CCR-19-3507

45. De la Iglesia R, Valenzuela-Heredia D, Andrade S, Correa J, González B. Composition dynamics of epilithic intertidal bacterial communities exposed to high copper levels. *FEMS Microbiol ecology* (2012) 79(3):720–7. doi: 10.1111/j.1574-6941.2011.01254.x

46. Guo W, Zhang X, Lin L, Wang H, He E, Wang G, et al. The disulfiram/copper complex induces apoptosis and inhibits tumour growth in human osteosarcoma by activating the ROS/JNK signalling pathway. *J Biochem* (2021) 170(2):275–87. doi: 10.1093/jb/mvab045

47. Cremasco V, Astarita JL, Grauel AL, Keerthivasan S, MacIsaac K, Woodruff MC, et al. FAP delineates heterogeneous and functionally divergent stromal cells in immune-excluded breast tumors. *Cancer Immunol Res* (2018) 6(12):1472–85. doi: 10.1158/2326-6066.CIR-18-0098

48. Canzonetta C, Pelosi A, Di Matteo S, Veneziani I, Tumino N, Vacca P, et al. Identification of neuroblastoma cell lines with uncommon TAZ+/mesenchymal stromal cell phenotype with strong suppressive activity on natural killer cells. *J immunother Cancer* (2021) 9(1):1055. doi: 10.1136/jitc-2020-001313

49. Turley SJ, Cremasco V, Astarita JL. Immunological hallmarks of stromal cells in the tumour microenvironment. *Nat Rev Immunol* (2015) 15(11):669–82. doi: 10.1038/nri3902

50. Nishio N, Diaconu I, Liu H, Cerullo V, Caruana I, Hoyos V, et al. Armed oncolytic virus enhances immune functions of chimeric antigen receptor-modified T cells in solid tumors. *Cancer Res* (2014) 74(18):5195–205. doi: 10.1158/0008-5472.CAN-14-0697

51. Pinna A, Solinas G, Giancipoli E, Porcu T, Zinellu A, D'Amico-Ricci G, et al. Glucose-6-Phosphate dehydrogenase (G6PD) deficiency and late-stage age-related macular degeneration. *Int J Med Sci* (2019) 16(5):623–9. doi: 10.7150/ijms.30155

52. Yang HC, Wu YH, Yen WC, Liu HY, Hwang TL, Stern A, et al. The redox role of G6PD in cell growth, cell death, and cancer. *Cells.* (2019) 8(9):e001313. doi: 10.3390/cells8091055

53. Ghergurovich JM, Esposito M, Chen Z, Wang JZ, Bhatt V, Lan T, et al. Glucose-6-Phosphate dehydrogenase is not essential for K-Ras-Driven tumor growth or metastasis. *Cancer Res* (2020) 80(18):3820–9. doi: 10.1158/0008-5472.CAN-19-2486

54. Lu M, Lu L, Dong Q, Yu G, Chen J, Qin L, et al. Elevated G6PD expression contributes to migration and invasion of hepatocellular carcinoma cells by inducing epithelial-mesenchymal transition. *Acta Biochim Biophys Sinica* (2018) 50(4):370–80. doi: 10.1093/abbs/gmy009

55. Yamawaki K, Mori Y, Sakai H, Kanda Y, Shiokawa D, Ueda H, et al. Integrative analyses of gene expression and chemosensitivity of patient-derived ovarian cancer spheroids link G6PD-driven redox metabolism to cisplatin chemoresistance. *Cancer letters* (2021) 521:29–38. doi: 10.1016/j.canlet.2021.08.018

56. Ju HQ, Lu YX, Wu QN, Liu J, Zeng ZL, Mo HY, et al. Disrupting G6PD-mediated redox homeostasis enhances chemosensitivity in colorectal cancer. *Oncogene.* (2017) 36(45):6282–92. doi: 10.1038/onc.2017.227

57. Lu C, Yang D, Klement JD, Colson YL, Oberlies NH, Pearce CJ, et al. G6PD functions as a metabolic checkpoint to regulate granzyme b expression in tumor-specific cytotoxic T lymphocytes. *J immunother Cancer* (2022) 10(1):e003543. doi: 10.1136/jitc-2021-003543

58. Nakamura M, Nagase K, Yoshimitsu M, Magara T, Nojiri Y, Kato H, et al. Glucose-6-phosphate dehydrogenase correlates with tumor immune activity and programmed death ligand-1 expression in merkel cell carcinoma. *J immunother Cancer* (2020) 8(2):e001679. doi: 10.1136/jitc-2020-001679

59. Cao F, Luo A, Yang C. G6PD inhibits ferroptosis in hepatocellular carcinoma by targeting cytochrome P450 oxidoreductase. *Cell signalling* (2021) 87:110098. doi: 10.1016/j.cellsig.2021.110098

60. Hanahan D. Hallmarks of cancer: New dimensions. *Cancer discovery* (2022) 12(1):31–46. doi: 10.1158/2159-8290.CD-21-1059

61. Gassmann R, Carvalho A, Henzing AJ, Ruchaud S, Hudson DF, Honda R, et al. Borealin: A novel chromosomal passenger required for stability of the bipolar mitotic spindle. *J Cell Biol* (2004) 166(2):179–91. doi: 10.1083/jcb.200404001

62. Ruchaud S, Carmena M, Earnshaw WC. Chromosomal passengers: Conducting cell division. *Nat Rev Mol Cell Biol* (2007) 8(10):798–812. doi: 10.1038/nrm2257

63. Wang Y, Zhao Z, Bao X, Fang Y, Ni P, Chen Q, et al. Borealin/Dasra b is overexpressed in colorectal cancers and contributes to proliferation of cancer cells. *Med Oncol (Northwood London England)* (2014) 31(11):248. doi: 10.1007/s12032-014-0248-5

64. Dai C, Miao CX, Xu XM, Liu LJ, Gu YF, Zhou D, et al. Transcriptional activation of human CDCA8 gene regulated by transcription factor NF-y in embryonic stem cells and cancer cells. *J Biol Chem* (2015) 290(37):22423–34. doi: 10.1074/jbc.M115.642710

65. Santos SD, Wollman R, Meyer T, Ferrell JE. Spatial positive feedback at the onset of mitosis. *Cell.* (2012) 149(7):1500–13. doi: 10.1016/j.cell.2012.05.028

66. Nixon VL, Levasseur M, McDougall A, Jones KT. Ca(2+) oscillations promote APC/C-dependent cyclin B1 degradation during metaphase arrest and completion of meiosis in fertilizing mouse eggs. *Curr biology: CB.* (2002) 12 (9):746–50. doi: 10.1016/S0960-9822(02)00811-4

67. Bondi J, Husdal A, Bukholm G, Nesland JM, Bakka A, Bukholm IR. Expression and gene amplification of primary (A, B1, D1, D3, and e) and secondary (C and h) cyclins in colon adenocarcinomas and correlation with patient outcome. *J Clin pathology* (2005) 58(5):509–14. doi: 10.1136/jcp.2004.020347

68. Wang A, Yoshimi N, Ino N, Tanaka T, Mori H. Overexpression of cyclin B1 in human colorectal cancers. *J Cancer Res Clin Oncol* (1997) 123(2):124–7. doi: 10.1007/BF01269891

69. Wang Q, Moyret-Lalle C, Couzon F, Surbiguet-Clippe C, Saurin JC, Lorca T, et al. Alterations of anaphase-promoting complex genes in human colon cancer cells. *Oncogene* (2003) 22(10):1486–90. doi: 10.1038/sj.onc.1206224

70. Zhao M, Kim YT, Yoon BS, Kim SW, Kang MH, Kim SH, et al. Expression profiling of cyclin B1 and D1 in cervical carcinoma. *Exp Oncol* (2006) 28(1):44–8.

71. Ikuerowo SO, Kuczyk MA, Mengel M, van der Heyde E, Shittu OB, Vaske B, et al. Alteration of subcellular and cellular expression patterns of cyclin B1 in renal cell carcinoma is significantly related to clinical progression and survival of patients. *Int J cancer* (2006) 119(4):867–74. doi: 10.1002/ijc.21869

72. Heald R, McLoughlin M, McKeon F. Human wee1 maintains mitotic timing by protecting the nucleus from cytoplasmically activated Cdc2 kinase. *Cell.* (1993) 74(3):463–74. doi: 10.1016/0092-8674(93)80048-J

73. Fotedar R, Flatt J, Gupta S, Margolis RL, Fitzgerald P, Messier H, et al. Activation-induced T-cell death is cell cycle dependent and regulated by cyclin b. *Mol Cell Biol* (1995) 15(2):932–42. doi: 10.1128/MCB.15.2.932

74. Sarafan-Vasseur N, Lamy A, Bourguignon J, Le Pessot F, Hieter P, Sesboüé R, et al. Overexpression of b-type cyclins alters chromosomal segregation. *Oncogene.* (2002) 21(13):2051–7. doi: 10.1038/sj.onc.1205257

75. Bayramoglu Akkoyun M, Temel Y, Bengü A, Akkoyun HT. Ameliorative effects of astaxanthin against copper(II) ion-induced alteration of pentose phosphate pathway and antioxidant system enzymes in rats. *Environ Sci pollut Res Int* (2021) 28(44):62919–26. doi: 10.1007/s11356-021-15017-8

76. Hanagata N, Zhuang F, Connolly S, Li J, Ogawa N, Xu M. Molecular responses of human lung epithelial cells to the toxicity of copper oxide nanoparticles inferred from whole genome expression analysis. *ACS nano* (2011) 5(12):9326–38. doi: 10.1021/nn202966t

77. Sun B, Yang D, Dai H, Liu X, Jia R, Cui X, et al. Eradication of hepatocellular carcinoma by NKG2D-based CAR-T cells. *Cancer Immunol Res* (2019) 7 (11):1813–23. doi: 10.1158/2326-6066.CIR-19-0026

78. Wang S, He Z, Wang X, Li H, Liu XS. Antigen presentation and tumor immunogenicity in cancer immunotherapy response prediction. *eLife* (2019) 8: e49020. doi: 10.7554/eLife.49020

79. Hu FF, Liu CJ, Liu LL, Zhang Q, Guo AY. Expression profile of immune checkpoint genes and their roles in predicting immunotherapy response. *Briefings Bioinf* (2021) 22(3):bbaa176. doi: 10.1093/bib/bbaa176

80. Rizvi NA, Hellmann MD, Snyder A, Kvistborg P, Makarov V, Havel JJ, et al. Cancer immunology. mutational landscape determines sensitivity to PD-1 blockade in non-small cell lung cancer. *Sci (New York NY)* (2015) 348 (6230):124–8. doi: 10.1126/science.aaa1348

frontiers | Frontiers in Immunology

TYPE Systematic Review
PUBLISHED 21 October 2022
DOI 10.3389/fimmu.2022.1013186



OPEN ACCESS

EDITED BY
Xiaoran Yin,
Second Affiliated Hospital of Xi'an Jiaotong University, China

REVIEWED BY
Zeguo Sun,
Icahn School of Medicine at Mount Sinai, United States
Han Yao,
Shanghai Jiao Tong University, China

*CORRESPONDENCE
Jun Li
ljadoctor@swmu.edu.cn
Yaling Li
lylapothecary@swmu.edu.cn

This article was submitted to Cancer Immunity and Immunotherapy, a section of the journal Frontiers in Immunology

SPECIALTY SECTION
RECEIVED 06 August 2022
ACCEPTED 10 October 2022
PUBLISHED 21 October 2022

CITATION
Kou L, Wen Q, Xie X, Chen X, Li J and Li Y (2022) Adverse events of immune checkpoint inhibitors for patients with digestive system cancers: A systematic review and meta-analysis.
*Front. Immunol.* 13:1013186.
doi: 10.3389/fimmu.2022.1013186



# Adverse events of immune checkpoint inhibitors for patients with digestive system cancers: A systematic review and meta-analysis

Liqiu Kou[1,2], Qinglian Wen[3], Xiaolu Xie[1,2], Xiu Chen[1,2], Jun Li[4]* and Yaling Li[1]*

[1]Department of Pharmacy, The Affiliated Hospital of Southwest Medical University, Luzhou, China, [2]School of Pharmacy, Southwest Medical University, Luzhou, China, [3]Department of Oncology, The Affiliated Hospital of Southwest Medical University, Luzhou, China, [4]Department of Traditional Chinese Medicine, The Affiliated Hospital of Southwest Medical University, Luzhou, China

**Objective:** To study the incidence and distribution of adverse events in immune checkpoint inhibitors (ICI) for digestive system cancers and to provide a reference for the safe, rational, and effective use of immune detection site inhibitors.

**Methods:** We searched for articles published in English between January 1, 2010, and May 18, 2022. All clinical trials of ICI-based therapies for digestive system cancers were investigated, including only randomized controlled trials that reported data on the overall incidence of treatment-related adverse events (trAEs) or immune-related adverse reactions (irAEs) or tables.

**Results:** We searched 2048 records, of which 21 studies (7108 patients) were eligible for inclusion. The incidence of ICI trAEs of any grade was 82.7% (95% CI 73.9-90.0), and the incidence of grade 3 or higher trAEs was 27.5% (95% CI 21.3-34.1). The pooled rate of ICI irAEs of any grade was 26.3% (95% CI 11.8-44.0), and the incidence of grade 3 or higher irAEs was 9.4% (95% CI 1.1-24.6). In multivariate analysis, the incidence, characteristics, and distribution of AEs varied by cancer type, combination therapy modality (single/two-drug), and different agent types.

**Conclusion:** Our meta-analysis summarizes AEs associated with ICI in digestive system cancers. The incidence, characteristics, and distribution of AEs vary by cancer type, combination therapy modality, and different agent types. These findings can be considered for the early identification of AEs and provide effective interventions to reduce the severity of these patients. It can provide a clinical reference and may contribute to clinical practice.

KEYWORDS

**immune checkpoint inhibitors, treatment-related adverse events, immune-related adverse events, digestive system cancers, systematic evaluation, advance intervention**

# Introduction

Immune checkpoint inhibitors (ICIs) works by blocking tumor cells [programmed cell death 1 Ligand-1 (PD-L1)] or T lymphocytes [programmed cell death protein-1 (PD-1) or cytotoxic T lymphocyte-associated protein 4 (CTLA-4)], resulting in an effective anti-tumor response in patients (1). In 2011, the CTLA-4 inhibitor Ipilimumab was approved for marketing by the FDA, becoming the world's first approved immune checkpoint inhibitor drug (2). The discovery and clinical implementation of ICIs have revolutionized cancer treatment, bringing a new era of cancer therapy and improving the prognosis of patients with a variety of advanced cancers with this groundbreaking new approach (3). Currently, the FDA-approved immune checkpoint inhibitors are anti-CTLA-4 (Ipilimumab, tremelimumab, etc.), anti-PD-1 (pembrolizumab, toripalimab, nivolumab, etc.), and anti-PD-L (atezolizumab, durvaluma, etc.) (4).

ICIs have shown exciting clinical results in many tumor types (5, 6), but the practical application process is full of adverse effects, mainly including irAEs and trAEs. The mechanism of action of ICIs involves nonspecific activation of the immune system, and therefore, disruption of the critical role of checkpoint molecules in immune homeostasis may lead to autoimmune complications (7). IrAEs affect almost every organ in the body, most commonly the skin, gastrointestinal tract, lungs, endocrine, musculoskeletal and other systems (8). TrAEs are therapeutically relevant and appear mainly after treatment of malignancies with immune checkpoint inhibitors and encompass a larger spectrum than irAEs. TrAEs may cause by immune checkpoint inhibitors or other concomitant reactions (9). TrAEs may manifest in the hematological system, the skin, the Respiratory system, the urinary system, systemic reactions, etc (10). Some fatal toxicities can occur in 0.4%-1.2% of patients, such as myocarditis, meningitis, myasthenia gravis, and various neuropathies. Although relatively rare, they often exhibit significant diagnostic complexity and may be underestimated (11, 12). Given the potential for long-term survival, ICI-related adverse events become a particularly relevant consideration (13). For patients receiving ICI for cancer, most AEs are reversible if diagnosed and treated promptly (14). Therefore, understanding AEs are critical to ensure timely diagnosis and effective management of these potentially severe adverse events (15).

With the increasing clinical use of ICIs, there have been numerous reports of adverse events associated with ICIs (16–18). As the indications for ICIs continue to expand, ICIs have been widely used in gastric, hepatic, esophageal, and gastroesophageal junction cancers (19–21). But the AEs associated with ICIs for the treatment of digestive system cancers have not been systematically evaluated. Given the increasing use of ICI-based immunotherapies in patients with digestive system cancers shortly, clinicians must have a comprehensive understanding of the toxicity associated with these therapies. Here, we aim to provide clinicians and clinical pharmacists with an evidence-based basis for immunosuppression in the treatment of gastrointestinal tumors by conducting a systematic evaluation and meta-analysis of published randomized controlled trials in the field of the digestive system regarding the trAEs of ICI.

# Methods

## Search strategy and selection criteria

We did a systematic review and meta-analysis to identify published RCTs using ICI therapy for digestive system cancers that reported treatment-related adverse events. Papers published between January 1, 2010, and May 18, 2022, were searched in PubMed, Embase, Web of Science, and Cochrane databases for the subject terms "Immune Checkpoint Inhibitors", "PD-1", "PD-L1", "CTLA-4"," Stomach Neoplasms", "Esophageal Neoplasms", "Colorectal Neoplasms", "Liver Neoplasms", "Gastroesophageal junction carcinoma", "Appendiceal Neoplasms", "Splenic Neoplasms", "Pancreatic Neoplasms", and "Randomized Controlled Trials" (Supplementary Table 1). Relevant references, related reviews, and article references were also checked manually to avoid missing relevant articles. Two researchers (Kou Liqiu, Xie Xiaolu) conducted the literature search and data extraction independently. All conflicts were resolved by discussion with a third partner (Chen Xiu) to reach a consensus.

This study was done in accordance with the guidance of the PRISMA statement.

We used the following selection criteria: (1) Studies of randomized controlled trials which were published before May 18, 2022. (2) Participants diagnosed with digestive system (colorectal, liver, stomach, esophagus, gastroesophageal junction, pancreatic, spleen, appendix) cancers who were treated with at least one PD-1, PD-L1, or CTLA-4 inhibitor (e.g., Nivolumab, Pembrolizumab, Atezolizumab, Ipilimumab, Camrelizumab, etc.). (3) Clinical trials that report overall incidence or tabular data for trAE or irAE profiles, and (4) Studies published in English. Exclusion criteria: (1) Received treatment other than PD-1, PD-L1, or CTLA-4 inhibitors (e.g., chemotherapy, targeted therapy drugs); (2) Repeat publications (only the most recent publications were retained); (3) Case reports, letters, conference abstracts, animal studies, reviews, expert opinions, etc.

## Data extraction

Two investigators (Kou Liqiu, Wen Qinglian) independently obtained the following basic information from each included study: first author, year of publication, country, clinical trial

number, cancer classification, median age, and enrollment, outcomes (total number of patients participating in safety analysis, number of patients discontinued and died due to treatment or immune-related AEs). AE terms are coded according to the Medical Dictionary of Regulatory Activities, and severity is graded according to the National Cancer Institute Common Terminology Criteria for Adverse Events. In this study, those AEs described as being of special interest were also extracted as irAE.

## Risk of bias and quality assessments

The Cochrane Collaboration tool was used to assess the risk of bias in the RCTs that were part of our study. Each trial was judged to be at low, unclear, or high risk for random sequence generation, allocation concealment, blinding of participants, personnel, and outcome assessors, incomplete outcome data, and selective outcome reporting. Two authors (Kou Liqiu, Chen Xiu) independently performed this process, and disagreements in ratings were resolved by a third investigator (Xie Xiaolu).

## Statistical analysis

We performed a meta-analysis of the overall incidence of ICI for the treatment of digestive system cancers. The primary study was the incidence of AEs, which was calculated by dividing the number of AEs by the total number of patients, the summary measure of the primary outcome was the incidence (95% CI). Before the meta-analysis, the incidence was logit converted and classic correction of 0.5 was added to zero events. Additionally, Subgroup analyses of AE incidence were performed according to type of cancer, type of combination of single ICI or dual ICI, and type of different agent. Multivariate multilevel meta-analysis models were performed to assess risk factors for AE, with the primary outcome of interest being the overall AE incidence. The putative predictors evaluated, including cancer type, combination type, type of ICI agent, were chosen as moderators. Effect sizes for all comparative analyses were assessed using the odds ratio (95%). The $\chi 2$ test and $I^2$ statistic were applied to estimate between-study heterogeneity. Significant heterogeneity was indicated for the $\chi 2$ test $p<0.10$ or $I^2>50\%$, and the random effects model was applied to the combined analysis. Otherwise, we applied a fixed-effects model. A random effects model was applied to the pooled analysis of the odds ratio. Statistical significance was considered when $p<0.05$. Publication bias detection was performed by Egger. If there was significant publication bias, pruning and filling were used to verify the robustness of the meta-analysis results. All analyses were done using SPSS statistical software (version 26.0) and R software (version 4.2.0).

# Results

## Search results

Our systematic search of PubMed, Embase, Web of Sciences, and Cochrane databases identified 2048 records (Figure 1), from which we selected 21 eligible studies involving 7108 patients for quantitative analysis. The main characteristics of the included studies are shown in Table 1 and Main characteristics of ICI arms included in the meta-analysis for AEs comparison (Supplementary Table 2).

## Risk of bias assessment

Two independent reviewers (Kou Liqiu, Xie Xiaolu) assessed the quality of evidence from 21 studies of RCTs using the Cochrane Collaboration's tool. The overall risk of bias was low in the included studies. 2 studies did not perform allocation concealment and 8 studies did not provide relevant information. 1 study did not conceal it from patients and staff. 3 studies were not blinding of outcome assessment. In addition, 13 studies were open-label studies and therefore may have had some publication bias. The risk of bias status is summarized in (Supplementary Table 3).

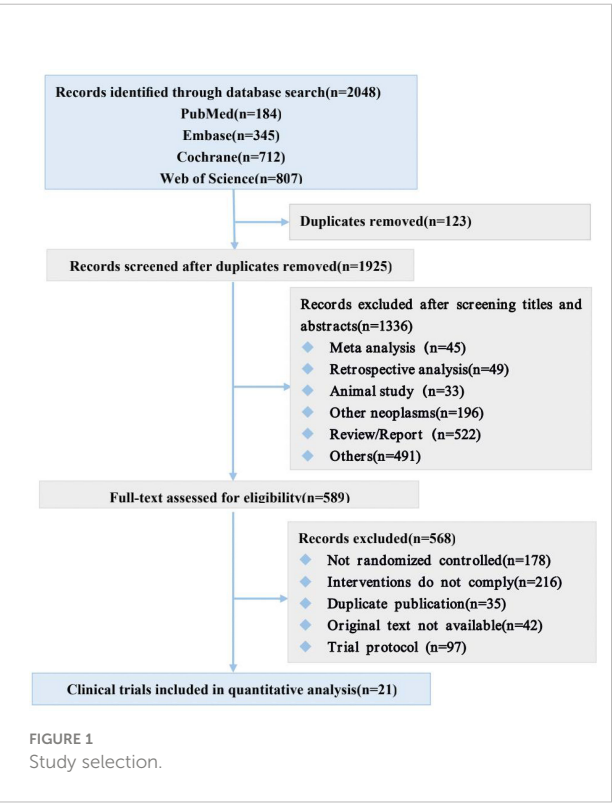


FIGURE 1
Study selection.

10.3389/fimmu.2022.1013186

TABLE 1 Characteristics of studies included in the Meta-analysis.

| Study | Year | Country | Trials identifier | Cancer type | Agents in arms | No.of.arms | Median age | Enrollment |
|---|---|---|---|---|---|---|---|---|
| Eng C (22) | 2019 | North,America, Europe, Asia,et al | NCT02788279 | Colorectal Cancer | Atezolizumab+Cobimetinib *vs.* Atezolizumab *vs.* Regorafenib | 1 | 56 (51–64) | 363 |
| André T (23) | 2020 | Asia,Western Europe, North America,et al | NCT02563002 | Colorectal Cancer | Pembrolizumab *vs.* Chemotherapy | 1 | 63 (24–93) | 307 |
| Chen EX (24) | 2020 | Canada | NCT02870920 | Colorectal Cancer | Tremelimumab+Durvaluma *vs.*BSC | 1 | 65 (39-87) | 180 |
| Hu H (25) | 2022 | China | NCT03926338 | Colorectal Cancer | Toripalimab *vs.* Toripalimab+Celecoxib | 1 | 53 (45–60) | 34 |
| Finn RS (26) | 2020 | Argentina,Australia, Canada,et al | NCT02702401 | Liver cancer | Pembrolizumab *vs.*Placebo | 1 | 67 (18-91) | 413 |
| Kelley RK (27) | 2021 | Japan | NCT02519348 | Liver cancer | Tremelimumab+Durvaluma | 4 | 66 (26-86) | 332 |
| Yau T (28) | 2022 | United States, Canada,Europe,et al | NCT02576509 | Liver cancer | Nivolumab *vs.* Sorafenib | 1 | 65 (19–89) | 743 |
| Kaseb AO (29) | 2022 | African-American, Asian | NCT03222076 | Liver cancer | Nivolumab *vs.* Nivolumab +Ipolimumab | 2 | 64 (56–68) | 27 |
| Qin S (30) | 2020 | China | NCT02989922 | Liver cancer | Camrelizumab *vs.* Camrelizumab | 2 | 48 (41–56) | 303 |
| Lee MS (31) | 2020 | Asian,Hawaiian, African American,et al | NCT02715531 | Liver cancer | Atezolizumab+Bevacizumab *vs.*Atezolizumab | 1 | 63 (23–85) | 104 |
| Yau T (32) | 2020 | United States, Italy,Spain,et al | NCT01658878 | Liver cancer | Nivolumab+Ipolimumab | 3 | 60 (52.5-66.5) | 148 |
| Shah MA (33) | 2021 | America,Europe, Australian | NCT02864381 | Gastric Cancer | Nivolumab *vs.* Andecaliximab | 1 | 62 (23–80) | 144 |
| Shitara K (34) | 2020 | Europe,North, America, Australian,et al | NCT02494583 | Gastric Cancer | Pembrolizumab *vs.* Pembrolizumab+Chemotherapy vs.Chemotherapy+Placebo | 1 | 62 (20-87) | 763 |
| Shitara K (35) | 2018 | Europe, Israel, North America,et al | NCT02370498 | Gastroesophageal junction cancer | Pembrolizumab *vs.* Paclitaxel | 1 | 62·5 (54–70) | 592 |
| Satoh T (36) | 2019 | Japan,Korea,Taiwan. China | NCT02267343 | Gastroesophageal junction cancer | Nivolumab *vs.* Placebo | 1 | 62 (20–83) | 493 |
| Kelly RJ (37) | 2020 | Europe,United States, Canada,et al | NCT02743494 | Gastroesophageal junction cancer | Nivolumab *vs.* Placebo | 1 | 62 (26–82) | 792 |
| Chung HC (38) | 2022 | China,Malaysia,Korea | NCT03019588 | Gastroesophageal junction cancer | Pembrolizumab *vs.* Paclitaxel | 1 | 61 (32-75) | 94 |
| Bang YJ (39) | 2017 | Asia,Row,et al | NCT01585987 | Gastroesophageal junction cancer | Ipilimumab *vs.* BSC | 1 | 65 (34–86) | 143 |
| Kojima T (40) | 2020 | Argentina,Australia, Brazil,et al | NCT02564263 | Esophageal cancer | Pembrolizumab *vs.* Chemotherapy | 1 | 63 (23-84) | 628 |
| Park S (41) | 2022 | Korea | NCT02520453 | Esophageal cancer | Durvaluma *vs.* Placebo | 1 | 64 (39-76) | 86 |
| Kato K (42) | 2019 | China,Denmark, Germany,et al | NCT02569242 | Esophageal cancer | Nivolumab *vs.*Chemotherapy | 1 | 64 (57–69) | 419 |

BSC, best supportive care.

## Studies evaluating the incidence of trAEs and irAEs

A total of 21 (22–42) trials were included, all reporting the incidence of trAEs and 6 (23, 26, 34–36, 39) trials reporting the incidence of irAEs. The overall incidence of trAEs of any grade was 82.7% (95% CI 73.9-90.0) in the 21 (22–27, 29, 30, 32, 34–40) study arms, and the incidence of trAEs of grade 3 or higher was 27.5% (95% CI 21.3-34.1) in the 28 (22–42) study arms. There were 6 (23, 26, 34–36, 39) arms of the study reported irAEs of any grade, with an overall incidence of irAEs of any grade was 26.3% (95% CI 11.8-44.0), respectively, and 6 (23, 26, 34–36, 39) arms of the study reported irAEs of grade 3 or higher, and the incidence was 9.4% (95% CI 1.1-24.6) (Figure 2).

## Assessment of the occurrence profile of AEs

We performed a pooled analysis of the incidence of AEs in ICI for the treatment of digestive system cancers. The most common trAEs of any grade were hypoalbuminemia (79.7% [95% CI 72.3-87.0]), lactate dehydrogenase increase (77.1% [95% CI 69.4-84.8]), lymphopenia (72.0% [95% CI 63.8-80.3]). (Supplementary Figure 1). We only reported trAEs of any grade with an incidence of 10% or more. TrAEs with grade 3 or higher were most common for lymphopenia (22.0% [95% CI 14.4-29.6]), lactate dehydrogenase increase (16.9% [95% CI 10.1-23.8]), hyponatremia (16.5% [95% CI 11.1-21.8]). (Supplementary Figure 2).

Among the adverse events associated with irAEs, the most common in any class were rash (26.4% [95% CI 19.2-33.5]), hypothyroidism (9.5% [95% CI 7.6-11.4]), diarrhea (6.8% [95% CI 3.3-10.3]). (Supplementary Figure 3). The incidence of irAEs of grade 3 or higher was lower, with the most common being diarrhea (5.4% [95% CI 2.3-5.1]), rash (5.1% [95% CI 0.7-9.4]), hepatitis (4.1% [95% CI 2.6-5.7]). (Supplementary Figure 4).

## TrAEs incidence by cancer type, combination types(single- or two-drug), and type of ICI agent

In the analysis of the incidence of trAEs in different cancer types, we found that gastric cancer had the highest incidence of trAEs of any grade (95.3% [95% CI 91.9-97.5]), followed by colorectal cancer (90.4% [95% CI 64.5-100.0]), liver cancer (81.0% [95% CI 71.5-89.0]), gastroesophageal junction cancer (78.1% [95% CI 54.1-94.8]), and the lowest incidence was esophageal cancer (63.7% [95% CI 58.1-69.0]). Among the incidence rates of grade 3 or higher, colorectal cancer (40.9% [95% CI 19.1-64.8]) had the highest incidence rate, followed by gastric cancer (34.0% [95% CI 5.1-72.5]), liver cancer (29.6% [95% CI 21.3-38.7]), gastroesophageal junction cancer (19.5% [95% CI 12.0-28.4]), and esophageal cancer (17.4% [95% CI 14.3-20.5]) had the lowest incidence (Figure 3).

In different combination types(single- or two-drug), trAEs was higher with two ICIs combined than with ICIs alone. The incidence of pooling of any grade was 81.0%, and the incidence of grade 3 or higher was 24.5% when treated with a single ICI drug. The incidence of any grade was 87.2%, and the incidence of grade 3 or higher was 41.0% with the combination of two ICIs (Figure 3).

Among the different types of ICI agents, the highest incidence of trAEs for any grade of anti-PD-L1 (88.7% [95% CI 79.6-95.3]), and the highest incidence of trAEs for grade 3 or higher was for anti-PD-1 (27.6% [95% CI 17.6-36.9]). The lowest incidence of trAEs of any grade (65.5% [95% CI 53.9-76.3]) was anti-CTLA-4, and the lowest incidence of grade 3 or higher was anti-PD-L1 (20.0% [95% CI 5.4-40.7]). Additionally, the different types of ICI combined (PD-1/PD-L1+CTLA-4) increased the risk of trAEs. The risk of the combination of anti-PD-L1 and anti-CTLA-4 is most evident in trAEs of any grade (89.3% [95% CI 61.2-100.0]) and trAEs of grade 3 or higher(41.7%[95%CI20.3-64.9]) (Figure 3).

## IrAEs incidence by cancer type, single- or two-drug(PD-1/PD-L1+CTLA-4) combinations, and type of ICI agent

There were no trials reporting irAEs for esophageal cancer in the included studies. Colorectal cancer had the highest incidence of irAEs at 30.7% for any grade, and 9.4% for grade 3 or higher. The lowest incidence of irAEs at any grade was for liver cancer (18.3%), and the lowest incidence of irAEs at grade 3 or higher was for gastric cancer (5.9%) (Figure 4).

The incidence of irAEs with two ICI combine therapy was not reported in the included studies. There were 6 studies reporting irAEs of any grade and irAEs of grade 3 or higher. The incidence of irAEs of any grade with single-agent ICI was

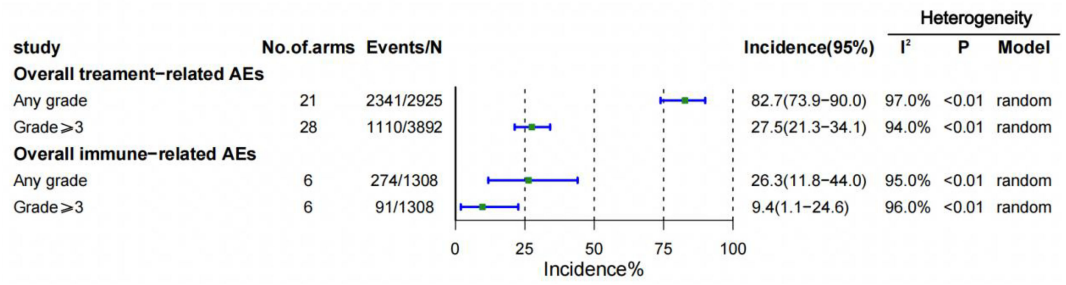


FIGURE 2
Overall incidences of treatment-related and immune-related adverse events (AEs). CI = confidence interval.

10.3389/fimmu.2022.1013186

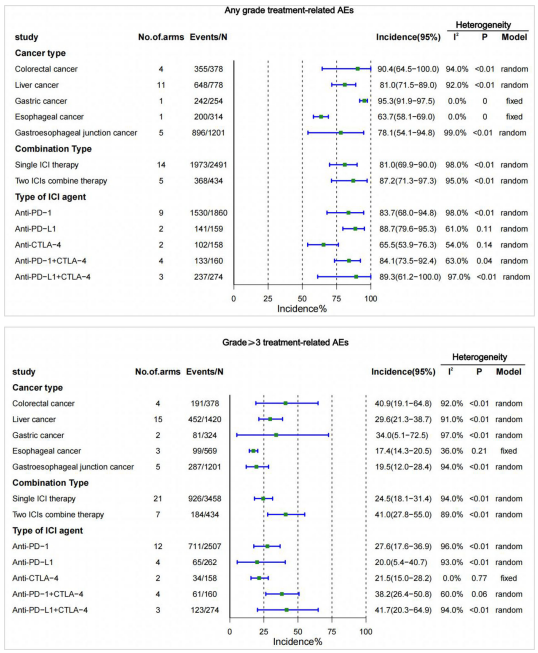


FIGURE 3
Incidence of treatment-related adverse events (trAEs) by cancer type, single- or two-drug combinations, and type of ICI agent. CI, confidence interval; ICI, immune checkpoint inhibitor.

26.3% and the incidence of grade 3 or higher irAEs was 9.4% (Figure 4).

The occurrence of irAEs was reported only in the anti-PD-1 and anti-CTLA-4 treatment groups among the different types of ICI drugs. The incidence of irAEs was higher for anti-CTLA-4 of any grade (70.2% [95% CI 57.9-82.4]), and for grade 3 or higher (54.4% [95% CI 41.1-67.7]) than for anti-PD-1 (Figure 4).

## Multivariable regression analysis

Colorectal cancer has a significantly higher risk of trAEs and irAEs than most other cancers of the digestive system. However, it is noteworthy that the incidence of trAEs at any grade was higher in gastric cancer than in colorectal cancer (OR:2.59,95% CI:1.34-5.01, P=0.0048). Two ICI drug therapy was associated with an increased risk of trAEs compared with a single ICI drug therapy. Combination therapy with two ICIs was associated with an increased risk of trAEs of any grade (OR:1.46, 95% CI:1.11-1.94, P=0.0075) and grade 3 or higher (OR:3.72, 95% CI:3.03-4.56, P<0.0001).

In addition, different types of ICI drugs are associated with trAEs and irAEs. We found that CTLA-4 had the lowest incidence of trAEs (OR: 0.39, 95% CI: 0.28-0.56, P<0.0001 for any grade and OR:1.55,95% CI:1.05-2.88, P=0.0257 for grade ≥3), but the highest incidence of irAEs (OR: 10.23, 95% CI: 5.70-

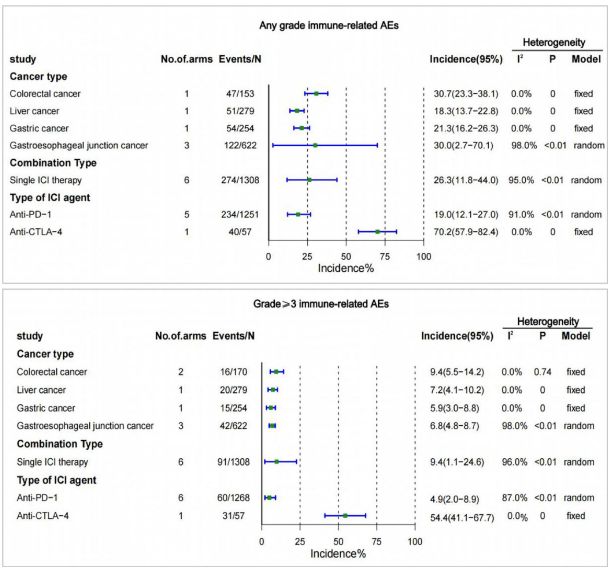


FIGURE 4
Incidence of treatment-related adverse events (irAEs) by cancer type, single- or two-drug combinations, and type of ICI agent. CI, confidence interval; ICI, immune checkpoint inhibitor.

18.36, P<0.0001 for any grade and OR: 23.19, 95% CI: 12.98-41.44, P<0.0001 for grade ≥3). Furthermore, the combination of PD-1 and CTLA-4 immune checkpoint inhibitors was associated with a higher risk of trAEs (OR:4.60, 95% CI: 3.58-5.92, P<0.0001 for grade≥3). The evaluation results are shown in (Table 2).

## Assessment of the occurrence profile of single and two-ICI AEs

In a multivariate analysis, we found that the incidence of AEs was higher with two drug therapy than with monotherapy. Therefore, we performed a comprehensive analysis of this influencing factor, and the top three incidences of monotherapy of any grade of AEs occurred were abdominal pain, alanine aminotransferase increase, and fatigue, while two ICIs were hypoalbuminemia, anaemia, and lactate dehydrogenase increase. Among AEs of grade 3 or higher, the highest incidence of single agents was hyponatremia, blood bilirubin increased, and hypertension, and the two ICIs were lymphopenia, hyponatremia, and lactate dehydrogenase increase (Figure 5).

## Assessment of the occurrence profile of different types of ICI agents AEs

Among adverse reactions of any grade, the most common adverse reactions to anti-PD-1 were maculopapular rash (30.8% [95% CI 1.7-59.8]), fatigue (19.2% [95% CI 17.1-21.2]), the most common adverse reactions to anti-PD-L1 were pruritus (10.8% [95% CI 4.7-16. 9]), hypothyroidism (9.9% [95% CI 4.0-15.8]), and the most common adverse reactions to anti-CTLA-4 were constipation (37.9% [95% CI 29.5-46.3]), cough (34.7% [95% CI 26.0-43.5]), while the most common adverse reaction to different types of ICI combination therapy with anti-PD-1 + anti-CTLA-4 was aspartate aminotransferase increased (50.0% [95% CI 20.0-80.0]), alanine aminotransferase increased (50.0% [95% CI 20.0-80.0]), and the most common adverse reactions of anti-PD-L1 +anti-CTLA-4 were anemia (83.9% [95% CI 77.2-90.6]), hypoalbuminemia (79.7% [95% CI 72.3- 87.0]).

Of the trAEs of grade 3 or higher, the most common adverse reactions to anti-PD-1 were blood bilirubin increase (7.5% [95% CI 4.4-10.6]), hypertension (7.2% [95% CI 5.3-11.3]), anti-PD-L1 most common adverse reactions were abdominal pain (4.4% [95% CI 0.1-8.8]), aspartate aminotransferase increase (3.4% [95% CI 1.4-8.3]), anti-CTLA-4 the most common adverse reactions were diarrhea (8.7% [95% CI 3.7-13.7]), AST increase (8.7% [95% CI 1.9-15.5]) and anti-PD-1+ anti-CTLA-4 the most common adverse reactions were aspartate aminotransferase increase (28.6% [95% CI 1.5-55.6]), and alanine aminotransferase (28.6% [95% CI 1.5-55.6]), and the most common adverse reactions to anti-PD-L1+anti-CTLA-4 were lymphopenia (22.0% [95% CI 14.4-29.6]) and hyponatremia (22.0% [95% CI 14.4-29.6]).

The most common adverse effects of anti-PD-1 in irAEs of any grade were hypothyroidism (9.0% [95% CI 6.9-11.1]), hyperthyroidism (4.1% [95% CI 2.7-4.6]), and anti-PD-1 + anti-

TABLE 2 Analysis of factors associated with the occurrence of treatment-related adverse events (trAEs) and immune-related adverse events (irAEs).

| Variables | trAES | | | | | | irAEs | | | | | |
|---|---|---|---|---|---|---|---|---|---|---|---|---|
| | Any grade | | | Grade≥3 | | | Any grade | | | Any grade | | |
| | OR | 95%CI | P value | OR | 95%CI | P value | OR | 95%CI | P value | OR | 95%CI | P value |
| **Cancer type** | | | | | | | | | | | | |
| Colorectal cancer | | Referent | | | Referent | | | Referent | | | Referent | |
| Liver cancer | 0.64 | (0.44-0.93) | 0.0177 | 0.46 | (0.36-0.58) | <0.0001 | 0.50 | (0.32-0.8) | 0.0034 | 0.74 | (0.37-1.48) | 0.40 |
| Gastric cancer | 2.59 | (1.34-5.01) | 0.0048 | 0.33 | (0.24-0.45) | <0.0001 | 0.61 | (0.39-0.96) | 0.0032 | 0.60 | (0.29-1.26) | 0.1777 |
| Esophageal cancer | 0.23 | (0.15-0.33) | <0.0001 | 0.21 | (0.15-0.28) | <0.0001 | 0.55 | (0.37-0.82) | 0.0031 | 0.70 | (0.38-1.27) | 0.2403 |
| Gastroesophageal junction cancer | 0.38 | (0.27-0.53) | <0.0001 | 0.31 | (0.24-0.39) | <0.0001 | Na | Na | Na | Na | Na | Na |
| **Combination Type** | | | | | | | | | | | | |
| Single ICI therapy | | Referent | | | Referent | | | Referent | | | Referent | |
| Two ICI combine therapy | 1.46 | (1.11-1.94) | 0.0075 | 3.72 | (3.03-4.56) | <0.0001 | Na | Na | Na | Na | Na | Na |
| **Type of ICI agent** | | | | | | | | | | | | |
| Anti–PD-1 | | Referent | | | Referent | | | Referent | | | Referent | |
| Anti–PD-L1 | 1.69 | (1.02-2.80) | 0.0417 | 1.87 | (1.39-2.5) | <0.0001 | Na | Na | Na | Na | Na | Na |
| Anti–CTLA-4 | 0.39 | (0.28-0.56) | <0.0001 | 1.55 | (1.05-2.88) | 0.0257 | 10.23 | (5.70-18.36) | <0.0001 | 23.19 | (12.98-41.44) | <0.0001 |
| Anti–PD-1+CTLA-4 | 1.38 | (0.96-1.99) | 0.0837 | 4.60 | (3.58-5.92) | <0.0001 | Na | Na | Na | Na | Na | Na |
| Anti–PD-L1+CTLA-4 | 1.06 | (0.69-1.63) | 0.7827 | 3.48 | (2.51-4.84) | <0.0001 | Na | Na | Na | Na | Na | Na |

Na, Not available.

CTLA-4 were rash (26.4% [95% CI 19.2-33.5]), hypothyroidism (11.2% [95% CI 6.9-15.6]). Among irAEs of grade 3 or higher, the most common adverse reactions to anti-PD-1 were hepatitis (1.8% [95% CI 0.6-3.0]), adrenal insufficiency (1.3% [95% CI -0.5-3.1]), while the most common adverse reactions to anti-PD-1+ anti-CTLA-4 were fatigue (3.5% [95% CI -1.4-8.4]), diarrhea (5.4% [95% CI 2.3-8.5]) (Supplementary Figures 5-18 summarizes the 20 most common AEs reported for different ICI agent types).

## Publication bias

We tested for publication bias in the occurrence profiles of treatment-related and immune-related adverse events of any grade and grade 3 or higher, and publication bias was present in all except for trAEs published at grade 3 or above (p=0.056). We modified the funnel plot by the pruning and filling method, and the results were still biased. We analyzed the following reasons: (1) We included five types of digestive system cancers, and there were differences in the responsiveness of different cancers to ICI drugs. (2) Different types of drug combinations may also make a difference in the occurrence of adverse events (Supplementary Figure 19).

# Discussion

This systematic evaluation and meta-analysis included 21 randomized controlled trials examining the incidence and profile of adverse events associated with immune checkpoint inhibitor-based therapies for digestive system cancers. Overall, our pooled analysis reported 82.7% and 27.5% incidence of trAEs of any grade and grade 3 or higher. These results showed a reduction in the incidence of trAEs compared with the incidence reported in previous studies of risk across cancer types(including cancer of the gastric or gastroesophageal junction) (43). In previous meta-analysis, the trAEs of different ICI in various cancer types were analyzed, with 86.8% and 35.9% of trAEs of any grade and grade 3 or higher, respectively, but the incidence of irAEs was not systematically evaluated in that article (43). However, some of the irAEs may be severe and lead to permanent disease (44). Hence, the incidence of irAEs was pooled in our meta-analysis and there were 26.3% and 9.4% of irAEs of any grade and grade 3 or higher. So it's necessary to focus on irAEs to reduce potential short- and long-term complications and optimize quality of life and long-term outcomes.

There were some interesting findings from multivariate analysis. First, the incidence of AE subgroups based on cancer type had the highest risk of trAEs and irAEs in colorectal cancer. That may be due to the following reasons: while ICI therapy has shown an unusually high depth and frequency of durable response in clinical trials in patients with mismatch repair-deficient(MMR-D) colorectal cancer with much fewer treatment-related adverse events (45, 46), whereas MMR occurs more frequently in early-stage tumors than in late-stage tumors (47), two of the four colorectal cancer studies included in

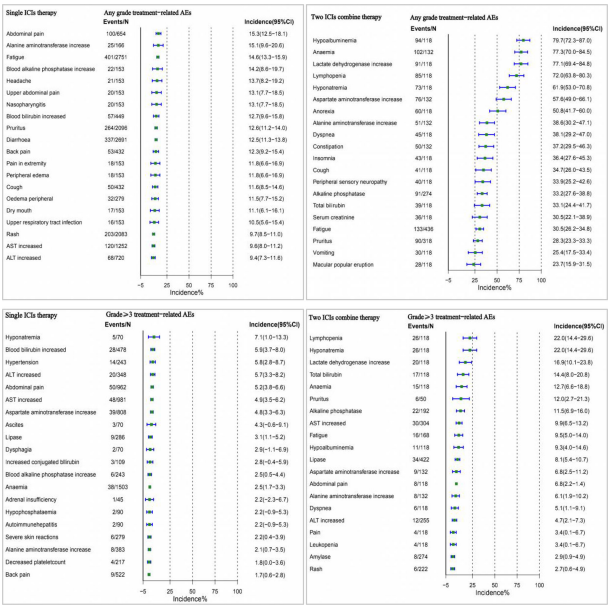


FIGURE 5
Overview of single and two ICI AEs.

this study were in advanced MMR-D colorectal cancer and one was metastatic colorectal cancer; In addition, Venderbosch et al. found that the incidence of dMMR in metastatic colorectal cancer was only 5%, which was lower than that of early-stage colorectal cancer (19.72%) (48). Second, ICI combination therapy(single or two drugs) was associated with an increased risk of trAEs, more pronounced in trAEs of any grade. That's consistent with the findings of Janjigian YY (49), Gubens MA (50), et al. Although the incidence of trAEs was higher with the combination of two ICIs than with a single ICI, it was still lower or similar to conventional treatment (chemotherapy and targeted therapy) (51, 52), thus, they can be managed appropriately through close monitoring and early recognition of relevant signs and symptoms. The included ICI combination therapy trials did not report the occurrence of irAEs, which may be due to the fact that most of the pilot studies focused on efficacy. Thirdly, Across the different types of ICI drugs, our meta-analysis found that anti-CTLA-4 had the lowest incidence of trAEs but the highest incidence of irAEs (53), and increased the risk of trAEs when combined with PD-1, which was consistent with the study by Osipov A et al (54). Therefore, TRAE, especially TRAE of grade 3 or higher, becomes one of the major issues that cannot be ignored in combination therapy. Take special care of lymphopenia when using PD-1 and CTLA-4. Lymphopenia is a predictive indicator and has a significant impact on survival. It is usually used with the addition of steroids (55).

Immune-related adverse reactions (irAEs) are immune activations caused by regulatory T-cell activity that can cause immune-related adverse reactions, resulting in symptoms associated with the corresponding organs (56). The most common irAEs include rash, colitis, hepatitis, endocrine disorders, and pneumonia (57). In this study, the most common incidence of irAEs at any level was found to be rash, hypothyroidism, and diarrhea, which is generally similar to the study by Wu, et al (17). However, Wu et al. studied the incidence of adverse events in ICI for urologic cancers, suggesting that irAEs are primarily drug-related and do not differ significantly concerning the type of cancer. In addition, grade 3 or higher irAEs are most commonly associated with diarrhea, rash, and hepatitis. Hepatitis is potentially fatal toxicity and immune-related hepatitis has a good prognosis but often requires treatment discontinuation, high-dose steroids, and second-line immunosuppression (58, 59). Most irAEs can be controlled and reversed by discontinuing dosing or using corticosteroids (60), With infliximab, for example, most of the adverse immune system reactions are eliminated with proper management (57).

This study has several advantages: 1) This systematic evaluation and meta-analysis included 21 randomized controlled trials that examined the incidence and distribution of adverse events associated with immune checkpoint inhibitor therapies for digestive system cancers. 2) The AEs associated with ICI in digestive system cancers were summarized by meta-analysis, which found that the incidence, characteristics, and distribution of AEs varied by cancer type, combination therapy modality, and different types of agents. 3) A comprehensive analysis of adverse events in ICI combination therapy can be used as an early identification to provide patients with effective interventions to reduce their severity. It may provide a clinical reference and may contribute to clinical practice. However there are some limitations: (1) We included only clinical randomized controlled trials, limiting the generalizability of our results to the general population of patients in real-world settings. (2) We found considerable heterogeneity when performing the test for heterogeneity, and despite doing subgroup analyses, we were still unable to find significant sources of heterogeneity, and some unobserved confounding factors may hinder the interpretation of the overall incidence in each subgroup, so the results need to be treated with caution. (3) Adverse events were recorded in clinical trials using MedDRA, but in some cases, the definitions of MedDRA overlapped. For example, patients with liver symptoms may be recorded as having hepatitis, autoimmune hepatitis, or elevated liver enzymes in a different clinical trial, thereby impeding knowledge of the actual incidence of adverse events. (4) Subgroup analysis revealed relatively small sample sizes for the Anti-PD-L1, Anti-CTLA-4, and Anti-PD-1 + CTLA-4 groups, so the results will have to be considered with caution and justified by a large sample of high-quality trials.

## Conclusion

This meta-analysis summarizes the profile of ICI-based treatment of common trAEs and irAEs in cancers of the digestive system. Different cancer types, combined treatment methods and different drug types are associated with incidence and AE characteristics, such a comprehensive analysis of adverse events in ICI combination therapy can be used as an early identification to provide effective interventions to reduce the severity of these patients. It may provide a clinical reference and may contribute to clinical practice. Further large-scale studies are needed to confirm our findings.

## Author contributions

YL, JL and QW have the concept of the study. LK and XC developed and implemented the search strategy. LK and XX independently screened the titles and abstracts of all retrieved records. LK and XC performed the data extraction. LK conducted the meta-analysis. LK wrote the draft manuscript. All authors contributed to the article and approved the submitted version.

## Funding

This study was supported by the Sichuan Provincial Department of Education (SCYG2020-04, SCYG2019-04).

## Acknowledgments

Thanks to all the authors of this article for their contributions to this article.

## Conflict of interest

The authors declare that the research was conducted in the absence of any commercial or financial relationships that could be construed as a potential conflict of interest.

## Publisher's note



## Supplementary material

The Supplementary Material for this article can be found online at: https://www.frontiersin.org/articles/10.3389/fimmu.2022.1013186/full#supplementary-material

## References

1. Mahoney KM, Rennert PD, Freeman GJ. Combination cancer immunotherapy and new immunomodulatory targets. *Nat Rev Drug Discov* (2015) 14(8):561–84. doi: 10.1038/nrd4591

2. Sharma P, Wagner K, Wolchok JD, Allison JP. Novel cancer immunotherapy agents with survival benefit: recent successes and next steps. *Nat Rev Cancer* (2011) 11(11):805–12. doi: 10.1038/nrc3153

3. Kraehenbuehl L, Weng CH, Eghbali S, Wolchok JD, Merghoub T. Enhancing immunotherapy in cancer by targeting emerging immunomodulatory pathways. *Nat Rev Clin Oncol* (2022) 19(1):37–50. doi: 10.1038/s41571-021-00552-7

4. Bagchi S, Yuan R, Engleman EG. Immune checkpoint inhibitors for the treatment of cancer: Clinical impact and mechanisms of response and resistance. *Annu Rev Pathol* (2021) 16:223–49. doi: 10.1146/annurev-pathol-042020-042741

5. Doki Y, Ajani JA, Kato K, Xu JM, Wyrwicz LJ, Motoyama S, et al. Nivolumab combination therapy in advanced esophageal squamous-cell carcinoma. *N Engl J Med* (2022) 386(5):449–62. doi: 10.1056/NEJMoa2111380

6. Chalabi M, Fanchi LF, Dijkstra KK, Fanchi FL, Dijkstra KK, Berg GJ, et al. Neoadjuvant immunotherapy leads to pathological responses in MMR-proficient and MMR-deficient early-stage colon cancers. *Nat Med* (2020) 26(4):566–76. doi: 10.1038/s41591-020-0805-8

7. Sangro B, Chan SL, Meyer T, Reig M, El-Khoueiry A, Galle PR. Diagnosis and management of toxicities of immune checkpoint inhibitors in hepatocellular carcinoma. *J Hepatol* (2020) 72(2):320–41. doi: 10.1016/j.jhep.2019.10.021

8. Brahmer JR, Lacchetti C, Schneider BJ, Atkins MB, Brassil KJ, Caterino JM. National comprehensive cancer network. management of immune-related adverse events in patients treated with immune checkpoint inhibitor therapy: American society of clinical oncology clinical practice guideline. *J Clin Oncol* (2018) 36 (17):1714–68. doi: 10.1200/JCO.2017.77.6385

9. Shen Y, Chen Y, Wang D, Zhu Z. Treatment-related adverse events as surrogate to response rate to immune checkpoint blockade. *Med (Baltimore)* (2020) 99(37):e22153. doi: 10.1097/MD.0000000000022153

10. Liu T, Jin B, Chen J, Wang H, Lin SY, Dang J, et al. Comparative risk of serious and fatal treatment-related adverse events caused by 19 immune checkpoint inhibitors used in cancer treatment: a network meta-analysis. *Ther Adv Med Oncol* (2020) 12:1758835920940927. doi: 10.1177/1758835920940927

11. Moslehi J, Lichtman AH, Sharpe AH, Galluzzi L, Kitsis RN. Immune checkpoint inhibitor-associated myocarditis: manifestations and mechanisms. *J Clin Invest* (2021) 131(5):e145186. doi: 10.1172/JCI145186

12. Haugh AM, Probasco JC, Johnson DB. Neurologic complications of immune checkpoint inhibitors. *Expert Opin Drug Saf* (2020) 19(4):479–88. doi: 10.1080/14740338.2020.1738382

13. Johnson DB, Nebhan CA, Moslehi JJ, Balko JM. Immune-checkpoint inhibitors: long-term implications of toxicity. *Nat Rev Clin Oncol* (2022) 19 (4):254–67. doi: 10.1038/s41571-022-00600-w

14. Inno A, Metro G, Bironzo P, Grimaldi AM, Grego E, Di Nunno V, et al. Pathogenesis, clinical manifestations and management of immune checkpoint inhibitors toxicity. *Tumori* (2017) 103(5):405–21. doi: 10.5301/tj.5000625

15. Delaunay M, Caron P, Sibaud V, Godillot C, Collot S, Milia J, et al. Toxicité des inhibiteurs de points de contrôle immunitaires [Toxicity of immune checkpoints inhibitors]. *Rev Mal Respir* (2018) 35(10):1028–38. doi: 10.1016/j.rmr.2017.08.006

16. Jing Y, Yang J, Johnson DB, Moslehi JJ, Han L. Harnessing big data to characterize immune-related adverse events. *Nat Rev Clin Oncol* (2022) 19(4):269–80. doi: 10.1038/s41571-021-00597-8

17. Wu Z, Chen Q, Qu L, Li M, Wang L, Mir MC, et al. Adverse events of immune checkpoint inhibitors therapy for urologic cancer patients in clinical trials: A collaborative systematic review and meta-analysis. *Eur Urol* (2022) 81(4):414–25. doi: 10.1016/j.eururo.2022.01.028

18. Nadelmann ER, Yeh JE, Chen ST. Management of cutaneous immune-related adverse events in patients with cancer treated with immune checkpoint inhibitors: A systematic review. *JAMA Oncol* (2022) 8(1):130–8. doi: 10.1001/jamaoncol.2021.4318

19. Janjigian YY, Shitara K, Moehler M, Garrido M, Salman P, Shen L, et al. First-line nivolumab plus chemotherapy versus chemotherapy alone for advanced gastric, gastro-oesophageal junction, and oesophageal adenocarcinoma (CheckMate 649): a randomised, open-label, phase 3 trial. *Lancet* (2021) 398 (10294):27–40. doi: 10.1016/S0140-6736(21)00797-2

20. Llovet JM, Castet F, Heikenwalder M, Maini MK, Mazzaferro V, Pinato DJ, et al. Immunotherapies for hepatocellular carcinoma. *Nat Rev Clin Oncol* (2022) 19 (3):151–72. doi: 10.1038/s41571-021-00573-2

21. Doki Y, Ajani JA, Kato K, Xu J, Wyrwicz L, Motoyama S, et al. CheckMate 648 trial investigators. Nivolumab combination therapy in advanced esophageal squamous-cell carcinoma. *N Engl J Med* (2022) 386(5):449–62. doi: 10.1056/NEJMoa2111380

22. Eng C, Kim TW, Bendell J, Argilés G, Tebbutt NC, Di Bartolomeo M. IMblaze370 investigators. atezolizumab with or without cobimetinib versus regorafenib in previously treated metastatic colorectal cancer (IMblaze370): a multicentre, open-label, phase 3, randomised, controlled trial. *Lancet Oncol* (2019) 20(6):849–61. doi: 10.1016/S1470-2045(19)30027-0

23. André T, Shiu KK, Kim TW, Jensen BV, Jensen LH, Punt C. KEYNOTE-177 investigators. Pembrolizumab in microsatellite-Instability-High advanced colorectal cancer. *N Engl J Med* (2020) 383(23):2207–18. doi: 10.1056/NEJMoa2017699

24. Chen EX, Jonker DJ, Loree JM, Kennecke HF, Berry SR, Couture F. Effect of combined immune checkpoint inhibition vs best supportive care alone in patients with advanced colorectal cancer: The Canadian cancer trials group CO.26 study. *JAMA Oncol* (2020) 6(6):831–8. doi: 10.1001/jamaoncol.2020.0910

25. Hu H, Kang L, Zhang J, Wu Z, Wang H, Huang M. Neoadjuvant PD-1 blockade with toripalimab, with or without celecoxib, in mismatch repair-deficient

or microsatellite instability-high, locally advanced, colorectal cancer (PICC): a single-centre, parallel-group, non-comparative, randomised, phase 2 trial. *Lancet Gastroenterol Hepatol* (2022) 7(1):38–48. doi: 10.1016/S2468-1253(21)00348-4

26. Finn RS, Ryoo BY, Merle P, Kudo M, Bouattour M, Lim HY. KEYNOTE-240 investigators. pembrolizumab as second-line therapy in patients with advanced hepatocellular carcinoma in KEYNOTE-240: A randomized, double-blind, phase III trial. *J Clin Oncol* (2020) 38(3):193–202. doi: 10.1200/JCO.19.01307

27. Kelley RK, Sangro B, Harris W, Ikeda M, Okusaka T, Kang YK. Safety, efficacy, and pharmacodynamics of tremelimumab plus durvalumab for patients with unresectable hepatocellular carcinoma: Randomized expansion of a phase I/II study. *J Clin Oncol* (2021) 39(27):2991–3001. doi: 10.1200/JCO.20.03555

28. Yau T, Park JW, Finn RS, Cheng AL, Mathurin P, Edeline J. Nivolumab versus sorafenib in advanced hepatocellular carcinoma (CheckMate 459): a randomised, multicentre, open-label, phase 3 trial. *Lancet Oncol* (2022) 23 (1):77–90. doi: 10.1016/S1470-2045(21)00604-5

29. Kaseb AO, Hasanov E, Cao HST, Xiao L, Vauthey JN, Lee SS. Perioperative nivolumab monotherapy versus nivolumab plus ipilimumab in resectable hepatocellular carcinoma: a randomised, open-label, phase 2 trial. *Lancet Gastroenterol Hepatol* (2022) 7(3):208–18. doi: 10.1016/S2468-1253(21)00427-1

30. Qin S, Ren Z, Meng Z, Chen Z, Chai X, Xiong J. Camrelizumab in patients with previously treated advanced hepatocellular carcinoma: a multicentre, open-label, parallel-group, randomised, phase 2 trial. *Lancet Oncol* (2020) 21(4):571–80. doi: 10.1016/S1470-2045(20)30011-5

31. Lee MS, Ryoo BY, Hsu CH, Numata K, Stein S, Verret W. GO30140 investigators. atezolizumab with or without bevacizumab in unresectable hepatocellular carcinoma (GO30140): an open-label, multicentre, phase 1b study. *Lancet Oncol* (2020) 21(6):808–20. doi: 10.1016/S1470-2045(20)30156-X

32. Yau T, Kang YK, Kim TY, El-Khoueiry AB, Santoro A, Sangro B. Efficacy and safety of nivolumab plus ipilimumab in patients with advanced hepatocellular carcinoma previously treated with sorafenib: The CheckMate 040 randomized clinical trial. *JAMA Oncol* (2020) 6(11):e204564. doi: 10.1001/jamaoncol.2020.4564

33. Shah MA, Cunningham D, Metges JP, Van Cutsem E, Wainberg Z, Elboudwarej E. Randomized, open-label, phase 2 study of andecaliximab plus nivolumab versus nivolumab alone in advanced gastric cancer identifies biomarkers associated with survival. *J Immunother Cancer* (2021) 9(12):e003580. doi: 10.1136/jitc-2021-003580

34. Shitara K, Van Cutsem E, Bang YJ, Fuchs C, Wyrwicz L, Lee KW. Efficacy and safety of pembrolizumab or pembrolizumab plus chemotherapy vs chemotherapy alone for patients with first-line, advanced gastric cancer: The KEYNOTE-062 phase 3 randomized clinical trial. *JAMA Oncol* (2020) 6 (10):1571–80. doi: 10.1001/jamaoncol.2020.3370

35. Shitara K, Özgüroğlu M, Bang YJ, Di Bartolomeo M, Mandalà M, Ryu MH. KEYNOTE-061 investigators. pembrolizumab versus paclitaxel for previously treated, advanced gastric or gastro-oesophageal junction cancer (KEYNOTE-061): a randomised, open-label, controlled, phase 3 trial. *Lancet* (2018) 392 (10142):123–33. doi: 10.1016/S0140-6736(18)31257-1

36. Satoh T, Kang YK, Chao Y, Ryu MH, Kato K, Cheol Chung H. Exploratory subgroup analysis of patients with prior trastuzumab use in the ATTRACTION-2 trial: a randomized phase III clinical trial investigating the efficacy and safety of nivolumab in patients with advanced gastric/gastroesophageal junction cancer. *Gastric Cancer* (2020) 23(1):143–53. doi: 10.1007/s10120-019-00970-8

37. Kelly RJ, Ajani JA, Kuzdzal J, Zander T, Van Cutsem E, Piessen G. CheckMate 577 investigators. adjuvant nivolumab in resected esophageal or gastroesophageal junction cancer. *N Engl J Med* (2021) 384(13):1191–203. doi: 10.1056/NEJMoa2032125

38. Chung HC, Kang YK, Chen Z, Bai Y, Wan Ishak WZ, Shim BY. Pembrolizumab versus paclitaxel for previously treated advanced gastric or gastroesophageal junction cancer (KEYNOTE-063): A randomized, open-label, phase 3 trial in Asian patients. *Cancer* (2022) 128(5):995–1003. doi: 10.1002/cncr.34019

39. Bang YJ, Cho JY, Kim YH, Kim JW, Di Bartolomeo M, Ajani JA. Efficacy of sequential ipilimumab monotherapy versus best supportive care for unresectable locally Advanced/Metastatic gastric or gastroesophageal junction cancer. *Clin Cancer Res* (2017) 23(19):5671–8. doi: 10.1158/1078-0432.CCR-17-0025

40. Kojima T, Shah MA, Muro K, Francois E, Adenis A, Hsu CH. KEYNOTE-181 investigators. randomized phase III KEYNOTE-181 study of pembrolizumab versus chemotherapy in advanced esophageal cancer. *J Clin Oncol* (2020) 38 (35):4138–48. doi: 10.1200/JCO.20.01888

41. Park S, Sun JM, Choi YL, Oh D, Kim HK, Lee T. Adjuvant durvalumab for esophageal squamous cell carcinoma after neoadjuvant chemoradiotherapy: a placebo-controlled, randomized, double-blind, phase II study. *ESMO Open* (2022) 7(1):100385. doi: 10.1016/j.esmoop.2022.100385

42. Kato K, Cho BC, Takahashi M, Okada M, Lin CY, Chin K. Nivolumab versus chemotherapy in patients with advanced oesophageal squamous cell carcinoma refractory or intolerant to previous chemotherapy (ATTRACTION-3): a multicentre, randomised, open-label, phase 3 trial. *Lancet Oncol* (2019) 20 (11):1506–17. doi: 10.1016/S1470-2045(19)30626-6

43. Zhou X, Yao Z, Bai H, Duan J, Wang Z, Wang X. Treatment-related adverse events of PD-1 and PD-L1 inhibitor-based combination therapies in clinical trials: a systematic review and meta-analysis. *Lancet Oncol* (2021) 22(9):1265–74. doi: 10.1016/S1470-2045(21)00333-8

44. Ramos-Casals M, Brahmer JR, Callahan MK, Flores-Chávez A, Keegan N, Khamashta MA. Immune-related adverse events of checkpoint inhibitors. *Nat Rev Dis Primers* (2020) 6(1):38. doi: 10.1038/s41572-020-0160-6

45. Overman MJ, Lonardi S, Wong KYM, Lenz HJ, Gelsomino F, Aglietta M. Durable clinical benefit with nivolumab plus ipilimumab in DNA mismatch repair-Deficient/Microsatellite instability-high metastatic colorectal cancer. *J Clin Oncol* (2018) 36(8):773–9. doi: 10.1200/JCO.2017.76.9901

46. Diaz LAJr, Shiu KK, Kim TW, Jensen BV, Jensen LH, Punt C. KEYNOTE-177 investigators. pembrolizumab versus chemotherapy for microsatellite instability-high or mismatch repair-deficient metastatic colorectal cancer (KEYNOTE-177): final analysis of a randomised, open-label, phase 3 study. *Lancet Oncol* (2022) 23(5):659–70. doi: 10.1016/S1470-2045(22)00197-8

47. Zhao P, Li L, Jiang X, Li Q. Mismatch repair deficiency/microsatellite instability-high as a predictor for anti-PD-1/PD-L1 immunotherapy efficacy. *J Hematol Oncol* (2019) 12(1):54. doi: 10.1186/s13045-019-0738-1

48. Venderbosch S, Nagtegaal ID, Maughan TS, Smith GC, Cheadle JP, Fisher D, et al. Mismatch repair status and BRAF mutation status in metastatic colorectal cancer patients: a pooled analysis of the CAIRO, CAIRO2, COIN, and FOCUS studies. *Clin Cancer Res* (2014) 20(20):5322–30. doi: 10.1158/1078-0432.CCR-14-0332

49. Janjigian YY, Bendell J, Calvo E, Kim JW, Ascierto PA, Sharma P. CheckMate-032 study: Efficacy and safety of nivolumab and nivolumab plus ipilimumab in patients with metastatic esophagogastric cancer. *J Clin Oncol* (2018) 36(28):2836–44. doi: 10.1200/JCO.2017.76.6212

50. Gubens MA, Sequist LV, Stevenson JP, Powell SF, Villaruz LC, Gadgeel SM. Pembrolizumab in combination with ipilimumab as second-line or later therapy for advanced non-small-cell lung cancer: KEYNOTE-021 cohorts d and h. *Lung Cancer* (2019) 130:59–66. doi: 10.1016/j.lungcan.2018.12.015

51. Hellmann MD, Paz-Ares L, Bernabe Caro R, Zurawski B, Kim SW, Carcereny Costa E. Nivolumab plus ipilimumab in advanced non-Small-Cell lung cancer. *N Engl J Med* (2019) 381(21):2020–31. doi: 10.1056/NEJMoa1910231

52. Motzer RJ, Tannir NM, McDermott DF, Arén Frontera O, Melichar B, Choueiri TK. CheckMate 214 investigators. nivolumab plus ipilimumab versus sunitinib in advanced renal-cell carcinoma. *N Engl J Med* (2018) 378(14):1277–90. doi: 10.1056/NEJMoa1712126

53. Weinmann SC, Pisetsky DS. Mechanisms of immune-related adverse events during the treatment of cancer with immune checkpoint inhibitors. *Rheumatol (Oxford)* (2019) 58(Suppl 7):vii59–67. doi: 10.1093/rheumatology/kez308

54. Osipov A, Lim SJ, Popovic A, Azad NS, Laheru DA, Zheng L, et al. Tumor mutational burden, toxicity, and response of immune checkpoint inhibitors targeting PD(L)1, CTLA-4, and combination: A meta-regression analysis. *Clin Cancer Res* (2020) 26(18):4842–51. doi: 10.1158/1078-0432.CCR-20-0458

55. Tomsitz D, Schlaak M, Zierold S, Pesch G, Schulz TU, Müller G, et al. Development of lymphopenia during therapy with immune checkpoint inhibitors is associated with poor outcome in metastatic cutaneous melanoma. *Cancers (Basel)* (2022) 14(13):3282. doi: 10.3390/cancers14133282

56. Morad G, Helmink BA, Sharma P, Wargo JA. Hallmarks of response, resistance, and toxicity to immune checkpoint blockade. *Cell* (2021) 184(21):5309–37. doi: 10.1016/j.cell.2021.09.020

57. Friedman CF, Proverbs-Singh TA, Postow MA. Treatment of the immune-related adverse effects of immune checkpoint inhibitors: A review. *JAMA Oncol* (2016) 2(10):1346–53. doi: 10.1001/jamaoncol.2016.1051

58. Zen Y, Yeh MM. Hepatotoxicity of immune checkpoint inhibitors: a histology study of seven cases in comparison with autoimmune hepatitis and idiosyncratic drug-induced liver injury. *Mod Pathol* (2018) 31(6):965–73. doi: 10.1038/s41379-018-0013-y

59. Patrinely JRJr, McGuigan B, Chandra S, Fenton SE, Chowdhary A, Kennedy LB. A multicenter characterization of hepatitis associated with immune checkpoint inhibitors. *Oncoimmunology* (2021) 10(1):1875639. doi: 10.1080/2162402X.2021.1875639

60. Chhabra N, Kennedy J. A review of cancer immunotherapy toxicity: Immune checkpoint inhibitors. *J Med Toxicol* (2021) 17(4):411–24. doi: 10.1007/s13181-021-00833-8

frontiers | Frontiers in Immunology

TYPE Original Research
PUBLISHED 13 December 2022
DOI 10.3389/fimmu.2022.944286



OPEN ACCESS

EDITED BY
Xiaoran Yin,
Second Affiliated Hospital of Xi'an Jiaotong University, China

REVIEWED BY
Liang Feng,
China Pharmaceutical University, China
Liang Ma,
Shanghai Institute of Materia Medica (CAS), China

*CORRESPONDENCE
Decai Tang
talknow@njucm.edu.cn
Junfei Gu
gujunfei@njucm.edu.cn

†These authors have contributed equally to this work

SPECIALTY SECTION
This article was submitted to Cancer Immunity and Immunotherapy, a section of the journal Frontiers in Immunology

RECEIVED 15 May 2022
ACCEPTED 25 November 2022
PUBLISHED 13 December 2022

CITATION
Liang Z, Sun R, Tu P, Liang Y, Liang L, Liu F, Bian Y, Yin G, Zhao F, Jiang M, Gu J and Tang D (2022) Immune-related gene-based prognostic index for predicting survival and immunotherapy outcomes in colorectal carcinoma. *Front. Immunol.* 13:944286. doi: 10.3389/fimmu.2022.944286



# Immune-related gene-based prognostic index for predicting survival and immunotherapy outcomes in colorectal carcinoma

Zhongqing Liang[1†], Ruolan Sun[1†], Pengcheng Tu[2,3†], Yan Liang[1], Li Liang[1], Fuyan Liu[1], Yong Bian[1,4], Gang Yin[1], Fan Zhao[1], Mingchen Jiang[1], Junfei Gu[1*] and Decai Tang[1*]

[1]School of Chinese Medicine, School of Integrated Chinese and Western Medicine, Nanjing University of Chinese Medicine, Nanjing, Jiangsu, China, [2]Affiliated Hospital of Nanjing University of Chinese Medicine, Nanjing, Jiangsu, China, [3]Laboratory of New Techniques of Restoration & Reconstruction of Orthopedics and Traumatology, Nanjing University of Chinese Medicine, Nanjing, Jiangsu, China, [4]Laboratory Animal Center, Nanjing University of Chinese Medicine, Nanjing, Jiangsu, China

**Introduction:** Colorectal cancer shows high incidence and mortality rates. Immune checkpoint blockade can be used to treat colorectal carcinoma (CRC); however, it shows limited effectiveness in most patients.

**Methods:** To identify patients who may benefit from immunotherapy using immune checkpoint inhibitors, we constructed an immune-related gene prognostic index (IRGPI) for predicting the efficacy of immunotherapy in patients with CRC. Transcriptome datasets and clinical information of patients with CRC were used to identify differential immune-related genes between tumor and para-carcinoma tissue. Using weighted correlation network analysis and Cox regression analysis, the IRGPI was constructed, and Kaplan–Meier analysis was used to evaluate its predictive ability. We also analyzed the molecular and immune characteristics between IRGPI high-and low-risk subgroups, performed sensitivity analysis of ICI treatment, and constructed overall survival-related receiver operating characteristic curves to validate the IRGPI. Finally, IRGPI genes and tumor immune cell infiltration in CRC model mice with orthotopic metastases were analyzed to verify the results.

**Results:** The IRGPI was constructed based on the following 11 hub genes: ADIPOQ, CD36, CCL24, INHBE, UCN, IL1RL2, TRIM58, RBCK1, MC1R, PPARGC1A, and LGALS2. Patients with CRC in the high-risk subgroup showed longer overall survival than those in the low-risk subgroup, which was confirmed by GEO database. Clinicopathological features associated with cancer progression significantly differed between the high- and low-risk subgroups. Furthermore, Kaplan–Meier analysis of immune infiltration showed that the increased infiltration of naïve B cells, macrophages M1, and

regulatory T cells and reduced infiltration of resting dendritic cells and mast cells led to a worse overall survival in patients with CRC. The ORC curves revealed that IRGPI predicted patient survival more sensitive than the published tumor immune dysfunction and rejection and tumor inflammatory signature

**Discussion:** Thus, the low-risk subgroup is more likely to benefit from ICIs than the high-risk subgroup. CRC model mice showed higher proportions of Tregs, M1 macrophages, M2 macrophages and lower proportions of B cells, memory B cell immune cell infiltration, which is consistent with the IRGPI results. The IRGPI can predict the prognosis of patients with CRC, reflect the CRC immune microenvironment, and distinguish patients who are likely to benefit from ICI therapy.

KEYWORDS

colorectal carcinoma, immune-related gene prognostic index (IRGPI), tumor immune microenvironment (TIM), immune-related gene (IRG), immune checkpoint inhibitor (ICI)

## Introduction

According to the Global Statistical Report on Cancer in 2020 (1), colorectal carcinoma (CRC) is one of the most common malignant tumors, ranking third in morbidity and second in mortality. More than 1.9 million new CRC cases and 935,000 CRC-related deaths were estimated to occur in 2020. The 5-year survival rate of patients with metastatic CRC is low at approximately 14% (2), and approximately 50% of patients who receive treatment develop metastases (3, 4).

Immunotherapy is a cutting-edge option for treating cancer that involves stimulation of specific immune responses to utilize the body's own immune system to suppress and kill tumor cells, thereby reducing tumor recurrence and metastasis. Immune checkpoint inhibitors (ICIs) are promising agents for treating a variety of solid tumor malignancies such as melanoma and lung cancer. Pembrolizumab and nivolumab are ICIs targeting programmed cell death protein 1 and have both been approved by the U.S. Food and Drug Administration for the treatment of microsatellite instability-high/DNA mismatch repair-deficient CRC (5, 6). However, this tumor type accounts for only 5% of metastatic CRCs, and the remaining patients show poor responses to ICI (7, 8). Various factors, including immunoassay sites and the tumor immune microenvironment (TIME), affect the effectiveness of ICIs, and the analysis of TIME can lead to the development of methods for improving the reactivity to immunotherapy (9).

Only few biomarkers have been identified for predicting patient prognosis. Therefore, more biomarkers that can reflect the benefit of immunotherapy as a clinical reference for predicting the survival and prognosis of patients with CRC are needed. In this study, we constructed a CRC-related prognostic marker using 11 genes that could predict the prognosis of immunotherapy, as shown in Figure 1. Based on the differential immune-related genes in the transcriptome data of patients with CRC in TCGA (The Cancer Genome Atlas), we identified immune-related hub genes and weighting coefficients related to patient prognosis, constructed the immune-related gene prognostic index (IRGPI), and verified its power reliability using multiple datasets. We then characterized the molecular and immune signatures between high- and low-risk subgroups determined using the IRGPI, examined their prognostic power in patients following immunotherapy, and compared them with other biomarkers, tumor immune dysfunction and rejection (TIDE), and tumor inflammatory signature (TIS). To simulate the characteristic environment in patients with CRC, we established an animal model of CRC to verify the prediction ability of the IRGPI. Our results suggest that IRGPI is a promising prognostic biomarker in patients being administered conventional immunotherapy and immunotherapy.

**Abbreviations:** AUC, area under the receiver operating characteristic curve; CRC, colorectal cancer; CTLA-4, cytotoxic T-lymphocyte-associated protein-4; FC, fold change; GEO, Gene Expression Omnibus; GO, Gene Ontology; ICI, immune checkpoint inhibitor; IC, immune checkpoint; IRG, immune-related gene; IRGPI, immune-related gene prognostic index; KEGG, Kyoto Encyclopedia of Genes and Genomes; K–M, Kaplan–Meier; PD-1, programmed cell death protein-1; PD-L1/2, programmed death protein ligand 1/2; OS, overall survival; ROC, receiver operating characteristic; TCGA, The Cancer Genome Atlas; TIDE, tumor immune dysfunction and rejection; TIME, tumor immune microenvironment; TIS, tumor inflammatory signature.

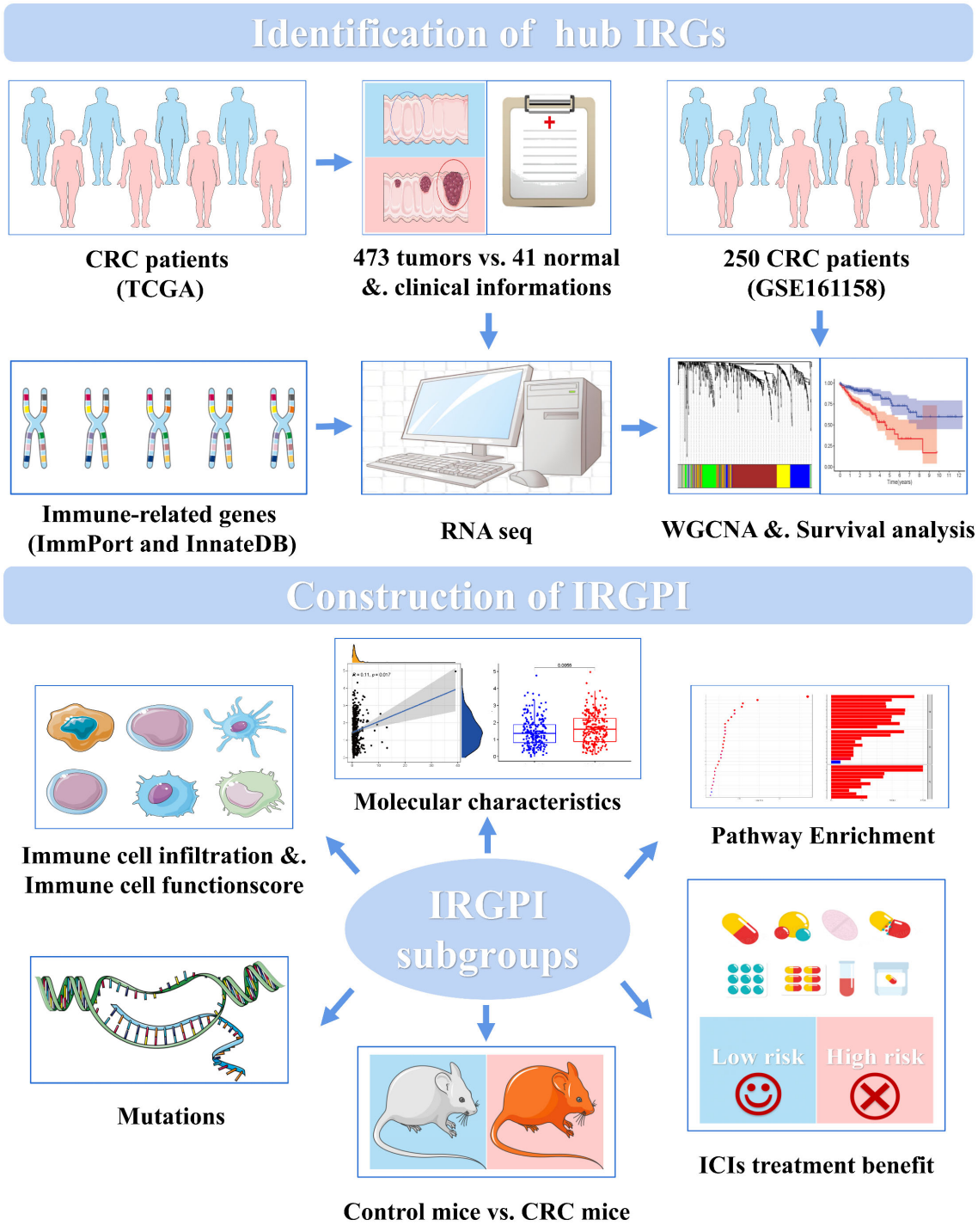


FIGURE 1
CRC IRGPI experimental technical roadmap.

# Materials and methods

## Collection of sample information

As the test group, transcript data and clinicopathological information were downloaded from the TCGA database (https://portal.Gdc.cancer.gov/), including 41 cases of para-tumors, 473 cases of CRC tumors, and 452 clinical cases. The TCGA data matrix was used to establish IRGPI in the following series of studies.

As the train group, survival and transcriptional data for 250 CRC cases were downloaded from the GEO database (https://www.ncbi.nlm.nih.gov/geo/). The transcript dataset GSE161158 was uploaded in November 2020 by the Moffitt Cancer Research Center, University of Miami (10). The GEO survival analysis was used to validate the results of IRGPI.

Lists of immune-related genes were downloaded from ImmPort (https://www.immport.org/home) and Innate DB (https://www.innatedb.ca/). KEGG (http://www.gsea-msigdb.org/gsea/index.jsp) gene sets and all Gene Ontology (GO) gene sets were used as gene symbols. Gene mutation information was downloaded from the cBioPortal (http://www.cbioportal.org/).

## Identification of immune-related differential genes

Limma package was used to analyze the differential expression of immune-related genes in para-tumor and tumor tissues. The ratio of expression between two samples (groups) [Log2fold-change (FC) = log2(treat mean/control mean)] and the *p*-value were calculated. A Log2FC >0 indicated that the gene is upregulated in the tumor tissue, whereas a Log2FC<0 indicated that the gene is downregulated in the tumor tissue. The false discovery rate was obtained by correcting the *p*-value (|Log2FC| >1 and false discovery rate<0.05). Differential immune-related genes (IRGs) identified using TCGA were analyzed for GO terms and KEGG pathway enrichment. The filter was adjusted to $p< 0.05$, and circles, bar plots, and bubble plots were drawn.

## Weighted gene co-expression network analysis to identify immune-related hub genes

The differential IRG dataset was selected to eliminate samples with data fluctuation and free and missing data, and the mean value of repeated data was determined. The Pearson correlation coefficient between any two genes was calculated; if the coefficient was higher than the threshold of 0.3, the two genes were considered as similar. The weighted value of the correlation coefficient was used in the analysis, taking the IRG correlation coefficient to the 20th power so that the connection between the genes obeyed the scale-free network distribution (11). These data were then converted into a topological matrix that described the degree of association between genes using a topological overlap metric. The genes were clustered using 1 – topological overlap metric as the distance, and a dynamic pruning tree was constructed to identify the modules (12). Finally, five modules were identified by setting the merge clipping threshold to 0.25. Univariate Cox regression analysis was performed on module (blue, brown, and yellow) genes significantly associated with CRC, and the correlation between the module genes and overall survival (OS) was determined. Thirty-four immune-related hub genes showing significant associations with survival were selected for further analysis.

## Establishment and verification of IRGPI

For the 34 immune-related hub genes, multivariate Cox regression analysis was used to construct the IRGPI. The risk score of each patient was obtained by the coefficient of multiplying the expression data of IRGs, and the patients were divided into high- and low-risk groups according to the median value of the risk score. The prognosis of subgroup patients defined using the IRGPI was assessed using the Kaplan–Meier (K–M) survival curve and log-rank test of TCGA and GEO cohorts. Prognostic univariate and multivariate Cox regression analyses were performed for age, sex, stage, and risk score to determine whether the risk score was affected by other factors. To detect associated genetic alterations, somatic mutations in patients between the high- and low-risk subgroups were analyzed using the maftools package in R software (The R Project for Statistical Computing, Vienna, Austria).

## Assessment of immune cell infiltration and immune characteristics

CIBERSORT was used to calculate the immune cell infiltration of samples from the TCGA dataset (13). According to the risk score, differences in immune cell infiltration between the high- and low-risk subgroups were counted, a boxplot was obtained, and the survival curves of the two groups were plotted. The immune function scores of samples in the high- and low-risk subgroups were calculated to obtain immune-related function scores for each sample. Higher scores indicated weaker immune function and *vice versa*. In addition, IC gene expression and risk analyses were performed in the high- and low-risk groups using the IRGPI.

## IRGPI and TIDE score

The TIDE score table, including the TIDE score, exclusion immune rejection, and dysfunction, was obtained from the TIDE database (http://tide.dfci.harvard.edu/) according to TCGA transcriptome files. Wilcoxon test was performed on the TIDE scores in the high- and low-risk subgroups, and a violin plot was drawn according to the results. The OS-related receiver operating characteristic (ROC) curves of TIDE, TIS, and IRGPI were plotted to compare the predictive powers of these values. The ROC curve of IRGPI related to OS at 1, 2, and 3 years was drawn; a larger area under the curve indicated that the model had higher prediction sensitivity.

## IRGPI gene expression in the CRC murine model

Specific pathogen-free BALB/c male mice, 6–8 weeks old with a body mass of 20 ± 5 g, were purchased from the Huaxing Experimental Animal Farm of Huiji District (Zhengzhou City, China), under the experimental animal license No. SCXK (Yu) 2019-0002. All animal experiments were approved by the Experimental Mouse Ethics Committee of the Nanjing University of Traditional Chinese Medicine (No. 202010A026).

The mice were randomly divided into the control group and the CRC model group, with 10 mice per group. Five BALB/c male mice were used as tumor-bearing mice, into which $1 \times 10^7$ CT26 cells were subcutaneously injected into the left axilla and sacrificed 1 week later. The subcutaneous tumor was removed under sterile conditions, placed in sterile phosphate-buffered saline, and divided into several 1-$mm^3$ masses. Under sterile conditions, the two groups of mice were dissected to expose the colon; the 1-$mm^3$ tumor mass was fixed to the colon of the CRC model group with tissue glue, whereas the control group was not fixed, and then the abdomen from mice in the two groups was sutured. After 3 days of postoperative recovery, the mice were weighed, and micro-computed tomography scanning was performed on day 26 (under isoflurane respiratory anesthesia). On day 27, the mice were sacrificed under anesthesia with 2% sodium pentobarbital. Total RNA was extracted from the colon of the control group and tumor tissue of the CRC model group using a FastPure Cell/Tissue Total RNA Isolation Kit (Vazyme, Nanjing, China, Cat#RC101-01). The RNA was reverse-transcribed into cDNA using HiScript® III RT SuperMix for quantitative PCR (Vazyme, Cat#R323-01), and then real-time PCR was performed to detect the expression of IRCPI genes in each group using Blastaq™ Green 2× qPCR MasterMix (abm, Richmond, British Columbia, Canada, Cat#G891). The primer sequences are listed in Table S4.

## Immune infiltration in the CRC murine model

The liver, colon, tumor, and mesentery of paraffin-embedded mice were sectioned, stained with hematoxylin–eosin, and photographed using an upright white light photographic microscope (Eclipse Ci-L, Nikon, Tokyo, Japan).

TIME immune cells were detected using flow cytometry. Peripheral blood mononuclear cells were extracted using RBC lysate (Cat#FMS-RBC500, FcMACS, Nanjing, China). At least $5 \times 10^6$ cell suspensions (100 µl) were incubated with FC blocker at 4°C for 10 min and then anti-human/mouse CD11b FITC antibody (Cat#03221-50, PeproTech, Rocky Hill, NJ, USA), PE-Cy™7 rat anti-mouse CD86 antibody (Cat#560582, BD Pharmingen™, San Diego, CA, USA), and Alexa Fluor® 488 anti-mouse CD206 antibody (Cat#141710, BioLegend, San Diego, CA, USA) were used to detect macrophages. Alexa Fluor® 488 anti-mouse CD19 antibody (REF#11-0193-81, Invitrogen, Carlsbad, CA, USA) and PE/Cy7 anti-mouse/rat/human CD27 antibody (Cat#124216, BioLegend) were used to detect B cells. Anti-mouse CD4 APC-cyanine7 (Cat#06122-87, PeproTech), anti-mouse CD8a FITC antibody (Cat#10122-50, PeproTech), anti-mouse CD25 APC antibody (Cat#07312-80, PeproTech), and anti-mouse/rat FOXP3 PE antibody (Cat#83422-60, PeproTech) were used to detect T cells. The cells were detected on an Amnis FlowSight flow cytometer (Merck Millipore, Billerica, MA, USA), and immunocyte subsets were analyzed using the IDEAS software (Merck Millipore). Figure S7 shows the strategy used to analyze the IRGPI immunocyte subsets using flow cytometry.

## Statistical methods

Independent *t*-tests were performed to compare continuous variables between the two groups. Data for various clinicopathological factors were analyzed using chi-square test. The TIDE scores between the groups were compared using Wilcoxon test. Univariate survival analysis was performed using K–M survival analysis and log-rank test. Univariate and multivariate Cox regression analyses were performed using the R package "survival" with hazard ratios and 95% confidence intervals. $p < 0.05$ indicated a significant difference between the two groups. The software Strawberry-perl-5.30.2.1, Rx64 4.1.0 (R Project), and GraphPad Prism 8 (GraphPad, Inc., La Jolla, CA, USA) were used in these analyses.

10.3389/fimmu.2022.944286

# Results

## CRC differential immune-related genes

A total of 7,780 differentially expressed genes (473 tumors versus 41 para-tumor samples) were identified in TCGA-differential expression analysis, among which 5,502 and 2,278 genes were up- and downregulated, respectively, in tumor samples compared to the genes in para-tumor samples (Tables S1 and S2). By intercrossing these genes with immune-related genes obtained from ImmPort and InnateDB, 649 differential immune-related genes were obtained, among which 256 and 393 genes were up- and downregulated, respectively, in tumor samples compared to those in para-tumor samples (Figure S1A).

Enrichment analysis of 649 immune-related differentially expressed genes screened from the TCGA dataset revealed significant correlations in 1,295 GO terms ($p< 0.001$) and 66 KEGG pathways ($p< 0.05$). The top 30 GO terms and KEGG pathways are shown in Figure S1B. The top three pathways enriched in GO analysis were humoral immune response, complement activation, and classical pathway (Figure S2A). The top three pathways enriched in KEGG analysis were cytokine–cytokine receptor interaction, viral protein interaction with cytokine and cytokine receptor, and chemokine signaling pathway (Figure S2B).

## Construction of IRCPI with 11 CRC immune-related hub genes

Weighted gene co-expression network analysis was used to analyze immune-related differential genes ($n$ = 649), and immune-related hub genes were identified (Figure S3A). The logarithm log($k$) of the node with connectivity $k$ and logarithm log of the node probability [$P(k)$] were negatively correlated, with a correlation coefficient >0.9 and an optimal soft threshold of 4. A total of 649 genes were assigned to the five modules. According to the Pearson correlation coefficients between modules and sample features, the blue, brown, and yellow modules were closely associated with CRC and positively correlated (Figure S3C). Genes in these modules were selected for further analyses. Thirty-four hub genes were significantly associated with OS according to univariate Cox regression analysis ($p< 0.05$) (Figure 2A, Table S3). Next, multivariate Cox regression analysis was performed, and 11 hub genes were obtained to establish prognostic indicators. This result was validated in the K–M analysis, as shown in Figure S3D ($p< 0.05$). Specifically, the IRGPI risk score was calculated using the gene expression levels multiplied by the weights of the 11 genes, as shown in Table 1.

## Molecular characteristics of CRC-related high- and low-risk IRGPI subgroups

The IRGPI was established by multiplying the expression data for the hub IRGs by the multivariate Cox regression coefficients, as follows: $risk\ \ score = \sum_{n=11}^{1}(gene\ \ expression\ \ data \times coef)$. Based on the median risk score, the samples were divided into high- and low-risk groups. There was a significant difference in the survival period between high- and low-risk patients ($p< 0.05$), as shown in Figure 2D. Univariate and multivariate Cox regression analyses were performed on the risk scores and clinical traits of the two groups, respectively. The risk scores showed significant differences ($p< 0.001$) related to the stage, features/extent of the primary tumor (T), regional lymph node involvement (N), and distant metastases (M) ($p< 0.001$), but not sex or age (Figures 2B, C). We then explored the signatures of 34 immune-related hub genes. As shown in Figure S4A, in 28.32% of the 399 samples, 34 immune-related hub genes showed amplifications, deep deletions, and missense mutations. As we all know, targeted somatic mutation (TSM) reflects the immunotherapy resistance, and a higher TSM represents a worse immunotherapy outcome.

We selected the top 20 genes with mutation in the high- and low-risk groups (Figure S4A), and we found that the low-risk group had a higher altered rate. The mutation of *APC*, *TP53*, *TTN*, and *LRP2* was more common in the IRGPI-high subgroup, whereas the mutation of *SYNE1*, *PIK3CA*, *MUC16*, *FAT4*, *ZFHX4*, *RYR2*, *OBSCN*, *DNAH5*, *PCLO*, *LRP1B*, and *DNAH11* was more common in the IRGPI-low subgroup (Figure S4B). The result demonstrated the low-risk group with more universality of germline and somatic mutations in DNA mismatch repair (MMR) genes that have a chance to overcome the genomic instability.

KEGG pathway enrichment analysis of 11 IRGPI hub genes showed that the high-risk group was significantly enriched in cell adhesion, extracellular matrix, focal adhesion, and PPAR signaling pathways, which were associated with CRC progression and metastasis and indicated a worse prognosis (Figure S4C).

## Prediction of immune cell infiltration in the CRC microenvironment with IRGPI

CIBERSORT was used to analyze the infiltration of immune cells in the IRGPI subgroups. We detected more follicular helper T cells in the IRCPI high-risk subgroup, whereas CD4+ memory resting T cells and activated mast cells were more abundant in the low-risk subgroup ($p< 0.05$) (Figure 3A). Features associated with the immune landscape, including the clinicopathological features of different IRGPI subgroups, are shown in Figures 3B, D. Dendritic cells, human leukocyte antigen, macrophages, T helper cells, tumor-infiltrating lymphocytes (TIL), and type I

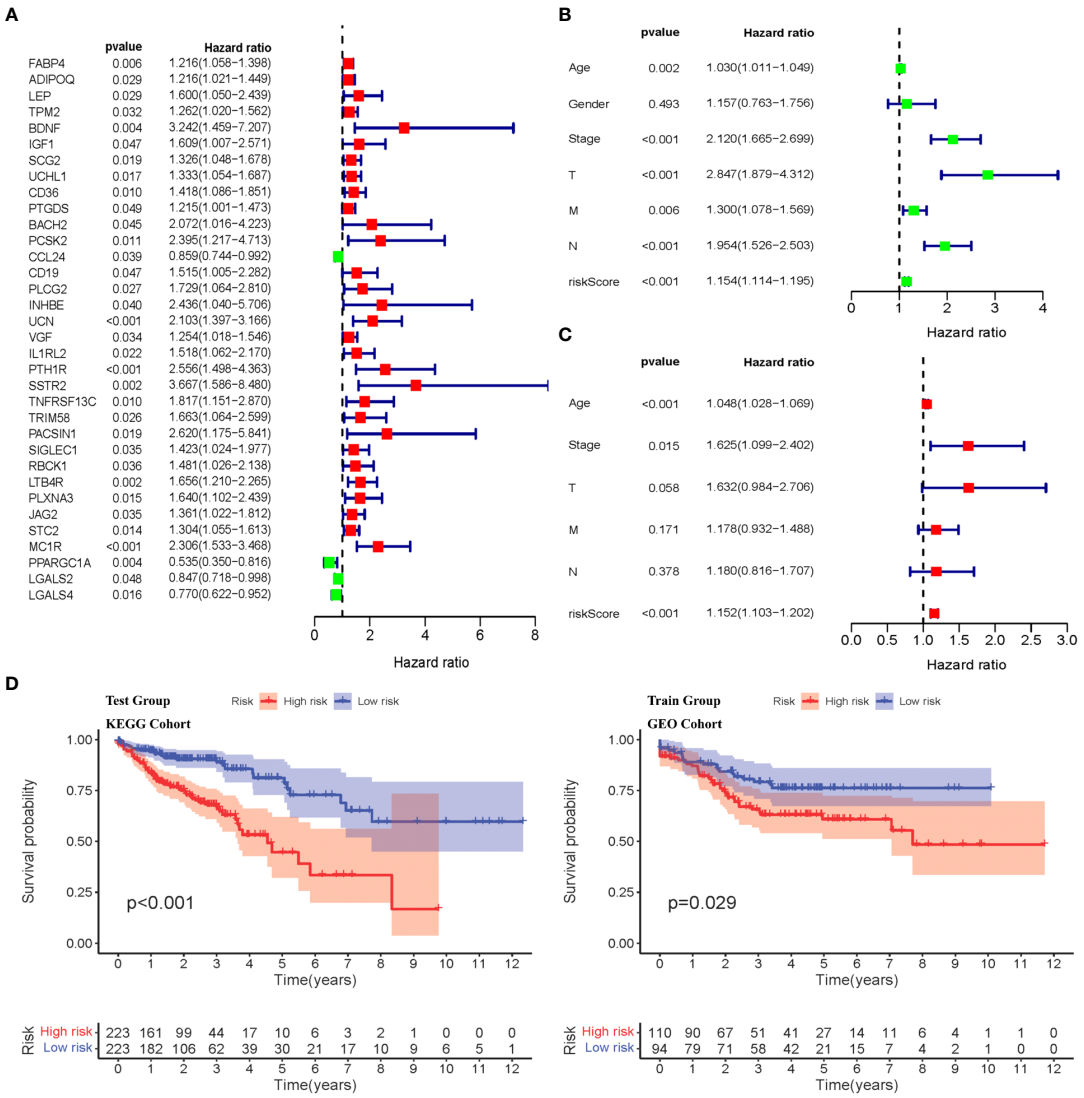


FIGURE 2
Identification of immune-related diffrentional genes *via* Cox regression and K-M analysis of IRGPI subgroups. **(A)** Univariate Cox analysis of 34 immune-related hub genes ($p< 0.05$). **(B, C)** Univariate and multivariate Cox regression analysis on IRGPI riskscore and other clinicopathologic variables. **(D)** Kaplan–Meier survival analysis between IRGPI subgroups in the TCGA cohort and GEO cohort ($p< 0.05$).

interferon responses showed higher immune function scores ($p< 0.05$) in the high-risk IRCPI subgroup (Figure 3C). Immune function scores are correlated with the prognosis of patients with multiple tumors, and patients with high immune scores have a poorer prognosis compared to patients with low scores.

To further investigate whether the prognostic value of IRGPI is based on immune cell infiltration, we performed differential immune cell-related and immune function-related K–M analyses. As shown in Figure 3E, five types of immune cells were significantly associated with OS. Patients with more naïve B cells, macrophages M1, and T-cell regulatory (Treg) infiltration had poor OS, whereas patients with more resting dendritic cells and activated mast immune cell infiltration had a longer OS ($p< 0.05$).

## IRGPI is significantly associated with CRC progression

To explore the relationship between IRGPI and various clinicopathological factors, 445 patients in the high- and low-risk IRGPI subgroups were evaluated using chi-square test to determine the distribution of different clinical features, as shown

TABLE 1 The 11 immune-related hub genes used to compute the IRGPI risk score.

| ID | Coef | HR | HR.95L | HR.95H | *p*-value |
|---|---|---|---|---|---|
| **ADIPOQ** | −0.2869 | 1.21605 | 1.02064 | 1.44886 | 0.02863 |
| **CD36** | 0.77205 | 1.41784 | 1.08580 | 1.85140 | 0.01033 |
| **CCL24** | −0.15359 | 0.85923 | 0.74388 | 0.99247 | 0.03914 |
| **INHBE** | 1.041035 | 2.43576 | 1.03974 | 5.70616 | 0.04039 |
| **UCN** | 0.584717 | 2.10328 | 1.39728 | 3.16602 | 0.00037 |
| **IL1RL2** | 0.310954 | 1.51794 | 1.06197 | 2.16971 | 0.02203 |
| **TRIM58** | 0.599037 | 1.66316 | 1.06424 | 2.59914 | 0.02553 |
| **RBCK1** | 0.322746 | 1.48107 | 1.02588 | 2.13822 | 0.03605 |
| **MC1R** | 0.526967 | 2.30592 | 1.53315 | 3.46820 | 0.00006 |
| **PPARGC1A** | −0.78226 | 0.53452 | 0.35002 | 0.81627 | 0.00373 |
| **LGALS2** | −0.2145 | 0.84689 | 0.71843 | 0.99832 | 0.04771 |

in Figure 4A. Between the two subgroups, patients in the T, N, and M stages showed more severe cancer progression ($p< 0.01$), whereas age and sex were unrelated to progression. These results indicate that the prognostic value of IRGPI is related to CRC progression.

## IRGPI risk scores correlate with immunotherapy biomarkers

Some biomarkers are used in clinical immunotherapy, including programmed cell death protein-1 (PD-1), programmed death protein ligand 1/2 (PD-L1/2), cytotoxic T-lymphocyte-associated protein-4 (CTLA-4), and lymphocyte-activation gene 3 (LAG-3) (14). In addition to PD-L1/2 and CTLA4, CD27 and FOXP3 are biomarkers of activated B cells and Tregs, which can reflect the activity of immunocytes to some extent. We next explored the relationship between the IRGPI score and these biomarkers. As shown in Figure 4B and Figure S6B, the IRGPI score was positively correlated with PD-1, PD-L1/2, CTLA-4, and LAG-3. Pearson's correlation coefficient (*R* value) between the IRGPI risk score and PD1 was 0.14, with a *p*-value of 2.3e-03 (PD-L1: $R = 0.079$, $p = 9.4e-02$; PD-L2: $R = 0.11$; $p = 2.2e-02$; CTLA-4: $R = 0.1$, $p = 3.4e-02$; LAG3: $R = 0.15$, $p = 1.2e-03$; CD27: $R = 0.11$, $p = 1.7e-02$; FOXP3: $R = 0.12$, $p = 9.6e-03$). In addition, the expression of IC genes in the high-risk subgroup was higher than that in the low-risk subgroup ($p< 0.05$), as shown in Table S6. Combined with the previous results of mutation, these results suggest that there were more immunosuppressive signals and tumor progression- and tumor metastasis-related signals in the high-risk group; meanwhile, there was more active immunity and damage repair in the low-risk group, which was consistent with the results of immune cell infiltration. In conclusion, the IRGPI low-risk group is more likely to develop an efficiently immune response from immunotherapy.

## IRGPI predicts benefits from immunotherapy

We used TIDE to assess the potential clinical efficacy of immunotherapy in different IRGPI subgroups. The TIDE score can evaluate the efficacy of immunotherapy for tumors, with a higher score representing a higher risk of immune evasion, suggesting that patients are less likely to benefit from ICI therapy (15). Our results show that the IRGPI high-risk subgroup had a higher TIDE score than the IRGPI low-risk subgroup ($p< 0.05$), with a higher T-cell dysfunction and exclusion score (Figure 4C). These results indicate that at-risk patients with a high IRGPI benefit less from ICI therapy compared to patients with a low IRGPI.

Analysis of the predictive power of IRGPI showed that its sensitivity was significantly higher than those of the TIDE and TIS scores (Figure 4D, area under the ROC curve: IRGPI = 0.744 > TIDE = 0.541 > TIS = 0.483). These results suggest that the IRGPI score is a suitable biomarker for predicting the immunotherapy response. In addition, the reliability of the IRGPI was determined using the time-dependent ROC curve (Figure 4D); we also tested the ROC curve using the TCGA dataset, as shown in Figure 4D. The areas under the 1-, 2-, and 3-year ROC curves were 0.723, 0.724, and 0.744, respectively, indicating that the IRGPI is useful for monitoring the survival rate.

## The CRC murine model verified the IRGPI predictive power

To support the predictive power of the IRGPI, we established a CRC mouse model and tested IRGPI gene and immune cell infiltration in the TME. The weight changes in the two groups were recorded. Mice in the CRC model group showed weight loss at later stages of CRC ($p< 0.05$) (Figure 5B). We scanned the abdominal cavity using micro-computed tomography to determine the morphology of the CRC tumors (Figure 5D). The

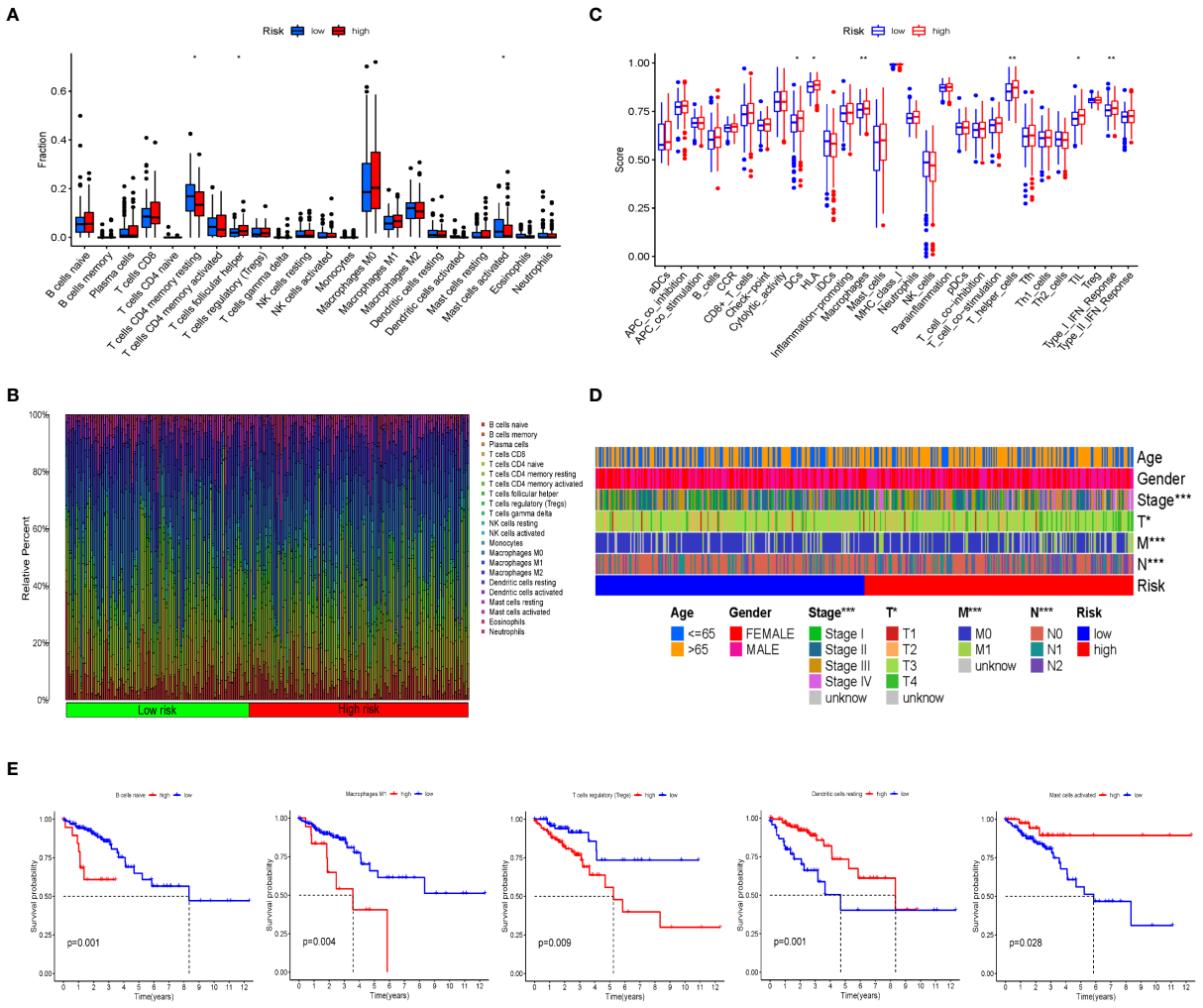


FIGURE 3
Immune cell infiltration and immune function scores between IRGPI subgroups. **(A)** Comparison of tumor immune cell infiltration between two IRGPI subgroups. Significant statistical differences between the two subgroups were assessed using the Wilcoxon test (*$p$< 0.05, **$p$< 0.01). **(B)** The proportions of TIME immune cells in different IRGPI subgroups. **(C)** Comparison of immune function score between two IRGPI-related CRC subgroups. Significant statistical differences between the two subgroups were assessed using the Wilcoxon test (*$p$< 0.05, **$p$< 0.01). **(D)** Clinicopathological information of the IRGPI-related CRC subgroups in the TCGA cohort. Age, gender, tumor stage, and T, M, and N are shown as patient annotations (*$p$< 0.05, **$p$< 0.01, ***$p$< 0.001). **(E)** Kaplan–Meier survival analysis of the TME cells and immune function IRGPI subgroups in the TCGA cohort.

results confirmed sufficient maturity of the CRC murine model. Pathological sections of the liver, colon, tumor with colon cancer, and mesentery were obtained (Figure 5C). Compared to the normal group, mesentery lymph nodes in CRC model mice were degenerated and reduced, with focal infiltration of local lymphocytes. Compared with the colon tissue arranged in a compact and orderly manner, tumor cells in the colon from the model group showed nuclei atypia, a high nuclear–cytoplasmic ratio, inconspicuous nucleoli, more mitotic phase (black arrow), a large area of tissue necrosis (green arrow), deep staining and fragmentation of nucleus shrinkage, and enhanced eosinophilic cytoplasm (yellow arrow). The liver is the first metastatic organ affected by CRC. As shown in Figure 5C, compared with normal mice, the liver of CRC mice contained a large number of hepatocytes with granular degeneration and loose cytoplasm around the central vein, bile duct area, and liver parenchyma, with loose and light-stained granular cytoplasm (black arrow), along with a lymphocytic infiltrate around the local bile duct (blue arrow). IRGPI gene expression was detected in both groups. We observed higher expression levels of Il1rl2, Rbck1, and Ppargc1a in tumor tissues of the CRC group and higher expression levels of Adipoq and Ucn in the colon of the control group (Figure 4E). The risk coefficient of IRGPI is the comprehensive score calculated by the expression levels of 11 genes and their risk coefficients, through

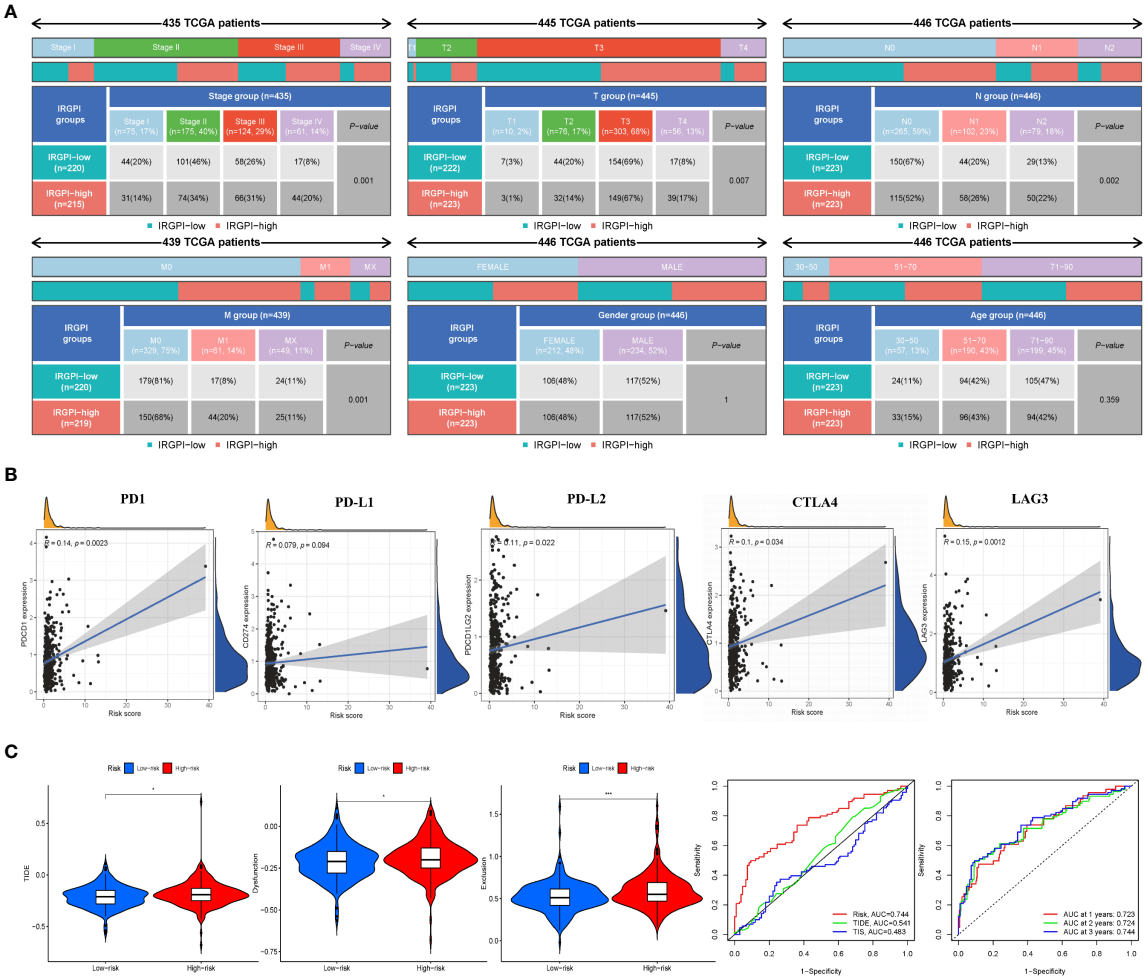


FIGURE 4
IRGPI signifcantly correlates with clinicopathological factors in CRC patients and the analysis of immunotherapy responses. **(A)** Heatmap and table showing the distribution of multiple clinicopathological factors in CRC patients between two IRGPI subgroups. **(B)** Scatter plots coordinated by IRGPI risk score with immune checkpoint PD-1, PD-L1, PD-L2, CTLA4, and LAG3, respectively. **(C)** TIDE, dysfunction, and T-cell exclusion score in different IRGPI subgroups. The scores between the two IRGPI subgroups were compared through the Wilcoxon test (*$p$< 0.05, ***$p$< 0.001). **(D)** Performance comparison between IRGPI risk, TIDE, and TIS in predicting 1-year OS in the TCGA cohort. Time-dependent ROC curve and AUC values in the TCGA cohort.

a complex process. It is worth noting that the IRGPI in the two kinds of mice may still have significance due to the distinction in the expression levels of the differential genes, in spite of the fact that there were no difference in some genes.

## Immune cell infiltration in the immune microenvironment of the CRC murine model has a negative impact on prognosis

To investigate whether the IRGP1 could predict changes in immune cell infiltration in CRC, we detected some immune cells in the peripheral blood of both groups of mice, as shown in Figure 6. An independent $t$-test was used to analyze the proportion of immune cells in the two groups. The proportions of Tregs CD4+CD8+FOXP3+ ($p$ = 0.0056), M1 macrophages CD11b+CD86+ ($p$ = 0.0017), and M2 macrophages CD11b+CD206+ ($p$ = 0.0393) in CRC model mice were higher than those in the control group. The proportions of B cells CD19+ ($p$ = 0.0090) and memory B cells CD19CD27+ ($p$ = 0.0430) in the CRC group were significantly lower, whereas helper T lymphocyte CD4+ and cytotoxic T lymphocyte CD8+ cells in the CRC group tended to be lower than those in the control group.

These results indicate that changes related to T cells, B cells, and macrophages occur in the TIME of CRC, which is similar to

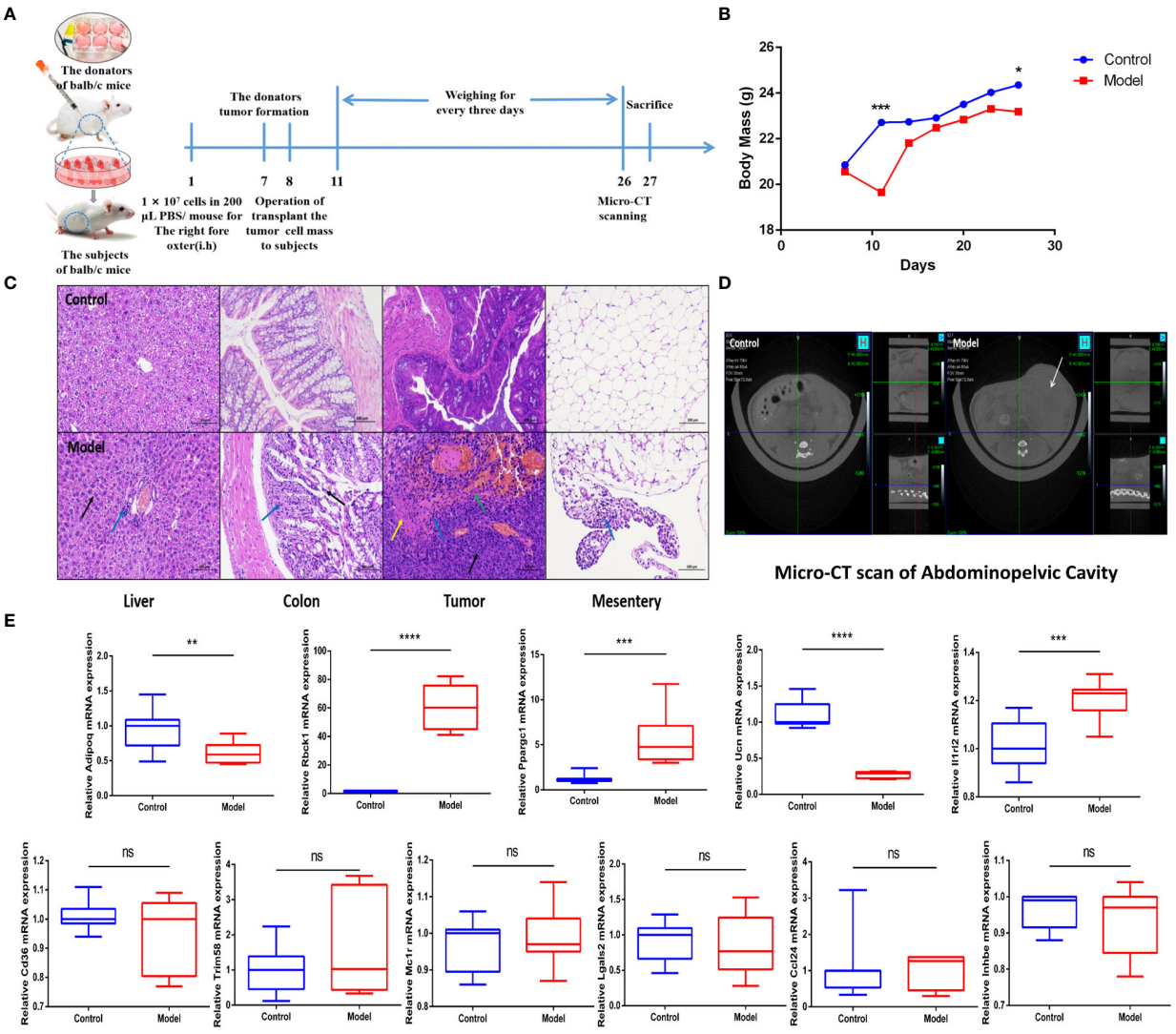


FIGURE 5
IRGPI gene expression situation in the identified murine CRC model. **(A)** Experimental scheme to establish the murine conlon transplant CRC metastasis model. **(B)** Curve of murine body mass change trends ($n$ = 10, *$p$< 0.05, ***$p$< 0.001). **(C)** Inflammatory changes within liver, colon, tumor, and mesentery were measured by H&E staining (scale bar = 100 μm; the blue arrow points to the inflammatory cell infiltration; the black arrow points to the cellular damage; the yellow arrow points to the tumor cells nuclear abnormalities and cytoplasm eosinophilic; the green arrow points to the necrosis and hemorrhage). **(D)** Micro-CT scan images of abdominal cavity between control and model groups (the white arrow points to the tumor in abdominal cavity). **(E)** Relative IRGPI gene expression detection by RT-PCR between control and model groups. (Values are presented as $2^{-\Delta\Delta CT}$ mean ± SEM, $n$ = 3 replicates per group, ns: not significant, *$p$< 0.05, **$p$< 0.01, ***$p$< 0.001, ****$p$< 0.0001.

the prediction results of the IRGPI. These results confirm the accurate prediction ability of the IRGPI.

## Discussion

In recent years, immunotherapy has been widely examined as a treatment for CRC, including ICIs, immunization, and adoptive T-cell therapy (16). An increasing number of ICI monotherapy or combination strategies is being designed to treat CRC. ICI therapy is an effective treatment for relapsed or refractory CRC (17). For example, PD-1 combined with a CTLA-4 blocker is clinically effective and well-tolerated in patients with advanced CRC having a defective DNA mismatch repair (18). However, CRC, like breast and ovarian cancers, is generally considered as a hypo-immunoreactive cancer (19), with limited infiltration of immune cells or extensive infiltration of immunosuppressive T cells; therefore, not all patients with CRC may benefit from these

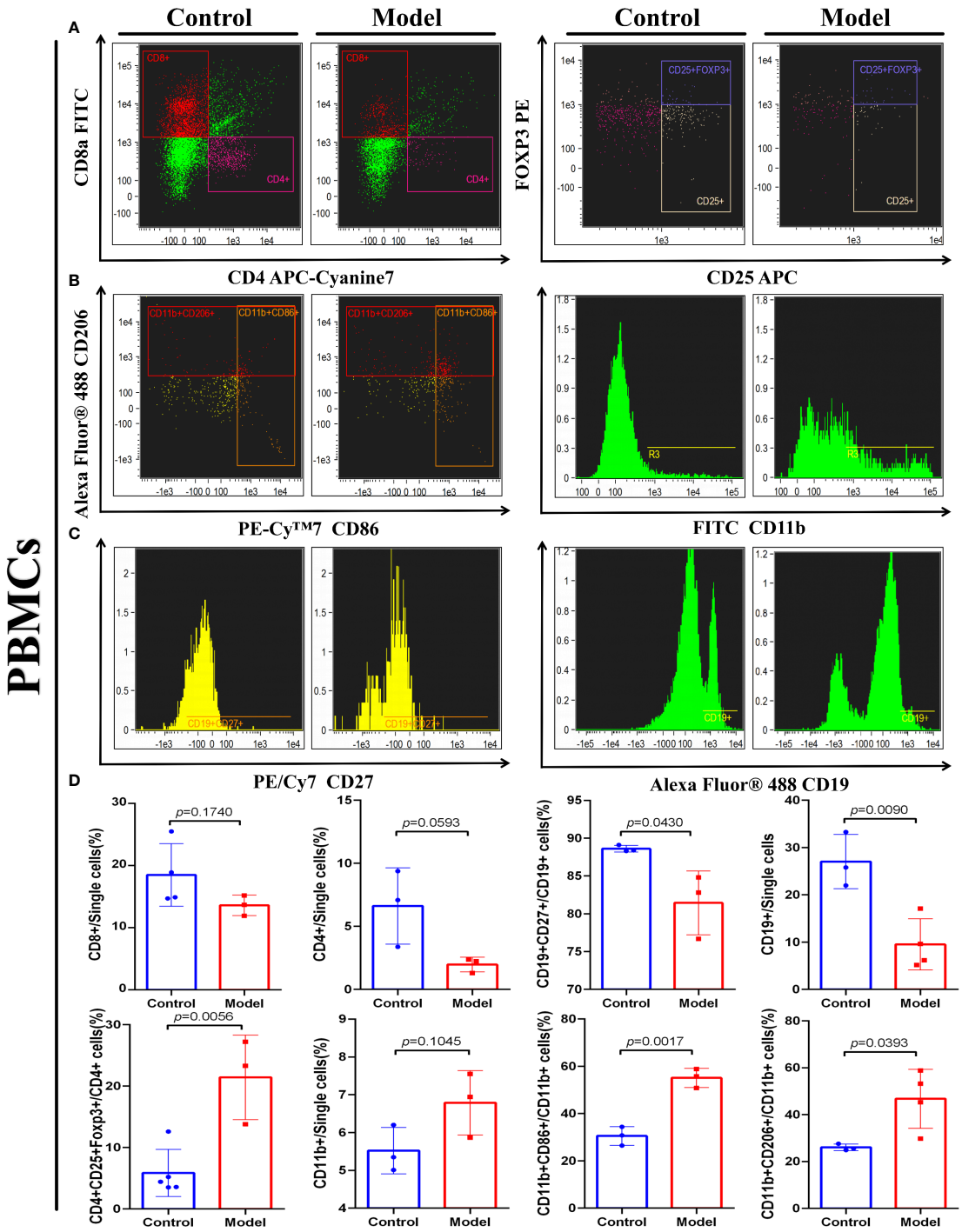


FIGURE 6
IRGPI-related immune cell discrepancy between CRC model mice with control mice. Flow cytometry determined the proportion of a series of immune-related cells that existed in murine peripheral blood. **(A)** T cells, **(B)** Macrophages, and **(C)** B cells. **(D)** Unpaired *t*-test analysis of the proportion of the immune-related cells: Cytotoxic T lymphocytes (CD8+), Helper T lymphocytes (CD4+) and Tregs cells (CD4+CD25+FOXP3+), B cells (CD27+), memory B cells (CD27+CD19+), Macrophages (CD11b+), M1 Macrophages (CD11b+CD86+), and M2 Macrophages (CD11b +CD206+) between control and the CRC model group. (Values are presented as mean ± SEM, *n* = 3 per group.).

treatments (20). Therefore, it is crucial to establish a characteristic classification for effectively targeting specific CRC subtypes and screening patients who may benefit the most from ICI treatment. Widely used biomarkers such as PD-L1 levels, TMB (tumor mutational burden), TIDE, and high microsatellite instability are not always reliable (21), highlighting the need to identify prognostic biomarkers for CRC immunotherapy.

In this study, 649 differential IRGs of CRC were selected from patient information to construct the IRGPI. The most relevant biological processes and signaling pathways were "humoral immune response" and "cytokine–cytokine receptor interaction," respectively, which is consistent with the pathological process of the CRC immune response reported in the literature (22). IRGs were fitted into five modules, and 11 IRGs were screened out, confirmed the independent and effective prognostic factors, and performed OS analysis to verify this result. We also confirmed that IRGPI is closely associated with clinicopathological factors. Specifically, patients with CRC having a low IRGPI risk score showed a better prognosis, whereas those with a high IRGPI risk score had a worse prognosis.

After that, we found that the low-risk group had a higher mutation rate, whereas the largest difference in mutations between groups was in *TP53* mutations, which were more common in IRGPI-high samples than IRGPI-low samples (60% vs. 46%). As we all know, the TP53 mutation was linked to more aggressive disease and poorer patient outcomes in CRC through the p53/HRK/XEDAR signaling pathway (23, 24). Therefore, IRGPI-high patients with high *TP53* mutations have a worse outcome than IRGPI-low patients with low *TP53* mutations, in agreement with our survival results. Meanwhile, the more MMR in the low-risk group means more likely benefits from ICIs. The ICs related with the differential immune cells and immune function. Classically, CTLA-4 interacting with the B7 molecules, including PD-1 (programmed death-1), PD-L1 (programmed death ligand-1) (B7-H1), and PD-L2 (B7-DC), results in decreased T-lymphocyte activity and regulates the immune response (23, 24). Similarly, PD-1 interactions with PD-L1 and PD-L2 downmodulate T-cell immune responses (25). FOXP3 (Forkhead box protein 3), commonly used as a marker in Treg (regulatory T cells) cells, is an important transcription factor in the immunosuppressive function of CRC (26). LAG-3 (lymphocyte-activation gene 3) is associated with the immune resistance of CD4+ cells in patients with CRC (27). CD27 is a member of the TNF-receptor superfamily. This receptor plays a key role in regulating B-cell activation and immunoglobulin synthesis (28). According to the difference of the expression of these IC genes between the two IRGPI subgroups, we can conclude that ICs are closely related to the immune function of T cells and B cells.

In the next study, we found that macrophages, T helper cells, and type I IFN responses showed obvious higher immune function scores in the IRGPI-high group; meanwhile, there are significant differences in T cells between the IRGPI-high group and the IRGPI-low group. To further explore the key immune cell interactions that produced differences between the high- and low-risk groups, we performed differential immune cell-related and immune function-related K–M analyses. As a result, patients with more naïve B cells, M1 macrophages, and T-cell regulatory (Treg) infiltration had poor OS, whereas patients with more resting dendritic cells and activated mast immune cell infiltration had a longer OS. From the above results, we can draw a conclusion—the key immune cell interactions that produced different prognoses between the high- and low-IRGPI groups may be related to three immune cells: macrophages, T cells, and B cells. Therefore, in the next experiment, we selected these three immune cells for further study in a murine CRC model.

Immune cell infiltration is important for tumor progression; however, it is an underrated factor for evaluating the efficacy of ICI treatment (29). Increasing evidence has shown that the interaction between tumors and the microenvironment is critical for the progression of CRC and effectiveness of immunotherapy (30). Therefore, we assessed the relative proportions of 22 immune cells in the high- and low-risk subgroups of CRC samples, including immune cell infiltration and immune function scores and the roles of various immune cells to explain the low response to ICI in patients with CRC. In general, large numbers of activated memory CD4+ T cells, cytotoxic T cells, and CD8+ T cells contribute to the immune response and are associated with better prognosis (31), whereas resting immune cells indicate a state of immune failure (32). Interestingly, a recent study (33) described that mast cells play important roles in ICI therapy. We found that activated mast cells prolonged OS, suggesting a more active anti-tumor immune response in low-risk patients. Follicular helper T cells are a distinct subset of CD4+ helper T cells that activate B cells, generate specific antibody responses, and play important roles in the progression of autoimmune diseases (34). Follicular helper T cells suppress the development of regulatory B cells, indicating a poor prognosis for digestive system cancers (35). Therefore, high infiltration in the high-risk subgroup suggests an immunosuppressive tendency. High-risk patients with more naïve B cells, macrophages M1, and Tregs, which suppress the tumor immune response, have a shorter OS.

To understand the constitutive mechanism of the IRGPI coefficient, we explored the constitutive genes of IRGPI. RBCK1 not only reduces chemosensitivity (36) but also reduces lymphocyte activity *via* MALT1 (37). CD36 regulates cytokine production, antigen presentation, phagocytosis, and immune tolerance. Because inflammation triggers the initiation, proliferation, invasion, and metastasis of tumor cells, reducing CD36-mediated sterile inflammation may become a new mode of anti-tumor treatment (38). CD36 can also participate in tumor pathogenesis by regulating the PPAR pathway and inhibiting the mitochondrial

biogenesis regulator gene *PPARGC1A* (39). Aberrant methylation of *TRIM58* has become a biomarker in multiple cancer prognostic models (40–42). IL1RL2 binding to IL-36 orchestrates an innate-adaptive immune linkage to control enteropathogenic bacterial infections (43) and promotes intestinal fibrosis in mice with chronic intestinal inflammation (44). MC1R promotes UV-induced DNA damage repair (45), and its frequent mutations are associated with an increased risk of CRC (46). In contrast, CCL24 is highly expressed in patients with CRC, is associated with a better prognosis (47), and specifically induces M1 macrophage chemotaxis (48). *LGALS2* is an oxidative stress-responsive gene that inhibits colon tumor growth (49). ADIPOQ is secreted by adipocytes in the tumor microenvironment, is widely present in the intestinal tract, and has been shown to activate cytotoxic autophagy induced by cancer cells; thus, elevated ADIPOQ levels are associated with decreased cancer growth (50). The results of these previous studies are consistent with those of the current study, showing that the correlation coefficients of immune-related oncogenes can be used when calculating IRGPI risk scores.

In summary, the IRGPI constructed based on 11 genes can accurately predict the survival rate of patients with CRC, reflect their immune microenvironment, and predict the sensitivity of immunotherapy. The mouse model of CRC constructed to observe IRGPI-related genes and immune cells in the CRC tumor microenvironment also showed differences in the expression of 11 IRGPI genes, supporting the validity of the IRGPI. Immune cells with immunosuppressive functions, including Tregs, M1 macrophages, and M2 macrophages, showed higher proportions in CRC mice than normal mice. Normal mice showed a higher proportion of active anti-tumor immune effector cells, such as B cells and memory B cells, and tended to have increased levels of helper T lymphocytes and cytotoxic T lymphocytes. These results confirm the expression changes of IRGPI genes in CRC tumor tissue and showed that the IRGPI accurately reflects the level of immune cell infiltration in CRC tumors.

Several biomarkers, such as TIDE and TIS, have been reported to predict patient responses to immunotherapy (51, 52). TIDE scores can predict prognosis more accurately compared to other biomarkers, such as PD-L1 levels and mutation burden, in patients with melanoma treated with first-line ICIs (15). Higher TIDE scores are associated with poorer outcomes (53). We observed higher TIDE scores in the IRGPI high-risk subgroup than in the IRGPI low-risk subgroup, suggesting that patients with low IRGPI benefited more from ICI treatment than those with high IRGPI. However, TIDE and TIS only focus on the function and state of T cells, which cannot fully reflect the complexity of immunocytes involved in immunotherapy in the TIME (54). Therefore, the IRGPI not only predicted differences in immune infiltration and immune function in the TIME of patients with CRC, but also showed a more accurate predictive ability than TIDE and TIS and better prediction of OS during long-term follow-up.

In conclusion, IRGPI is a promising immune-related prognostic marker that can intuitively predict the prognosis and immunotherapy effects in CRC (55, 56). In the era of precision medicine, biomarkers based on IRGs are expected to become effective tools for the clinical treatment of CRC. However, animal experiments, such as in mice, are needed to further evaluate the use of ICIs for treating CRC, observe and analyze the relationship between survival status and IRGPI-related genes and immune cell infiltration, and verify the effectiveness of IRGPI. Moreover, larger numbers of patients with CRC should be evaluated in prospective studies to validate and improve our approach.

## Data availability statement

The datasets presented in this study can be found in online repositories. The names of the repository/repositories and accession number(s) can be found below: https://figshare.com/, https://figshare.com/articles/dataset/data_for_IRGPI/19534810.

## Ethics statement

All experimental procedures were performed in accordance with the National Institutes of Health Guidelines for Laboratory Animals and approved by the Animal Ethics Committee of Nanjing University of Chinese Medicine (202010A026).

## Author contributions

DT and JG conceived the concept and critically reviewed the manuscript; ZL and PT collected and assembled the data and finished the manuscript; RS and YL performed the experiments; FL, LL, YB, MJ, FZ and GY provided experimental assistance. All authors contributed to the article and approved the submitted version.

## Funding

This research was supported by grants from the National Natural Science Foundation of China (No. 82274116, No. 81873021, and No. 81904059), the TCM Science and Technology Development Special Project of Jiangsu Province (No. 2020ZX01), the Natural Science Research in Jiangsu Province (No. BK20190803), the Youth Project of Nanjing University of Chinese Medicine (No. NZY81904059), and the Innovation Program for Graduate Students of Jiangsu Province (No. KYCX22_1885 and No. KYCX21_1763).

## Conflict of interest

The authors declare that the research was conducted in the absence of any commercial or financial relationships that could be construed as a potential conflict of interest.

## Publisher's note

All claims expressed in this article are solely those of the authors and do not necessarily represent those of their affiliated organizations, or those of the publisher, the editors and the reviewers. Any product that may be evaluated in this article, or claim that may be made by its manufacturer, is not guaranteed or endorsed by the publisher.

## Supplementary material

The Supplementary Material for this article can be found online at: https://www.frontiersin.org/articles/10.3389/fimmu.2022.944286/full#supplementary-material

## References

1. Sung H, Ferlay J, Siegel RL, Laversanne M, Soerjomataram I, Jemal A, et al. Global cancer statistics 2020: GLOBOCAN estimates of incidence and mortality worldwide for 36 cancers in 185 countries. *CA Cancer J Clin* (2021) 71(3):209–49. doi: 10.3322/caac.21660

2. Siegel RL, Miller KD, Fedewa SA, Ahnen DJ, Meester RGS, Barzi A, et al. Colorectal cancer statistics, 2017. *CA Cancer J Clin* (2017) 67:177–93. doi: 10.3322/caac.21395

3. Siegel RL, Miller KD, Jemal A. Colorectal cancer statistics, 2020. *CA Cancer J Clin* (2020) 70(1):7–30. doi: 10.3322/caac.21590

4. Tolba MF. Revolutionizing the landscape of colorectal cancer treatment: The potential role of immune checkpoint inhibitors. *Int J Cancer* (2020) 147(11):2996–3006. doi: 10.1002/ijc.33056

5. Almquist DR, Ahn DH, Bekaii-Saab TS. The role of immune checkpoint inhibitors in colorectal adenocarcinoma. *BioDrugs* (2020) 34(3):349–62. doi: 10.1007/s40259-020-00420-3

6. Thomas J, Leal A, Overman MJ. Clinical development of immunotherapy for deficient mismatch repair colorectal cancer. *Clin Colorectal Cancer* (2020) 19 (2):73–81. doi: 10.1016/j.clcc.2020.02.002

7. Lin A, Zhang J, Luo P. Crosstalk between the MSI status and tumor microenvironment in colorectal cancer. *Front Immunol* (2020) 11:2039. doi: 10.3389/fimmu.2020.02039

8. Miller KD, Nogueira L, Mariotto AB, Rowland JH, Yabroff KR, Alfano CM, et al. Cancer treatment and survivorship statistics, 2019. *CA Cancer J Clin* (2019) 69 (5):363–85. doi: 10.3322/caac.21565

9. Picard E, Verschoor CP, Ma GW, Pawelec G. Relationships between immune landscapes, genetic subtypes and responses to immunotherapy in colorectal cancer. *Front Immunol* (2020) 11:369. doi: 10.3389/fimmu.2020.00369

10. Szeglin BC, Wu C, Marco MR, Park HS, Zhang Z, Zhang B, et al. A SMAD4-modulated gene profile predicts disease-free survival in stage II and III colorectal cancer. *Cancer Rep (Hoboken)* (2022) 5(1):e1423. doi: 10.1002/cnr2.1423

11. Langfelder P, Horvath S. WGCNA: an r package for weighted correlation network analysis. *BMC Bioinf* (2008) 9:559. doi: 10.1186/1471-2105-9-559

12. Shuai M, He D, Chen X. Optimizing weighted gene co-expression network analysis with a multi-threaded calculation of the topological overlap matrix. *Stat Appl Genet Mol Biol* (2021) 20(4-6):145–53. doi: 10.1515/sagmb-2021-0025

13. Newman AM, Liu CL, Green MR, Gentles AJ, Feng W, Xu Y, et al. Robust enumeration of cell subsets from tissue expression profiles. *Nat Methods* (2015) 12 (5):453–7. doi: 10.1038/nmeth.3337

14. Toor SM, Murshed K, Al-Dhaheri M, Khawar M, Abu Nada M, Elkord E. Immune check-points in circulating and tumor-infiltrating CD4+ T cell subsets in colorectal cancer patients. *Front Immunol* (2019) 10:2936. doi: 10.3389/fimmu.2019.02936

15. Jiang P, Gu S, Pan D, Fu J, Sahu A, Hu X, et al. Signatures of T cell dysfunction and exclusion predict cancer immunotherapy response. *Nat Med* (2018) 24(10):1550–8. doi: 10.1038/s41591-018-0136-1

16. Lichtenstern CR, Ngu RK, Shalapour S, Karin M. Immunotherapy, inflammation and colorectal cancer. *Cells* (2020) 9(3):618. doi: 10.3390/cells9030618

17. Le DT, Kim TW, Van Cutsem E, Geva R, Jäger D, Hara H, et al. Phase II open-label study of pembrolizumab in treatment-refractory, microsatellite instability-High/Mismatch repair-deficient metastatic colorectal cancer: KEYNOTE-164. *J Clin Oncol* (2020) 38(1):11–9. doi: 10.1200/JCO.19.02107

18. Kanani A, Veen T, Søreide K. Neoadjuvant immunotherapy in primary and metastatic colorectal cancer. *Br J Surg* (2021) 108(12):1417–25. doi: 10.1093/bjs/znab342

19. Majidpoor J, Mortezaee K. The efficacy of PD-1/PD-L1 blockade in cold cancers and future perspectives. *Clin Immunol* (2021) 226:108707. doi: 10.1016/j.clim.2021.108707

20. Tauriello DVF, Palomo-Ponce S, Stork D, Berenguer-Llergo A, Badia-Ramentol J, Iglesias M, et al. TGFβ drives immune evasion in genetically reconstituted colon cancer metastasis. *Nature* (2018) 554(7693):538–43. doi: 10.1038/nature25492

21. Ciardiello D, Vitiello PP, Cardone C, Martini G, Troiani T, Martinelli E, et al. Immunotherapy of colorectal cancer: Challenges for therapeutic efficacy. *Cancer Treat Rev* (2019) 76:22–32. doi: 10.1016/j.ctrv.2019.04.003

22. Fidelle M, Yonekura S, Picard M, Cogdill A, Hollebecque A, Roberti MP, et al. Resolving the paradox of colon cancer through the integration of genetics, immunology, and the microbiota. *Front Immunol* (2020) 11:600886. doi: 10.3389/fimmu.2020.600886

23. Fife BT, Bluestone JA. Control of peripheral T-cell tolerance and autoimmunity *via* the CTLA-4 and PD-1 pathways. *Immunol Rev* (2008) 224:166–82. doi: 10.1111/j.1600-065X.2008.00662.x

24. Salomon B, Bluestone JA. Complexities of CD28/B7: CTLA-4 costimulatory pathways in autoimmunity and transplantation. *Annu Rev Immunol* (2001) 19:225–52. doi: 10.1146/annurev.immunol.19.1.225

25. Rakké YS, Carrascosa LC, van Beek AA, de Ruiter V, van Gemerden RS, Doukas M, et al. GITR ligation improves anti-PD1-mediated restoration of human MMR-proficient colorectal carcinoma tumor-derived T cells. *Cell Mol Gastroenterol Hepatol* (2022) 15(1):77–97. doi: 10.1016/j.jcmgh.2022.09.007

26. Sanborn RE, Pishvaian MJ, Callahan MK, Weise A, Sikic BI, Rahma O, et al. Safety, tolerability and efficacy of agonist anti-CD27 antibody (varlilumab) administered in combination with anti-PD-1 (nivolumab) in advanced solid tumors. *J Immunother Cancer* (2022) 10(8):e005147. doi: 10.1136/jitc-2022-005147

27. Alsalman A, Al-Mterin MA, Murshed K, Alloush F, Al-Shouli ST, Toor SM, et al. Circulating and tumor-infiltrating immune checkpoint-expressing CD8+ Treg/T cell subsets and their associations with disease-free survival in colorectal cancer patients. *Cancers (Basel)* (2022) 14(13):3194. doi: 10.3390/cancers14133194

28. Wang Q, He Y, Li W, Xu X, Hu Q, Bian Z, et al. Soluble immune checkpoint-related proteins in blood are associated with invasion and progression in non-small cell lung cancer. *Front Immunol* (2022) 13:887916. doi: 10.3389/fimmu.2022.887916

29. Kealey J, Düssmann H, Llorente-Folch I, Niewidok N, Salvucci M, Prehn JHM, et al. Effect of TP53 deficiency and KRAS signaling on the bioenergetics of colon cancer cells in response to different substrates: A single cell study. *Front Cell Dev Biol* (2022) 10:893677. doi: 10.3389/fcell.2022.893677

30. Tomicic MT, Dawood M, Efferth T. Epigenetic alterations upstream and downstream of p53 signaling in colorectal carcinoma. *Cancers (Basel)* (2021) 13 (16):4072. doi: 10.3390/cancers13164072

31. Liu C, Liu R, Wang B, Lian J, Yao Y, Sun H, et al. Blocking IL-17A enhances tumor response to anti-PD-1 immunotherapy in microsatellite stable colorectal cancer. *J Immunother Cancer* (2021) 9(1):e001895. doi: 10.1136/jitc-2020-001895

32. Galli F, Aguilera JV, Palermo B, Markovic SN, Nisticò P, Signore A. Relevance of immune cell and tumor microenvironment imaging in the new era of immunotherapy. *J Exp Clin Cancer Res* (2020) 39(1):89. doi: 10.1186/s13046-020-01586-y

33. Shi W, Dong L, Sun Q, Ding H, Meng J, Dai G. Follicular helper T cells promote the effector functions of CD8+ T cells *via* the provision of IL-21, which is downregulated due to PD-1/PD-L1-mediated suppression in colorectal cancer. *Exp Cell Res* (2018) 372(1):35–42. doi: 10.1016/j.yexcr.2018.09.006

34. Boissière-Michot F, Lazennec G, Frugier H, Jarlier M, Roca L, Duffour J, et al. Characterization of an adaptive immune response in microsatellite-instable colorectal cancer. *Oncoimmunology* (2014) 3:e29256. doi: 10.4161/onci.29256

35. Li H, Xiao Y, Li Q, Yao J, Yuan X, Zhang Y, et al. The allergy mediator histamine confers resistance to immunotherapy in cancer patients *via* activation of the macrophage histamine receptor H1. *Cancer Cell* (2022) 40(1):36–52.e9. doi: 10.1016/j.ccell.2021.11.002

36. Xu F, Zhang H, Chen J, Lin L, Chen Y. Immune signature of T follicular helper cells predicts clinical prognostic and therapeutic impact in lung squamous cell carcinoma. *Int Immunopharmacol* (2020) 81:105932. doi: 10.1016/j.intimp.2019.105932

37. Overacre-Delgoffe AE, Bumgarner HJ, Cillo AR, Burr AHP, Tometich JT, Bhattacharjee A, et al. Microbiota-specific T follicular helper cells drive tertiary lymphoid structures and anti-tumor immunity against colorectal cancer. *Immunity* (2021) 54(12):2812–2824.e4. doi: 10.1016/j.immuni.2021.11.003

38. Douanne T, Gavard J, Bidère N. The paracaspase MALT1 cleaves the LUBAC subunit HOIL1 during antigen receptor signaling. *J Cell Sci* (2016) 129 (9):1775–80. doi: 10.1242/jcs.185025

39. Liu ML, Zang F, Zhang SJ. RBCK1 contributes to chemoresistance and stemness in colorectal cancer (CRC). *BioMed Pharmacother* (2019) 118:109250. doi: 10.1016/j.biopha.2019.109250

40. Wang J, Li Y. CD36 tango in cancer: signaling pathways and functions. *Theranostics* (2019) 9(17):4893–908. doi: 10.7150/thno.36037

41. Zhang X, Yao J, Shi H, Gao B, Zhang L. LncRNA TINCR/microRNA-107/CD36 regulates cell proliferation and apoptosis in colorectal cancer *via* PPAR signaling pathway based on bioinformatics analysis. *Biol Chem* (2019) 400(5):663–75. doi: 10.1515/hsz-2018-0236

42. Diaz-Lagares A, Mendez-Gonzalez J, Hervas D, Saigi M, Pajares MJ, Garcia D, et al. A novel epigenetic signature for early diagnosis in lung cancer. *Clin Cancer Res* (2016) 22(13):3361–71. doi: 10.1158/1078-0432.CCR-15-2346

43. Li R, Yin YH, Jin J, Liu X, Zhang MY, Yang YE, et al. Integrative analysis of DNA methylation-driven genes for the prognosis of lung squamous cell carcinoma using MethylMix. *Int J Med Sci* (2020) 17(6):773–86. doi: 10.7150/ijms.43272

44. Xu R, Xu Q, Huang G, Yin X, Zhu J, Peng Y, et al. Combined analysis of the aberrant epigenetic alteration of pancreatic ductal adenocarcinoma. *BioMed Res Int* (2019) 2019:9379864. doi: 10.1155/2019/9379864

45. Ngo VL, Abo H, Kuczma M, Szurek E, Moore N, Medina-Contreras O, et al. IL-36R signaling integrates innate and adaptive immune-mediated protection against enteropathogenic bacteria. *Proc Natl Acad Sci U S A* (2020) 117 (44):27540–8. doi: 10.1073/pnas.2004484117

46. Scheibe K, Kersten C, Schmied A, Vieth M, Primbs T, Carlé B, et al. Inhibiting interleukin 36 receptor signaling reduces fibrosis in mice with chronic intestinal inflammation. *Gastroenterology* (2019) 156(4):1082–1097.e11. doi: 10.1053/j.gastro.2018.11.029

47. Guida S, Guida G, Goding CR. MC1R functions, expression, and implications for targeted therapy. *J Invest Dermatol* (2022) 142(2):293–302.e1. doi: 10.1016/j.jid.2021.06.018

48. Peng L, Chang J, Liu X, Lu S, Ren H, Zhou X, et al. MC1R is a prognostic marker and its expression is correlated with MSI in colorectal cancer. *Curr Issues Mol Biol* (2021) 43(3):1529–47. doi: 10.3390/cimb43030108

49. Korbecki J, Kojder K, Simińska D, Bohatyrewicz R, Gutowska I, Chlubek D, et al. CC chemokines in a tumor: A review of pro-cancer and anti-cancer properties of the ligands of receptors CCR1, CCR2, CCR3, and CCR4. *Int J Mol Sci* (2020) 21 (21):8412. doi: 10.3390/ijms21218412

50. Chung SJ, Nagaraju GP, Nagalingam A, Muniraj N, Kuppusamy P, Walker A, et al. ADIPOQ/adiponectin induces cytotoxic autophagy in breast cancer cells through STK11/LKB1-mediated activation of the AMPK-ULK1 axis. *Autophagy* (2017) 13(8):1386–403. doi: 10.1080/15548627.2017.1332565

51. Li H, Zhao L, Lau YS, Zhang C, Han R. Genome-wide CRISPR screen identifies LGALS2 as an oxidative stress-responsive gene with an inhibitory function on colon tumor growth. *Oncogene* (2021) 40(1):177–88. doi: 10.1038/s41388-020-01523-5

52. Xuan W, Qu Q, Zheng B, Xiong S, Fan GH. The chemotaxis of M1 and M2 macrophages is regulated by different chemokines. *J Leukoc Biol* (2015) 97(1):61–9. doi: 10.1189/jlb.1A0314-170R

53. Danaher P, Warren S, Lu R, Samayoa J, Sullivan A, Pekker I, et al. Pan-cancer adaptive immune resistance as defined by the tumor inflammation signature (TIS): results from the cancer genome atlas (TCGA). *J Immunother Cancer* (2018) 6 (1):63. doi: 10.1186/s40425-018-0367-1

54. Danaher P, Warren S, Ong S, Elliott N, Cesano A, Ferree S. A gene expression assay for simultaneous measurement of microsatellite instability and anti-tumor immune activity. *J Immunother Cancer* (2019) 7(1):15. doi: 10.1186/s40425-018-0472-1

55. Zheng H, Liu H, Ge Y, Wang X. Integrated single-cell and bulk RNA sequencing analysis identifies a cancer associated fibroblast-related signature for predicting prognosis and therapeutic responses in colorectal cancer. *Cancer Cell Int* (2021) 21(1):552. doi: 10.1186/s12935-021-02252-9

56. Qiu C, Shi W, Wu H, Zou S, Li J, Wang D, et al. Identification of molecular subtypes and a prognostic signature based on inflammation-related genes in colon adenocarcinoma. *Front Immunol* (2021) 12:769685. doi: 10.3389/fimmu.2021.769685

frontiers | Frontiers in Oncology

TYPE Review
PUBLISHED 25 January 2023
DOI 10.3389/fonc.2023.1011810



OPEN ACCESS

EDITED BY
Xiaoran Yin,
Second Affiliated Hospital of Xi'an Jiaotong University, China

REVIEWED BY
Ilaria Attili,
European Institute of Oncology (IEO), Italy
Yudong Wang,
Fourth Hospital of Hebei Medical University, China

*CORRESPONDENCE
Fang Wu
wufang4461@csu.edu.cn

†These authors have contributed equally to this work

SPECIALTY SECTION
This article was submitted to Cancer Immunity and Immunotherapy, a section of the journal Frontiers in Oncology

RECEIVED 04 August 2022
ACCEPTED 04 January 2023
PUBLISHED 25 January 2023

CITATION
Peng Y, Li Z, Fu Y, Pan Y, Zeng Y, Liu J, Xiao C, Zhang Y, Su Y, Li G and Wu F (2023) Progress and perspectives of perioperative immunotherapy in non-small cell lung cancer.
*Front. Oncol.* 13:1011810.
doi: 10.3389/fonc.2023.1011810



# Progress and perspectives of perioperative immunotherapy in non-small cell lung cancer

Yurong Peng[1†], Zhuo Li[2†], Yucheng Fu[1], Yue Pan[1], Yue Zeng[1], Junqi Liu[1], Chaoyue Xiao[1], Yingzhe Zhang[1], Yahui Su[3], Guoqing Li[3] and Fang Wu[1*]

[1]Department of Oncology, the Second Xiangya Hospital, Central South University, Changsha, Hunan, China, [2]The Ophthalmologic Center of the Second Xiangya Hospital, Central South University, Changsha, Hunan, China, [3]XiangYa School of Public Health, Central South University, Changsha, Hunan, China

Lung cancer is one of the leading causes of cancer-related death. Lung cancer mortality has decreased over the past decade, which is partly attributed to improved treatments. Curative surgery for patients with early-stage lung cancer is the standard of care, but not all surgical treatments have a good prognosis. Adjuvant and neoadjuvant chemotherapy are used to improve the prognosis of patients with resectable lung cancer. Immunotherapy, an epoch-defining treatment, has improved curative effects, prognosis, and tolerability compared with traditional and ordinary cytotoxic chemotherapy, providing new hope for patients with non-small cell lung cancer (NSCLC). Immunotherapy-related clinical trials have reported encouraging clinical outcomes in their exploration of different types of perioperative immunotherapy, from neoadjuvant immune checkpoint inhibitor (ICI) monotherapy, neoadjuvant immune-combination therapy (chemoimmunotherapy, immunotherapy plus antiangiogenic therapy, immunotherapy plus radiotherapy, or concurrent chemoradiotherapy), adjuvant immunotherapy, and neoadjuvant combined adjuvant immunotherapy. Phase 3 studies such as IMpower 010 and CheckMate 816 reported survival benefits of perioperative immunotherapy for operable patients. This review summarizes up-to-date clinical studies and analyzes the efficiency and feasibility of different neoadjuvant therapies and biomarkers to identify optimal types of perioperative immunotherapy for NSCLC.

KEYWORDS

**perioperative period perioperative immunotherapy, neoadjuvant therapies, immunotherapy, neoadjuvant immune monotherapy, adjuvant therapy, biomarkers, NSCLC, lung cancer**

## 1 Introduction

Lung cancer is the leading cause of death in men and women among neoplastic diseases globally. Nearly 85% of lung cancers are non-small cell lung cancer (NSCLC) (1). Surgical resection is the standard of practice for patients with operable early-stage and locally advanced NSCLC. However, 25%–70% of surgical patients (which varies by stage)

eventually relapse despite complete resection, yielding a 5-year survival rate of 35%-65% (2). Distant metastasis is the most common form of lung cancer postoperative recurrence (3).

Perioperative treatments (adjuvant and neoadjuvant treatment) for NSCLC have the potential to improve disease outcomes. Three randomized controlled trials, namely, International Adjuvant Lung Cancer Trial (IALT), JBR.10, and Adjuvant Navelbine International Trialist Association (ANITA), and the pooled analysis in Lung Adjuvant Cisplatin Evaluation (LACE), studied the efficacy of adjuvant chemotherapy (4–6). Both adjuvant and neoadjuvant chemotherapy had an approximate 5-year survival benefit of 5% and did not significantly improve the time to local recurrence. However, additional regimens must be evaluated, and there is no phase III study of any perioperative targeted therapy.

Immune checkpoint inhibitors (ICIs) are mainstream of immunotherapy, with good clinical results in patients with advanced NSCLC (7–10). The PACIFIC study introduced immunotherapy to stage III NSCLC (11), reporting that patients with negative drive gene mutations can benefit from ICIs. The estimated 5-year overall survival (OS) of early-stage lung cancer was 23.2% for treatment-naive patients with pembrolizumab, and 15.5% *vs.* 16% for pembrolizumab versus nivolumab in previously treated patients (12).

Following the profound application of immunotherapy in NSCLC, there has been tremendous potential benefit to combining immunotherapy with surgery, as has been applied to some recent phase Ib/II and III clinical trials. The CheckMate159 trial was the first study that evaluated neoadjuvant immunotherapy, showing that neoadjuvant therapy with a single-drug programmed cell death protein 1 (PD-1) inhibitor (nivolumab) achieved a major pathological response (MPR) and pathological complete response (pCR) in 45% and 15% of participants, respectively (13). CheckMate-816 was the first phase III clinical trial to demonstrate the benefit of neoadjuvant immunotherapy (nivolumab) in resectable NSCLC patients, reporting a median event-free survival of nivolumab plus chemotherapy that was 10.8 months longer than with chemotherapy alone in addition to a pCR of 24.0% *vs.* 2.2%, respectively (14). This review incorporates the latest evidence to assess efficacy and feasibility of neoadjuvant immune monotherapy, immune-combination therapy, and biomarkers for neoadjuvant immunotherapy to identify the optimal perioperative immunotherapy for NSCLC (Figure 1).

## 2 Neoadjuvant immunotherapy

### 2.1 Neoadjuvant ICIs monotherapy

The earliest study of immunotherapy as perioperative neoadjuvant therapy for NSCLC was CheckMate 159, which enrolled 21 patients treated with nivolumab for two cycles before surgery. That trial opened a new era of perioperative immunotherapy, reporting an MPR rate of nivolumab neoadjuvant therapy of 45%, a 24-month relapse-free survival (RFS) of 70%, and a pCR of 10%. It also confirmed the clinical efficacy and safety of neoadjuvant ICI monotherapy (15). Despite initially promising results, the MPR rates reported by other studies that used single-agent neoadjuvant

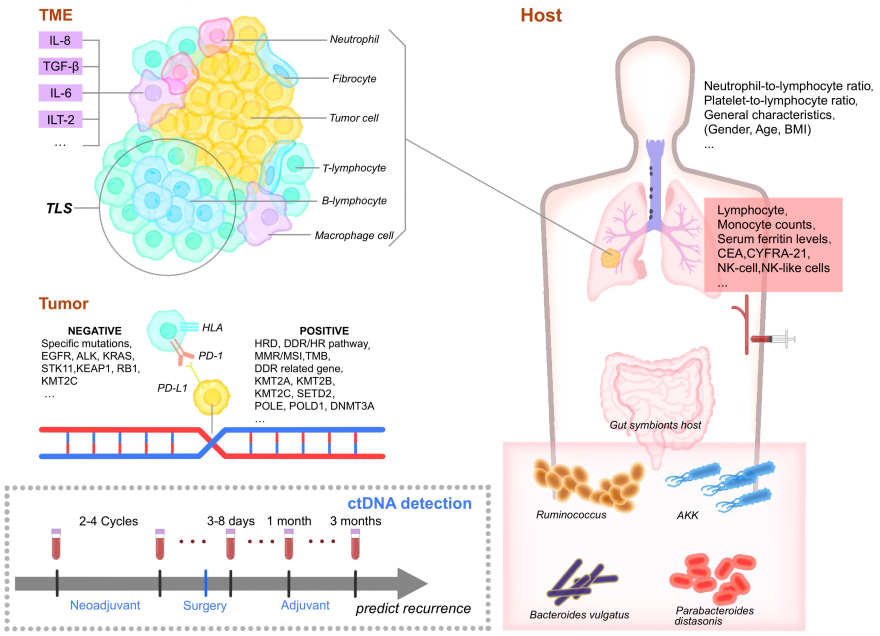


FIGURE 1
Biomarkers of perioperative immunotherapy. TME, Tumor microenvironment. IL-8, interleukin-8. TGF-β, Transforming growth factor. IL-6, interleukin-6. ILT-2, Ig-like transcript 2. TLS, Tertiary lymphoid structures. TIL, tumor-infiltrating lymphocytes. EGFR, epidermal growth factor receptor. HLA, human leukocyte antigen. PD-1, programmed cell death protein 1. PD-L1, Programmed cell death ligand 1. HRD, Homologous recombination deficiency. DDR, DNA-damage response/HR, homologous recombination pathway, MMR, mismatch repair. MSI, microsatellite instability. TMB, tumor mutation burden. KMT2A/B/C, Lysine methyltransferase 2A/B/C. POLE, polymerase epsilon. DNMT3A, DNA methyltransferases 3A. BMI, body mass index. CEA, carcinoembryonic antigen. NK, natural killer cells. AKK, Akkermansia muciniphila. NK, natural killer cells. CD4, cluster of differentiation 4. CD8+, cluster of differentiation 8. Treg, regulatory T cells. DC, dendritic cells. CTL, cytotoxic T lymphocyte.

immunotherapy were not as encouraging. For instance, the LCMC3 study of neoadjuvant atezolizumab in patients with resectable stage IB-IIIB NSCLC with epidermal growth factor receptor (EGFR) or anaplastic lymphoma kinase (ALK) genetic aberrations attained a 21% of MPR at the time of resection and a pCR of 7%, while the use of atezolizumab in another neoadjuvant study yielded an MPR rate of only 13% and a pCR of 7%. These data suggest that atezolizumab has a survival advantage compared with historical outcomes, but more convincing evidence is needed to validate its curative effect.

When Nivolumab single-agent treatment was evaluated in the NEOSTAR study, the MPR rate was only 17% and the pCR was 9% (16). Moreover, the use of sintilimab in 49 patients in ChiCTR-OIC-17013726 and durvalumab in 46 patients in IONESCO as single-agent treatment with an ICI in the neoadjuvant setting reported MPR rates of 40% and 17% and pCRs of 16% and 7%, respectively (17–19). The TOP1501 study showed that pembrolizumab was efficacious and well tolerated as neoadjuvant therapy in 30 patients (20). These results indicate that different monotherapies with anti-PD-L1 agents are being attempted, but more clinical studies are required to establish the ability for neoadjuvant immunotherapy to improve the survival of patients with early-stage NSCLC (Table 1).

To summarize, the MPR ratio of perioperative ICI monotherapy of 14%–45% is significantly higher than that of neoadjuvant chemotherapy with cisplatin (MPR between 10% and 15%), but the clinical benefit rate of these treatments was not as high.

TABLE 1 Preoperative phase I or II neoadjuvant immunotherapy in operable NSCLC.

| | Clinical trial | Phase | Stage | Intervention used | Estimated sample size | Primary endpoints | Secondary endpoints | Estimated completion date |
|---|---|---|---|---|---|---|---|---|
| Neoadjuvant ICIs monotherapy | ChiCTR-OIC-17013726 | I | IA-IIIB | Sintilimab 2C + S | 40 | Safety | ORR,MPR, DFS | 05/2020 |
| | MK3475-223 (NCT02938624) | I | I-II | Pembrolizumab 1C/2C+ S | 28 | Toxicity, MPR | mOS, mTR | 04/2021 |
| | CheckMate 159 (NCTO2259621) | II | l-IIIA | Nivolumab 2C + S | 45 | Safety | PR, RdR | 01/2023 |
| | IONESCO (NCT03030131) | II | IB-II | Durvalumab 3C + S | 81 | R0 resection | RR, DFS,OS | 08/2019 |
| | Columbia University (NCT02716038) | II | IB-IIIA | Atezolizumab 4C + S | 30 | MPR | NA | 12/2021 |
| | PRICNEPS (NCT02994576) | II | IB-IIIA | Atezolizumab 1C + S | 60 | Toxicity | NA | 12/2022 |
| | NEOMUN (NCT03197467) | II | II-IIIA | Pembrolizumab 2C +S | 30 | AEs | DFS, OS | 10/2023 |
| | LCMC3 (NCT02927301) | II | IB-IIIA | Atezolizumab 2C+ S | 180 | MPR | ORR | 05/2025 |
| | TOP1501 (NCT02818920) | II | IB-IIIA | Pembrolizumab+ S | 35 | SFR | ORR, DFS | 03/2026 |
| Neoadjuvant ICIs immune-combination therapy | NeoCOAST (NCT03794544) | II | I-IIIA | Durvalumab ± Oleclumab (MEDI9447) or Monalizumab (IPH2201) or Danvatirsen+ S | 160 | MPR | pCR | 01/2021 |
| | CANOPY-N (NCT03968419) | II | IB-IIIA | Canakinumab + Pembrolizumab/ Canakinumab/Pembrolizumab | 88 | MPR | ORR | 08/2022 |
| | NADIM (NCT03081689) | II | I-IIIA | Chemotherapy + Nivolumab *vs.* Chemotherapy+ S | 46 | PFS | OS, Toxicity | 06/2023 |
| | SAKK 16/14 (NCT02572843) | II | IIIA (N2) | Durvalumab 2C + Chemotherapy 3C+ S | 68 | EFS | OS, OR, pCR | 12/2024 |
| | NEOSTAR (NCT03158129) | II | l-IIIA | Nivolumab ± Ipilimumab or Chemotherapy | 88 | MPR | RFS | 07/2022 |
| | TOP1201 (NCT01820754) | II | IB-IIIA | Chemotherapy 1C + (Ipilimumab + Chemotherapy) 2C + S | 24 | CTCs | Toxicity, mDFS | 04/2018 |
| | EAST ENERGY (NCT04040361) | II | IB-IIIA | Pembrolizumab + Ramucirumab + S | 24 | MPR | Safety, pCR, OS, ORR | 11/2025 |

NSCLC, non-small cell lung cancer; C: cycle; S: surgery; y: year; ORR, objective response rate; MPR, major pathological response; DFS, disease-free survival; mOS, median overall survival; mTR, median time-to-recurrence; PR, pathological response; RdR, radiographic response; RR, response rate; R0 resection; OS, overall survival; NA, not mentioned; patient percentage of surgical resection R0 after a maximum of three cycles of immune therapy; AEs, adverse events; CTCs, circulating T cells; EFS, event-free survival; PFS: progression-free survival; pCR, pathological complete response; SFR, surgical feasibility rate; RFS, recurrence-free survival; R0, resection.

## 2.2 Neoadjuvant immune-combination therapy

It is generally felt that neoadjuvant immune-combination therapy is a great step forward in perioperative immunotherapy. Versatile forms of combination therapy, such as neoadjuvant chemoimmunotherapy, neoadjuvant immunotherapy plus antiangiogenic therapy, neoadjuvant dual immunotherapy, neoadjuvant immunotherapy plus radiotherapy or concurrent chemoradiotherapy, and neoadjuvant immunotherapy plus chemoradiotherapy, are currently being investigated (Tables 1, 2).

### 2.2.1 Neoadjuvant chemoimmunotherapy

Neoadjuvant chemoimmunotherapy accounts for the majority of neoadjuvant immunotherapy clinical trials and generally reports an improved pathological response, with a higher pCR and MPR compared with single-agent neoadjuvant immunotherapy, thereby prolonging OS.

There may be some synergy between neoadjuvant immunotherapy and chemotherapy. Chemotherapy can induce tumor cell gene mutations, thereby producing new epitopes that can in turn enhance tumor immunogenicity and improve the efficacy of immunotherapy (21).

In a phase II trial of 30 patients with stage IB–IIIA NSCLC, neoadjuvant atezolizumab combined with chemotherapy achieved

TABLE 2 Ongoing clinical trials of neoadjuvant immunotherapy plus radiotherapy in operable NSCLC.

| Clinical trial | Phase | Stage | Drugs | Intervention used | Estimated sample size | Primary end-points | Secondary endpoints | Estimated completion date |
|---|---|---|---|---|---|---|---|---|
| NCT04287894 | I | II–III | Durvalumab | Durvalumab 2C+ Chemotherapy + Radiotherapy + S + Durvalumab | 34 | Safety | DFS, OS, DCR | 01/2021 |
| NCT05157542 | I | III | Durvalumab | Durvalumab 2C + Chemotherapy + Radiotherapy + S | 9 | Safety, AEs, SAEs | ORR, EFS, MPR | 06/2023 |
| NCT02987998 | I | IIIA | Pembrolizumab | Pembrolizumab + Chemotherapy + Radiotherapy + S + Pembrolizumab | 9 | Safety | PFS, ORR | 01/2024 |
| NCT03237377 | II | IIIA | Durvalumab or Tremelimumab (CTLA-4) | Durvalumab 3C + Radiotherapy + S *vs.* Durvalumab 3C + Tremelimumab(CTLA-4)+ Radiotherapy + S | 32 | Safety, feasibility | SMM, PR rate | 09/2021 |
| NCT03217071 | II | I-IIIA | Pembrolizumab | Pembrolizumab 2C + S *vs.* Pembrolizumab 2C + Radiotherapy(SRT) + S | 40 | number of infiltrating CD3+ T cells/μm2 | AEs, OS, RFS | 12/2021 |
| NCT02904954 | II | IB-IIIA | Durvalumab | Durvalumab 2C + S + Durvalumab 1y *vs.* Durvalumab 2C + Radiotherapy + S + Durvalumab 1y | 60 | MPR | DFS, ORR | 04/2022 |
| NCT04085250 | II | III | Nivolumab | Nivolumab 2C + Chemotherapy +Radiotherapy + S + Nivolumab 1y | 264 | PFS | OS, ORR, AEs | 11/2023 |
| NCT04933903 | II | IB-III | ipilimumab +Nivolumab | Ipilimumab + Nivolumab + SBRT+ S | 25 | MPR, pCR | AEs | 01/2024 |
| NCT03110978 | II | I-IIA | Radiotherapy (SBRT) + Nivolumab *vs.* Radiotherapy | SBRT *vs.* SBRT+ Nivolumab 3C | 140 | EFS, secondary malignancy, and death | OS, AEs | 06/2022 |
| NCT04245514 | II | T1-4>7 N2 | Durvalumab | Durvalumab 1C + Chemotherapy 3C +Radiotherapy+ S + Durvalumab 13C | 90 | EFS | RFS, OS, pCR, MPR | 03/2025 |

NSCLC, non-small cell lung cancer; C: cycle; S: surgery; y: year; DCR, 1-year disease control rate; CTLA-4, immunoglobulin-related receptors that are responsible for various aspects of T-cell immune regulation; SRT, stereotactic radiation therapy; SBRT, stereotactic body radiation therapy; AEs, adverse events; SAEs, serious adverse events; ORR, objective response rate; RFS, relapse-free survival; EFS, event-free survival; DFS, disease-free survival; SMM, surgical morbidity and mortality; PR rate, pathological response; PFS, progression-free survival; MPR, major pathological response; pCR, pathological complete response; EFS, event-free survival; OS, overall survival; T1–4>7 N2: i.e., T1–3 N2 or T4 N2 but T4 only allowed if due to size >7cm, not allowed if due to invasion or nodule in different ipsilateral lobe.

MPR and pCR rates of 57% (17/30) and 33% (10/30), respectively (22). Of the 55 patients with stage IIIA NSCLC in the SAKK 16/14 study who underwent surgical resection followed by the treatment of cisplatin or docetaxel followed by durvalumab, the MPR rate was 62% (34/55), the pCR rate was 18% (10/55), and the 1-year event-free survival (EFS) rate reached 73.3% (23). Toripalimab plus platinum-based doublet chemotherapy for patients with stage III NSCLC yielded a high MPR rate of 66.7% and a pCR rate of 50% (24). Although neoadjuvant chemoimmunotherapy had good therapeutic efficacy, treatment-related adverse events are worth mentioning. A single-arm trial of 21 patients who underwent two cycles of neoadjuvant nivolumab every 2 weeks before surgery was associated with few side effects, no delay in surgery, and an MPR of 45% (9/20) (15).

The NADIM study with nivolumab plus paclitaxel and carboplatin achieved strong clinical results, with an MPR of 83% (34/41), a pCR of 63% (26/41), a 2-year progression-free survival (PFS) rate of 77.1%, and a 2-year OS of 89.9%. However, 93% (43/46) of the patients had treatment-related adverse events, 30% (14/46) of which were in grade ≥ 3. However, none of the adverse events were associated with surgery delays or treatment-related deaths (25). The SAKK 16/14 study also reported grade ≥ 3 adverse events in 59 (88%) patients, including two fatal adverse events that were judged to not be treatment related (23).

The first phase III study to evaluate neoadjuvant chemoimmunotherapy, CheckMate-816, with neoadjuvant nivolumab plus chemotherapy achieved an approximately 10-fold meaningful increase, with a pCR of 24% (95% CI, 18.0–31.0) compared with 2.2% (95% CI, 0.6–5.6) among patients treated with chemotherapy alone. The EFS of the experimental group was 31.6 months compared with 20.8 months in the single-agent chemotherapy group, representing a significant improvement. The US Food and Drug Administration recently approved CheckMate-816's regimen, which could represent a new standard of care for NSCLC patients with tumors ≥4 cm or who are node positive (14). Several other relevant phase III clinical trials are currently underway, such as the AEGEAN study, which focuses on durvalumab combined with chemotherapy, and their results are highly anticipated (26).

The treatment intervals between cycles varied among all of the above study designs. The interval between toripalimab, nivolumab, tislelizumab, durvalumab, and camrelizumab cycles were generally 2 weeks before surgery, while for pembrolizumab and atezolizumab, it was 3 weeks. As a result of comprehensive consideration of various factors, most studies chose two to four immune treatment cycles to ensure its efficacy and patient compliance, but more clinical evidence is required to identify the optimal medication regimen (27–29).

### 2.2.2 Neoadjuvant immunotherapy plus antiangiogenic therapy

Previous studies have demonstrated that antiangiogenic drugs (Endostar) combined with chemotherapy in patients treated with neoadjuvant therapy can increase therapeutic efficacy without increasing adverse effects in stage IIIA-N2 NSCLC patients (30). Several recent clinical studies evaluated neoadjuvant immunotherapy combined with antiangiogenic therapy. The phase 2 study NCT04040361 administered two cycles of pembrolizumab and ramucirumab before surgery, with MPR defined as the primary outcome measure. Anlotinib was combined with pembrolizumab in a neoadjuvant study (NCT04762030). Additional future trials may evaluate other ICIs along with various antiangiogenic drugs. The optimal combination of these therapies, the ideal target population, and therapy choice in the setting of disease progression require further study.

### 2.2.3 Neoadjuvant dual immunotherapy

Cascone et al. sought to examine the efficacy of neoadjuvant immune-immune therapy through the NeoSTAR, which evaluated anti-PD-1 plus anti-CTLA-4 in the treatment of early-stage NSCLC. Compared with nivolumab, nivolumab plus ipilimumab had higher MPR (22% *vs*. 38%) and pCR rates (10% *vs*. 38%), suggesting that dual immunotherapy has significant potential during the perioperative period in patients with operable NSCLC (16). The recent NeoCOAST study paired neoadjuvant durvalumab with three investigational drugs, namely, oleclumab, monalizumab, and danvatirsen, reporting that combination strategies may boost the programmed cell death ligand 1 (PD-L1) inhibitor durvalumab's neoadjuvant efficacy, resulting in MPR rates of 19%, 30%, and 31.3% with oleclumab, monalizumab, and danvatirsen, respectively, compared with durvalumab monotherapy (11.1%) (31). Ongoing clinical studies are evaluating the efficacy and safety of two cycles of neoadjuvant durvalumab immunotherapy plus ramucirumab (anti-angiogenic) (NCT04040361), durvalumab combined with FL-101 (anti-IL-1β, NCT04758949), oleclumab (anti-CD73) plus chemotherapy, and monalizumab (anti-NKG2A) plus chemotherapy (NCT05061550).

### 2.2.4 Neoadjuvant immunotherapy plus radiotherapy or concurrent chemoradiotherapy

Radiotherapy is a standard treatment for many tumors. Radiotherapy cannot only kill the inhibitory stromal cells, indirectly improving the body's anti-tumor activity, but also induce immunogenic cell death and expose the surface of calpain cells. The release of immunostimulatory components such as High Mobility Group Box 1 (HMGB1) and adenosine triphosphate (ATP) activates dendritic cells and effector T cells, which in turn increase the body's anti-tumor abilities. Radiotherapy can also induce the expression of various proinflammatory cytokines, such as interleukin-1β (IL-1β) and tumor necrosis factor α (TNF α), which can induce the tumor's inflammatory microenvironment and increase its immune tumor necrosis factor (32, 33).

Neoadjuvant immunotherapy plus radiotherapy achieved positive results in recent clinical trials. A study of neoadjuvant chemoradiation and durvalumab in patients with potentially resectable phase III NSCLC tumors reported a 77.8% MPR rate (14/18, 95% CI, 54.3%–91.5%) and a 38.9% pCR rate (7/18, 95% CI, 20.2%–61.5%). Seventy-five percent (18/24) of patients underwent surgery after neoadjuvant therapy (34). Neoadjuvant durvalumab with or without stereotactic body radiotherapy (SBRT) also achieved better outcomes, with MPR observed in 16 of 30 patients (53.3%) in the durvalumab plus radiotherapy group *vs*. 2 of 30 patients (6.7%) in the durvalumab monotherapy group (35). These results suggest that neoadjuvant immunotherapy plus radiotherapy or chemoradiotherapy are more

effective than neoadjuvant ICI monotherapy. However, this concept is being further evaluated (Table 2).

## 3 Adjuvant immunotherapy

Postoperative adjuvant therapy can eliminate undetectable residual "micrometastatic" tumor cells that may exist in lymph nodes, blood vessels, or lymphatic vessels, delaying or reducing postoperative recurrence and metastasis, prolonging PFS and OS, and improving patient quality of life. Adjuvant immunotherapy for perioperative patients includes adjuvant immune monotherapy and combination therapy (36).

With respect to adjuvant chemo-immunotherapy therapy, atezolizumab after adjuvant chemotherapy is a promising treatment option for patients with resectable early-stage NSCLC. The Impower010 study, the first to incorporate immunity into early-stage lung cancer treatment (atezolizumab), achieved a 34% improvement in disease-free survival (DFS) in stage II–IIIA patients with PD-L1≥1%, an improvement also supported by the OS interim analysis of atezolizumab at the 2022 American Society of Clinical Oncology Meeting (37). Based on the success of Impower010 study and the approval of the Food and Drug Administration (FDA), postoperative auxiliary immunotherapy became the standard guidance (38).

Patients with stage II–IIIA PD-L1-positive tumors and PD-L1 tumor proportion scores (TPS) ≥ 50% are considered the key targets for immune adjuvant therapy. Keynote-091, a randomized, triple-blinded, phase III trial, enrolled a total of 1,177 patients who were randomized 1:1 to receive either pembrolizumab or placebo. The study's dual primary end points were DFS in all-comers and PD-L1 TPS ≥50% groups. It was announced at the 2022 European Society for Medical Oncology virtual plenary meeting that the study had reached one of the two primary endpoints (39). Pembrolizumab significantly improved the cohort's DFS regardless of the PD-L1 expression level (53.6 *vs*. 42.0 months; HR, 0.76; 95% CI, 0.63–0.91; p = 0.0014). These results suggest that immunotherapy is an effective adjuvant treatment for NSCLC and could significantly prolong the postoperative DFS of NSCLC patients. It also laid the foundation for further studies seeking to evaluate adjuvant immunotherapy after surgery.

Other phase III clinical trials that are currently underway are evaluating the efficacy of adjuvant immunotherapy in patients with resected stage IB–IIIA NSCLC (Table 3).

## 4 Neoadjuvant and adjuvant immunotherapy

Prior to resection, the patient's tumor is large and neoantigen abundant and their immune system is relatively intact. Anti-PD-1 therapy at this stage can induce the expansion of mutation-associated neoantigen-specific T-cell clones in the peripheral blood (13). It can also fully enhance the activity of anti-tumor immune T cells *in vivo*. However, the surgery can contribute to change in cytokines, growth factors, and immune cells because of inflammation and neuroendocrine and postoperative complications, resulting in immunosuppression (40).

Adjuvant therapy will be primarily used in patients with resectable stage l and II NSCLC, but neoadjuvant therapy is more preferred for patients with stage IIIA to IIIC disease (41).

Moreover, the interval between neoadjuvant therapy and surgery is of great importance. A preclinical study in mouse models of spontaneously metastatic mammary cancer reported that a short duration (4–5 days) between the first administration of neoadjuvant immunotherapy and resection of the primary tumor was necessary to achieve optimal efficacy. The authors also found that changes in the immune microenvironment, including differences in the proportion of tumor-specific T cells and their ability to produce interferon gamma (IFNγ), influence operative timing (42).

NADIM, NADIM II, and CheckMate 816 all reported a consistent and reproducible improvement in the rate of pathological response in patients treated with neoadjuvant immunotherapy in combination with chemotherapy (14, 25). NADIM II demonstrated superior pCR in patients with resectable stage IIIA NSCLC treated with chemotherapy combined with immunotherapy. Patients were only included in the adjuvant immune treatment (nivolumab) cohort if they were R0 and received their first drug administration between the third to eighth week after surgery and over a 6-month period. Results showed that neoadjuvant nivolumab plus chemotherapy significantly increased pCR compared with chemotherapy in the intent-to-treat patients (ITT, 36.2% *vs*. 6.8%) and reported an improved MPR rate (52% *vs*. 14%) and ORR (74% *vs*. 48%) versus chemotherapy alone (43).

Neoadjuvant and adjuvant immunotherapy combined with chemotherapy has been studied clinically. The majority of these studies evaluated two to four cycles of neoadjuvant treatment and 1 year for effective adjuvant therapy. Tislelizumab was evaluated for 8 cycles and atezolizumab 16 cycles. Ongoing phase III trials are exploring the safety and feasibility of neoadjuvant immunotherapy combined with chemotherapy for NSCLC. Different drugs (pembrolizumab, nivolumab, atezolizumab, tislelizumab, toripalimab, and sintilimab) were evaluated in combination with chemotherapy versus chemotherapy alone, mostly using EFS as the primary endpoint (Table 3).

## 5 Biomarkers for perioperative immunotherapy

Immunotherapy biomarkers for patients with resectable NSCLC can be roughly divided into four groups: tumor-cell-associated biomarkers, tumor-microenvironment (TME)-associated biomarkers, host-associated biomarkers, and blood cell and liquid biopsy-related biomarkers.

### 5.1 Tumor-cell-associated biomarkers

Tumor biomarkers for NSCLC are substances present in or produced by the tumor itself or the host microenvironment in

TABLE 3 Ongoing phase III clinical trials of neoadjuvant and adjuvant immunotherapy in operable NSCLC.

| | Clinical trial | Stage | Drugs | Intervention used | Estimated sample size | Phase | Primary endpoints | Estimated completion date |
|---|---|---|---|---|---|---|---|---|
| Adjuvant Immunotherapy | IMpower010 (NCT02486718) | IB (tumors ≥4 cm) to IIIA | Atezolizumab | S+ Atezolizumab + Chemotherapy/Chemotherapy alone | 1280 | III | DFS | 12/2027 |
| | PEARLS/ KEYNOTE-091 (NCT02504372) | IB (tumors ≥4 cm) to IIIA | Pembrolizumab (MK-3475) | S+ Pembrolizumab 1y/placebo | 1177 | III | DFS | 02/2024 |
| | ANVIL (NCT02595944) | IB (tumors ≥4 cm) to IIIA | Nivolumab | S+ Nivolumab 1y/placebo | 903 | III | DFS | 07/2024 |
| | IFCT-1401 (NCT02273375) | IB (tumours ≥4 cm) to IIIA | MEDI4736 | S+ MEDI4736 1y/placebo | 1415 | III | DFS | 01/2024 |
| | MERMAID 1 (NCT04385368) | II-III | Durvalumab | Durvalumab + SoC Chemotherapy/placebo | 86 | III | DFS | 12/2026/ |
| | MERMAID 2 (NCT04642469) | II-III | Durvalumab | S+durvalumab(1y)/placebo | 284 | III | DFS | 10/2027 |
| Neoadjuvant Immunotherapy +Chemotherapy | AEGEAN (NCT03800134) | IIA -IIIB | Durvalumab | Durvalumab+Chemotherapy + S | 800 | III | MPR | 01/2024 |
| | CheckMate 816 (NCT02998528) | IB-IIIA | Nivolumab | Nivolumab+Chemotherapy/ Nivolumab+Ipilimumab/ Chemotherapy + S | 350 | III | EFS, pCR | 11/2028 |
| Neoadjuvant + Adjuvant Immunotherapy +Chemotherapy | KEYNOTE-671 (NCT03425643) | IIB-IIIA | Pembrolizumab | Pembrolizumab+Chemotherapy S + Pembrolizumab | 786 | III | EFS, OS | 06/2026 |
| | CheckMate 77T (NCT04025879) | II-IIIB (T3N2) | Nivolumab | Nivolumab+Chemotherapy S + Nivolumab | 452 | III | EFS | 09/2024 |
| | IMpower 030 (NCT03456063) | II-IIIB (T3N2) | Atezolizumab | Atezolizumab+Chemotherapy S + Atezolizumab | 450 | III | MPR, EFS | 11/2024 |
| | RATIONALE 315 (NCT04379635) | II-IIIA | Tislelizumab | Tislelizumab+Chemotherapy S + Tislelizumab | 380 | III | MPR, EFS | 02/2021 |
| | JS001-029 (NCT04158440) | IIIA | Toripalimab | Toripalimab+Chemotherapy S + Toripalimab | 406 | III | MPR, EFS | 10/2024 |
| | NCT05116462 | IIB-IIIB | Sintilimab | Sintilimab+Chemotherapy S + Sintilimab | 800 | III | EFS, pCR | 06/2026 |

NSCLC, non-small cell lung cancer; C, cycle; S, surgery; y, year; SoC, Standard of care DFS, disease-free survival; MPR, major pathologic response; EFS, event-free survival; pCR, pathologic complete response; OS, overall survival.

response to tumorigenesis and progression. The tumor-cell-related biomarkers of interest to perioperative immunotherapy include PD-L1, TMB, the DNA–damage response (DDR) pathway, the homology-dependent recombination (HR) pathway, homologous recombination deficiency (HRD), specific genetic mutations (e.g., the interferon gamma pathway, KRAS, and STK11 mutations), and neo-antigens. All of the above may be related to the efficacy of perioperative immunotherapy (44).

### 5.1.1 Programmed cell death ligand 1

PD-L1 antibody blocking immune checkpoints have revolutionized the treatment of advanced NSCLC (15).

CheckMate159 study was the first to report a correlation between PD-L1 expression and MPR/RFS in immune single-agent neoadjuvant therapy. PD-L1 expression was associated with pathological remission, and PD-L1-positive tumors trended towards improved RFS. LCMC3 study reported on the pathological and imaging response to different levels of PD-L1 expression as secondary endpoints, finding that high levels of PD-L1 expression was associated with MPR from neoadjuvant immunotherapy in patients with early stage NSCLC (45). A meta-analysis that studied 10 neoadjuvant immunotherapy studies and included a total of 461 NSCLC patients associated high levels of PD-L1 expression with an improved pathological response, noting 50% PD-L1 as a stronger predictive cutoff than 1% expression. A report presented at the 2022 ASCO meeting reported that neoadjuvant nivolumab treatment of tumors with high PD-L1 expression may predict long-term response. However, larger prospective studies are required (46).

PD-L1 expression was also found meaningful when considering adjuvant immunotherapy. Impower010 showed that patients with PD-L1 expression≥xprhad a greater DFS benefit, especially in patients high expression levels (38).

There is no consensus on the use of PD-L1 to estimate the efficacy of neoadjuvant treatment. CheckMate-816 reported that patients with ≥1% PD-L1 expression had a considerably higher treatment benefit than those with <1% expression (14). Similarly, NADIM II reported pCR rates of patients with PD-L1 expression 1%-49% or TPS ≥ 50% of 41.7% and 61.1%, respectively, compared with 15% in patients with PD-L1 expression <1%. Moreover, patients with high levels of PD-L1 expression and TPS ≥ 1% were more likely to achieve pCR after nivolumab plus chemotherapy (43). ChiCTR-OIC-17013726's 3 year results found that patients with PD-L1 ≥ 1% had more favorable clinical outcomes than other subgroups (HR, 0.275; 95% CI, 0.078–0.976) (19). Another study of neoadjuvant durvalumab alone or combined with SBRT reported that MPR was achieved independent of PD-L1 tumor status after adjusting for PD-L1 baseline expression as assessed with immunohistochemistry (IHC). Furthermore, no significant changes in PD-L1 expression were observed when comparing pretreatment and surgical resection tumor specimens in both trial groups and between patients with and without MPR (35). A further study showed that there was no significant association between PD-L1 expression and PFS (47).

### 5.1.2 Tumor mutation burden

TMB is defined as the number of somatic mutations per million bases in the coding region of the tumor genome. In patients with advanced NSCLC being treated with immunotherapy, TMB is closely related to the efficacy and prognosis of immune checkpoint inhibitors. This is not as well shown in patients with early NSCLC who receive perioperative immunotherapy, with current studies still in the exploratory stage. However, it is generally accepted that TMB is closely related to the efficacy and prognosis of ICIs (48).

A study of neoadjuvant nivolumab for patients with stage I–IIIA NSCLC reported an MPR rate of 45%, with 311 patients with MPR and 74 patients without, which was statistically significant ($p = 0.01$). Furthermore, it showed that there was a significant correlation between pathological response and the pretreatment tumor mutational burden (15). A recent meta-analysis suggests that TMB may be associated with better pathological response to neoadjuvant immunotherapy, and although there are different neoadjuvant and adjuvant regimens and different TMB detection methods [next-generation sequencing (NGS) and whole-exome sequencing (WES)], high TMB is always associated with high MPR and pCR rates (49). In LCMC3, patients with high TMB values tended to have a better pathological response, and a high TMB immune response was associated with better PFS. This indicates that TMB is a potential predictive biomarker for MPR during neoadjuvant immunotherapy. After it was found in KENOTE-158 that patients with a high TMB performed significantly better than those with a low TMB, pembrolizumab monotherapy was approved by the FDA for patients with a high TMB, defined as ≥10 mutations/Mb, those with disease progression after previous treatments, and for patients with solid metastatic tumors. However, in another study on neoadjuvant immunotherapies, the MPR of nivolumab combined with ipilimumab was only 33%, indicating that the pathological response was not associated with TMB (50). The predictive value of TMB for neoadjuvant immunotherapy therefore requires further study.

### 5.1.3 Homologous recombination deficiency

HRD are biomarkers that may be highly predictive of the therapeutic outcomes of neoadjuvant immunotherapy in NSCLC patients. Mutations of tumor suppressor genes in the DNA damage repair (DDR) and homology-dependent recombination (HR) pathways were more common in MPR patients, suggesting that better responders were likely to have HRD events. Moreover, HR pathway mutations were associated with better responding immunotherapy patients regardless of the treatment regimen and clinicopathological characteristics. It has also been observed that patients on immunotherapy with HR mutations have higher a TMB and longer survival in addition to a substantial number HR pathway alternations in multiracial treatment-free samples (51, 52).

Mismatch repair (MMR) is one of the multiple pathways that compose the DDR system. The proteins of MMR are related to apoptosis, indicating that the TME can indirectly promote the survival of tumor cells by inhibiting some DDR pathways. Defects in MMR genes that result in microsatellite instability-high (MSI-H) status result in the accumulation of mutations and the production of neoantigens, which can enhance the anti-cancer immune response (53). DDR-related genes such as KMT2A, KMT2B, KMT2C, SETD2, POLE, POLD1, and DNMT3A may also be predictive biomarkers for immunotherapy outcomes in patients with resectable NSCLC (52).

### 5.1.4 Oncogenic driver mutations

NSCLC patients with mutations in major driver genes, such as EGFR and ALK, are excluded or represent a very small proportion of the cohorts used in most immunotherapy clinical studies. This indicates that conventional immunotherapy is not recommended for driver-gene-positive NSCLC patients, especially during neoadjuvant period (27).

KEYNOTE-010, a phase III randomized clinical trial comparing pembrolizumab to docetaxel, found in its subgroup analysis of EGFR-mutated NSCLC patients that pembrolizumab did not improve OS compared with docetaxel. Only a modest proportion of patients benefited from targeted treatment, and while no additional benefits

from ICI therapy were observed, drug toxicity and side effects were report (54). Neoadjuvant single-agent immunotherapy in patients with potentially negative factors, such as EGFR-sensitive mutations/ALK fusions, should be used with caution. EGFR/ALK mutations are promising predictive biomarkers.

In the NADIM study, patients with driver gene EGFR/STK11/KEAP1/RB1 mutations had shorter PFS than wild-type patients, suggesting that patients with these mutations are less likely to benefit from neoadjuvant immune-chemotherapy (25).

With respect to STK11 mutation status, KEYNOTE-042 showed that patients who received pembrolizumab monotherapy had better PFS and OS than those who received standard chemotherapy. It is unclear if a STK11 mutation is a prognostic or predictive factor in patients with NSCLC who are receiving PD-1/PD-L1 inhibitor therapy (10).

## 5.2 Tumor-microenvironment-associated biomarkers

The overall immune microenvironment can be considered a biomarker of immunotherapy efficacy. A growing body of evidence suggests that microbiome is associated with ICIs and could certainly influence the efficacy of neoadjuvant immunotherapy. Tumor-microenvironment-associated biomarkers include tumor-infiltrating immune cells and immune status scores (55). The former consists of immune cells with specific phenotypes (e.g., cluster of differentiation 4+, CD4+ T cells, cluster of differentiation 8+, CD8+ T cells, and FOXP3+ T cells) and the diversity of the immune repertoire (e.g., T-cell receptor library).

Early studies have shown that massive infiltration of CD4+ and CD8+ T cells is associated with better tumor survival and prognosis (56). In the excised specimens of patients who achieved pCR from immune-neoadjuvant therapy, a large number of infiltrated CD8+ T cells, PD-1+ lymphocytes, CD68+ macrophages, FoxP3+ regulatory T cells, and tertiary lymphocytes were observed in the visual field. Higher levels of CD3+ tumor-infiltrating lymphocytes (TILs) and tissue-resident memory T cells were also seen in surgical specimens (50). Similarly, CD3+ and PD-1+ T cells were increased in patients with MPR in LCMC3 (NCT02927301) (45). Findings from CheckMate159, which evaluated nivolumab single-agent neoadjuvant therapy, suggested that T-cell enrichment could be a potential biomarker, as patients who achieved MPR after receiving neoadjuvant therapy with nivolumab had higher levels of CD8+ T-cell infiltration after treatment compared with before treatment. This suggests that PD-1 inhibitors may enhance anti-tumor T-cell activation (13). In another study cohort, high CD8+ TILs IHC expression was associated with better OS (9.4 *vs.* 5.6 months) (47). It is important to note that in the resected specimens obtained for PCR, the field was heavily infiltrated with CD8 + T cells, PD-1 + lymphocytes, CD68 + macrophages, FoxP3 + regulatory T cells, and tertiary lymphoid structures (TLS) (50).

Later research used RNA sequencing analysis of multiple immune cell subtypes in the tumor microenvironment to predict the efficacy of neoadjuvant immunotherapy. In the LCMC3 study (45), Ig-like transcript 2 (ILT2) was positively correlated with MPR by single-cell sequencing surgically resected specimens. ILT2 was mostly expressed in dendritic cells, monocytes, and macrophages, and was correlated with PD-L1 expression. A linear correlation suggested that LIT2 was co-expressed with PD-L1 on the same cells. The study also reported that early decreases in serum interleukin-8 (IL-8) were associated with longer overall survival ($p = 0.015$) (57). Low systemic inflammation, including interleukin-6 (IL-6), IL-8, and high levels of IFN-γ, was observed in patients who had a long-term response to ICI treatment (58). Transforming growth factor (TGF)-β signaling also functioned importantly in the regulation of TME. TGF-β promotes tumor invasion and metastasis by inducing the epithelial–mesenchymal transition (EMT) of NSCLC and can predict the clinical outcomes of patients with lung adenocarcinoma (LUAD) who are treated with immunotherapy (59, 60).

## 5.3 Host-associated biomarkers

Host-related biomarkers include general characteristics (such as gender, age, and body fat distribution.), gut symbionts, and host germline genetic characteristics (such as human leukocyte antigen, HLA, diversity, and other specific mutations). The immune microenvironment is different after immunotherapy. By comparing the gene expression profiles of surgically resected specimens with normal lung samples, it is possible to use the NSCLC immune microenvironment to predict surgical outcomes. Peripheral T-cell receptor sequencing may also prove useful in predicting a patient's response to immunotherapy. An increased abundance of gut *Ruminococcus* and *Akkermansia* spp. was associated with MPR to dual therapy (16). Another study that performed a microbial analysis found that *Parabacteroides distasonis* and *Bacteroides vulgatus* abundance was higher in anti-PD-1 blockade responders than in non-responders (61).

A high neutrophil-to-lymphocyte ratio (NLR) and platelet-to-lymphocyte ratio (PLR) are indicators of host inflammation and associated with worse overall survival (OS) in NSCLC. Elevated pretreatment NLR and PLR are also associated with shorter OS and PFS and worse response rates in patients with metastatic NSCLC treated with nivolumab independent of other prognostic factors (62). Carcinoembryonic antigen (CEA) and cytokeratin-19 fragment (CYFRA 21-1), which have been used for decades to monitor the efficacy of antitumor therapy, may also be useful in predicting NSCLC patient outcome (63, 64).

## 5.4 Blood cell and liquid biopsy-related biomarkers

### 5.4.1 Circulating tumor DNA monitoring during perioperative immunotherapy

Cell-free DNA in plasma is called circulating cell-free DNA (cfDNA). cfDNA exists in various body fluids of the human body, and its concentration changes with tissue damage, cancer, and inflammatory reactions, where cells from tumor patients are released into the body (65). Circulating cfDNA is ctDNA. Postoperative ctDNA is non-invasive mode of minimal residual disease (MRD) detection *via* liquid biopsy and has been widely used as a prognostic biomarker in patients with early NSCLC

(66). A study that dynamically tracked 40 NSCLC patients with stage I–III disease after radical treatment using CAPP-Seq technology showed that all 20 ctDNA-positive patients at any time point had disease recurrence, with a median advance prediction time of 5.2 months (67, 68).

Comparing ctDNA levels before and after surgery may help identify patients at a high risk for disease recurrence. A retrospective study including 22 patients with stage IB–IIIA NSCLC who received neoadjuvant immunotherapy combined with chemotherapy, double immunotherapy, or chemotherapy alone used lung cancer-MRD sequencing panels for ctDNA detection before and after neoadjuvant therapy postoperatively and during follow-up. Patients who were ctDNA detection positive after neoadjuvant therapy and before surgery had a poorer RFS prognosis (HR, 7.41; 95% CI, 0.91–60.22, p=0.03). ctDNA was detected in 31.8% of patients 3–8 days after surgery and was found to be an independent risk factor for recurrence (HR, 5.37; 95% CI, 1.27–22.67, p=0.01). ctDNA detection 3 months after surgery suggests that it could predict recurrence, with a sensitivity and specificity of 83% and 90%, respectively (69). Another study of patients with higher stage (III/IV) disease found that those who were preoperative ctDNA positive had a significantly lower RFS (HR = 3.812, p = 0.0005) and OS (HR = 5.004, p = 0.0009), with ctDNA detection ahead of radiographic findings by a median of 12.6 months (41).

Early findings from NADIM study suggest that ctDNA clearance may be superior to radiological assessment at predicting survival and that neoadjuvant nivolumab combined with chemotherapy for resectable NSCLC could achieve a long-term survival benefit (70). CheckMate 816 also suggested that ctDNA may predict long-term DFS and OS and that higher pCR and longer EFS can be seen in patients with ctDNA clearance (14). A prospective, multicenter cohort enrolled 950 plasma samples obtained at three perioperative time points (before surgery and 3 days and 1 month after surgery) of 330 stage I–III NSCLC patients. Perioperative ctDNA analysis was found to be effective in the early detection of MRD and relapse risk stratification and hence could benefit NSCLC patient management (71).

A study reported at the 2022 ASCO Annual Meeting revealed that ctDNA detection after surgery could indicate an increased risk of recurrence risk when monitoring the effects of adjuvant therapy in patients with resectable NSCLC. The recurrence ratio was 33.33% (4/12) in patients with detectable ctDNA and 4.34% (1/23) in patients with undetectable ctDNA before adjuvant therapy. After a median follow-up of 9.47 months, 6 patients relapsed. All patients who were ctDNA negative were disease-free after adjuvant therapy (11/11), while those who were ctDNA positive had a 33.33% (1/3) recurrent rate (72). The outcomes of IMpower010 showed that adjuvant atezolizumab combined with chemotherapy had a DFS benefit in patients who were ctDNA positive. Adding adjuvant atezolizumab can reduce the risk of recurrence by 28% and in both ctDNA-positive and ctDNA-negative patients. Adjuvant Atezo plus chemotherapy was effective only in patients with positive PD-L1 expression (38). Yilong Wu et al. recently explored the prognostic value of MRD detection in patients with NSCLC after surgery, reporting a negative predictive value of 96.8%. This might represent potentially cured patients regardless of stage and adjuvant therapy (73).

Several clinical studies are under way to assess the perioperative use of ctDNA. NCT04966663 is attempting to use ctDNA detection to help in predicting if giving adjuvant treatment after surgery can decrease the chance of lung cancer recurrence, while NCT04585477 explores if the administration of durvalumab can reduce the number of circulating cancer cells in the blood after testing positive for residual cancer after standard treatment. Other studies have attempted to use ctDNA as a biomarker with different immunological agents like nivolumab (NCT03770299) and atezolizumab (NCT04267237) added to standard of care therapy (SOC) after surgery to test their effectiveness compared with SOC alone. The MEDAL study (NCT03634826) is trying to prospectively confirm the value of circulating tumor DNA and its aberrant methylation in their longitudinal monitoring of surgical lung cancer patients.

Despite the prognostic advantages of ctDNA, it is not highly sensitive (20%) and may not predict the MRD of patients with brain metastases (73). Additional studies are needed to explore the underlying mechanism behind this phenomenon.

### 5.4.2 Peripheral blood cells and other molecular biomarkers

Additional biomarkers are related to peripheral blood cells (e.g., CD45RO+/CD8+T cells, circulating tumor cells, CTCs, and other molecular markers such as exosomes) (74). Exploration of peripheral blood immune phenotypes in the prediction of MPR and innate immune cells such as natural killer (NK) cells and NK-like T cells expressing ILT2 and NKG2A in the peripheral blood may be able to quantify the efficacy of neoadjuvant immunotherapy.

CheckMate 159 explored the relationship between the efficacy and specific expansion of tumor-specific T cells in the peripheral blood and found that tumor-specific T-cell subtypes continue to increase with treatment and continued disease-free status in MPR patients but decreased in patients with recurrent disease or who did not achieve MPR (75). In LCMC3, a lower frequency of ILT2+NKG2A+ and ILT2+NKG2A natural killer (NK) cells and ILT2+ NK-like T cells in pretreatment peripheral blood was significantly associated with MPR, suggesting that ILT2 has a negative effect on the HLA-G and/or NKG2A/HLA-E axis. NKG2D expression on NK cells correlated with lymph node involvement, whereas expression on NK-like T cells and T cells correlated with no lymph node involvement, suggesting that the NKG2D/NKG2D-L axis plays a role in tumor immune escape. These immunophenotypic data identify new potential immune escape mechanisms and new potential biomarkers and therapeutic targets (45).

## 6 Discussion

Current clinical research findings suggest that the use of a PD-1 inhibitor combined with chemotherapy (neoadjuvant chemotherapy immunotherapy) is superior to neoadjuvant PD-1 monotherapy and dual immunotherapy (76).

During the perioperative period, treatment strategies should be classified according to their precise modality. Accurate TNM staging is beneficial to identifying the appropriate treatment strategy. The pathological classification of tumors can help guide the scope of surgical resection. Qiu presented at the 2022 ASCO meeting that the MPR rate of squamous cell carcinoma patients (51.6%, 16/31) was significantly higher than those with non-squamous cell carcinoma (12.5%, 3/24) (p = 0.002) (77). Furthermore, the tumor microenvironment can predict tumor evolution and development,

while molecular sub-types represent their heterogeneity. The endpoints assessed for neoadjuvant and perioperative therapy were EFS, pCR, and MPR, while those for adjuvant therapy were DFS and OS.

Lung cancer postoperative recurrence and metastasis is still a major problem. The more advanced the stage, the higher the risk of recurrence and metastasis (14).

The 5-year survival rate of stage I patients was 90% after surgical treatment, with similar local and distant recurrence rates of approximately 5% each. In contrast, the local recurrence rate of stage IIB–IIIA patients is 12%–15%, with a distant recurrence rate of 40%–60% (15). Adjuvant therapy is therefore recommended for perioperative patients with stage II–IIIA disease and may also be recommended for select stage IB patients as well. Although important clinical trials are still ongoing, already completed trials have yielded exciting preliminary results for immunotherapy, with an MPR of 22%–45% for immune monotherapy and 50%–83% for immunotherapy combined with chemotherapy (15–17, 31). The safety of immunotherapy is good, indicating that neoadjuvant immunotherapy is a promising treatment strategy for patients with resectable lung cancers. Compared with the adjuvant approach, neoadjuvant therapy can help eliminate micrometastases early on. However, despite effective treatment, the study arm was terminated early due to toxicity (50).

Surgical safety after neoadjuvant immunotherapy is of interest to surgeons, but there are no current indicators that immunotherapy impact surgical outcomes. A prior work showed that neoadjuvant immunotherapy alone or in combination with chemotherapy did not result in many delayed surgical events, with an overall mean surgical resection rate of 88.7%. There was also no increase in surgical difficulty and perioperative risk. The mean incidence of surgical complications was 20.6%, with most patients having good prognosis. Deaths had almost nothing to do with drug treatment (30).

Immune single-agent neoadjuvant studies, such as CheckMate 159, LCMC3, PRINCEPS, TOPlS01, IoNESCO, and ChicTR-OIC-17013726, included patients with stage I–IIIb NSCLC. After one to three cycles of treatment, MPR ranged from 14% to 45%. Neoadjuvant immune combined chemotherapy (NADIM, NCT02716038, SAKK 16/14) studies enrolled patients with stage Ib–IIIa disease for two to four cycles. The MPR rate of the NADIM study was as high as 85.36%, and pCR reached 71.4%. The MPR of both the other studies was approximately 60%. The double immune neoadjuvant study (NEOSTAR) enrolled patients with stage I–IIIA lung cancer for three cycles of treatment, yielding an MPR rate of 24% (16). CheckMate 816 is currently the first phase III study to reach its primary endpoint, and we are eagerly awaiting the release of more detailed data (14).

In order to explore correlations between pathological endpoints and long-term benefit and as more trials use MPR and pCR as surrogates for the clinical benefit of neoadjuvant therapy, there is an urgent need to clearly demonstrate to what extent these pathological endpoints reflect survival benefit. A retrospective analysis showed that patients who achieved MPR after neoadjuvant chemotherapy had significantly prolonged DFS and OS compared with those who did not. Thus, does this effect apply to immune combination therapy? In NADIM (nivolumab plus chemotherapy), the 24-month OS was 100% in patients who achieved MPR or pCR and 85.7% in patients with an incomplete pathological response (p=0.002). Another clinical trial of neoadjuvant immunotherapy plus chemotherapy (atezolizumab combined with chemotherapy) reported that the median DFS of patients who achieved versus who did not achieve MPR was 34.5 and 14.3 months, respectively (p=0.71) (25). The relationship between pCR, MPR, and OS still requires a large amount of clinical data to verify, and the definition of MPR needs to be further explored and standardized.

Delayed surgery may lead to tumor progression. Reasons why surgery may be delayed include differences in imaging judgment and treatment-related adverse reactions. Premature surgery may cause serious surgical complications in addition to the immune cell infiltration stimulated by immunotherapy during the anti-tumor response. It is therefore necessary to determine the optimal time interval between neoadjuvant immunotherapy and surgery. Too long or too short of an interval will reduce the efficacy of immunotherapy. Meanwhile, preclinical research indicates that changes in the immune microenvironment may assist with surgical timing, and the effects on surgery caused by prolonging the interval may be related to the proportion of tumor-specific T cells and IFNγ production (42).

It is still difficult to screen for immune responders using PD-L1, TMB, or other kinds of tumor immune microenvironment markers. Assessment of the pathological response using both the primary tumor and lymph nodes (LNs) may be important ways to judge the efficacy of neoadjuvant immunotherapy (78). Furthermore, is it important to question if the supplementation of MPR and pCR with surrogate or complementary indicators is the right way to monitor postoperative outcomes over the long term? Moreover, what are common microenvironmental changes that occur after immunotherapy? Available data from CheckMate816 showed a tumor PD-L1 expression level more than 1% and stage III resectable NSCLC are predictors of outcome (14). Furthermore, the sensitivity of single postoperative ctDNA MRD detection is <50%. Although continuous longitudinal ctDNA MRD detection can greatly improve its sensitivity, its sensitivity among patients with brain metastases is not high (20%) and MRD may not be detected (73). More clinical studies are needed to validate the predictive merits of any of these factors.

Current perioperative immunotherapy research study designs are not the same. Many issues such as the selection of neoadjuvant therapy, the use of a postoperative immune adjuvant, the duration of adjuvant therapy, the selection of the target population, and postoperative recurrence and metastasis monitoring still require further study. New long-term survival follow-up data are being released. The 5-year clinical outcome of neoadjuvant therapy with nivolumab was better than that of historical controls, with a 5-year OS of 80%, a 5-year RFS of 60%, and a median RFS of 67 months (46). The "International Expert Consensus on Neoadjuvant Immunotherapy for Non-Small Cell Lung Cancer" (27), the "Expert Consensus on Perioperative Immunotherapy for Locally Advanced Non-Small Cell Lung Cancer" (28), and the "Consensus on Postoperative Recurrence Prediction of Non-small Cell Lung Cancer Based on Molecular Markers" (29) have been published. We look forward to more results of phase III studies on neoadjuvant/adjuvant immunotherapy for NSCLC.

Compared with advanced tumors, perioperative treatment research over a large time span encompasses many significant changes during the treatment period. Many factors such as treatment drugs, treatment strategies, and population distribution may change dramatically, affecting research progress and results. A larger volume of research is needed to combat these potential biases (Figure 2).

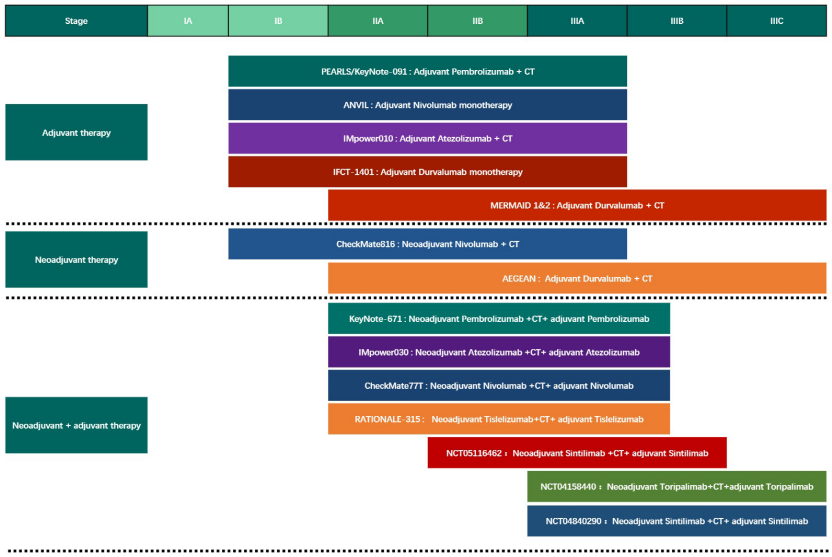


FIGURE 2
The Phase III clinical trials of different modes of perioperative immunotherapy for Non-Small Cell Lung Cancer. CT, chemotherapy.

## 7 Conclusion

In conclusion, perioperative neoadjuvant and adjuvant ICI monotherapy and immune-combination therapy have successfully improved the survival and prognosis of patients with resectable NSCLC. Recent clinical trial findings suggest that patients who receive neoadjuvant and adjuvant immunotherapy combined with chemotherapy had better outcomes and acceptable safety than other modalities. Perioperative immune-related drugs and interval cycles varied between studies, with most studies choosing two to four cycles to ensure its efficacy and patient compliance. More clinical evidence is required to identify the optimal regimen. Different tumor biomarkers such as TME, host associated, blood cell, and liquid biopsy were also evaluated. Additional studies and clinical research findings are needed to identify the ideal perioperative regimen.

## Author contributions

FW: Conceptualization, Supervision, Validation, Design the figure. YRP, ZL: Writing original draft, Design the figure and tables. YF: Drawing the figure. YP, YZ, JL, CX, YZZ, YS, GL: Review, Editing. All authors contributed to the article and approved the submitted version.

## Funding

This study was funded by the following: 1) 2022.01–2024.12, The effects and mechanism investigation of stress status on efficacy and prognosis of immune checkpoint blockade therapy in non-small cell lung cancer, supported by the Beijing Xisike Clinical Oncology Research Foundation (Grant No. Y-HS202102-0130), PI; 2) 2021.01–2024.12, The novel mechanism underlying the resistance to immune checkpoint blockade therapy in non-small cell lung cancer: focusing on β2-AR signaling in CD8+T cell, supported by the Hunan Provincial Science Fund for Excellent Young Scholars (Grant No. 2021JJ20088), PI; and 3) 2020.01–2022.12, The role of β2-AR pathway on the CD8+T cells within tumor microenvironment in the effect of immune checkpoint inhibitors therapy of non-small cell lung cancer, supported by the Chinese Thoracic Oncology Group (CTONG)-ROCHE Lung Cancer Research Foundation, PI.

## Acknowledgments

The authors would like to thank the multi-disciplinary team (MDT) for thoracic tumors of the Second Xiangya Hospital of Central South University for their inspiration and guidance.

## Conflict of interest

The authors declare that the research was conducted in the absence of any commercial or financial relationships that could be construed as a potential conflict of interest.

## Publisher's note

# References


1. Siegel RL, Miller KD, Fuchs HE, Jemal A. Cancer statistics, 2022. *CA Cancer J Clin* (2022) 72(1):7–33. doi: 10.3322/caac.21708

2. Molina JR, Yang P, Cassivi SD, Schild SE, Adjei AA. Non-small cell lung cancer: epidemiology, risk factors, treatment, and survivorship. *Mayo Clinic Proc* (2008) 83 (5):584–94. doi: 10.4065/83.5.584

3. Goldstraw P, Chansky K, Crowley J, Rami-Porta R, Asamura H, Eberhardt WE, et al. The IASLC lung cancer staging project: Proposals for revision of the TNM stage groupings in the forthcoming (Eighth) edition of the TNM classification for lung cancer. *J Thorac Oncol Off Publ Int Assoc Study Lung Cancer* (2016) 11(1):39–51. doi: 10.1016/j.jtho.2015.09.009

4. Arriagada R, Bergman B, Dunant A, Le Chevalier T, Pignon JP, Vansteenkiste J. Cisplatin-based adjuvant chemotherapy in patients with completely resected non-small-cell lung cancer. *New Engl J Med* (2004) 350(4):351–60. doi: 10.1056/NEJMoa031644

5. Winton T, Livingston R, Johnson D, Rigas J, Johnston M, Butts C, et al. Vinorelbine plus cisplatin vs. observation in resected non-small-cell lung cancer. *New Engl J Med* (2005) 352(25):2589–97. doi: 10.1056/NEJMoa043623

6. Douillard JY, Rosell R, De Lena M, Carpagnano F, Ramlau R, Gonzáles-Larriba JL, et al. Adjuvant vinorelbine plus cisplatin versus observation in patients with completely resected stage IB-IIIA non-small-cell lung cancer (Adjuvant navelbine international trialist association [ANITA]): a randomised controlled trial. *Lancet Oncol* (2006) 7 (9):719–27. doi: 10.1016/s1470-2045(06)70804-x

7. Garon EB, Hellmann MD, Rizvi NA, Carcereny E, Leighl NB, Ahn MJ, et al. Five-year overall survival for patients with advanced Non–Small-cell lung cancer treated with pembrolizumab: Results from the phase i KEYNOTE-001 study. *J Clin Oncol Off J Am Soc Clin Oncol* (2019) 37(28):2518–27. doi: 10.1200/jco.19.00934

8. Gandhi L, Rodríguez-Abreu D, Gadgeel S, Esteban E, Felip E, De Angelis F, et al. Pembrolizumab plus chemotherapy in metastatic non-Small-Cell lung cancer. *New Engl J Med* (2018) 378(22):2078–92. doi: 10.1056/NEJMoa1801005

9. Paz-Ares L, Luft A, Vicente D, Tafreshi A, Gümüş M, Mazières J, et al. Pembrolizumab plus chemotherapy for squamous non-Small-Cell lung cancer. *New Engl J Med* (2018) 379(21):2040–51. doi: 10.1056/NEJMoa1810865

10. Mok TSK, Wu YL, Kudaba I, Kowalski DM, Cho BC, Turna HZ, et al. Pembrolizumab versus chemotherapy for previously untreated, PD-L1-expressing, locally advanced or metastatic non-small-cell lung cancer (KEYNOTE-042): a randomised, open-label, controlled, phase 3 trial. *Lancet (London England)* (2019) 393 (10183):1819–30. doi: 10.1016/s0140-6736(18)32409-7

11. Antonia SJ, Villegas A, Daniel D, Vicente D, Murakami S, Hui R, et al. Durvalumab after chemoradiotherapy in stage III non-Small-Cell lung cancer. *New Engl J Med* (2017) 377(20):1919–29. doi: 10.1056/NEJMoa1709937

12. Topalian SL, Hodi FS, Brahmer JR, Gettinger SN, Smith DC, McDermott DF, et al. Five-year survival and correlates among patients with advanced melanoma, renal cell carcinoma, or non-small cell lung cancer treated with nivolumab. *JAMA Oncol* (2019) 5 (10):1411–20. doi: 10.1001/jamaoncol.2019.2187

13. Duan H, Wang T, Luo Z, Tong L, Dong X, Zhang Y, et al. Neoadjuvant programmed cell death protein 1 inhibitors combined with chemotherapy in resectable non-small cell lung cancer: an open-label, multicenter, single-arm study. *Trans Lung Cancer Res* (2021) 10(2):1020–8. doi: 10.21037/tlcr-21-130

14. Forde PM, Spicer J, Lu S, Provencio M, Mitsudomi T, Awad MM, et al. Neoadjuvant nivolumab plus chemotherapy in resectable lung cancer. *New Engl J Med* (2022) 386(21):1973–85. doi: 10.1056/NEJMoa2202170

15. Forde PM, Chaft JE, Smith KN, Anagnostou V, Cottrell TR, Hellmann MD, et al. Neoadjuvant PD-1 blockade in resectable lung cancer. *New Engl J Med* (2018) 378 (21):1976–86. doi: 10.1056/NEJMoa1716078

16. Cascone T, William WNJr., Weissferdt A, Leung CH, Lin HY, Pataer A, et al. Neoadjuvant nivolumab or nivolumab plus ipilimumab in operable non-small cell lung cancer: the phase 2 randomized NEOSTAR trial. *Nat Med* (2021) 27(3):504–14. doi: 10.1038/s41591-020-01224-2

17. Gao S, Li N, Gao S, Xue Q, Ying J, Wang S, et al. Neoadjuvant PD-1 inhibitor (Sintilimab) in NSCLC. *J Thorac Oncol Off Publ Int Assoc Study Lung Cancer* (2020) 15 (5):816–26. doi: 10.1016/j.jtho.2020.01.017

18. Mignard X, Antoine M, Moro-Sibilot D, Dayen C, Mennecier B, Gervais R, et al. [IoNESCO trial: Immune neoajuvant therapy in early stage non-small cell lung cancer]. *Rev Des maladies respiratoires* (2018) 35(9):983–8. doi: 10.1016/j.rmr.2018.08.006

19. Zhang F, Guo W, Zhou B, Wang S, Li N, Qiu B, et al. Research article: Three-year follow-up of neoadjuvant PD-1 inhibitor (Sintilimab) in non-small cell lung cancer. *J Thorac Oncol Off Publ Int Assoc Study Lung Cancer.* (2022) 17(7):909–20. doi: 10.1016/j.jtho.2022.04.012

20. Tong BC, Gu L, Wang X, Wigle DA, Phillips JD, Harpole DHJr., et al. Perioperative outcomes of pulmonary resection after neoadjuvant pembrolizumab in patients with non-small cell lung cancer. *J Thorac Cardiovasc Surg* (2022) 163(2):427–36. doi: 10.1016/j.jtcvs.2021.02.099

21. Wu J, Waxman DJ. Immunogenic chemotherapy: Dose and schedule dependence and combination with immunotherapy. *Cancer Lett* (2018) 419:210–21. doi: 10.1016/j.canlet.2018.01.050

22. Shu CA, Gainor JF, Awad MM, Chiuzan C, Grigg CM, Pabani A, et al. Neoadjuvant atezolizumab and chemotherapy in patients with resectable non-small-cell lung cancer: an open-label, multicentre, single-arm, phase 2 trial. *Lancet Oncol* (2020) 21 (6):786–95. doi: 10.1016/s1470-2045(20)30140-6

23. Rothschild SI, Zippelius A, Eboulet EI, Savic Prince S, Betticher D, Bettini A, et al. SAKK 16/14: Durvalumab in addition to neoadjuvant chemotherapy in patients with stage IIIA(N2) non-Small-Cell lung cancer-a multicenter single-arm phase II trial. *J Clin Oncol Off J Am Soc Clin Oncol* (2021) 39(26):2872–80. doi: 10.1200/jco.21.00276

24. Zhao ZR, Yang CP, Chen S, Yu H, Lin YB, Lin YB, et al. Phase 2 trial of neoadjuvant toripalimab with chemotherapy for resectable stage III non-small-cell lung cancer. *Oncoimmunology* (2021) 10(1):1996000. doi: 10.1080/2162402x.2021.1996000

25. Provencio M, Nadal E, Insa A, Garcia-Campelo MR, Casal-Rubio J, Domine M, et al. Neoadjuvant chemotherapy and nivolumab in resectable non-small-cell lung cancer (NADIM): an open-label, multicentre, single-arm, phase 2 trial. *Lancet Oncol* (2020) 21 (11):1413–22. doi: 10.1016/S1470-2045(20)30453-8

26. Heymach JV, Mitsudomi T, Harpole D, Aperghis M, Jones S, Mann H, et al. Design and rationale for a phase III, double-blind, placebo-controlled study of neoadjuvant durvalumab + chemotherapy followed by adjuvant durvalumab for the treatment of patients with resectable stages II and III non-small-cell lung cancer: The aegean trial. *Clin Lung Cancer* (2022) 23(3):e247–51. doi: 10.1016/j.cllc.2021.09.010

27. Liang W, Cai K, Chen C, Chen H, Chen Q, Fu J, et al. Expert consensus on neoadjuvant immunotherapy for non-small cell lung cancer. *Trans Lung Cancer Res* (2020) 9(6):2696–715. doi: 10.21037/tlcr-2020-63

28. Qiu B, Cai K, Chen C, Chen J, Chen KN, Chen QX, et al. Expert consensus on perioperative immunotherapy for local advanced non-small cell lung cancer. *Trans Lung Cancer Res* (2021) 10(9):3713–36. doi: 10.21037/tlcr-21-634

29. [Consensus on postoperative recurrence prediction of non-small cell lung cancer based on molecular markers]. *Zhongguo Fei Ai Za Zhi* (2022) 25(10):701–14. doi: 10.3779/j.issn.1009-3419.2022.102.44

30. Zhao X, Su Y, You J, Gong L, Zhang Z, Wang M, et al. Combining antiangiogenic therapy with neoadjuvant chemotherapy increases treatment efficacy in stage IIIA (N2) non-small cell lung cancer without increasing adverse effects. *Oncotarget* (2016) 7 (38):62619–26. doi: 10.18632/oncotarget.11547

31. Testing new neoadjuvant combos in NSCLC. *Cancer Discovery* (2022) 12(6):1400–1. doi: 10.1158/2159-8290.Cd-nb2022-0029

32. Deng L, Liang H, Burnette B, Beckett M, Darga T, Weichselbaum RR, et al. Irradiation and anti-PD-L1 treatment synergistically promote antitumor immunity in mice. *J Clin Invest* (2014) 124(2):687–95. doi: 10.1172/jci67313

33. Twyman-Saint Victor C, Rech AJ, Maity A, Rengan R, Pauken KE, Stelekati E, et al. Radiation and dual checkpoint blockade activate non-redundant immune mechanisms in cancer. *Nature* (2015) 520(7547):373–7. doi: 10.1038/nature14292

34. Hong MH, Ahn B, Kim HR, Lim SM, Lee S, Park SY, et al. FP03.02 interim analysis of neoadjuvant chemoradiotherapy and durvalumab for potentially resectable stage III non-small cell lung cancer (NSCLC). *J Thorac Oncol* (2021) 16(3):S194–5. doi: 10.1016/j.jtho.2021.01.084

35. Altorki NK, McGraw TE, Borczuk AC, Saxena A, Port JL, Stiles BM, et al. Neoadjuvant durvalumab with or without stereotactic body radiotherapy in patients with early-stage non-small-cell lung cancer: a single-centre, randomised phase 2 trial. *Lancet Oncol* (2021) 22(6):824–35. doi: 10.1016/s1470-2045(21)00149-2

36. Chaft JE, Shyr Y, Sepesi B, Forde PM. Preoperative and postoperative systemic therapy for operable non-Small-Cell lung cancer. *J Clin Oncol Off J Am Soc Clin Oncol* (2022) 40(6):546–55. doi: 10.1200/jco.21.01589

37. Wakelee H, Altorki N, Felip E, Vallieres E, Vynnychenko IO, Akopov A, et al. PL03.09 IMpower010:Overall survival interim analysis of a phase III study of atezolizumab vs best supportive care in resected NSCLC. *J Thorac Oncol* (2022) 17(9, Supplement):S2. doi: 10.1016/j.jtho.2022.07.013

38. Felip E, Altorki N, Zhou C, Csőszi T, Vynnychenko I, Goloborodko O, et al. Adjuvant atezolizumab after adjuvant chemotherapy in resected stage IB-IIIA non-small-cell lung cancer (IMpower010): a randomised, multicentre, open-label, phase 3 trial. *Lancet (London England)* (2021) 398(10308):1344–57. doi: 10.1016/s0140-6736(21)02098-5

39. Paz-Ares L, O'Brien MER, Mauer M, Dafni U, Oselin K, Havel L, et al. VP3-2022: Pembrolizumab (pembro) versus placebo for early-stage non-small cell lung cancer (NSCLC) following complete resection and adjuvant chemotherapy (chemo) when indicated: Randomized, triple-blind, phase III EORTC-1416-LCG/ETOP 8-15 – PEARLS/KEYNOTE-091 study. *Ann Oncol* (2022) 33(4):451–3. doi: 10.1016/j.annonc.2022.02.224

40. Nøst TH, Alcala K, Urbarova I, Byrne KS, Guida F, Sandanger TM, et al. Systemic inflammation markers and cancer incidence in the UK biobank. *Eur J Epidemiol* (2021) 36 (8):841–8. doi: 10.1007/s10654-021-00752-6

41. Peng M, Huang Q, Yin W, Tan S, Chen C, Liu W, et al. Circulating tumor DNA as a prognostic biomarker in localized non-small cell lung cancer. *Front Oncol* (2020) 10:561598. doi: 10.3389/fonc.2020.561598

42. Liu J, O'Donnell JS, Yan J, Madore J, Allen S, Smyth MJ, et al. Timing of neoadjuvant immunotherapy in relation to surgery is crucial for outcome. *Oncoimmunology* (2019) 8(5):e1581530. doi: 10.1080/2162402x.2019.1581530

43. Provencio-Pulla M, Nadal E, Larriba JLG, Martinez-Marti A, Bernabé R, Bosch-Barrera J, et al. Nivolumab + chemotherapy versus chemotherapy as neoadjuvant

treatment for resectable stage IIIA NSCLC: Primary endpoint results of pathological complete response (pCR) from phase II NADIM II trial. *J Clin Oncol* (2022) 40 (16_suppl):8501–1. doi: 10.1200/JCO.2022.40.16_suppl.8501

44. Pan Y, Fu Y, Zeng Y, Liu X, Peng Y, Hu C, et al. The key to immunotherapy: how to choose better therapeutic biomarkers for patients with non-small cell lung cancer. *biomark Res* (2022) 10(1):9. doi: 10.1186/s40364-022-00355-7

45. Oezkan F, Seweryn M, Pietrzak M, Byun WY, Owen D, Schulze K, et al. MA09.01 LCMC3: Immune cell subtypes predict nodal status and pathologic response after neoadjuvant atezolizumab in resectable NSCLC. *J Thorac Oncol* (2021) 16(10):S910–1. doi: 10.1016/j.jtho.2021.08.152

46. Rosner S, Reuss JE, Zahurak M, Taube JM, Broderick S, Jones DR, et al. Neoadjuvant nivolumab in early-stage non–small cell lung cancer (NSCLC): Five-year outcomes. *J Clin Oncol* (2022) 40(16_suppl):8537–7. doi: 10.1200/JCO.2022.40.16_suppl.8537

47. Fumet JD, Richard C, Ledys F, Klopfenstein Q, Joubert P, Routy B, et al. Prognostic and predictive role of CD8 and PD-L1 determination in lung tumor tissue of patients under anti-PD-1 therapy. *Br J Cancer* (2018) 119(8):950–60. doi: 10.1038/s41416-018-0220-9

48. E.C.o.T.V.-t.T. Chinese society of clinical oncology, E.C.o.N.-s.C.L.C. chinese society of clinical oncology, expert consensus on tumor mutational burden for immunotherapy in lung cancer. *Zhongguo Fei Ai Za Zhi* (2021) 24(11):743–52. doi: 10.3779/j.issn.1009-3419.2021.101.40

49. Deng H, Zhao Y, Cai X, Chen H, Cheng B, Zhong R, et al. PD-L1 expression and tumor mutation burden as pathological response biomarkers of neoadjuvant immunotherapy for early-stage non-small cell lung cancer: A systematic review and meta-analysis. *Crit Rev Oncol Hematol* (2022) 170:103582. doi: 10.1016/j.critrevonc.2022.103582

50. Reuss JE, Anagnostou V, Cottrell TR, Smith KN, Verde F, Zahurak M, et al. Neoadjuvant nivolumab plus ipilimumab in resectable non-small cell lung cancer. *J immunotherapy Cancer* (2020) 8(2):e001282. doi: 10.1136/jitc-2020-001282

51. Zhou Z, Ding Z, Yuan J, Shen S, Jian H, Tan Q, et al. Homologous recombination deficiency (HRD) can predict the therapeutic outcomes of immuno-neoadjuvant therapy in NSCLC patients. *J Hematol Oncol* (2022) 15(1):62. doi: 10.1186/s13045-022-01283-7

52. Jiang M, Jia K, Wang L, Li W, Chen B, Liu Y, et al. Alterations of DNA damage response pathway: Biomarker and therapeutic strategy for cancer immunotherapy. *Acta Pharm Sinica. B* (2021) 11(10):2983–94. doi: 10.1016/j.apsb.2021.01.003

53. Fanale D, Corsini LR, Scalia R, Brando C, Cucinella A, Madonia G, et al. Can the tumor-agnostic evaluation of MSI/MMR status be the common denominator for the immunotherapy treatment of patients with several solid tumors? *Crit Rev Oncol Hematol* (2022) 170:103597. doi: 10.1016/j.critrevonc.2022.103597

54. Herbst RS, Garon EB, Kim DW, Cho BC, Gervais R, Perez-Gracia JL, et al. Five year survival update from KEYNOTE-010: Pembrolizumab versus docetaxel for previously treated, programmed death-ligand 1-positive advanced NSCLC. *J Thorac Oncol Off Publ Int Assoc Study Lung Cancer* (2021) 16(10):1718–32. doi: 10.1016/j.jtho.2021.05.001

55. Kockx MM, McCleland M, Koeppen H. Microenvironmental regulation of tumour immunity and response to immunotherapy. *J Pathol* (2021) 254(4):374–83. doi: 10.1002/path.5681

56. Hiraoka K, Miyamoto M, Cho Y, Suzuoki M, Oshikiri T, Nakakubo Y, et al. Concurrent infiltration by CD8+ t cells and CD4+ t cells is a favourable prognostic factor in non-small-cell lung carcinoma. *Br J Cancer* (2006) 94(2):275–80. doi: 10.1038/sj.bjc.6602934

57. Sanmamed MF, Perez-Gracia JL, Schalper KA, Fusco JP, Gonzalez A, Rodriguez-Ruiz ME, et al. Changes in serum interleukin-8 (IL-8) levels reflect and predict response to anti-PD-1 treatment in melanoma and non-small-cell lung cancer patients. *Ann Oncol Off J Eur Soc Med Oncol* (2017) 28(8):1988–95. doi: 10.1093/annonc/mdx190

58. Kauffmann-Guerrero D, Kahnert K, Kiefl R, Sellmer L, Walter J, Behr J, et al. Systemic inflammation and pro-inflammatory cytokine profile predict response to checkpoint inhibitor treatment in NSCLC: a prospective study. *Sci Rep* (2021) 11 (1):10919. doi: 10.1038/s41598-021-90397-y

59. Yu Q, Zhao L, Yan XX, Li Y, Chen XY, Hu XH, et al. Identification of a TGF-β signaling-related gene signature for prediction of immunotherapy and targeted therapy for lung adenocarcinoma. *World J Surg Oncol* (2022) 20(1):183. doi: 10.1186/s12957-022-02595-1

60. Paz-Ares L, Kim TM, Vicente D, Felip E, Lee DH, Lee KH, et al. Bintrafusp alfa, a bifunctional fusion protein targeting TGF-β and PD-L1, in second-line treatment of patients with NSCLC: Results from an expansion cohort of a phase 1 trial. *J Thorac Oncol Off Publ Int Assoc Study Lung Cancer* (2020) 15(7):1210–22. doi: 10.1016/j.jtho.2020.03.003

61. Huang J, Liu D, Wang Y, Liu L, Li J, Yuan J, et al. Ginseng polysaccharides alter the gut microbiota and kynurenine/tryptophan ratio, potentiating the antitumour effect of antiprogrammed cell death 1/programmed cell death ligand 1 (anti-PD-1/PD-L1) immunotherapy. *Gut* (2022) 71(4):734–45. doi: 10.1136/gutjnl-2020-321031

62. Diem S, Schmid S, Krapf M, Flatz L, Born D, Jochum W, et al. Neutrophil-to-Lymphocyte ratio (NLR) and platelet-to-Lymphocyte ratio (PLR) as prognostic markers in patients with non-small cell lung cancer (NSCLC) treated with nivolumab. *Lung Cancer (Amsterdam Netherlands)* (2017) 111:176–81. doi: 10.1016/j.lungcan.2017.07.024

63. Grunnet M, Sorensen JB. Carcinoembryonic antigen (CEA) as tumor marker in lung cancer. *Lung Cancer (Amsterdam Netherlands)* (2012) 76(2):138–43. doi: 10.1016/j.lungcan.2011.11.012

64. Dal Bello MG, Filiberti RA, Alama A, Orengo AM, Mussap M, Coco S, et al. The role of CEA, CYFRA21-1 and NSE in monitoring tumor response to nivolumab in advanced non-small cell lung cancer (NSCLC) patients. *J Trans Med* (2019) 17(1):74. doi: 10.1186/s12967-019-1828-0

65. Wan JCM, Massie C, Garcia-Corbacho J, Mouliere F, Brenton JD, Caldas C, et al. Liquid biopsies come of age: towards implementation of circulating tumour DNA, nature reviews. *Cancer* (2017) 17(4):223–38. doi: 10.1038/nrc.2017.7

66. Wu Y-l, Lu S, Cheng Y, Zho Qh, Wang C-l, Wang Lh, et al. Expert consensus of molecular residual disease for non-small cell lung cancer. *J Evidence-Based Med* (2021) 21 (3):129–35. doi: 10.12019/j.issn.1671-5144.2021.03.001

67. Chaudhuri AA, Chabon JJ, Lovejoy AF, Newman AM, Stehr H, Azad TD, et al. Early detection of molecular residual disease in localized lung cancer by circulating tumor DNA profiling. *Cancer Discovery* (2017) 7(12):1394–403. doi: 10.1158/2159-8290.Cd-17-0716

68. Li N, Wang BX, Li J, Shao Y, Li MT, Li JJ, et al. Perioperative circulating tumor DNA as a potential prognostic marker for operable stage i to IIIA non-small cell lung cancer. *Cancer* (2022) 128(4):708–18. doi: 10.1002/cncr.33985

69. Yue D, Liu W, Chen C, Zhang T, Ma Y, Cui L, et al. Circulating tumor DNA predicts neoadjuvant immunotherapy efficacy and recurrence-free survival in surgical non-small cell lung cancer patients. *Trans Lung Cancer Res* (2022) 11(2):263–76. doi: 10.21037/tlcr-22-106

70. Provencio M, Serna-Blasco R, Nadal E, Insa A, García-Campelo MR, Casal Rubio J, et al. Overall survival and biomarker analysis of neoadjuvant nivolumab plus chemotherapy in operable stage IIIA non-Small-Cell lung cancer (NADIM phase II trial). *J Clin Oncol Off J Am Soc Clin Oncol* (2022) 40(25):2924–33. doi: 10.1200/jco.21.02660

71. Xia L, Mei J, Kang R, Deng S, Chen Y, Yang Y, et al. Perioperative ctDNA-based molecular residual disease detection for non-small cell lung cancer: A prospective multicenter cohort study (LUNGCA-1). *Clin Cancer Res an Off J Am Assoc Cancer Res* (2022) 28(15):3308–17. doi: 10.1158/1078-0432.Ccr-21-3044

72. Tian X, Wang R, Qian K, Li Y, Wang T, Liu L, et al. Postoperative ctDNA in indicating the recurrence risk and monitoring the effect of adjuvant therapy in surgical non–small cell lung cancers. *J Clin Oncol* (2022) 40(16_suppl):8533–3. doi: 10.1200/JCO.2022.40.16_suppl.8533

73. Zhang JT, Liu SY, Gao W, Liu SM, Yan HH, Ji L, et al. Longitudinal undetectable molecular residual disease defines potentially cured population in localized non-small cell lung cancer. *Cancer Discovery* (2022) 12(7):1690–701. doi: 10.1158/2159-8290.CD-21-1486

74. Paskeh MDA, Entezari M, Mirzaei S, Zabolian A, Saleki H, Naghdi MJ, et al. Emerging role of exosomes in cancer progression and tumor microenvironment remodeling. *J Hematol Oncol* (2022) 15(1):83. doi: 10.1186/s13045-022-01305-4

75. Joshua E, Kellie N, Valsamo A, Jiajia Z, Marianna Z, Justina X, et al. Neoadjuvant nivolumab in resectable non-small cell lung cancer: extended follow-up and molecular markers of response. *J Clin Oncol* (2019) 37:8524. doi: 10.1200/jco.2019.37.15_suppl.8524

76. Saw SPL, Ong B-H, Chua KLM, Takano A, Tan DSW. Revisiting neoadjuvant therapy in non-small-cell lung cancer. *Lancet Oncol* (2021) 22(11):e501–16. doi: 10.1016/S1470-2045(21)00383-1

77. Qiu F, Fan J, Shao M, Yao J, Zhao L, Zhu L, et al. Two cycles versus three cycles of neoadjuvant sintilimab plus platinum-doublet chemotherapy in patients with resectable non-small-cell lung cancer (neoSCORE): A randomized, single center, two-arm phase II trial. *J Clin Oncol* (2022) 40(16_suppl):8500–0. doi: 10.1200/JCO.2022.40.16_suppl.8500

78. Ling Y, Li N, Li L, Guo C, Wei J, Yuan P, et al. Different pathologic responses to neoadjuvant anti-PD-1 in primary squamous lung cancer and regional lymph nodes. *NPJ Precis Oncol* (2020) 4(1):32. doi: 10.1038/s41698-020-00135-2

frontiers | Frontiers in Oncology

TYPE Case Report
PUBLISHED 14 September 2023
DOI 10.3389/fonc.2023.912168



OPEN ACCESS

EDITED BY
Yuyan Wang,
Beijing Cancer Hospital, China

REVIEWED BY
Lei Kang,
Peking University, China
Carlo Genova,
University of Genoa, Italy
Kevin Sheng-Kai Ma,
School of Public Health, Harvard University, United States

*CORRESPONDENCE
Ru-peng Wang
wrp71@163.com
Yi Zhou
zhouy2011@163.com

RECEIVED 04 April 2022
ACCEPTED 04 August 2023
PUBLISHED 14 September 2023

CITATION
Li X, Li G, Chen D, Su L, Wang R-p and Zhou Y (2023) Case Report: sintilimab-induced Stevens-Johnson Syndrome in a patient with advanced lung adenocarcinoma.
*Front. Oncol.* 13:912168.
doi: 10.3389/fonc.2023.912168



# Case Report: sintilimab-induced Stevens-Johnson Syndrome in a patient with advanced lung adenocarcinoma

Xueqin Li[1], Guanghui Li[1], Diangang Chen[1], Linxi Su[2], Ru-peng Wang[3]* and Yi Zhou[1]*

[1]Institute of Cancer, Xinqiao Hospital, Army Medical University, Chongqing, China, [2]Department of Pathology, Xinqiao Hospital, Army Medical University, Chongqing, China, [3]Department of Rheumatology and Dermatology, Xinqiao Hospital, Army Medical University, Chongqing, China

Immune checkpoint inhibitors (ICIs) have been widely applicated in clinical therapy in recent years. Skin-related adverse reaction is one of the most common adverse events for ICIs. Stevens-Johnson syndrome (SJS) is one of the serious cutaneous reactions threatening the life. Here, we reported a case of 76-year-old male patient with poorly differentiated metastatic lung adenocarcinoma, after 9 weeks exposure of sintilimab (3 doses) combined with paclitaxel liposome after concurrent chemotherapy/radiotherapy, experienced Stevens-Johnson syndrome involving limbs, trunk, lip and the oral mucosa. Biopsy of the skin tissue showed infiltration of CD4 and CD8 positive T lymphocytes. We also found PD-L1 expression in the glands and the basal layer of the skin. This finding is distinct from the previously reported expression of PD-L1 on the surface of epidermal keratinocytes in patients with SJS due to immunotherapy.

KEYWORDS

**immunotherapy, adverse events, Stevens-Johnson Syndrome, sintilimab, case report**

## 1 Introduction

Immune checkpoint inhibitors (ICIs) are effective in the treatment of tumors and have been widely explored in recent years. ICIs kills tumors by activating autoimmune cells that may damage tissue. Due to their uniqueness, the side effects of ICIs are different from those of radiotherapy and chemotherapy. Skin toxicity is one of the most common adverse reactions for ICIs. Here, we presented a case of Stevens-Johnson syndrome (SJS) with poorly differentiated lung adenocarcinoma after being treated by sintilimab. Biopsy of the skin tissue showed infiltration of CD4 and CD8 positive T lymphocytes and PD-L1 expression in the glands and the basal layer of the skin.

## 2 Case description

On March 2020, a 76-year-old male with a long history of heavy smoking (about 75 pack-years) started to develop irritating cough, nausea, and paroxysmal chest tightness. These symptoms gradually worsened in the following months. On June 2020, positron emission tomography/computed tomography (PET/CT) scan was performed, revealing a lesion in the apical segment of the upper lobe of the right lung (5.1cm× 3.3 cm), encircling the superior vena cava and right pulmonary artery, with possible mediastinal, and right upper and lower clavicular lymph node metastases. Tumor marker carcinoembryonic antigen (CEA) was 183.4ng/mL. An electrocardiogram was also conducted, suggesting anterior interstitial and anterior wall old myocardial infarction, but the patient has no symptoms. Then, we performed a biopsy of the right supraclavicular lymph nodes, and histopathologic analysis suggested a poorly differentiated carcinoma, with immunohistochemical staining showing CK (+), CK 7(−), CK20 (−), P63 (−), TTF-1 (−), NAPSINA (−), Ki-67 (60%+) (Figures 1A–D). Next-generation sequencing (NGS) analysis was performed and identified. The results were obtained: EGFR, ALK, RET, MET, ROS1 without positive driver genes, the tumor proportion score (TPS) of PD-L1 protein expression was less than one percent, microsatellite state was stable (MSS), and tumor mutation burden (TMB) was 22.19 mutations/Mb. The clinical stage was cT4N3M0. Concurrent chemotherapy/radiotherapy was administered from July 24 to August 13, 2020. The radiotherapy target included the lung mass, right hilar, mediastinal, supraclavicular and subclavian lymph nodes and the dose of PGTV was 45Gy/15F. On July 20 and August 12, 2020, two cycles of paclitaxel liposome and carboplatin were performed. There were no obvious side effects during the treatment. One month after chemoradiotherapy, chest CT scan was performed to evaluate efficacy and the tumor regression degree was 31.4%. Then, the treatment was converted to paclitaxel liposome combined with sintilimab immunotherapy on September 17. After three cycles, the lesion was assessed as stable.

On November 19, 2020, patient began to develop painful erosion of the lips and the oral mucosa, dark red erythema localized to the chest wall, back, hands and feet. Hands and feet started to be swollen and blistered (Figure 2). On November 24, 2020, the patient was admitted to our dermatology department. TOX IgM, FZ IgM, CMV IgM, DP IgM were all negative. HCMV-DNA, EBV nucleic acid, BK virus nucleic acid, and JC virus nucleic acid were also all negative. After treated with antihistamines and compound glycyrrhizin anti-inflammatory therapy, the symptoms were not relieved and the pain of the lips and oral mucosa was getting worse. A pathological examination of the right forearm was performed on November 26, 2020. It showed epidermal necrosis and subepidermal split (Figures 3A, B), consistent with SJS. Immunofluorescence showed granular IGM and linear deposits on the basement membrane zone. Staphylococcus aureus was detected in the pustules. Severe drug rash with infection was considered and intravenous shock treatment was administered with methylprednisolone 50 mg/day (1 mg/kg/day) and infusion of immunoglobulin (Supplementary Table S1). Mupirocin ointment was applied to the infected area. 20 days later, the skin erythema became lighter, and the erosion and desquamation appeared on the chest, back and upper extremities. Some of the toenails became yellow and thickened before falling off. The dose of prednisone was reduced to 40 mg/day orally, until discontinuation on January 11, 2021. However, the dorsum of the left foot and the left external ankle were still erosional, the wound discharge was reviewed without bacterial or fungal growth. A medical wound nursing membrane was applied to promote healing, and the erosion had improved but still persisted. The erosion was somewhat resistant to local corticosteroids. Then we analyzed the patient's right forearm skin biopsy to assess for PD-1 and PD-L1. The results were positive for both PD-1 (Figure 3C) and PD-L1 expression (22C3 pharmDx assay, Agilent Technologies), particularly with PD-L1 expression in the basal layer of the skin (Figure 3D) and in the glands (Figure 3E). PD-L1 expression in tonsil tissue was used as a control to verify antibody specificity (Supplementary Figure 1). We also performed CD4 and CD8 positive T lymphocyte expression assay, and the

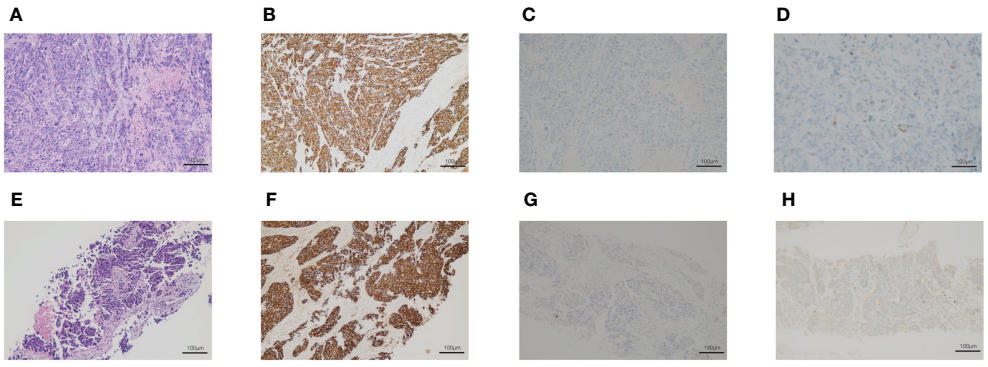


FIGURE 1
The biopsy of the right supraclavicular lymph node. **(A–D)** The first biopsy of the right supraclavicular lymph node. **(A)** Hematoxylin and eosin-stained staining of the right supraclavicular lymph node. **(B)** Immunohistochemical staining of CK. **(C)** Immunohistochemical staining of p63. **(D)** Immunohistochemical staining of TTF-1. **(E–H)** The second biopsy of the right supraclavicular lymph nodes. **(E)** Hematoxylin and eosin-stained section of the right supraclavicular lymph node. **(F)** Immunohistochemical staining of CK. **(G)** Immunohistochemical staining of p63. **(H)** Immunohistochemical staining of TTF-1.

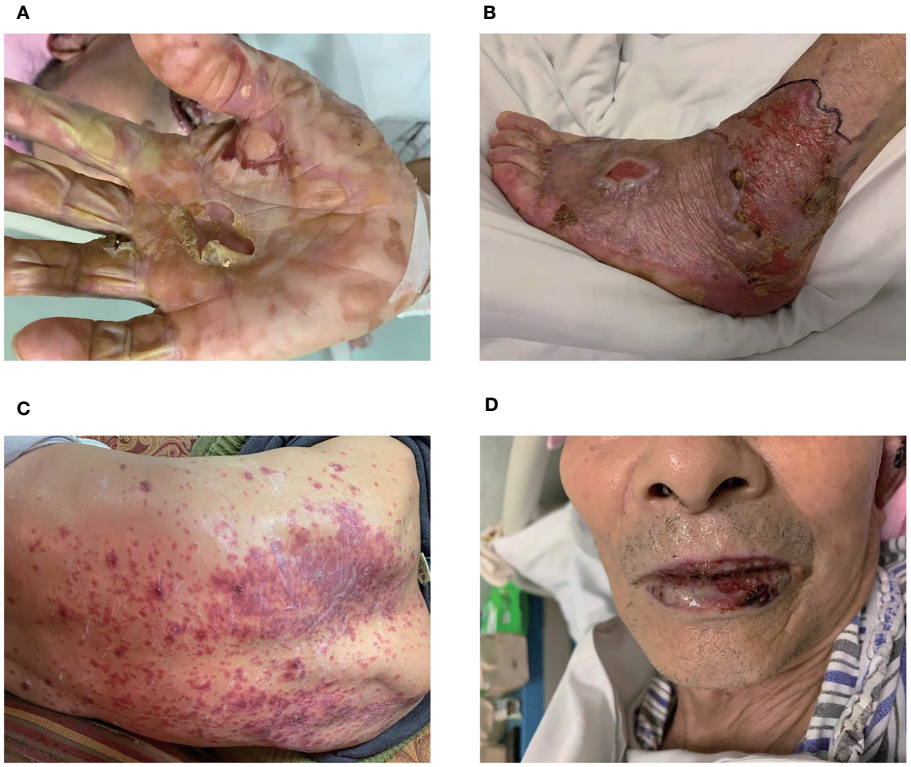


FIGURE 2
Skin and lips mucosa injury. The localized skin lesions presented with erosions on hands **(A)** and feet **(B)**. **(C)** The erythema was on the back. **(D)** The lips mucosa had painful erosions.

results showed positive CD4 (Figure 3F) and CD8 (Figure 3G) positive T lymphocyte infiltration.

After two months, chest CT revealed that the right lung lesion and right supraclavicular lymph nodes were significantly larger than before. We performed a second biopsy of the right supraclavicular lymph node and confirmed a poorly differentiated adenocarcinoma with immunohistochemical staining results showing CK 7(−), TTF-1 (+), NAPSINA (−), P40 (−), P63(−), CK5/6(−), 35BH11(+), CK (+), Ki-67 (70%+) (Figures 1E–H). Two cycles of chemotherapy with pemetrexed were administered, however the tumors continued to grow and the patient's physical state was not adequate for further chemotherapy. On July, 2021, chest CT revealed tumor progressed. On August, 2021, the right lung lesion and right supraclavicular lymph node were implanted with radioactive iodine-125 particles.

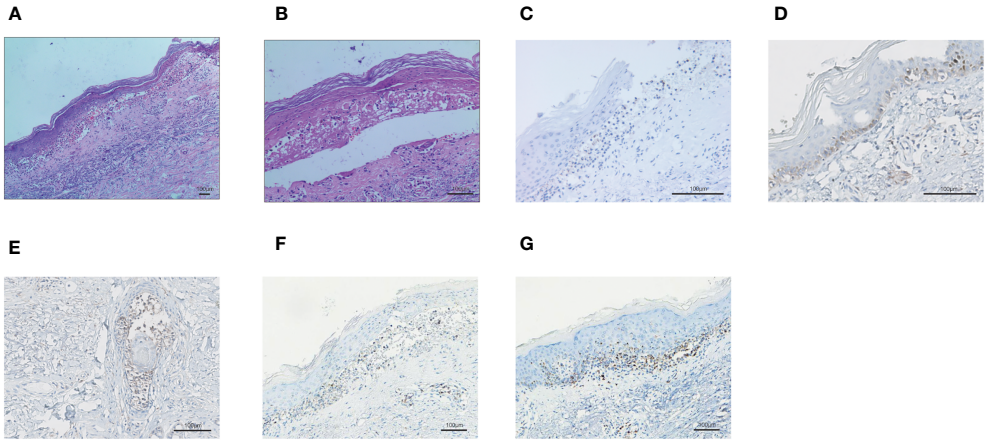


FIGURE 3
The biopsy of the skin lesion of right forearm. **(A-B)** Hematoxylin and eosin-stained staining of skin biopsy. The biopsy of the skin lesion showed local keratinocytic necrosis **(A)** and subepidermal split **(B)**. **(C)** PD-1 expression in skin lesion. **(D)** PD-L1 expression in the basal layer of the skin. **(E)** PD-L1 expression in the glands of the skin. **(F)** CD4+ T lymphocyte infiltration in the skin. **(G)** CD8+ T lymphocyte infiltration in the skin.

The patient was followed up by telephone in December 2021, and he was in a good condition.

## 3 Timeline

On June 2020, the patient was diagnosed with poorly differentiated lung cancer and the clinical stage was cT4N3M0. From July to August 2020, concurrent chemotherapy/radiotherapy was administered. Paclitaxel liposome and sintilimab were administered for three cycles from September 2020. Unfortunately, SJS-induced by sintilimab on November 2020. Then, the treatments for SJS were performed. on March 2021, the right lung lesion and supraclavicular lymph node were significantly larger than before, two cycles of chemotherapy with pemetrexed were administered. On July 2021, the tumor was progression again and the radioactive iodine-125 particles were implanted (Figure 4).

## 4 Diagnostic assessment

On June 28, 2020, the mass in right lung approximately 5.1cm × 3.3 cm. On September 15, 2020, the tumor regression degree was 31.4% after chemoradiotherapy (approximately 3.5 cm × 2.2 cm). On November 2, 2020, the tumor assessment was stability (approximately 3.5 cm × 2.2 cm). On March 9, 2021, the tumor mass of right lung (approximately 4.2 cm ×2.8 cm) and right supraclavicular lymph nodes were significantly larger than before. On July 28, 2021, the tumor of right lung was significantly larger than previous detection (approximately 7.2 cm ×3.6 cm) (Figure 4).

## 5 Discussion

ICIs, including the PD-1, PD-L1, and CTLA-4 monoclonal antibodies, can result in impressive response rates and durable disease remission in patients with cancer and have thus revolutionized the treatment of advanced cancer patients. There are several biomarkers that can be used to predict the efficacy of immunotherapy, including PD-L1, TMB, MSI, and dMMR. Checkmate-227 study on non-small cell lung cancer (NSCLC) showed that high TMB is a positive predictor for the efficacy of PD-1 antibodies, especially with the use of combination therapy (1). In this case, tumor tissue NGS analysis before treatment suggested high TMB, and we provided treatment with sintilimab, which is a monoclonal antibody against PD-1 and had been performed to treat non-small cell lung cancer (2).

Cutaneous adverse reactions have been the most common and increase with continued use of ICIs. The common skin manifestations are maculopapular rash, pruritus, and vitiligo-like lesions. Other potentially severe cutaneous adverse events include multiforme-like drug reaction, Stevens-Johnson syndrome (SJS), and drug rash with eosinophilia and systemic symptoms (DRESS syndrome) (3–5). SJS was severe adverse cutaneous drug reactions that predominantly involve the skin and mucous membranes. The damage is primarily to the body surfaces, with painful red spots and blisters forming on the skin, eyes, mouth, and genitals. Ma et al. reported ocular side effects of 8 cancer patients in whom SJS/TEN developed during ICIs treatment. The ocular manifestations included no involvement in 3 patients (37.5%), mild involvement in 2 patients (25%), and most severe involvement in 3 patients (37.5%) (6). In our study, the disease mainly affected the chest, back, limbs and lip, but did not involve the patient's eyes. According to the patient's clinical stage, we formulated a treatment plan of concurrent chemotherapy/radiotherapy followed by immunotherapy maintenance (7). For PD-L1 <1%, durvalumab has no or insignificant benefit from available data (8), so we adopted the mode of chemotherapy combined with immunotherapy. Due to the efficacy, cost - effective and accessibility of drugs, we chose sintilimab (2). The patient developed painful erosion of the lips and the oral mucosa, severe and extensive skin lesions after 3 cycles of treatment with sintilimab, a pathological examination of right forearm showed epidermal necrosis and subepidermal split, which was consistent with SJS. Generally speaking, IGM deposit was undetected in SJS. Autoimmune-related indexes were tested and the result showed SSA antibody (3+), RO-52 (3+), antinuclear antibody titer (1:100) and ANA-PH-S (coarse particle type). These might lead to granular IGM and linear deposits of Immunofluorescence on the basement membrane zone.

According to the literature, many different classes of drugs have been found to cause SJS/TEN. Drugs that bear a high risk for SJS/TEN including antileptics (carbamazepine, lamotrigine, phenobarbital and phenytoin), anti-infective drugs (sulfonamides, sulfasalazine and nevirapine), NSAIDs (piroxicam) and allopurinol. Other drugs are moderate risk for SJS/TEN, such as antibiotics (cephalosporins, macrolides, Quinolones, Tetracyclines) and NSAIDs (diclofenac) (9). PD-1 inhibitors can also cause SJS (10),

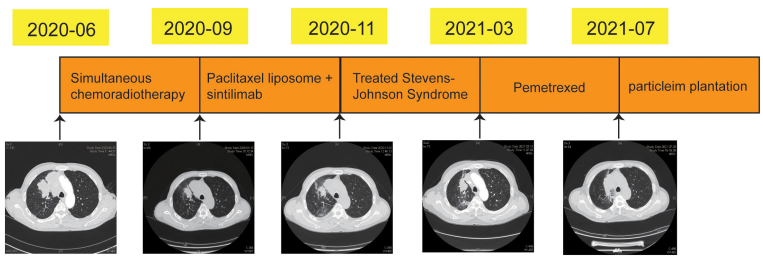


FIGURE 4
Timeline of treatment and diagnostic assessment of lung lesions during treatment.

and the most reported agents were nivolumab and pembrolizumab. The most common drugs to cause chemotherapy-induced SJS include lenalidomide, methotrexate, docetaxel, and thalidomide. SJS happened concomitantly or within 8 weeks of the chemotherapeutic agents exposed. The immune checkpoint inhibitors latency period for inducing SJS/TEN ranged from 7 days to 140 days. A recent systematic review reported that SJS/TEN-like reactions caused by nivolumab had median onset time of 3 weeks in seven cases, whereas pembrolizumab had median onset time of 11 weeks in five cases, the average latency of SJS as 8.9 weeks (11). The patient had no drug allergies before, he had been treated with atorvastatin for several months, and he had no exposure to new compounds other than sintilimab. During the checkpoint inhibitor therapy, lichenoid drug eruption is one of common skin-related adverse reaction. Some cases are associated with severe erosive or bullous lesions. The lesions of bullous lichenoid drug eruption were epidermolytic, mild mucosal involvement, protracted disease course and relatively good overall health, but histological findings were not consistent with SJS. The histology of both lichenoid drug eruptions and SJS characterized by necrotic keratinocytes and subepidermal cleft formation. However, the more prominent lymphocytic infiltrate, along with jagged acanthosis (often with parakeratosis), is suggestive of lichenoid drug eruption. This histological findings in our case consistent with SJS (12, 13). Paraneoplastic syndrome can also manifest as cutaneous adverse reactions, but cutaneous manifestations usually occur months or years before tumor diagnosis (although they can appear simultaneously), and in this case the patient had no rash at the time of disease onset. Given the temporal relationship between initiation of immunotherapy and the onset of SJS, paraneoplastic SJS is less likely. Skin reactions caused by radiotherapy are usually localized radiation dermatitis in the radiation field. Radiotherapy may lead to a hypersensitivity reaction by preferentially impairing T suppressor cells. The hypersensitivity reaction induced by radiotherapy may have had synergistic and/or complementary contributions to the immune dysregulation. Many studies have shown that genetic factors contribute to differences in drug sensitivity. Chung et al. had demonstrated a strong association between the HLA-B*1502 and SJS induced by carbamazepine in Han Chinese (14). Furthermore, the HLA-A*02:07 and HLA-B*46:01 alleles were significantly associated with severe ocular complications among Han Chinese patients with SJS resulted by ICIs (15). However, genomic test for the patient did not detect these HLA subtypes. An MDT (multidisciplinary team) meeting was conducted by Dermatologists, pharmacologists, pathologists, oncologists and immunologists. Given the patient's symptoms and history, SJS-induced by sintilimab was diagnosed, which is an uncommon and harmful adverse effect of sintilimab therapy. SJS is characterized by total epidermal necrosis due to extensive keratinocyte apoptosis.

Previously, sintilimab has been associated with myositis-myasthenia overlap syndrome (16), autoimmune diabetes mellitus (17), cytokine release syndrome, pulmonary fibrosis, hypothyroidism, and encephalitis (18–21). Now we report SJS caused by sintilimab. Knowing that the main cause of adverse reactions by ICIs is overactivation of immunity, but the mechanism is incompletely understood. Moreover, TMB, MSI, and dMMR were not present in the somatic cells; thus, we speculated whether it was the high expression of PD-L1 or PD-1 in the skin cells that led to SJS via the immune cells simultaneously attacking the tumor and the skin cells. Therefore, we performed tissue PD-1 and PD-L1 assays on the skin lesions, and the results showed that the skin biopsies were positive for both PD-1 and PD-L1 expression. PD-L1 is usually undetectable in skin cells, but anti-PD1 therapy could increase the expression of PD-L1 in keratinocytes and permit the activated CD8+ cytotoxic T cells to target keratinocytes, leading to keratinocyte apoptosis (22). Ziemer et al. also observed PD-L1 expression on the surface of deceased epidermal keratinocytes from all SJS/TEN patients (23). In the current patient, we detected PD-L1 expression in the glands and in the basal layer of the skin, and it appeared to be specific in the glands. Additionally, CD4 and CD8 positive T lymphocytes were infiltrated, indicating active immune response. CD8-positive T cells infiltration leaded to keratinocyte apoptosis and SJS. Whether more infiltration of immune cells after SJS is not clear and needs to be further studied in the future. Previous studies have suggested that the surge of PD-L1 expression in the epidermis may represent an antagonistic lymphocyte (22). The gene expression profile between anti-PD-1 medicines treated patients and SJS/TEN patients was similar, with upregulation of CXCL9, CXCL10, CXCL11, PRF1, GZMB, and FASLG. The relationship between dose or time of exposure to ICIs and cutaneous adverse reactions has not been fully elucidated (24). The onset of adverse reactions may continue for months or even years after discontinuation, and clinicians need to remain vigilant (25). The patient's rash gradually improved through hormone shock therapy and infusion of immunoglobulin to achieve immunosuppressive and immunomodulatory effects, alleviating the patient's symptoms.

In conclusion, sintilimab-associated SJS in lung cancer treatment is a very rare adverse event, but the consequences are serious. During and after treatment with anti-PD-1 agents, it is imperative to monitor the skin adverse reactions.

## Patient perspective

The patient expressed his gratitude to the medical staff for all their efforts during the treatment.

## Data availability statement

The datasets presented in this study can be found in online repositories. The names of the repository/repositories and accession number(s) can be found in the article/Supplementary Material.

## Ethics statement

Ethical review and approval was not required for the study on human participants in accordance with the local legislation and institutional requirements. The patients/participants provided their written informed consent to participate in this study. Written

informed consent was obtained from the individual(s) for the publication of any potentially identifiable images or data included in this article.

## Author contributions

YZ and RW designed the concept and investigation. XL collected and analyzed data and wrote this paper, DC and GL analyzed data, LS provided assistance. All authors contributed to the article and approved the submitted version.

## Funding

This study was supported by the Scientific Research Project of Army Medical University (2021XQN21).

## Acknowledgments

We would like to thank the patient in this case and all the medical staff for their careful care during the treatment.

## Conflict of interest

The authors declare that the research was conducted in the absence of any commercial or financial relationships that could be construed as a potential conflict of interest.

## Publisher's note



## Supplementary material

The Supplementary Material for this article can be found online at: https://www.frontiersin.org/articles/10.3389/fonc.2023.912168/full#supplementary-material

## References

1. Hellmann MD, Ciuleanu TE, Pluzanski A, Lee JS, Otterson GA, Audigier-Valette C, et al. Nivolumab plus ipilimumab in lung cancer with a high tumor mutational burden. *N Engl J Med* (2018) 378:2093–104. doi: 10.1056/NEJMoa1801946

2. Yang Y, Wang Z, Fang J, Yu Q, Han B, Cang S, et al. Efficacy and safety of sintilimab plus pemetrexed and platinum as first-line treatment for locally advanced or metastatic nonsquamous NSCLC: a randomized, double-blind, phase 3 study (Oncology pRogram by InnovENT anti-PD-1-11). *J Thorac Oncol* (2020) 15:1636–46. doi: 10.1016/j.jtho.2020.07.014

3. Saw S, Lee HY, Ng QS. Pembrolizumab-induced Stevens–Johnson syndrome in non-melanoma patients. *Eur J Cancer* (2017) 81:237–9. doi: 10.1016/j.ejca.2017.03.026

4. Mirza S, Hill E, Ludlow SP, Nanjappa S. Checkpoint inhibitor-associated drug reaction with eosinophilia and systemic symptom syndrome. *Melanoma Res* (2017) 27:271–3. doi: 10.1097/CMR.0000000000000326

5. Nomura H, Takahashi H, Suzuki S, Kurihara Y, Chubachi S, Kawada I, et al. Unexpected recalcitrant course of drug-induced erythema multiforme-like eruption and interstitial pneumonia sequentially occurring after nivolumab therapy. *J Dermatol* (2017) 44:818–21. doi: 10.1111/1346-8138.13810

6. Ma KS, Saeed HN, Chodosh J, Wang CW, Chung YC, Wei LC, et al. Ocular manifestations of anti-neoplastic immune checkpoint inhibitor-associated Stevens-Johnson syndrome/toxic epidermal necrolysis in cancer patients. *Ocul Surf* (2021) 22:47–50. doi: 10.1016/j.jtos.2021.06.010

7. Antonia SJ, Villegas A, Daniel D, Vicente D, Murakami S, Hui R, et al. Durvalumab after chemoradiotherapy in stage III non-small-cell lung cancer. *N Engl J Med* (2017) 377:1919–29. doi: 10.1056/NEJMoa1709937

8. Spigel DR, Faivre-Finn C, Gray JE, Vicente D, Planchard D, Paz-Ares L, et al. Five-year survival outcomes from the PACIFIC trial: durvalumab after chemoradiotherapy in stage III non-small-cell lung cancer. *J Clin Oncol* (2022) 40:1301–11. doi: 10.1200/JCO.21.01308

9. Paulmann M, Mockenhaupt M. Severe skin reactions: clinical picture, epidemiology, etiology, pathogenesis, and treatment. *Allergo J Int* (2019) 28:311–26. doi: 10.1007/s40629-019-00111-8

10. Creamer D, Walsh SA, Dziewulski P, Exton LS, Lee HY, Dart JK, et al. UK Guidelines for the management of Stevens–Johnson syndrome/toxic epidermal necrolysis in adults 2016. *Br J Dermatol* (2016) 174:1194–227. doi: 10.1111/bjd.14530

11. Maloney NJ, Ravi V, Cheng K, Worswick S. Stevens-Johnson syndrome and toxic epidermal necrolysis-like reactions to checkpoint inhibitors: a systematic review. *Int J Dermatol* (2020) 59:183–8. doi: 10.1111/ijd.14811

12. Ziemer M, Fries V, Paulmann M, Mockenhaupt M. Epidermal necrolysis in the context of immuno-oncologic medication as well as kinase inhibitors and biologics. *J Dtsch Dermatol Ges* (2022) 20(6):777–86. doi: 10.1111/ddg.14711

13. Reschke R, Mockenhaupt M, Simon JC, Ziemer M. Severe bullous skin eruptions on checkpoint inhibitor therapy - in most cases severe bullous lichenoid drug eruptions. *J Dtsch Dermatol Ges* (2019) 17(9):942–8. doi: 10.1111/ddg.13876

14. Chung WH, Hung SI, Hong HS, Hsih MS, Yang LC, Ho HC, et al. Medical genetics: a marker for Stevens-Johnson syndrome. *Nature* (2004) 428:486. doi: 10.1038/428486a

15. Ma KS, Chung WH, Hsueh YJ, Chen SY, Tokunaga K, Kinoshita S, et al. Human leucocyte antigen association of patients with Stevens-Johnson syndrome/toxic epidermal necrolysis with severe ocular complications in Han Chinese. *Br J Ophthalmol* (2022) 106(5):610–5. doi: 10.1136/bjophthalmol-2020-317105

16. Xing Q, Zhang ZW, Lin QH, Shen LH, Wang PM, Zhang S, et al. Myositis-myasthenia gravis overlap syndrome complicated with myasthenia crisis and myocarditis associated with anti-programmed cell death-1 (sintilimab) therapy for lung adenocarcinoma. *Ann Transl Med* (2020) 8:250. doi: 10.21037/atm.2020.01.79

17. Wen L, Zou X, Chen Y, Bai X, Liang T. Sintilimab-induced autoimmune diabetes in a patient with the anti-tumor effect of partial regression. *Front Immunol* (2020) 11:2076. doi: 10.3389/fimmu.2020.02076

18. Gao C, Xu J, Han C, Wang L, Zhou W, Yu Q. An esophageal cancer case of cytokine release syndrome with multiple-organ injury induced by an anti-PD-1 drug: a case report. *Ann Palliat Med* (2020) 9:2393–9. doi: 10.21037/apm-20-1310

19. Ni J, Zhang L, Zhang X. Marked elevation of creatine phosphokinase alone caused by sintilimab beware of hypothyroid myopathy. *Eur J Cancer* (2020) 128:57–9. doi: 10.1016/j.ejca.2019.12.030

20. Kang K, Zheng K, Zhang Y. Paraneoplastic encephalitis and enteric neuropathy associated with anti-Hu antibody in a patient following immune-checkpoint inhibitor therapy. *J Immunother* (2020) 43:165–8. doi: 10.1097/CJI.0000000000000314

21. Hu J, Li Y, Chen X, Luo C, Zuo X. Pulmonary fibrosis and cytokine release syndrome after hyperactivation with sintilimab. *J Clin Pharm Ther* (2020) 45:1474–7. doi: 10.1111/jcpt.13217

22. Goldinger SM, Stieger P, Meier B, Micaletto S, Contassot E, French LE, et al. Cytotoxic cutaneous adverse drug reactions during anti-PD-1 therapy. *Clin Cancer Res* (2016) 22:4023–9. doi: 10.1158/1078-0432.CCR-15-2872

23. Ziemer CM, Miedema J, Smith CJ, Liu Z, Thomas NE, Googe PB. Immunohistochemical expression of PD-L1 is increased in lesional epidermal keratinocytes in Stevens–Johnson syndrome/toxic epidermal necrolysis. *Am J Dermatopathol* (2021) 43:318–20. doi: 10.1097/DAD.0000000000001816

24. Ernstoff MS, Gandhi S, Pandey M, Puzanov I, Grivas P, Montero A, et al. Challenges faced when identifying patients for combination immunotherapy. *Future Oncol* (2017) 13:1607–18. doi: 10.2217/fon-2017-0218

25. Pennock GK, Chow LQ. The evolving role of immune checkpoint inhibitors in cancer treatment. *Oncologist* (2015) 20:812–22. doi: 10.1634/theoncologist.2014-0422

# Frontiers in Immunology

**Explores novel approaches and diagnoses to treat immune disorders.**

The official journal of the International Union of Immunological Societies (IUIS) and the most cited in its field, leading the way for research across basic, translational and clinical immunology.

## Discover the latest Research Topics

See more →


**Frontiers**

Avenue du Tribunal-Fédéral 34
1005 Lausanne, Switzerland
frontiersin.org

**Contact us**

+41 (0)21 510 17 00
frontiersin.org/about/contact